

**The University of Sheffield**  
Department of Chemistry



Development of electroactive polymers for  
application in anti-corrosion formulations.

**Ryan Nicholas Rees**

A thesis submitted for the degree of Doctor of Philosophy

March 2016

Dedicated to my loving Girlfriend, Parents and Family

*“After this, there is no turning back.....You quit – the story end, you wake up in your bed and believe whatever you want to believe. You carry on and finish it – you stay in Wonderland and you’ll see how deep the rabbit-hole goes!”*

-Dialogue sourced from The Matrix and modified as a motivational speech, a close friend.

*“You have to let it all go. Fear, doubt, and disbelief. Free your mind.”*  
-Morpheus, The Matrix (Warner Bros. Pictures, 1999).

*"Live as if you were to die tomorrow. Learn as if you were to live forever."*  
- Mahatma Gandhi

# Declaration

This thesis is submitted for the degree of doctorate of philosophy at the University of Sheffield, having been submitted for no other degree. The research discussed and presented in this thesis is original work undertaken by myself at the University of Sheffield from October 2007 to September 2012 unless otherwise stated.

Ryan Nicholas Rees

March 2016

# Abstract

Corrosion is a major environmental and economic problem with many modern manmade structures heavily relying on the utilisation of metals and alloys due to their extraordinary strength, mechanical and physical properties. Applications such as those seen in the construction industry, aerospace and marine industries, all of which need a constant protection and barriers against the harsh environmental conditions. Current methods of protection employ the use of chromates in paint formulations for the active anti-corrosive paints or the uses of non-active polymeric paints acting solely as a physical barrier preventing the diffusion of ions through to the metal surface. However ideas have recently come forward regarding the use of conductive and electro-active polymers. Theorised to not only prevent the diffusions of ions on a physical level but to also act as an electrochemical barrier by passivating the surface of the metal so that it can protect itself from further degradation caused by corrosive agents, one such polymer that has been put forward is Polyaniline (PANI). Through the process of doping, PANI can be made to conduct an electrical current through the formation of charge carriers by oxidising the PANI with a protonic acid which can be functionalised. Further investigation has found that the functionalisation of these acids can dramatically change the once insoluble material in common solvents soluble, increasing the processability and possible increase the applications of this materials.

This thesis reports the synthetic routes used to obtain functionalised Sulphonic acids based on the precursor 5-Sulphoisophthalic acid by acid catalysed esterification's are described. With the synthesis phosphoric acid diester carried out by several named reported methods and both series were progressed forward to dope PANI (polyaniline). The optical properties were analysed for all doped PANI in DCM showing that branched side chains produced the highest optical absorption at around 944 nm and some as thin films (21) and (25), showing optical band gaps of 1.21 eV.

This thesis also reports the anti-corrosions properties for the doped PANI systems. Films were cast coating mild carbon steel and copper plates, along with a range of acrylic resin/doped PANI composite films, PVC/doped PANI composite films and a set of films for an epoxide resin/doped PANI (17) composite. Samples were subjected to accelerated corrosion tests and showed that the application of PANI to the metal surfaces was beneficial and displayed efficacious anti-corrosion properties, not only in the doped state (emeraldine salt) but also in its native undoped state (emeraldine base) where the polymer undergoes redox reactions at the metal interface passivating the surface and creating an electrochemical barrier system which the polymer itself is a component however corrosion inhibition is only truly effective when a physical barrier is used in combination.

The results of the dopant synthesis, doped PANI systems and their composites in resins and the data from NMR spectroscopy, IR, elemental analysis, LC-Mass spectroscopy, mass spectroscopy, UV-Vis spectroscopy are presented in this thesis. The accelerated corrosion tests and the data from scanning electron microscopy (SEM) are also presented within this thesis.

# Acknowledgements

The use of please and thank you cost nothing to express but the impact can mean so much to a fellow neighbour. There are many people I am indebted for their guidance, assistance, support, friendship and love throughout the whole project. Without them I feel that I would have completed this thesis but my mental state may have been in question.

First of all I would like to acknowledge my supervisor Dr. Ahmed Iraqi for whom I would like to show my deepest gratitude for his support and guidance. Always there to help giving words of wisdom. This thesis would not exist had it not been for ICI who later became known as Akzo Nobel, their funding made this project possible allowing Dr. Shaun Wright to conduct the initial research that created the basis for my work. Appreciation should be made to the Iraqi group, for their repartee and help, namely; Dr. Hunan Yi, Abdul-Aziz, Mohammed, Richard, Soliman and Sani. Other people who deserve mention that are from other groups are Paul Bonner, Adam Ellis, Georgia Mann, Anika Clifton, Tom Swift who became a very close friend, Katie Brown, Andrew McKenzie and Kayleigh Cox-Nowak. A mention must go to Rob Hansen and Simon Thorpe for their help with the analytical services, Sue Bradshaw for NMR spectra measurements, Mel Hannah our lab technician who quickly came to know me as the bane of the lab due to some of my experiments. Pete Farran and Nick Smith from the chemistry stores and 'Paul the Porter', deserve my appreciation for whom when I felt at a low point during the research I could find go to and find an escape for a brief time.

Other factors made my time in Sheffield among the best years of my life. Les Mills International, who have a range of fitness classes which I later became qualified to teach; BodyATTACK, BodyPUMP, CXWorx and Les Mills Grit™ expelling all my troubles during the class. Music kept me sane throughout and Saturday nights at The Corporation 'Corp' Rock and Heavy Metal nightclub deserve the highest accolade.

Finally my Family, Girlfriend and close friends who I also consider family, were always naturally there for me being moral support and pillar for me to lean on when I was at my lowest encouraging me to go on and continue strong on the path to completion of this postgraduate degree.

# Table of Contents

DECLARATION .....	III
ABSTRACT .....	IV
ACKNOWLEDGEMENTS .....	V
TABLE OF CONTENTS .....	VI
TABLE OF FIGURES .....	XII
TABLE OF SCHEMES .....	XVI
TABLE OF MECHANISMS .....	XVII
TABLE OF EQUATIONS .....	XVIII
TABLE OF TABLES .....	XIX
TABLE OF APPENDICES .....	XX
<b>CHAPTER 1 INTRODUCTION</b> .....	<b>1</b>
1.1 FOUNDATIONS AND THE HISTORY OF POLYMER SCIENCE .....	1
1.1.1 <i>History of Polymers</i> .....	1
1.1.2 <i>Current applications of Polymers</i> .....	2
1.2 CONJUGATED POLYMERS .....	2
1.1.3 <i>The development of conductive polymers</i> .....	4
1.1.3.1 Historical Perspective of Conjugated polymers .....	4
1.1.4 <i>Properties of Conjugated and Conductive Polymers</i> .....	6
1.1.4.1 Electronic properties of conjugated polymers .....	8
1.1.4.2 Physical properties of conjugated polymers .....	9
1.1.4.3 Band gaps .....	9
1.1.4.3.1 Peierls Effect/Distortion .....	12
1.1.4.4 Manipulating the Band gaps of polymers .....	15
1.1.5 <i>Concept of Doping</i> .....	16
1.1.5.1 Mechanisms and Methods of Doping Polymeric Materials .....	17
1.1.5.3.1 Redox Methods of Doping .....	17
1.1.5.3.1.1 <i>p</i> -type doping .....	18
1.1.5.3.1.1.1 Chemical Doping .....	19
1.1.5.3.1.1.2 Electrochemical Doping .....	21
1.1.5.3.1.2 <i>n</i> -Type chemical doping .....	22
1.1.5.3.1.2.1 Chemical Reduction/Doping .....	22
1.1.5.3.1.2.2 Electrochemical Reduction/Doping .....	22
1.1.5.3.1.3 Charge Injection doping .....	23
1.1.5.3.1.4 Photo Induced Doping .....	23
1.1.5.3.2 Non redox doping .....	24
1.1.6 <i>Charge Transport Mechanism</i> .....	25
1.1.6.1 Solitons .....	27
1.1.6.2 Polarons .....	29
1.1.6.3 Bipolarons .....	30
1.1.6.4 Charge Hopping .....	31
1.2 POLYANILINE .....	32
1.2.1 <i>Properties of Polyaniline</i> .....	32
1.2.2 <i>Synthesis of Polyaniline</i> .....	38

1.2.3	<i>Doping of Polyaniline</i> .....	38
1.2.3.1	Functionalised Dopants.....	42
1.2.3.1.1	Secondary solvent doping effects .....	43
1.2.4	<i>Conduction Mechanism of Polyaniline</i> .....	44
1.2.5	<i>Uses of Polyaniline</i> .....	44
1.3	<b>CORROSION AND THE USE OF POLYANILINE IN ANTI-CORROSIVE PAINTS.</b> .....	45
1.3.1	<i>Corrosion of Metallic materials.</i> .....	46
1.3.2	<i>Corrosion of Steel</i> .....	48
1.3.3	<i>Corrosion of Copper</i> .....	49
1.3.4	<i>Corrosion of Aluminium</i> .....	51
1.3.5	<i>Use of Polyaniline in anti-corrosive paints.</i> .....	53
1.3.5.1	Mechanism of protection. ....	54
1.3.5.2	Solubility issues and possible solutions .....	55
1.3.5.3	Matrices, and their properties .....	56
1.3.5.4	Current corrosion protection paints utilising PANI.....	57
<b>CHAPTER 2 AIMS AND OBJECTIVES</b> .....		59
2.1	PURPOSE.....	59
2.1.1	<i>Polyaniline and doping</i> .....	60
2.2	PROPOSAL.....	60
2.2.1	<i>Phase One: The Development of Functionalised Dopants.</i> .....	62
2.2.2	<i>Phase 2/3: Corrosion testing of Metal substrates coated with various degrees of doped Polyaniline and its analysis.</i> .....	64
<b>CHAPTER 3 EXPERIMENTAL</b> .....		66
3.1	GENERAL PROCEDURES .....	66
3.1.1	<i>Materials</i> .....	66
3.1.2	<i>Analysis Techniques</i> .....	66
3.1.2.1	Thin Layer Chromatography.....	66
3.1.2.2	Elemental Analysis .....	66
3.1.2.3	Mass Spectroscopy (MS) and Liquid Chromatography Mass Spectroscopy (LC-MS).....	66
3.1.2.4	Infra-Red Absorption Spectroscopy (IR).....	67
3.1.2.5	UV-Visible Absorption Spectroscopy .....	67
3.1.2.6	NMR Spectroscopy.....	67
3.1.2.7	Accelerated Corrosion Testing.....	67
3.1.2.8	Electron Microscopy.....	68
3.2.	DOPANT SYNTHESIS .....	68
3.2.1.	<i>Sulphonic Acid series of Dopants.</i> .....	68
3.2.1.1	Bis(8-hydroxyoctyl) 5-sulphoisophthalic acid (1) (SIPAOO).....	68
3.2.1.2	Bis(8-acryloxy octyl)-5- Sulphoisophthalic acid(2) (SIPAOA).....	69
3.2.1.3	Bis[2-(2-hydroxy-ethoxy)-ethyl]-5-sulphoisophthalic acid (3). .....	70
3.2.1.4	Bis(8-methacryloxy octyl)-5-Sulphoisophthalic acid (4).....	70
3.2.2.	<i>Hydrogen phosphate diester dopant Series.</i> .....	71
3.2.2.1	Bis(8-acryloyloxy octyl) hydrogen phosphate (DAOHP) (5).....	71
3.2.2.2	Bis(8-methacryloyloxy octyl) hydrogen phosphate(6) (DMOHP).....	73
3.2.3.	<i>Other Compounds and Intermediate compounds for Dopant synthesis.</i> .....	74
3.2.3.1	8-hydroxyoctyl acrylate (7) .....	74
3.2.3.2	8-hydroxyoctyl methacrylate (8) .....	75
3.2.3.3	2-Chloromethyl-4-nitrophenyl phosphorodichloridate (9) .....	76
3.2.3.4	2-Chloromethyl-4-nitrophenyl phosphorodi(octyl acrylate) (10) .....	77
3.2.3.5	2-Chloromethyl-4-nitrophenyl bis(8-methacryloxy octyl) phosphoridate (11).....	78
3.2.4	OTHER SYNTHESIS .....	78

3.2.4.1	2-(N,N-Dimethylamino)-4-nitrophenol hydrochloride (12)	78
3.3	POLYMER DOPING	79
3.3.1	<i>Procedure for doping PANI with dopants.</i>	79
3.3.1.1	Doping of PANI with bis(8-hydroxy octyl)-5-sulphoisophthalic acid (1) in dichloroacetic Acid (DCAA) (17)	80
3.3.1.2	Doping of PANI with bis(8-acryloxy octyl)-5-sulphoisophthalic acid (2) in dichloroacetic Acid (DCAA) (18)	80
3.3.1.3	Doping of PANI bis[2-(2-hydroxy-ethoxy)-ethyl]-5-sulphoisophthalic acid (3) in dichloroacetic Acid (DCAA) (19)	81
3.3.1.4	Doping of PANI with bis(8-methacryloxy octyl)-5-sulphoisophthalic acid (4) in dichloroacetic Acid (DCAA) (20)	81
3.3.1.5	Doping of PANI with bis(8-methacryloxy octyl) hydrogen phosphate (6) in dichloroacetic acid (DCAA) (21)	82
3.3.1.6	Doping of PANI with dodecylbenzene sulphonic acid (14) in dichloroacetic Acid (DCAA) (22)	82
3.3.1.7	Doping of PANI with bis(2-ethyl hexyl) hydrogen phosphate (15) in dichloroacetic Acid (DCAA) (23)	83
3.3.1.8	Doping of PANI with bis(2-methacryloxy ethyl) hydrogen phosphate (16) in dichloroacetic Acid (DCAA) (24)	83
3.4	PREPARATION OF POLYMER COATING SOLUTIONS	83
3.4.1	<i>Preparation of polyaniline composites.</i>	83
3.4.1.1	General preparation of PANI/PVC composite Solutions	83
3.4.1.1.1	Doped PANI (17)/PVC 1 wt% film	84
3.4.1.1.2	Doped PANI (18)/PVC 1 wt% film	84
3.4.1.1.3	Doped PANI (20)/PVC 1 wt% film	84
3.4.1.1.4	Doped PANI (21)/PVC 1 wt% film	84
3.4.1.1.5	Doped PANI (22)/PVC 1 wt% film	84
3.4.1.1.6	Doped PANI (23)/PVC 1 wt% film	84
3.4.3	<i>General preparation of PANI/epoxy resin composite solutions.</i>	84
3.4.4	<i>General preparation of epoxy resin composite solutions.</i>	85
3.4.4.1	Preparation of Epikote 828 for a 20wt%	85
3.4.4.2	Preparation of Epikote 828 for a 10wt%	85
3.4.4.3	Preparation of Epikote 828 for a 5wt%	85
3.4.4.4	Preparation of Epikote 828 for a 2wt%	85
3.4.4.5	Preparation of Epikote 828 for a 1wt%	86
3.4.5	<i>General preparation of acrylic resin/PANI composite solutions.</i>	86
3.4.5.1	Doped PANI (18)/acrylate resin film 1 wt%	86
3.4.5.2	Doped PANI (20)/acrylic resin film 1 wt%	86
3.4.5.3	Doped PANI (21)/acrylic resin film 1 wt%	86
3.4.5.4	Doped PANI (23)/acrylic resin film 1 wt%	86
3.5	PREPARATION OF METAL PLATES	86
3.5.1	<i>Preparation of mild carbon steel plates.</i>	86
3.5.2	<i>Preparation of pure copper plates.</i>	87
3.6	PREPARATION OF SOLVENT CAST FILMS	87
3.6.1	<i>Preparation of polyaniline films.</i>	87
3.6.2	<i>Preparation of PVC films.</i>	87
3.6.3	<i>Preparation of polyaniline/PVC composite films.</i>	87
3.6.4	<i>Preparation of polyaniline/epoxy resin composites</i>	87
3.6.4.1	Preparation of polyaniline – epoxy resin composite (20wt%)	88
3.6.4.2	Preparation of polyaniline – epoxy resin composite (10wt%)	88
3.6.4.3	Preparation of polyaniline – epoxy resin composite (5wt%)	88
3.6.4.4	Preparation of polyaniline – epoxy resin composite (2wt%)	88
3.6.4.5	Preparation of polyaniline – epoxy resin composite (1wt%)	88

3.6.5	<i>Preparation of polyaniline – acrylic resin composites.</i>	88
3.7	CORROSION INHIBITION TESTING.	88
<b>CHAPTER 4 RESULTS AND DISCUSSION: DOPANTS SYNTHESIS AND DOPING STUDIES</b>		
		90
4.1	SYNTHESIS OF SULPHONIC ACID SERIES OF DOPANTS.	90
4.1.1	<i>The synthesis of bis(8-hydroxyoctyl) 5-sulphoisophthalic acid (1) (SIPAOH).</i>	90
4.1.1.1	The alcohol dehydration of bis(8-hydroxyoctyl) 5-sulphoisophthalic acid (1) with excess 1, 8 – octanediol in hot, dry low pressure conditions.	94
4.1.2	<i>The synthesis of bis(8-acryloxy octyl)-5-sulphoisophthalic acid (2) (SIPAOA) and bis(8-methacryloxy octyl) 5-sulphoisophthalic acid (4) (SIPAOMA).</i>	96
4.1.3	<i>The synthesis of bis[2-(2-hydroxy-ethoxy)-ethyl]-5-sulphoisophthalic acid (3) (SIPADEG).</i>	99
4.2	SYNTHESIS OF PHOSPHORIC ACID DIESTERS SERIES OF DOPANTS.	100
4.2.1	<i>The synthesis of bis(8-acryloxy octyl) hydrogen phosphate (DAOHP) (5) and the synthesis of bis(8-methacryloxy octyl) hydrogen phosphate (DMOHP) (6).</i>	100
4.2.1.1	The synthesis of bis(8-acryloxy octyl) hydrogen phosphate (5) via original developed methods (Method 1).	100
4.2.1.2	The synthesis of bis(8-acryloxy octyl) hydrogen phosphate (5) and bis(8-methacryloxy octyl) hydrogen phosphate (6) via a modified method of Muhika et al <sup>104,105</sup> (Method 2).	102
4.2.1.3	The synthesis of bis(8-acryloxy octyl) hydrogen phosphate (5) via a modified method of Jang and Jeong <sup>106</sup> (Method 3).	106
4.2.1.4	Problems encountered during the synthesis of the phosphodiester.	108
4.3	SYNTHESIS OF ADDITIONAL AND AUXILIARY COMPOUNDS.	109
4.3.1	<i>The synthesis of 8-hydroxyoctyl acrylate (7) and the 8-hydroxyoctyl methacrylate (8).</i>	109
4.3.3	<i>2-Chloromethyl-4-nitrophenyl phosphorodichloridate (9).</i>	110
4.3.4	<i>The synthesis of 2-chloromethyl-4-nitrophenyl phosphorodi(octyl acrylate) (10) and 2-chloromethyl-4-nitrophenyl bis(8-methacryloxy octyl) phosphoridate (11).</i>	112
4.3.6	<i>2-(N, N-Dimethylamino)-4-nitrophenol protecting group (12).</i>	113
4.4	POLYMER DOPING	114
4.4.1	<i>The doping of PANI with the sulphonic acid and phosphoric acid diesters (17 – 25).</i>	115
4.4.2	<i>The preparation of doped PANI composites with PVC.</i>	117
4.4.3	<i>The preparation of doped PANI composites with epoxide resin.</i>	118
4.4.5	<i>The preparation of doped PANI composites with acrylic resin.</i>	120
4.5	UV/VIS SPECTROSCOPY OF DOPED POLYANILINE.	125
4.5.1	<i>Electronic and optical properties of the sulphonic acid and phosphoric acid doped series of PANI in solution and cast films.</i>	126
4.5.1.1	Analysis of the sulphonic acid doped PANI series in solutions of DCM.	128
4.5.1.1.1	Electronic properties of bis(8-hydroxy octyl) 5-sulphoisophthalic acid doped PANI (17) (PANI-SIPAOH).	130
4.5.1.1.2	Electronic properties of bis(8-acryloxy octyl) 5-sulphoisophthalic acid doped PANI (18) (PANI- SIPAOA).	132
4.5.1.1.3	Electronic properties of bis[2-(2-hydroxy-ethoxy)-ethyl]-5-sulphoisophthalic acid doped PANI (19) (PANI- SIPADEG).	133
4.5.1.1.4	Electronic properties of bis(8-methacryloxy octyl)-5-sulphoisophthalic acid doped PANI (20) (PANI-SIPAOMA).	133
4.5.1.1.5	Electronic properties of dodecylbenzene sulphonic acid doped PANI (22) (PANI-DBSA).	134
4.5.1.2	Analysis of the phosphoric acid diester doped PANI series in solutions of DCM.	136

4.5.1.2.1 Electronic properties of bis(8-methacryloyloxy octyl) hydrogen phosphate doped PANI (21) (PANI-DMOHP).....	140
4.5.1.2.2 Electronic properties of bis(2-ethylhexyl) hydrogen phosphate doped PANI (23) (PANI-DEHHP).....	142
4.5.1.2.3 Electronic properties of bis(2-methacryloyloxy ethyl) hydrogen phosphate doped PANI (24) (PANI-DMEHP).....	143
4.5.1.2.4 Electronic properties of bis(8-acryloyloxy octyl) hydrogen phosphate doped PANI (25) (PANI-DAOHP).....	144
4.5.1.3 Analysis of the phosphoric acid diester doped PANI series cast films from DCM solutions. ...	145
4.5.1.3.1 Optical properties of bis(8-methacryloyloxy octyl) hydrogen phosphate doped PANI (21) (PANI-DMOHP) Films.....	146
4.5.1.3.2 Optical properties of bis(8-acryloyloxy octyl) hydrogen phosphate doped PANI (25) (PANI-DAOHP) cast film.....	148
4.5.2 Electronic and optical properties of doped PANI series PVC films.....	151
4.5.3 Solvent effects on doping and electronic properties of PANI.....	153
4.5.3.1 Electronic and optical properties induced by DCAA.....	154
4.5.3.2 Electronic and optical properties induced by <i>m</i> -cresol.....	155
4.5.3.3 Electronic and Spectroscopic effects induced by NMP.....	159
4.5.3.4 Electronic and optical properties of doped PANI (21) films cast from different Solvents..	162

**CHAPTER 5 RESULTS AND DISCUSSION: ACCELERATED CORROSION STUDIES. 166**

5.1 ACCELERATED CORROSION TESTING.....	166
5.1.1 Scanning Electron Microscope (SEM).....	166
5.1.2 Accelerated corrosion of the experiment standards for benchmarking.....	167
5.1.2.1 Accelerated corrosion of uncoated metal and morphology results.....	168
5.1.2.2 PVC Alone Accelerated corrosion tests and morphology of the coating.....	169
5.1.2.3 Accelerated corrosion tests and morphology of the Epikote 828™ films.....	171
5.1.2.4 Accelerated corrosion tests using acrylic resin alone films.....	172
5.1.3 Accelerated corrosion of metal coated with doped PANI.....	173
5.1.3.1 Films cast with Sulphonic acid series doped PANI.....	174
5.1.3.1.1 Films cast with hydroxyl functionalised sulphonic acid doped PANI.....	174
5.1.3.1.1.1 The morphology of hydroxyl functionalised sulphonic acid dopants.....	175
5.1.3.1.2 Films cast with acrylic functionalise sulphonic acid doped PANI.....	176
5.1.3.1.2.1 The morphology of acrylic functionalised sulphonic acid dopants.....	177
5.1.3.1.3 Films cast with dodecylbenzene sulphonic acid doped PANI.....	178
5.1.3.1.3.1 Morphology of dodecylbenzene sulphonic acid films.....	179
5.1.3.2 Films cast with Phosphoric acid diester series of doped PANI.....	180
5.1.3.2.1 Morphology of films phosphoric acid diester series.....	183
5.1.3.2.2 Literature standard phosphoric acid diester's films and their morphology.....	186
5.1.4 PANI/Polymer resin composites.....	189
5.1.4.1 Doped PANI/PVC composites film accelerated corrosion.....	189
5.1.4.1.1 Doped PANI/PVC composite film morphology.....	193
5.1.4.2 Doped PANI/epoxy resin composite film accelerated corrosion.....	194
5.1.4.2.1 Morphology of doped PANI/epoxy resin composite film accelerated corrosion.....	197
5.1.4.3 Doped PANI/acrylate resin composite film accelerated corrosion.....	198
5.1.4.3.1 Morphology of doped PANI/acrylic resin complex coated samples.....	201

**CHAPTER 6 CONCLUSIONS AND FUTURE WORK..... 205**

6.1 GENERAL PROCEDURES.....	205
6.1.1 Dopant synthesis.....	205
6.1.2 Doping of PANI.....	208
6.1.3 UV studies of doped PANI (17 – 25).....	209

6.1.4	<i>Composites</i> .....	212
6.1.5	<i>Corrosion testing</i> .....	214
6.1.6	<i>Corrosion results</i> .....	216
6.1.7	<i>Overall conclusion</i> .....	217
6.2	FUTURE WORK.....	219
<b>REFERENCES</b> .....		221
<b>APPENDIX</b> .....		229
1.	UV/VISIBLE SPECTROSCOPY (SUPPLEMENTARY).....	229
2.	ACCELERATED CORROSION (SUPPLEMENTARY).....	234
3.	ELECTRON MICROSCOPY IMAGES (SUPPLEMENTARY).....	241

# Table of Figures

FIGURE 1: REPEATING UNITS OF A RANGE OF CONJUGATED POLYMERS; ILLUSTRATING SIMPLE, HETEROCYCLIC AND COMPLEX REPEATING UNITS. ....	3
FIGURE 2: STRUCTURE OF POLY (SULPHUR NITRIDE).....	4
FIGURE 3: THE ISOMERIC FORMS OF POLY (ACETYLENE).....	5
FIGURE 4: CONDUCTIVITY RANGES OF VARIOUS KNOWN MATERIALS, SHOWING REGIONS OF CONDUCTIVITIES AND ELECTRONIC REGIMES OF MATERIALS <sup>19</sup> .....	7
FIGURE 5: THREE REPRESENTATIONS OF POLYACETYLENE; IN DEGENERATE GROUND STATE, ELECTRON DELOCALISATION OF THE $\pi$ -BONDING ALONG THE POLYMER CHAIN AND ELECTRON LOCALISATION SHOWING THAT EACH CARBON HAS AN ELECTRON WHICH CAN BE DONATED INTO THE $\pi$ -SYSTEM. ....	8
FIGURE 6: COMPARISON OF ENERGY LEVELS AND BAND GAPS BETWEEN THE ELECTRONIC STATES OF MATERIALS.....	10
FIGURE 7: ENERGY LEVEL DIAGRAM, ILLUSTRATING THE FORMATION OF BANGS GAPS UPON INCREASING CONJUGATION, WITH FORMATION FROM DISCREET ENERGY LEVELS TO ENERGY BANDS. ....	11
FIGURE 8: BOND LENGTHS OF <i>TRANS</i> -POLYACETYLENE <sup>20</sup> . ....	13
FIGURE 9: STRUCTURAL REPRESENTATIONS OF POLY (SULPHUR NITRIDE); A, THE SIMPLIFIED CHEMICAL STRUCTURE. B, REPRESENTATION OF THE STRUCTURE IN TERMS OF ELECTRON DELOCALISATION, AND C, REPRESENTATION OF THE LONE UNPAIRED ELECTRON LOCALISED TO THE NITROGEN ATOM.....	14
FIGURE 10:PHYSICAL STRUCTURE OF POLYSULPHUR NITRIDE <sup>26</sup> .....	14
FIGURE 11: THE OXIDATION OF PA IN THE PRESENCE OF BROMINE VAPOUR RESULTING IN THE UNDESIRABLE SATURATED BY PRODUCT. ....	18
FIGURE 12: STRUCTURAL DIFFERENCES BETWEEN BENZENOID AND QUINOID STRUCTURE. ....	19
FIGURE 13: THE ISOMERIC FORMS OF POLY (ACETYLENE).....	20
FIGURE 14: DOPING OF PA WITH IODINE VAPOUR AT ROOM TEMPERATURE.....	20
FIGURE 15: BAND GAPS UPON SUBJECTING TO <i>N</i> -TYPE AND <i>P</i> -TYPE DOPANTS.....	26
FIGURE 16: THE DIMERISED DEGENERATE GROUND STATES OF <i>TRANS</i> -POLYACETYLENE. ....	27
FIGURE 17: NEUTRAL SOLITON.....	28
FIGURE 18: SOLITONS; A) NEGATIVE SOLITON, B) POSITIVE SOLITON. SHOWING THE MID-GAP ENERGY LEVEL BETWEEN THE VALENCE BAND AND THE CONDUCTION BAND. ....	29
FIGURE 19: FORMATION OF POLARONS, BIPOLARON AND BIPOLARON BANDS UPON INCREASING DOPING LEVELS. MOST COMMON METHOD FOR OBTAINING THESE ELECTRONIC SPECIES BEING VIA OXIDATION DUE TO ELECTRON DENSITIES OF THE POLYMERIC MATERIAL.....	30
FIGURE 20: LINEAR CHARGE TRANSPORT ALONG THE POLYMER CHAIN.....	31
FIGURE 21: CHARGE HOPPING BETWEEN PARALLEL CHAINS.....	32
FIGURE 22: INTRACHAIN CARBON-CARBON BOND LENGTH AND INTERCHAIN SPACING DISTANCE. ....	32
FIGURE 23: OXIDATION STATES OF POLYANILINE <sup>3</sup> .....	34
FIGURE 24: ELECTROCHEMICAL ROUTES OF OBTAINING PANI IN DIFFERENT OXIDATION STATES. ....	35
FIGURE 25: <i>N</i> -DOPING OF POLYANILINE <sup>54</sup> .....	41
FIGURE 26: ELECTROSTATIC INTERACTION AT THE METAL/PANI INTERFACE <sup>81</sup> .....	55
FIGURE 27: STRUCTURES OF 4-SULPHOPHTHALIC ACID AND 5-SULPHOSIOPHTHALIC ACID.....	63
FIGURE 28: PROPOSED SERIES OF DOPANTS TO BE SYNTHESISED AND UTILISED FOR DOPING PANI, INCLUDING DOPANTS FOUND IN JOURNAL ARTICLES.....	63
FIGURE 29: BISPHENOL A DIGLYCIDYL ETHER FORM (EPIKOTE 828 <sup>TM</sup> ). ....	64
FIGURE 30: ILLUSTRATION OF THE EQUIPMENT USED FOR THE ACCELERATED CORROSION TESTING, A RUDIMENTARY METHOD USING A HEATED CULTIVATOR/PROPAGATOR OBTAINABLE FROM ANY	

GENERAL DIY OR GARDENING ESTABLISHMENT. AS SHOWN METAL SAMPLES WILL BE SUBMERGED AND EXPOSURE TO HUMID AND HARSH ENVIRONMENT.....	65
FIGURE 31: <sup>1</sup> H-NMR PORTION REPRESENTING THE LABELLED AREAS; A, B AND C. INTEGRATIONS INCLUDED FOR CALCULATING THE LEVELS OF ALCOHOL DEHYDRATION TO PRODUCE AN ETHER LINKAGE (C). .....	92
FIGURE 32: <sup>1</sup> H-NMR DISPLAYING SIDE PRODUCTS PRODUCED IN THE PRESENCE OF <i>P</i> -METHOXYPHENOL. ....	109
FIGURE 33: EXAMPLE OF A CROSS LINKED SEGMENT OF THE COMPOSITE WITH THE CURING AGENT (JEFFAMINE ®D230), SHOWN IN RED. ....	120
FIGURE 34: GENERALISED STRUCTURES OF THE POTENTIAL CROSSLINKING OF THE METHACRYLATE AND ACRYLATE FUNCTIONALISED DOPANTS. ....	123
FIGURE 35: UV-VISIBLE SPECTRA OF ALL THE SUCCESSFULLY DOPED POLYANILINE .....	126
FIGURE 36: PRECURSOR AND GENERAL ANALOGUE FOR; A) SULPHONIC ACID AND B) PHOSPHORIC ACID RANGE OF DOPANTS .....	128
FIGURE 37: SPECTRAL OVERLAYS OF POLYANILINE DOPED WITH A VARIETY OF DOPANTS BELONGING TO THE SULPHONIC ACID SERIES, MEASURED IN A SOLUTIONS OF DCM.....	128
FIGURE 38: STRUCTURE OF BISPHENOL A EPOXIDE RESIN. ....	131
FIGURE 39: STRUCTURE OF THE ALIPHATIC SIDE CHAIN FOR THE DOPANT USED IN DOPED PANI (17) .....	131
FIGURE 40: SPECTRAL OVERLAYS OF POLYANILINE DOPED WITH A VARIETY OF DOPANTS BELONGING TO THE PHOSPHORIC ACID DIESTER SERIES.....	137
FIGURE 41: SPECTRAL OVERLAYS OF THE PHOSPHORIC AND SULPHONIC ACID (FUNCTIONALISED WITH METHACRYLOYLOXY OCTYL CHAINS) DOPED PANI (21) AND (20) RESPECTIVELY.....	141
FIGURE 42: SIMPLE ILLUSTRATION TO SHOW THE SITES OF STERIC EFFECTS BETWEEN THE DOPANT AND THE POLYMER CHAIN (PANI). A) DISPLAYS THE EFFECTS SEEN WHEN PANI IS DOPED WITH A SULPHONIC ACID DOPANT (IN THIS CASE DBSA) AND B) IS THE SAME AS PREVIOUS BUT DEMONSTRATING THE SITES OF STERIC EFFECTS WHEN A PHOSPHORIC ACID DOPING SYSTEMS IS UTILISED, IN THIS CASE BIS(2-METHACRYLOYLOXY ETHYL) HYDROGEN PHOSPHATE (DMEHP). ....	144
FIGURE 43: SPECTRAL OVERLAYS OF THE PHOSPHORIC ACID (FUNCTIONALISED WITH METHACRYLOYLOXY OCTYL (21) AND ACRYLOYLOXY OCTYL (25) CHAINS) DOPED PANI (21) AND (25) RESPECTIVELY.....	145
FIGURE 44: UV/VIS SPECTROSCOPY DISPLAYING THE ELECTRONIC PROPERTIES OF POLYANILINE DOPED WITH BIS(8-METHACRYLOYLOXY OCTYL) HYDROGEN PHOSPHATE (PANI-DMOHP) (21) CAST AS A THIN FILM FROM A SOLUTION OF DCM ONTO A QUARTZ PLATE. ....	146
FIGURE 45: THE SPECTRAL OVERLAY OF DOPED PANI (21) IN A SOLUTION OF DCM AND ITS CORRELATING THIN FILM CAST FROM A SOLUTION OF DCM. ....	147
FIGURE 46: UV/VIS SPECTROSCOPY DISPLAYING THE ELECTRONIC PROPERTIES OF POLYANILINE DOPED WITH BIS(8-ACRYLOYLOXY OCTYL) HYDROGEN PHOSPHATE (PANI-DMOHP) (25) CAST AS A THIN FILM FROM A SOLUTION OF DCM ONTO A QUARTZ PLATE. ....	148
FIGURE 47: THE SPECTRAL OVERLAY OF DOPED PANI (25) IN A SOLUTION OF DCM AND ITS CORRELATING THIN FILM CAST FROM A SOLUTION OF DCM. ....	149
FIGURE 48: SPECTRAL OVERLAY OF THE OPTICAL PROPERTIES OF DOPED PANI (17 – 18, 20, 22 - 23, 25) INCORPORATED INTO A PVC MATRIX AND CAST AS A FILM ONTO QUARTZ GLASS. ....	151
FIGURE 49: SPECTRAL OVERLAYS OF DOPED PANI (PANI-ES) AND UN-DOPED PANI (PANI-EB) IN DCAA TO DEMONSTRATE ANY POTENTIAL EFFECTS THAT MAY BE EXHIBITED IN DCAA.....	154
FIGURE 50: SPECTRAL OVERLAYS OF DOPED PANI (PANI-ES) AND UN-DOPED PANI (PANI-EB) IN <i>M</i> -CRESOL TO DEMONSTRATE ANY POTENTIAL EFFECTS THAT MAY BE EXHIBITED BY THE SOLVENT. ....	155
FIGURE 51: ILLUSTRATION OF BAND GAPS IN THE CASE OF <i>M</i> -CRESOL.....	156
FIGURE 52: STRUCTURE OF <i>M</i> -CRESOL. ....	156

FIGURE 53: AROMATIC $\pi$ STACKING OF THE POLYANILINE BACKBONE IN A SOLUTION OF <i>m</i> -CRESOL, ILLUSTRATING SECONDARY DOPING EFFECTS. ....	157
FIGURE 54: STRUCTURE OF CAMPHOR SULPHONIC ACID. ....	158
FIGURE 55: MOLECULAR RECOGNITION (STERIC MATCHING) DOPED PANI IN <i>m</i> -CRESOL. DEMONSTRATING THE EXAMPLES OF FORCES INVOLVED IN THE DEVELOPMENT OF THE SUPRAMOLECULAR COMPLEX (PANI = GREEN, DOPANT = BLACK AND <i>m</i> -CRESOL = BLUE). ...	159
FIGURE 56: STRUCTURE OF <i>N</i> -METHYL-2-PYRROLIDONE (NMP).....	160
FIGURE 57: SPECTRUM OF DOPED PANI (21) IN NMP. ....	160
FIGURE 58: ILLUSTRATION OF THE NMP/PANI/DOPANT COMPLEX. ....	162
FIGURE 59: SPECTRAL OVERLAYS OF DOPED PANI (21) FILMS CAST FROM A VARIETY OF SOLVENTS ILLUSTRATING RED SHIFTS IN ABSORPTION FROM SOLUTIONS TO THIN FILMS. ....	163
FIGURE 60: A TYPICAL HEATED PROPAGATOR USED FOR THE ACCELERATED CORROSION TESTING. IMAGES OBTAINED FROM; <a href="http://www.britcrophydroponics.co.uk/components/com_virtuemart/shop_image/product/stewart_propagat_4cdd2f3a96c1c.jpg">HTTP://WWW.BRITCROPHYDROPONICS.CO.UK/COMPONENTS/COM_VIRTUEMART/SHOP_IMAGE/PRODUCT/STEWART_PROPAGAT_4CDD2F3A96C1C.JPG</a> AND <a href="http://www.bostockshomeandgarden.co.uk/webroot/bt/shops/store_002e_shop910/470b/772c/d366/14c2/f3c3/ac10/3d2a/ec93/large_electric_propagator.jpg">HTTP://WWW.BOSTOCKSHOMEANDGARDEN.CO.UK/WEBROOT/BT/SHOPS/STORE_002E_SHOP910/470B/772C/D366/14C2/F3C3/AC10/3D2A/EC93/LARGE_ELECTRIC_PROPAGATOR.JPG</a> ..	166
FIGURE 61: PHILIPS XL20 SCANNING ELECTRON MICROSCOPE. OPERATING VOLTAGES BETWEEN 8 AND 12 kV, RESOLUTION TO 4NM AND A MAXIMUM MAGNIFICATION OF X50,000. ....	167
FIGURE 62: PHOTOGRAPH OF MILD STEEL AND COPPER POST SUBMERSION IN A (3.5%) SALINE SOLUTION FOR 7 DAYS.....	168
FIGURE 63: A) MAGNIFIED UN-CORRODED AREA (LEFT), MAGNIFIED TO X3000 AND B) RUSTED AREA MAGNIFIED TO OVER 700 TIMES. ....	169
FIGURE 64: PHOTOGRAPHS OF PVC CAST FILM ONTO MILD STEEL; SAMPLING A) 7 DAYS AFTER BEING SPRAYED WITH A 3.5% SALINE SOLUTION AND B) 7DAYS AFTER BEING SUBMERGED INTO A 3.5% SALINE SOLUTION. ....	170
FIGURE 65: PVC CAST ONTO PRE-TREATED COPPER, ILLUSTRATING INTERNAL STRUCTURE OF A PORE ON A CAST FILM. ....	170
FIGURE 66: STRUCTURE OF BISPHENOL A DIGLYCIDYL ETHER FORM (EPIKOTE 828™) USED FOR THIS RESEARCH. ....	171
FIGURE 67: CLOSE UP OF SHOWING RUST/METAL INTERFACE UNDER THE EPOXIDE FILM. ....	171
FIGURE 68: CLOSE UP PATINA/COPPER INTERFACE. ....	172
FIGURE 69: STRUCTURE OF METHYL METHACRYLATE, UPON THE CROSSLINKING AND FREE RADICAL POLYMERISATION FORMS A VAST NETWORK WHICH RESULTS IN A THIN FILM (COATING). ....	172
FIGURE 70: METAL PLATES COATED IN ACRYLIC RESIN ALONE AFTER 7DAYS (168 HRS) OF ACCELERATED CORROSION TESTING. FROM LEFT TO RIGHT; STEEL SUBMERGED IN BRINE AND COPPER SUBMERGED IN BRINE, STEEL SPRAYED WITH SALINE AND COPPER SPRAYED WITH SALINE. ....	173
FIGURE 71: STRUCTURES OF THE SULPHONIC ACID SERIES OF DOPANTS USED TO DOPE PANI.....	174
FIGURE 72: POLYMERIC FILM SITTING ON THE EDGE OF A PATCH OF RUST. AN ILLUSTRATION OF POTENTIAL CRYSTALLINITY OF THE DOPED PANI. ....	176
FIGURE 73: PHOTOGRAPH OF A) MILD STEEL AFTER 24 HRS SUBMERSION IN 3.5% SALINE SOLUTION AND B) MILD STEEL AFTER 1 HR POST SALINE SPRAY, COATED WITH DOPED PANI (17). ....	177
FIGURE 74: MORPHOLOGY OF DOPED PANI (18); A) 350X MAG., B) 1339X MAG.....	178
FIGURE 75: PHOTOGRAPH OF BOTH STEEL AND COPPER SUBMERGED FOR 7 DAYS IN (3.5%) SALINE SOLUTION (LEFT AND MIDDLE IMAGE) AND EFFECTS 7 DAYS AFTER BEING SPRAYED WITH (3.5%) SALINE SOLUTION, COATED WITH DOPED PANI (22). ....	179
FIGURE 76: POLYANILINE DOPED WITH LITERATURE STANDARD DBSA. ....	180
FIGURE 77: STRUCTURES OF DOPANTS USED IN DOPED PANI (21) AND (23). ....	180
FIGURE 78: PHOTOGRAPH OF BOTH STEEL AND COPPER 24 HRS OF TESTING (TOP IMAGE) AND CORROSION NOTICED AFTER 7 DAYS; FROM LEFT TO RIGHT STEEL SUBMERGED, COPPER	

SUBMERGED, STEEL SPRAYED AND COPPER SPRAYED WITH (3.5%) SALINE SOLUTION AND COATED DOPED PANI (21). .....	181
FIGURE 79: PHOTOGRAPH OF BOTH STEEL AND COPPER 24 HRS OF TESTING (TOP IMAGE) AND CORROSION NOTICED AFTER 7 DAYS; FROM LEFT TO RIGHT STEEL SUBMERGED, COPPER SUBMERGED, STEEL SPRAYED AND COPPER SPRAYED WITH (3.5%) SALINE SOLUTION AND COATED DOPED PANI (23). .....	182
FIGURE 80: MORPHOLOGY OF DOPED PANI (21) FILM ON STEEL.....	183
FIGURE 81: COPPER SAMPLE COATED WITH DOPED PANI (21).....	184
FIGURE 82: CATHODIC DELAMINATION AT THE METAL/POLYMER INTERFACE. ....	186
FIGURE 83: STRUCTURES OF THE LITERATURE STANDARD PHOSPHORIC ACID DIESTER DOPANTS USED. ....	186
FIGURE 84: STEEL SHEET COATED WITH DOPED PANI (23).....	188
FIGURE 85: STEEL COATED WITH DOPED PANI (24).....	189
FIGURE 86: PHOTOGRAPH OF DOPED PANI (17) 1 WT% IN PVC, DIP COATED AND AIR DRIED. FROM LEFT TO RIGHT STEEL SUBMERGED, COPPER SUBMERGED IN A SALINE SOLUTION (3.5%) AFTER 120 HRS AND STEEL SPRAYED AND COPPER SPRAYED WITH (3.5%) SALINE SOLUTION AFTER 144 HRS. ....	190
FIGURE 87: PVC/DOPED PANI (22) 1 WT% CAST ONTO STEEL.....	193
FIGURE 88: SCHEMATIC OF CROSS-LINKED EPOXIDE RESIN WITH THE DOPED PANI (17). ....	194
FIGURE 89: PHOTOGRAPHS OF STEEL AND COPPER COATED IN DOPED PANI (17) 1 WT% IN EPIKOTE 828™, SAMPLED PRIOR TO ACCELERATED CORROSION TESTING. ....	195
FIGURE 90: PHOTOGRAPHS OF STEEL AND COPPER SAMPLES COATED IN DOPED PANI (17) 1 WT% IN EPIKOTE 828™, SAMPLED AFTER 7 DAYS OF ACCELERATED CORROSION TESTING, FROM LEFT TO RIGHT; STEEL SAMPLE SPRAYED, STEEL SAMPLE SUBMERGED AND FINALLY THE OPPOSITE SIDE OF THE SUBMERGED STEEL SAMPLE, BOTTOM LEFT; COPPER SPRAYED AND BOTTOM; COPPER SUBMERGED. ....	196
FIGURE 91: SCHEMATIC ILLUSTRATION OF THE ACCELERATED CORROSION SAMPLING, A) SIDE PROFILE AND B) A TOP ANGLED VIEW.....	197
FIGURE 92: EPOXY RESIN/DOPED PANI (17) 1 WT%, COMPLETELY CLEAR OF RUST. ....	198
FIGURE 93: PHOTOGRAPH OF DOPED PANI (20) 1 WT% IN ACRYLIC RESIN. FROM LEFT TO RIGHT STEEL SUBMERGED, COPPER SUBMERGED IN A SALINE SOLUTION (3.5%) AND STEEL SPRAYED AND COPPER SPRAYED WITH (3.5%) SALINE SOLUTION AFTER 7 DAYS (168 HRS). ....	199
FIGURE 94: PHOTOGRAPH OF DOPED PANI (21) 1 WT% IN ACRYLIC RESIN. FROM LEFT TO RIGHT STEEL SUBMERGED, COPPER SUBMERGED IN A SALINE SOLUTION (3.5%) AND STEEL SPRAYED AND COPPER SPRAYED WITH (3.5%) SALINE SOLUTION; AFTER 24 HRS (TOP IMAGE) AND AFTER 48 HRS FOR THE BOTTOM IMAGE SAMPLES. ....	200
FIGURE 95: THE CONTAMINATION OF THE SALINE SOLUTION USED IN THE ACCELERATED CORROSION STUDIES; FROM THE REACTION OF THE PHOSPHATE DOPED POLYMERS, THE METAL SUBSTRATES AND THE SALINE SOLUTION. ....	201
FIGURE 96: ACRYLATE RESIN/DOPED PANI (21) 1 WT% CAST FILM DISPLAYING DELAMINATION ....	202
FIGURE 97: ACRYLATE RESIN/DOPED PANI (23) 1 WT% CAST ONTO COPPER.....	204
FIGURE 98: UV/VIS SPECTROSCOPY DISPLAYING THE ELECTRONIC PROPERTIES OF POLYANILINE DOPED WITH BIS(2-METHACRYLOYLOXY ETHYL) HYDROGEN PHOSPHATE (PANI-DMEHP) (24). ....	233

# Table of Schemes

SCHEME 1: SYNTHESIS OF BIS(8-HYDROXYOCTYL) 5-SULPHOISOPHTHALIC ACID (1).....	90
SCHEME 2: THE SYNTHESIS OF BIS(8-ACRYLOXY OCTYL) 5-SULPHOISOPHTHALIC ACID (2). ....	96
SCHEME 3: SYNTHESIS OF 5-SULPHOISOPHTHALIC ACID BIS [2-(2-HYDROXY-ETHOXY)-ETHYL] ESTER (3) (SIPADEG). ....	99
SCHEME 4: THE SYNTHESIS OF BIS(8-ACRYLOXY OCTYL) HYDROGEN PHOSPHATE (5) BY METHOD 1. .....	100
SCHEME 5: THE SYNTHESIS OF BIS(8-ACRYLOXY OCTYL) HYDROGEN PHOSPHATE (5) VIA METHOD 2. .....	103
SCHEME 6: THE SYNTHESIS OF BIS(8-ACRYLOXY OCTYL) HYDROGEN PHOSPHATE (5) AND BIS(8- ACRYLOXY OCTYL) HYDROGEN PHOSPHATE (6) VIA A MODIFIED METHOD OF JANG AND JEONG <sup>106</sup> . METHOD 3. ....	107
SCHEME 7: THE SYNTHESIS OF 8-HYDROXYOCTYL ACRYLATE (7).....	110
SCHEME 8: THE SYNTHESIS OF 2-CHLOROMETHYL-4-NITROPHENYL PHOSPHORODICHLORIDATE (9).111	
SCHEME 9: THE SYNTHESIS OF 2-CHLOROMETHYL-4-NITROPHENYL PHOSPHORODI(OCTYL ACRYLATE) (10). ....	112
SCHEME 10: THE SYNTHESIS OF 2-( <i>N, N</i> -DIMETHYLAMINO)-4-NITROPHENOL PROTECTING GROUP (12). .....	113
SCHEME 11: THE DOPING OF POLYANILINE IN THE PRESENCE OF A PROTONIC ACID. ....	114
SCHEME 12: DOPING OF PANI WITH THE SULPHONIC ACID AND PHOSPHORIC ACID DIESTER SERIES OF DOPANTS. ....	115

# Table of Mechanisms

MECHANISM 1: THE MECHANISM OF ESTERIFICATION OF 1,8-OCTANEDIOL WITH 5-SULPHOISOPHTHALIC ACIDS LEADING TO THE EVENTUAL FORMATION OF BIS(8-HYDROXYOCTYL) 5-SULPHOISOPHTHALIC ACID (1). .....	91
MECHANISM 2: MECHANISM TO DEMONSTRATE THE FORMATION OF AN ETHER PRODUCT VIA ALCOHOL DEHYDRATION. ....	94
MECHANISM 3: EXAMPLE SHOWING PART OF THE ESTERIFICATION LEADING TO THE EVENTUAL FORMATION OF BIS(8-ACRYLOXY OCTYL) 5-SULPHOISOPHTHALIC ACID (2). ....	97
MECHANISM 4: THE SYNTHESIS OF BIS(8-ACRYLOXY OCTYL) HYDROGEN PHOSPHATE (5) IN THE PRESENCE OF WATER (METHOD 1). ....	101
MECHANISM 5: THE MECHANISM OF SYNTHESIS OF BIS(8-ACRYLOXY OCTYL) HYDROGEN PHOSPHATE (5) VIA ESTER PROTECTION. ....	105
MECHANISM 6: THE ESTERIFICATION OF PHOSPHORUS OXYCHLORIDE ACCORDING TO A MODIFIED METHOD OF JANG AND JEONG <sup>106</sup> .....	108
MECHANISM 7: THE ESTERIFICATION OF 2-CHLOROMETHYL-4-NITROPHENOL WITH PHOSPHORUS OXYCHLORIDE. ....	111
MECHANISM 8: METHYLATION MECHANISM OF 2-AMINO-4-NITROPHENOL. ....	114
MECHANISM 9: THE MECHANISM OF PROTONIC ACID DOPING, EXAMPLE USING SULPHONIC SERIES OF DOPANTS. ....	116
MECHANISM 10: THE MECHANISM FOR THE CURING OF THE EPOXY RESIN BY THE CURING AGENT JEFFAMINE D230. ....	119
MECHANISM 11: FREE RADICAL POLYMERISATION OF METHYL METHACRYLATE IN THE PRESENCE OF AIBN. ....	121
MECHANISM 12: THE MECHANISM OF DOPANT CROSSLINKING WITH THE ACRYLIC RESIN. ....	122
MECHANISM 13: THE CROSSLINKING AND BRIDGING OF POLY(METHYL METHACRYLATE) WITH ETHYLENE GLYCOL DIMETHACRYLATE (EGDMA). ....	124

# Table of Equations

EQUATION 1: CALCULATION TO DETERMINE THE BAND GAP OF A POLYMERIC MATERIAL. ( $E_{\text{OX, RED}}$ ) OXIDATION AND REDUCTION POTENTIALS, ( $S^{\pm}$ ) SOLVATION ENERGY OF THE IONISED MOLECULE SUBTRACTING THE SOLVATION ENERGY OF THE NEUTRAL MOLECULE, ( $\epsilon_{1,2}$ ) DIELECTRIC CONSTANT OF THE SOLUTION AND THE MOLECULAR SOLID RESPECTIVELY.....	11
EQUATION 2: <i>P</i> -TYPE DOPING OF A POLYMER WITH THE HALOGEN IODINE. ....	20
EQUATION 3: <i>P</i> -TYPE ELECTROCHEMICAL DOPING OF POLYMER. ....	22
EQUATION 4: <i>N</i> -TYPE CHEMICAL DOPING WITH SODIUM NAPHTHALIDE. ....	22
EQUATION 5: DOPING VIA CHARGE INJECTION.....	23
EQUATION 6: PHOTO DOPING OF A CONJUGATED POLYMER.....	24
EQUATION 7: NON REDOX DOPING VIA A PROTONIC ACID .....	24
EQUATION 8: THE OXIDATION OF STEEL (IRON) IN AIR PRODUCING AN IRON (III) SPECIES (SIMPLIFIED) <sup>70</sup> .....	48
EQUATION 9: OXIDATION OF STEEL IN THE PRESENCE OF WATER THE PRODUCTION OF HYDROGEN GAS BY-PRODUCT <sup>70</sup> .....	48
EQUATION 10: THE ELECTROCHEMICAL REACTION OF STEEL (IRON) IN THE PRESENCE OF OXYGEN AND WATER <sup>69</sup> .....	49
EQUATION 11: FURTHER OXIDATION OF IRON <sup>69</sup> .....	49
EQUATION 12: THE ELECTROCHEMICAL REACTION OF COPPER IN THE PRESENCE OF SULPHUR CONTAINING CORROSIVE SPECIES, INITIALLY FORMING THE OXIDE AND PROCEEDING TO FORM THE PATINA <sup>76</sup> .....	50
EQUATION 13: FORMATION OF SULPHATED PATINA IN THE PRESENCE OF SULPHURIC ACID. ....	50
EQUATION 14: FORMATION OF CHLORIDE PATINAS. ....	51
EQUATION 15: PASSIVATION OF ALUMINIUM, LEADING THE FORMATION OF ALUMINIUM OXIDE (ALUMINA).....	52
EQUATION 16: THE CORROSION OF ALUMINIUM IN A BASIC SOLUTION. ....	52
EQUATION 17: CORROSION OF ALUMINIUM VIA INTERMEDIATES. ....	52
EQUATION 18: CORROSION OF THE ALUMINIUM OXIDE (ALUMINA) IN A BASIC SOLUTION. ....	53
EQUATION 19: CALCULATION OF THE IMPURITIES USING THE INTEGRATIONS OBTAINED FROM THE <sup>1</sup> H- NMR.....	96
EQUATION 20: CALCULATION OF THE IMPURITIES USING THE PROTON INTEGRATIONS OBTAINED FROM THE <sup>1</sup> H-NMR DISPLAYING THE SIDE PRODUCT.....	109
EQUATION 21: EQUATION USED FOR THE CALCULATION OF THE OPTICAL BAND GAPS FROM THE $\Lambda_{\text{MAX}}$ ABSORPTION FOR THE DOPED POLYMERS ( $HC$ ) IS A FACTOR OF PLANK'S CONSTANT ( $6.626 \times 10^{-34}$ J.S) MULTIPLIED BY THE SPEED OF LIGHT IN A VACUUM ( $C = 2.998 \times 10^8$ M.S).....	147

# Table of Tables

TABLE 1: SUMMARY OF ABSORPTION DATA FROM UV-VISIBLE SPECTROSCOPY OF POLYANILINE DOPED WITH VARIOUS SULPHONIC ACID DOPANTS.....	129
TABLE 2: TABLE TO ILLUSTRATE THE VARIOUS LENGTHS OF THE DOPANT SIDE CHAINS IN ASCENDING ORDER OF LENGTH, CORRELATING THE LENGTH OF THE CHAINS TO THE OPTICAL PROPERTIES OBSERVED AND RECORDED. ....	136
TABLE 3: SUMMARY OF ABSORPTION DATA FROM UV-VISIBLE SPECTROSCOPY OF POLYANILINE DOPED WITH VARIOUS PHOSPHORIC ACID DIESTER DOPANTS. ....	138
TABLE 4: TABLE TO ILLUSTRATE THE VARIOUS LENGTHS OF THE DOPANT SIDE CHAINS OF THE PHOSPHORIC ACID DOPANTS IN ASCENDING ORDER OF LENGTH, CORRELATING THE LENGTH OF THE CHAINS TO THE OPTICAL PROPERTIES OBSERVED AND RECORDED. ....	139
TABLE 5: SUMMARY OF THE RECORDED OPTICAL PROPERTIES OF DOPED PANI (21) IN A SOLUTION OF DCM AND SOLID STATE CAST FROM A SOLUTION OF DCM.....	148
TABLE 6: SUMMARY OF THE RECORDED OPTICAL PROPERTIES OF DOPED PANI (25) IN A SOLUTION OF DCM AND SOLID STATE CAST FROM A SOLUTION OF DCM; INCLUDES THE SUMMARY OF THE OPTICAL PROPERTIES OF THE THIN FILMS FOR BOTH DOPED PANI (21) AND (25). ....	150
TABLE 7: OPTICAL PROPERTIES FOR THE THIN FILMS OF DOPED PANI SYSTEMS IN PVC COMPOSITE BLENDS AND THEIR RESPECTIVE OPTICAL PROPERTIES IN SOLUTION.....	153
TABLE 8: TABLE SUMMARISING THE ABSORPTION BANDS OF DOPED PANI (21) CAST FILMS IN COMPARISON TO DOPED PANI (21) IN SOLUTION. (*= NMP SAMPLE FILM CAST UNDER VACUUM AT 80°C.NB1; SAMPLE IS DOPED PANI (19) IN DCAA, NB2; SAMPLE IS DOPED PANI (19) IN <i>m</i> -CRESOL). ....	164
TABLE 9: TABLE TO ILLUSTRATE THE VARIOUS LENGTHS OF THE DOPANT SIDE CHAINS IN ASCENDING ORDER OF LENGTH, CORRELATING THE LENGTH OF THE CHAINS TO THE OPTICAL PROPERTIES OBSERVED AND RECORDED. TEXT IN RED CORRESPONDS TO THE SULPHONIC ACID DOPED PANI SYSTEMS AND THE BLUE TEXT REFERS TO THE PHOSPHORIC ACID DOPED PANI SYSTEMS. ....	210
TABLE 10: SUMMARY OF OPTICAL PROPERTIES FOR DOPED PANI (21) AND (25) THINS FILMS CAST ONTO QUARTZ PLATE FROM A SOLUTION OF DCM. ....	212

# Table of Appendices

APPENDIX 1: UV/VIS SPECTROSCOPY DISPLAYING THE ELECTRONIC PROPERTIES OF POLYANILINE DOPED WITH BIS(8-HYDROXYOCTYL)-5-SULPHOISOPHTHALIC ACID (17).....	229
APPENDIX 2: UV/VIS SPECTROSCOPY DISPLAYING THE ELECTRONIC PROPERTIES OF POLYANILINE DOPED WITH BIS(8-ACRYLOXY OCTYL) 5-SULPHOISOPHTHALIC ACID DOPED PANI (18) (PANI-SIPAOA) IN SOLUTION. ....	230
APPENDIX 3: UV/VIS SPECTROSCOPY DISPLAYING THE ELECTRONIC PROPERTIES OF POLYANILINE DOPED WITH BIS[2-(2-HYDROXY-ETHOXY)-ETHYL]-5-SULPHOISOPHTHALIC ACID (PANI-SIPAOA). ....	230
APPENDIX 4: UV/VIS SPECTROSCOPY DISPLAYING THE ELECTRONIC PROPERTIES OF POLYANILINE DOPED WITH BIS(8-METHACRYLOXY OCTYL)-5-SULPHOISOPHTHALIC ACID (PANI-SIPAOMA). ....	231
APPENDIX 5: UV/VIS SPECTROSCOPY DISPLAYING THE ELECTRONIC PROPERTIES OF POLYANILINE DOPED WITH DODECYLBENZENE SULPHONIC ACID DOPED PANI (22) (PANI-DBSA). ....	231
APPENDIX 6: UV/VIS SPECTROSCOPY DISPLAYING THE ELECTRONIC PROPERTIES OF POLYANILINE DOPED WITH BIS(8-METHACRYLOYLOXY OCTYL) HYDROGEN PHOSPHATE (PANI-DMOHP) (21). ....	232
APPENDIX 7: UV/VIS SPECTROSCOPY DISPLAYING THE ELECTRONIC PROPERTIES OF POLYANILINE DOPED WITH BIS(2-ETHYLHEXYL) HYDROGEN PHOSPHATE (PANI-DEHHP) (23). ....	232
APPENDIX 8: UV/VIS SPECTROSCOPY DISPLAYING THE ELECTRONIC PROPERTIES OF POLYANILINE DOPED WITH BIS(8-ACRYLOYLOXY OCTYL) HYDROGEN PHOSPHATE (PANI-DAOHP) (25).....	233
APPENDIX 9: PHOTOGRAPH OF A) MILD STEEL BEFORE ACID PICKLING AND B) AFTER ACID PICKLING. ....	234
APPENDIX 10: PHOTOGRAPH OF A) COPPER BEFORE ACID PICKLING AND B) AFTER ACID PICKLING	234
APPENDIX 11: PHOTOGRAPHS OF PVC CAST FILM ONTO COPPER; SAMPLING A) 7 DAYS AFTER BEING SPRAYED WITH A 3.5% SALINE SOLUTION AND B) 7DAYS AFTER BEING SUBMERGED INTO A 3.5% SALINE SOLUTION. ....	235
APPENDIX 12: METAL SAMPLES COATED IN EPOXIDE RESIN CAST FILMS, FROM LEFT TO RIGHT; MILD STEEL SUBMERGED, MILD STEEL SPRAYED (3.5% SALINE), COPPER SUBMERGED AND COPPER SPRAYED AFTER 7 DAYS INCUBATION.....	235
APPENDIX 13: METAL PLATES COATED IN ACRYLIC RESIN ALONE PRIOR TO ACCELERATED CORROSION TESTING, FROM LEFT TO RIGHT; STEEL THEN COPPER FOR SUBMERSION AND STEEL AND COPPER FOR SPRAYING. ....	235
APPENDIX 14: PHOTOGRAPH OF A) COPPER AFTER 48 HRS SUBMERSION IN 3.5% SALINE SOLUTION AND B) COPPER AFTER 1 HR POST SALINE SPRAY DOPED PANI (17). ....	236
APPENDIX 15: PHOTOGRAPH OF BOTH STEEL AND COPPER PRIOR TO TESTING (TOP IMAGE) AND CORROSION NOTICED AFTER 24HRS; FROM LEFT TO RIGHT STEEL SUBMERGED, COPPER SUBMERGED, STEEL SPRAYED AND COPPER SPRAYED WITH (3.5%) SALINE SOLUTION AND COATED DOPED PANI (18). ....	236
APPENDIX 16: : PHOTOGRAPH OF BOTH STEEL AND COPPER PRIOR TO TESTING (TOP IMAGE) AND CORROSION NOTICED AFTER 24HRS; FROM LEFT TO RIGHT STEEL SUBMERGED, COPPER SUBMERGED, STEEL SPRAYED AND COPPER SPRAYED WITH (3.5%) SALINE SOLUTION AND COATED DOPED PANI (20). ....	237
APPENDIX 17: PHOTOGRAPH OF BOTH STEEL AND COPPER COATED WITH DOPED PANI (18) 1 WT% IN PVC AFTER 7 DAYS (168 HRS) OF TESTING, FROM LEFT TO RIGHT; STEEL SUBMERGED, COPPER SUBMERGED IN A SALINE SOLUTION (3.5%) AND STEEL SPRAYED AND COPPER SPRAYED WITH (3.5%) SALINE SOLUTION. ....	237
APPENDIX 18: PHOTOGRAPH OF BOTH STEEL AND COPPER COATED WITH DOPED PANI (20) 1 WT% IN PVC AFTER 7 DAYS (168 HRS) OF TESTING, FROM LEFT TO RIGHT; STEEL SUBMERGED, COPPER	

SUBMERGED IN A SALINE SOLUTION (3.5%) AND STEEL SPRAYED AND COPPER SPRAYED WITH (3.5%) SALINE SOLUTION. ....	238
APPENDIX 19: PHOTOGRAPH OF DOPED PANI (22) 2 WT% IN PVC, DIP COATED AND AIR DRIED. FROM LEFT TO RIGHT STEEL SUBMERGED, COPPER SUBMERGED IN A SALINE SOLUTION (3.5%) AFTER 7 DAYS (168 HRS) AND STEEL SPRAYED AND COPPER SPRAYED WITH (3.5%) SALINE SOLUTION. AFTER 7 DAYS (168 HRS). ....	238
APPENDIX 20: PHOTOGRAPH OF DOPED PANI (22) 1 WT% IN PVC, DIP COATED AND AIR DRIED. FROM LEFT TO RIGHT STEEL SUBMERGED, COPPER SUBMERGED IN A SALINE SOLUTION (3.5%) AFTER 7 DAYS (168 HRS) AND STEEL SPRAYED AND COPPER SPRAYED WITH (3.5%) SALINE SOLUTION AFTER 7 DAYS (168 HRS). ....	238
APPENDIX 21: PHOTOGRAPH OF DOPED PANI (21) 1 WT% IN PVC, DIP COATED AND AIR DRIED. FROM LEFT TO RIGHT STEEL SUBMERGED, COPPER SUBMERGED IN A SALINE SOLUTION (3.5%) AFTER 7 DAYS (168 HRS) AND STEEL SPRAYED AND COPPER SPRAYED WITH (3.5%) SALINE SOLUTION AFTER 7 DAYS (168 HRS). ....	239
APPENDIX 22: PHOTOGRAPH OF DOPED PANI (23) 1 WT% IN PVC, DIP COATED AND AIR DRIED. FROM LEFT TO RIGHT STEEL SUBMERGED, COPPER SUBMERGED IN A SALINE SOLUTION (3.5%) AFTER 7 DAYS (168 HRS) AND STEEL SPRAYED AND COPPER SPRAYED WITH (3.5%) SALINE SOLUTION AFTER 7 DAYS (168 HRS). ....	239
APPENDIX 23: PHOTOGRAPH OF DOPED PANI (18) 1 WT% IN ACRYLIC RESIN. FROM LEFT TO RIGHT STEEL SUBMERGED, COPPER SUBMERGED IN A SALINE SOLUTION (3.5%) AND STEEL SPRAYED AND COPPER SPRAYED WITH (3.5%) SALINE SOLUTION AFTER 7 DAYS (168 HRS). ....	239
APPENDIX 24: PHOTOGRAPH OF DOPED PANI (23) 1 WT% IN ACRYLIC RESIN. FROM LEFT TO RIGHT STEEL SUBMERGED, COPPER SUBMERGED IN A SALINE SOLUTION (3.5%) AND STEEL SPRAYED AND COPPER SPRAYED WITH (3.5%) SALINE SOLUTION AFTER 24 HRS TOP IMAGE. AND AFTER 48 HRS FOR THE BOTTOM IMAGE SAMPLES. ....	240
APPENDIX 25: UNCOATED STEEL SAMPLE TAKEN AT THE EYELET, SITUATED AT THE TOP CENTRE OF THE PLATE. THE SURFACE OF THE METAL IN THIS ZONE ILLUSTRATES BOTH CORRODED (RUSTED) METAL, SEEN AS BRIGHTER AREAS AND THE DULLER AREAS REPRESENT RUST FREE ZONES. ....	241
APPENDIX 26: BARE COPPER SURFACE AT; A) 2748X MAGNIFICATION AND B) 169X MAGNIFICATION .....	241
APPENDIX 27: STEEL SAMPLE COATED WITH HYDROXYL FUNCTIONALISED DOPED PANI (17). IMAGE SHOWS POLYMER (DARK AREA) AND RUST (LIGHTER AREA). IMAGE OBTAINED AT 88X MAGNIFICATION. ....	242
APPENDIX 28: FURTHER MAGNIFICATION OF THE SAME AREA SHOWN IN (APPENDIX 27). 351X MAGNIFICATION. ....	242
APPENDIX 29: FURTHER MAGNIFICATION OF APPENDIX 28 DEMONSTRATING THE MORPHOLOGY OF THE POLYMER AND THE CORRODED STEEL AT THE INTERFACE. ....	243
APPENDIX 30: COPPER SAMPLE COATED WITH DOPED PANI (17). ....	243
APPENDIX 31: DOPED PANI (23) FILM ON COPPER. ....	244
APPENDIX 32: PVC (POLYVINYL CHLORIDE) CAST ONTO PRE-CLEANED STEEL. ....	244
APPENDIX 33: PVC/DOPED PANI (22) 1 WT% CAST ONTO STEEL. ....	245
APPENDIX 34: PRE-CLEANED COPPER SAMPLE WITH EPOXY RESIN MATRIX CAST FILM COATING. ....	245
APPENDIX 35: EPOXY RESIN/DOPED PANI (17) 1 WT%, DISPLAYING NO RUST AT THE EDGE OF METAL SHEET .....	246
APPENDIX 36: EPOXY RESIN CAST FILM ON PRE CLEANED STEEL SAMPLE. ....	246
APPENDIX 37: ACRYLATE RESIN/DOPED PANI (21) 1 WT% CAST FILM, DISPLAYING A) ORGANIC COAT DELAMINATION (TOP LEFT CORNER) AND B) RUST (MID-CENTRE TO THE RIGHT). ....	247
APPENDIX 38: INTACT ACRYLATE RESIN/DOPED PANI (21) 1 WT% CAST FILM ON STEEL .....	247

# Glossary of Abbreviations and Terms

## A

Å	Angstrom (unit equals to 0.1 nm)
A <sup>-</sup>	Dopant acid anion (conjugate base)
Abs	Absorption
AcOH	Acetic acid or ethanoic acid
AIBN	Azobisisobutyronitrile
Al	Aluminium
Al <sub>2</sub> O <sub>3</sub>	Alumina (aluminium oxide)
AMU	Atomic Mass Units
(aq)	Aqueous
ATR	Attenuated Total Reflectance

## B

bp	Boiling point
<i>n</i> -BuOH	Butanol

## C

<i>c</i>	Speed of light ( $2.997 \times 10^8 \text{ m s}^{-1}$ )
°C	Degrees Celsius (unit of temperature based on the freezing point of water).
CB	Conduction Band
CDCl <sub>3</sub> - <i>d</i> <sub>1</sub>	Deuterated chloroform
CHCl <sub>3</sub>	Chloroform
CHN	Carbon, Hydrogen and Nitrogen
CI	Chemical Ionisation (Mass spectroscopy)
cm	centimetre
Cm <sup>3</sup>	Centimetre cubed (volume equal to an ml)
CSA	Camphorsulphonic acid
Cu	Copper
Cu <sup>+</sup>	Cuprous
Cu <sup>2+</sup>	Cupric
CV	Cyclic voltammetry

## D

<i>d</i>	Doublet (NMR)
<i>dd</i>	Double Doublet (NMR)
<i>dt</i>	Double triplet (NMR)
D <sub>2</sub> O	Deuterated water or deuterium oxide (NMR)
DAOHP	Di or bis(8-acryloxy octyl) hydrogen phosphate
DBSA	Dodecylbenzene sulphonic acid
DC	Direct Current

DCAA (DCA)	Dichloroacetic acid
DCM	Dichloromethane
DEHHP	Di or bis(2-ethyl hexyl) hydrogen phosphate
DMF	<i>N, N</i> -Dimethylformamide
DMOHP	Di or bis(8-methacryloxy octyl) hydrogen phosphate
DMEHP	Di or bis(2-methacryloxy ethyl) hydrogen phosphate
DMSO- <i>d</i> <sub>6</sub>	Deuterated dimethyl sulphoxide
DMSO	Dimethyl sulphoxide
<b>E</b>	
<i>E</i>	Energy (measure of J or eV)
<i>e</i> <sup>-</sup>	Electron
<i>E</i> <sub>A</sub>	Electron affinity
<i>E</i> <sub>g</sub>	Electrochemical/Optical band gap
eV	Electron volts
EGDMA	Ethylene glycol dimethacrylate
EA	Ethyl acetate or ethyl ethanoate
EI+	Electron Ionisation (Mass spectroscopy)
ESI	Electrospray ionisation (Mass spectroscopy)
ESI-ToF	Electrospray ionisation Time of Flight mass spectroscopy
EtOH	Ethanol
Et <sub>2</sub> O	Diethyl ether
<b>F</b>	
Fe	Iron
Fe <sup>2+</sup>	Ferrous
Fe <sup>3+</sup>	Ferric
FT-IR	Fourier Transform Infra-Red spectroscopy
<b>G</b>	
g	Gram
<b>H</b>	
<i>h</i>	Planck constant ( $6.626 \times 10^{-34} \text{ kg m}^2 \text{ s}^{-1}$ )
<sup>1</sup> H-NMR	Proton/hydrogen Nuclear Magnetic resonance spectroscopy
c.HCl	Concentrated hydrochloric acid
HCl	Hydrochloric acid (other than concentrated)
c.HNO <sub>3</sub>	Concentrated nitric acid
HNO <sub>3</sub>	Nitric acid
HOMO	Highest Occupied Molecular Orbital
HPLC	High Performance Liquid Chromatography
hr (hrs)	Hour(s)
c.H <sub>2</sub> SO <sub>4</sub>	Concentrated sulphuric acid
H <sub>2</sub> SO <sub>4</sub>	Sulphuric acid

<b>I</b>	
$I_p$	Ionisation potential
ICP	Intrinsic conductive polymers
IPA	Isopropyl alcohol (Isopropanol)
IR	Infra-Red spectroscopy
<b>J</b>	
J	Joules (a unit measure of energy)
<b>K</b>	
K	Kelvin (scientific unit of temperature based on absolute zero)
kg	Kilogrammes
kV	Kilovolts
<b>L</b>	
$\lambda$	Lambda (unit of wavelength in nm)
$\lambda_{\max}$	Lambda max (Wavelength of maximum absorption)
LC-MS	Liquid chromatography mass spectroscopy
LED	Light Emitting Diode
LUMO	Lowest Unoccupied Molecular Orbital
<b>M</b>	
m	Metre (unit measurement of length)
m	multiplet (NMR)
<i>m-</i>	Meta (chemical moiety in Meta position)
M	Molar (concentration)
$M_n$	Number average molecular weight (polymers)
$M_w$	Weight average molecular weight (polymers)
MA	Methyl acrylate
MeCN (ACN)	Acetonitrile
MeOD- $d_4$	Deuterated methanol
MeOH	Methanol
MHz	Megahertz (frequency)
mmol	millimole (measure of amount)
MMA	Methyl methacrylate
Mpt (m.p)	Melting point
mg	milligram
MgSO <sub>4</sub>	Magnesium sulphate
MH <sup>+</sup>	Molecular ion positively charged (Mass spectroscopy)
ml or mL	millilitre
mmHg	Millimetre of mercury (measure of pressure or vacuum)
MS	Mass spectroscopy

<b>N</b>	
N <sub>2</sub>	Nitrogen
NaCl	Sodium chloride (salt)
NaHCO <sub>3</sub>	Sodium hydrogen carbonate (sodium bicarbonate)
NaOH	Sodium hydroxide
nm	nanometre
NH <sub>3</sub>	Ammonia
NH <sub>4</sub> OH	Ammonium hydroxide
NIR	Near Infra-Red
NUV	Near Ultra-violet
NMP	<i>N</i> -methyl pyrrolidone
NMR	Nuclear Magnetic Resonance spectroscopy
<b>O</b>	
OLED	Organic Light Emitting Diode
O <sub>x</sub> (Oxid)	Oxidation
<i>o</i> -	Ortho (chemical moiety in ortho position)
<b>P</b>	
π	Pi (3.14159) (constant)
π	Pi bond
π*	Pi star or anti-pi bond
<i>p</i> -	Para (positioning of a chemical moiety)
<sup>31</sup> P-NMR	Phosphorus Nuclear Magnetic Resonance Spectroscopy
PA	Polyacetylene
PANI (PAn)	Polyaniline
PANI-EB	Polyaniline emeraldine base (native state/undoped)
PANI-ES	Polyaniline emeraldine salt (doped)
P3AT	Poly-3-alkylthiophene
PD	Polydispersity (PD= $M_w/M_n$ )
P3HT	Poly-3-hexylthiophene
PMMA	Poly methyl methacrylate
ppm	Parts per million
PPP	Poly- <i>p</i> -phenylene
PPV	Poly- <i>p</i> -phenylenevinylene
PPy	Polypyrrole
POCl <sub>3</sub>	Phosphorus oxychloride
PT	Polythiophene
PVC	Polyvinyl chloride
<b>Q</b>	
q	Quartet (NMR)

<b>R</b>	
Red	Reduction
R <sub>f</sub>	Release Factor
RT	Retention Time
r.t.	Room temperature
<b>S</b>	
σ	sigma (molecular bond)
s	singlet (NMR)
s	Second (unit of time)
s <sup>-1</sup>	per second
S	Siemens (unit of electrical conductance)
S cm <sup>-1</sup>	Siemens per centimetre
SEM	Scanning electron microscopy
SIPA	5-Sulphoisophthalic acid
SIPA OH	Bis(8-hydroxy octyl) 5-sulphoisophthalic acid
SIPA OO	Bis(8-hydroxy octyl) 5-sulphoisophthalic acid
SIPA OA	Bis(8-acryloxy octyl) 5-sulphoisophthalic acid
SIPA OMA	Bis(8-methacryloxy octyl) 5-sulphoisophthalic acid
SIPA DEG	Bis[2-(2-hydroxy-ethoxy) 5-sulphoisophthalic acid
SN	Polysulphur nitride
S <sub>N</sub> <sup>2</sup>	Nucleophilic substitution
<b>T</b>	
t	Triplet (NMR)
TEA	Triethylamine
THF	Tetrahydrofuran
TLC	Thin Layer Chromatography
TsA	Tosic acid or <i>p</i> -toluene sulphonic acid
T <sub>g</sub>	Glass transition temperature (°C or K)
<b>U</b>	
UV/Vis	Ultra-violet/Visible light spectroscopy
<b>V</b>	
VB	Valence Band

# Chapter 1 INTRODUCTION

## 1.1 Foundations and the History of Polymer Science.

Polymer, derived from a conjugation of the Greek words; (*πολύς*) polis and (*μέρος*) meros meaning ‘much/many’ and ‘parts’, are a collection of repeating units building up to vast elongated structures which can be found naturally or can be synthetically produced. Industrially important, they have found roles in many areas such as the electronics industry to name but one. It is due to their vast range of desirable properties which have made them such an extensively utilised commodity. Generally polymers with their vast carbon backbone are insulators by nature, very often inert and for the most part environmentally stable, making polymeric material the material of the future.

### 1.1.1 History of Polymers

For thousands of years wood, bones, skin and other such other such naturally occurring polymer fibres have been utilised as devices and tools, however the scientific field regarding polymers is something of a 20<sup>th</sup> Century creation<sup>1</sup>, which compared to other aspects of chemistry is relatively new and growing field. Currently the field of polymer science has become a huge field of science both industrially and academically, with the applicability of these materials seen in broad applications which appear to be almost endless. It is seen now that a lot of manufacturers are producing tools which are in total, generally composed of polymers whether these are naturally sourced or synthetically created for their specific role and application.

Research worthy of noting, regarding the history and the progression of the polymer research are; Wallace Carolther of Du Pont who developed Nylon in 1935, Ziegler and Natta and their work on the catalytic methods of synthesising polymers in the 1950's which had major implications on the plastic manufacturing industry and finally Flory who also can be associated with the development of the now vast area of polymer science through his work on macromolecules. The latter researchers

have all received Nobel prizes for their contributions to the field of Macromolecule and Polymer Science<sup>1</sup>.

### 1.1.2 Current applications of Polymers

Looking around in the environment it can be said that many structures, tools and devices contain at least a small proportion of polymeric material, whether it is decorative paints to utensils found in the home, the uses are vast and ever increasing, in fact it is stated that the uses of polymers is far greater than any other class of material<sup>1</sup>, this is owed to the properties that the traditional and conventional polymers exhibit. Typically they are insulating materials<sup>2,3</sup> and transparent to visible light in most cases a fact that is attributed to the participation of all the four valence electrons of the carbons involvement in covalent bonds thus consisting of only  $\sigma$ -bands, inevitably resulting in large band gaps (electron energy gaps,  $E_g$ <sup>1,4</sup>). These having found use encapsulating electronics and isolating metallic conducting wires<sup>5</sup>. Mechanically they are characterised by their lightweight properties over other classes of materials manufactured for the same niche, flexible or rigid depending on what functionality the polymer is being marketed towards. Polymers ability to form good films<sup>6</sup>, holding attractive chemical properties and finally their high malleability and processability<sup>7,8</sup>.

## 1.2 Conjugated Polymers

Within the paradigm of Polymer science, research, interests and attentions have been directed towards conjugated polymers. Investigation is currently being undertaken by countless research groups as to their potential and possible applications of this subgroup of polymers. Investigating whether what may be theoretically postulated, may actually be practical. Currently they have been found to be incorporated into electronic devices, electro chromic displays, antistatic applications, shielding from electromagnetic radiation, anticorrosion application<sup>9</sup>, LED's, Batteries and sensor devices<sup>10</sup> to name but a few.

Due to their applications and the possibilities that have been hypothesised, there are currently large vested interests focussed on conjugated polymers and their properties. This new field opened up endless excitement, with research on the boundaries of both chemistry and 'condensed-matter' physics<sup>1</sup>. Several classes of conjugated polymers have been identified (Figure 1).

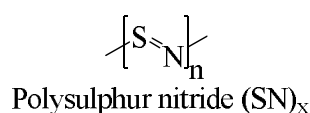
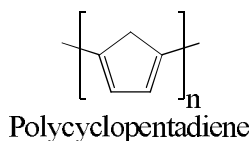
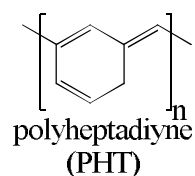
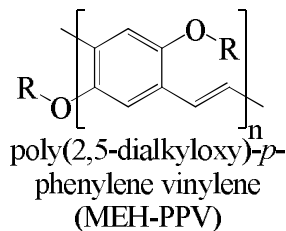
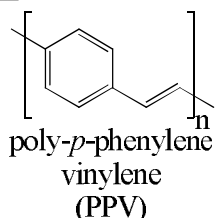
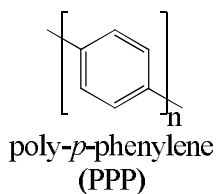
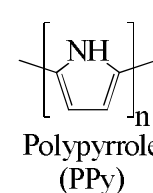
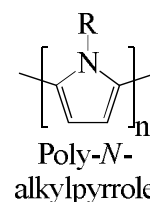
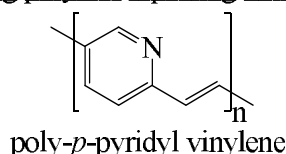
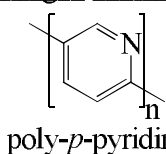
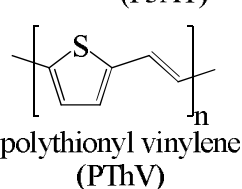
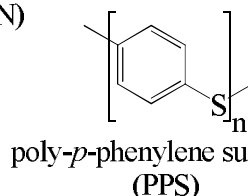
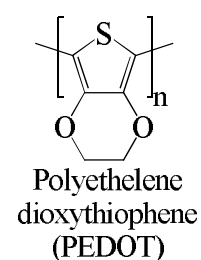
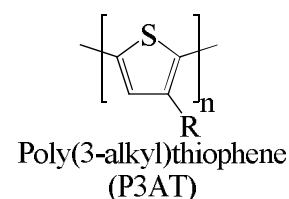
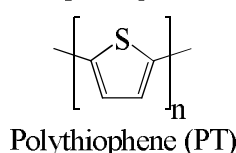
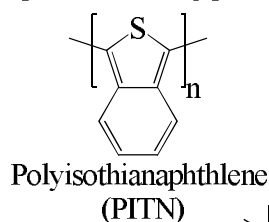
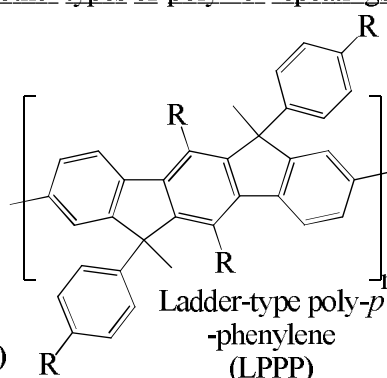
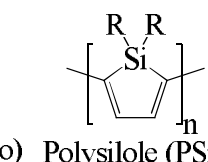
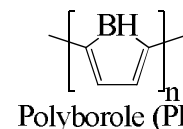
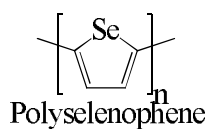
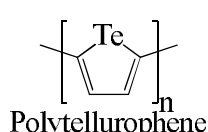
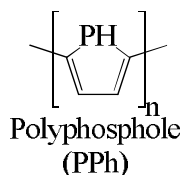
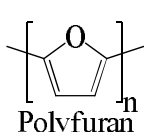
Simple polymer repeating unitsAromatic repeating unitsNitrogen containing polymer repeating unitsSulphur containing polymer repeating unitscomplex and other types of polymer repeatings units

Figure 1: Repeating units of a range of Conjugated Polymers; illustrating simple, heterocyclic and complex repeating units.

The field of polymer science is at present, quite vast, however with in this new field, there has been the emergence of new and exciting fields, with interests focussed on individual aspects of polymer science. One such emergence that has

come about since interests developed in the field of polymers is the research of conjugated polymers. As a new field of polymer science, there is a lot of vested interests and excitement currently placed on this relatively new area with research occurring only within the last 50 years and in particular there has been a massive drive since the late 1970's<sup>11</sup>.

Further division of polymer science has led to new research fields developing; such a field exists for conjugated polymers. These subtypes of polymers are characterised by their elongation and propagation of alternating  $\pi$ -bond system along the polymer backbone<sup>2,12</sup>.

### 1.1.3 The development of conductive polymers.

Over the years greater attentions have been placed on conjugated polymers as time has progressed, due to their properties and potential applications of these materials within the paradigm of science. The key property which has excited the polymer research community is the electro active properties and potential possibilities of creating conductive organic molecules, with conductivities in the region of many metallic elements. The true beginnings of such research which led to this can be said to have started in the 1960's<sup>4,13</sup>, Pohl *et al.* during the 1960's synthesised semiconducting and conjugated polymers, but it wasn't until the 1970's when interests in conductive polymers were directed at looking at conjugated polymers with the objectives of developing conductive material<sup>14</sup>.

#### 1.1.3.1 Historical Perspective of Conjugated polymers

In 1973 it was discovered that poly(sulphur nitride) (aka polysulphur nitride) or simply abbreviated to  $(SN)_x$  (Figure 2), an inorganic polymeric explosive<sup>13</sup> in previous applications, showed properties that excited researchers due to its electronic properties.

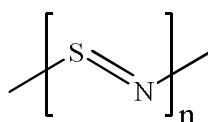


Figure 2: Structure of Poly (sulphur nitride)

Although the discovery of  $(SN)_x$  was not the driving force behind leading research into conjugated polymers it certainly was an initiator and opened the eyes of many researchers to the possibilities and potentials these materials held.

The most crucial and famous pioneering research that led to an excitement in conjugated polymer applications in electronic applications, belongs to the work conducted by Shirakawa et al.<sup>11,12,15,16</sup> Their pioneering has gone on to influence, direct and initiate extensive research into the different reaches of chemistry and physics regarding conjugated polymers, looking at both charged and neutral conjugated polymers.

Since 1977 when ideas and postulated theories were still in their infancy, Shirakawa and co-workers pioneering research looked at the synthetic methodologies of synthesising the simplest of conjugated polymers poly (acetylene) (abbr. PA) in both isomeric forms. Their work led to the serendipitous discovery of conductive polymers. They initially developed techniques of controlling the ratios at which the *cis*- and *trans*-isomers are produced. Both isomers (Figure 3) coincidentally looked metallic upon the isolation of thin films; the *cis*-isomer producing a film coloured and resembling copper and the *trans* isomer producing a film that was silver in colour<sup>11</sup>.

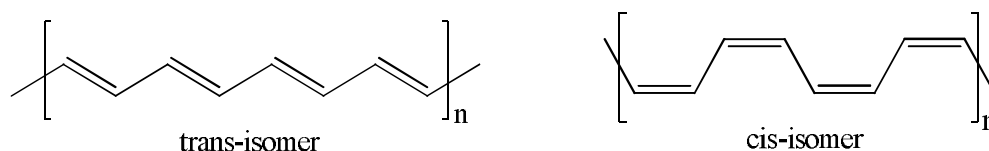


Figure 3: The isomeric forms of Poly (acetylene)

These isolated isomers were in the region of insulators and semi-conductors in their neutral states with conductivities measured at  $4.4 \times 10^{-5} \text{ S cm}^{-1}$  (semi-conductive) and  $1.7 \times 10^{-9} \text{ S cm}^{-1}$  (insulating) for the *trans* and *cis*-isomers respectively when measured at 273 K ( $0^\circ\text{C}$ ). However the interest arose when the films were exposed to chemical species that were either oxidative (electron accepting, Lewis Acid) or reducing agents (electron donor, Lewis Base) at ambient room temperatures for a few minutes, such species utilised were halogens (chlorine, bromine and iodine vapours), this process greatly increasing the conductivities over several orders of

magnitude<sup>11,12</sup>, from  $4.4 \times 10^{-5} \text{ S cm}^{-1}$  to a maximum quoted at  $10^5 \text{ S cm}^{-1,17}$  a conductivity that compares to metal.

This major breakthrough led to the extensive research of conjugated polymers looking at modifications via doping. Key figures that have since emerged in the field of conjugated and conductive polymers are Heeger and MacDiarmid<sup>16,18</sup>.

Well known for their research, they led the way to the discovery of new classes of conducting polymers. At present such polymers which are intrinsically semi-conducting, conductive polymers, conductive upon modification or electro-active polymers have become known within the polymer community as synthetic metals. With the existence of such a class of polymers, there is now a journal called 'synthetic metals' which solely and exclusively deals and publishes research focussed on conducting polymer research<sup>13</sup> with hundreds of articles published every year in this and various other journals. Heeger, Shirakawa and MacDiarmid's have since received recognition for their pioneering work and for their establishment of the conjugated polymer science, by being granted and awarded the Nobel Prize in Chemistry in 2000. They have also been accredited as being the 'founding fathers' of electro-active polymers<sup>12</sup>, however with any field of science more figures are becoming well known for their research and contributions.

#### 1.1.4 Properties of Conjugated and Conductive Polymers

Conjugated polymers by nature are insulating materials or at best are semiconducting materials, however these materials can be tuned and optimised to induce conductivity along the polymer chain that is within a region similar to metals<sup>7</sup>(Figure 4).

Any conjugated polymeric material which possess the electrical, magnetic and optical qualities that are commonly associated with metals, whilst retaining the mechanical properties of current conventional insulating polymers have been labelled as 'Synthetic Metals' or Intrinsic Conducting Polymers (ICP's). These however should not be confused with current 'conductive polymers' which are at present in use within the industry, these purely being a mixture of an insulating polymer/plastic with a dispersion of a conductive material, such as highly conducting metallic particles or Carbon black powder with the matrix material.

Regions of Conductivity	Conductivity (S cm <sup>-1</sup> )	Organic Molecules, Polymeric materials and Crystals	Metals and Inorganic compounds
Metals	10 <sup>6</sup>	Graphite, Polysulphur nitride <i>trans</i> -Polyacetylene (Doped)	Silver, Copper
	10 <sup>5</sup>		Mercury
	10 <sup>4</sup>		Iron
Semiconductors	10 <sup>3</sup>	<i>trans</i> -Polyacetylene (Undoped)	Magnesium
	10 <sup>2</sup>		Tin
	10 <sup>1</sup>		Indium
	10 <sup>0</sup>		Zinc Oxide
	10 <sup>-1</sup>		Germanium
	10 <sup>-2</sup>		Silicon
	10 <sup>-3</sup>		Boron
Insulators	10 <sup>-4</sup>	<i>cis</i> -Polyacetylene (undoped) Glass Diamond Nylon Quartz Polyvinyl chloride (PVC) Polystyrene PTFE (Teflon)	Water
	10 <sup>-5</sup>		Iodine
	10 <sup>-6</sup>		Silicon Dioxide (Sand)
	10 <sup>-7</sup>		
	10 <sup>-8</sup>		
	10 <sup>-9</sup>		
	10 <sup>-10</sup>		
	10 <sup>-11</sup>		
	10 <sup>-12</sup>		
	10 <sup>-13</sup>		
10 <sup>-14</sup>			
10 <sup>-15</sup>			
10 <sup>-16</sup>			
10 <sup>-17</sup>			
10 <sup>-18</sup>			
10 <sup>-19</sup>			
10 <sup>-20</sup>			

Figure 4: Conductivity ranges of various known materials, showing regions of conductivities and electronic regimes of materials<sup>19</sup>.

Exceptions to the concept that polymers are intrinsically semiconducting at most have been discovered with an example such as polysulphur nitride, an inorganic conjugated polymer that is truly within the metallic regime and resides within the conductive region en par with most metals<sup>15</sup>.

### 1.1.4.1 Electronic properties of conjugated polymers.

The structure of the polymer is one aspect that is crucial to conductivity of charge along the polymer chain. Conjugated polymers are seen to display a spatial and elongating  $\pi$ -bonding system that propagates along the polymer chain backbone, an array of alternating carbon-carbon single bonds and carbon-carbon double bonds, with the  $\pi$ -bonds being in the configuration of  $sp^2p_z$  and resulting in the overlapping of  $p_z$  orbitals of alternating carbons, this is not however localised to just carbon-carbon bonds, nitrogen is also seen to be a participant in the  $p_z$  orbital overlap which is seen in the case of polyaniline and allows further extension of electron delocalisation along the polymer backbone<sup>2,20</sup>.

This configuration has significant effect on the electronic properties of conjugated polymers, and is evident when comparing conjugated polymers with saturated polymers, where all the four valence electrons are implemented in covalent bonds, the net result and nature of the chemical bonding in conjugated polymers results in an unpaired electron per carbon atom (Figure 5). Localisation of the wavefunction is less stable and favourable in the scenario where the electron is localised to any one individual carbon atom thus the result is that the each carbon injects the unpaired electron into the electron rich and more stable  $\pi$ -system, stabilised by the delocalisation of the electrons. This is supplemented and facilitated by the overlap of the orbital's of alternate carbons which creates the vast and spatial array of  $\pi$ -bonds over the whole chain. The electronic delocalisation that is created by this system of  $\pi$ -bonds is suggested to provide the route or a sort of 'motorway network'<sup>4</sup>, allowing movement of the electrons to along chain therefore if this is true for electron migration the same can therefore be postulated for propagation of a charge along the chain<sup>6</sup> and thus achieving some levels of electronic activity, whether this be conductivity of an applied potential or optical activity.

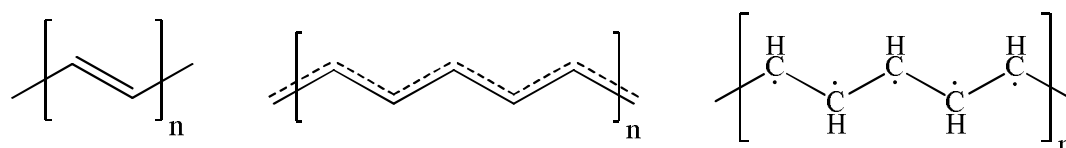


**Figure 5: Three representations of Polyacetylene; in degenerate ground state, electron delocalisation of the  $\pi$ -bonding along the polymer chain and electron localisation showing that each carbon has an electron which can be donated into the  $\pi$ -system.**

#### *1.1.4.2 Physical properties of conjugated polymers.*

It is important to understand just how critical and important the structure in its relation and its effects on the intrinsic conductivity of the polymer. In terms of describing the how the physical structure and the electronic properties are intertwined, this is excellently exemplified by the simplest of conjugated polymer, polyacetylene, and the highly conducting polymer, polysulphur nitride.

Conjugated polymers are intrinsically ‘quasi’-one dimensional in geometry, a result of that is resultant from the  $sp^2$  hybridised nature of the polymers producing a somewhat rigid and linear structure<sup>12</sup>. Further to the covalent bonding within the polymer chain there exist other weaker interactions between the parallel linear chains, namely Van der Waal forces<sup>20,21</sup>.

#### *1.1.4.3 Band gaps*

A band gap by definition is the difference in energy between the lowest energy levels of the conduction band, also known as  $\pi^*$  band (anti  $\pi$  band) or the Lowest Unoccupied Molecular Orbital (LUMO) and the highest energy levels of the valence band, also known by several alias's namely  $\pi$  band or the Highest Occupied Molecular Orbital (HOMO)<sup>22</sup>. This gap is seen to be a region of forbidden electron energy, whereby the electrons are incapable of moving from one band to another unless energy exceeding the forbidden energy is supplied into the system, this activation energy ( $E_a$ ) therefore promotes the electron to a higher electron orbital or in the case of conjugated polymers promoting the electron from the  $\pi$  band to the higher energy  $\pi^*$  band thus allowing for the electro-active properties that are seen under specific conditions. The trend in band gaps differs between different classes of materials, generally aliphatic saturated materials and polymers are seen to be insulating with huge band gaps, to an extent that electron migration from the one band to another is not a probable scenario due to the energy that would be needed to promote electrons, these materials are inherently insulating and transparent to visible light and potentially other forms of electro-magnetic radiation. Conjugated materials on the other hand are placed between the regions of insulating materials and crossing over into the regions of semiconducting materials, due to the delocalised wave function of the  $\pi$  electron, over all or at least portions of the chain. The  $E_a$  required for electron promotion into the conduction band is considerably less; principally these materials hold band gaps between 1 to 4 electron volts (eV).

Typically activation energy can come from several sources; electromagnetic radiation (visible light), applied electric fields to name a couple of examples and finally metallic materials and metallic elements have no band gaps to at a maximum a small band gap. Generally the bands are illustrated in two different manners; firstly some postulate and describe the bands in metallic materials as overlapping, where the valence band overlaps the conduction band. Concordantly it can be described that the bands of metals are in a state where the bands are half filled, however described they both allow for electron promotion from one band to the other without expenditure of large amounts of energy or any external source of energy such as light to activate and excite the electrons (Figure 6)<sup>4,22</sup>.

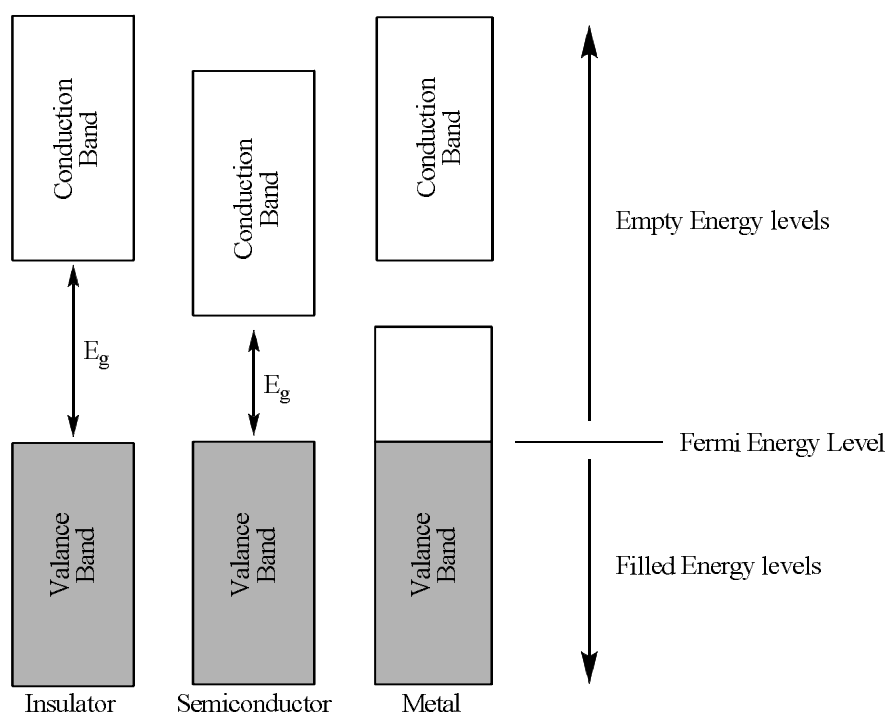


**Figure 6: Comparison of Energy levels and Band gaps between the electronic states of materials**

Determination of a band gap for any polymeric material is achievable via analytical and electrochemical means, techniques such as cyclic voltammetry (CV), where potentials are applied to the material giving readings for the oxidation and reduction potentials for the polymer. This is on the proviso that the interchain interactions are relatively small and have little effect on the readings (Equation 1)<sup>22</sup>.

$$E_g \approx (E_{ox} - E_{red}) + (S^+ + S^-) \left( \frac{1}{\epsilon_1} - \frac{1}{\epsilon_2} \right)$$

**Equation 1: Calculation to determine the Band gap of a Polymeric Material.** ( $E_{ox, red}$ ) Oxidation and Reduction potentials, ( $S^\pm$ ) Solvation energy of the ionised molecule subtracting the solvation energy of the neutral molecule, ( $\epsilon_{1,2}$ ) Dielectric constant of the solution and the molecular solid respectively.

The formation of the bands are consequently due to the extensive alternating  $\pi$ -bonding system that occurs along the backbone of the conjugated polymer (Figure 7) as is shown upon successively increasing the levels of conjugation along the polymer chain, a reduction and narrowing of the band gap occurs between the LUMO and the HOMO energy levels, until a point is reached where conjugation is infinite and the band gap reduces no more.

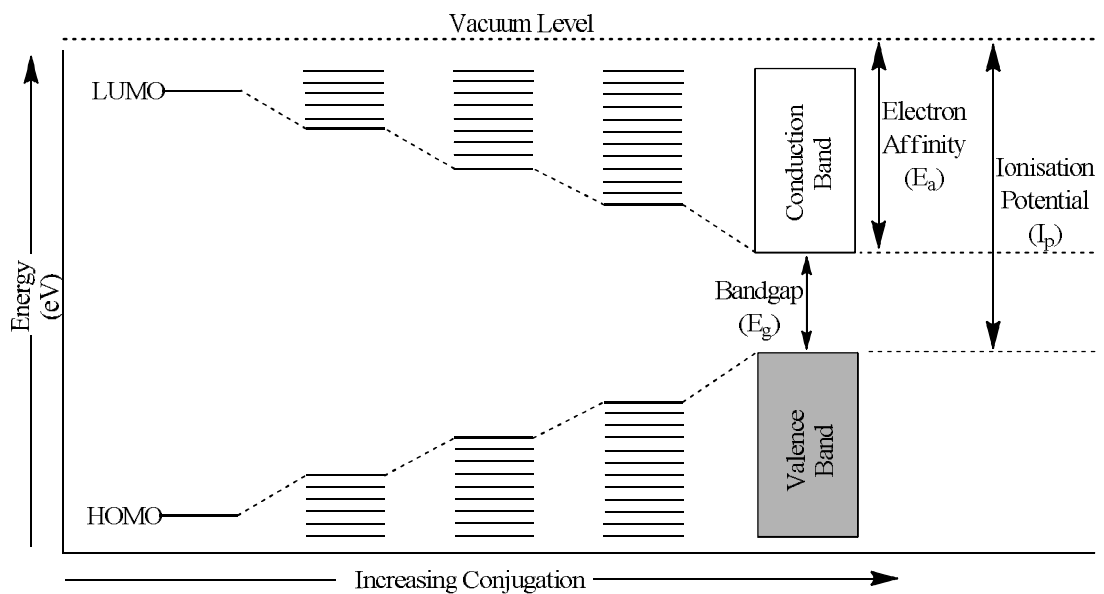


**Figure 7: Energy Level diagram, illustrating the formation of bands upon increasing conjugation, with formation from discrete energy levels to energy bands.**

Each  $\pi$ -bond consists of a  $\pi$  band and a  $\pi^*$  band (anti  $\pi$  band), both capable of holding two electrons per atom, a spin up and spin down electron. In the case of conjugated polymers the  $\pi$  band filled with two electrons whilst the  $\pi^*$  band remains empty. Differences in energy between the highest occupied molecular orbital (HOMO) and the lowest unoccupied molecular orbital (LUMO) results in an energy gap between the  $\pi - \pi^*$  band that if of sufficient contrast prevents electrons from migrating into the  $\pi^*$  band (LUMO). Previously stated the conductivity is

therefore dependent on whether the electrons can migrate to the  $\pi^*$  band or whether there is electrons already localised in the  $\pi^*$  band. However the electrons in conjugated polymers occupy and fill the lower energy band and with no electrons remaining, the  $\pi^*$  band remains empty. This situation can be manipulated, by the insertion of electrons into the polymer chain, electrons would be promoted into the  $\pi^*$  band due to the  $\pi$  band capacitating at its maximum, thus conductivity can be achieved. On the other hand removal of electrons from the polymer chain producing a half filled band conditions allowing for charge transport<sup>4,7,12,13,17,18,23,24</sup>.

Several influencing factors control the formation of band gaps in conjugated polymers with the energy difference between the gaps differing between different polymers based on several criteria. The main controlling factor appears to be the physical structure of the polymer. Characteristics such as bond lengths and the differences between the alternating  $\pi$  bond and  $\sigma$  bonds of the polymer, the torsion angles at which are exerted by the polymer chain which are seen to disrupt the conjugation, resonance energies of the polymer chain, substituent effects. In the case of aromatic systems additional effects such as inter ring torsion angles and the planarity of the polymer<sup>25</sup>.

#### 1.1.4.3.1 Peierls Effect/Distortion

The general assumption that full delocalisation occurs along the polymer chain may not be as accurate as thought, with the assumption made that if each carbon has an unpaired electron which is donated into a state of delocalisation, it would make the system more energetically favourable. Then the conductivity of an electrical charge would occur along the polymer backbone. However conjugated polymers, as previously stated are at best semi-conductors, the question that is then posed is why this is? There must be other factors affecting the electronic properties of these materials.

Several papers have placed the emphasis and the importance that the physical structure has on the electronic parameters of conjugated polymers. One such influencing factor that has been discussed is the Peierls Effect, an instability that is seen in all conjugated polymers. Using polyacetylene as an exemplary model, the peierls instability can be easily illustrated, placing into context the importance of the physical structure on the electronic properties.

Polyacetylene is the simplest of conjugated polymers structurally all the carbons participate in an  $\sigma$ -bond with both their adjacent carbons, are in possession of a hydrogen atom and each carbon harbours a  $\pi$ -electron. In a state such as this all the carbon-carbon bond lengths are almost certainly of equal distance throughout the polymer chain denoting the existence of a  $-(\text{CH})_n$  repeat unit (Figure 5). Considering the unpaired  $\pi$ -electron, it may be postulated that is present and potentially localised on each carbon. A consequence of this would by implication suggest that the polymer would be in a metallic state, with conductivities rivalling metals and in a true sense of the word would be a synthetic metal. The subsequent culmination would be a material that is antiferromagnetic and a Mott insulator. Contrary to this belief, neither of these qualities is seen, with facts such as the ease at which these materials dope into metallic states and the countless studies conducted on neutral conjugated polymers discrediting such possibilities and ideas.

The actual structure of polyacetylene is seen to be dimerised which accordingly leads to Peierls instability within the polymer chain. As a result the repeat structure is better represented as  $(\text{CH}=\text{CH})_n$ , with the overlap of the  $p_z$  orbital of successive carbons producing a  $\pi$ -bond, which inevitably utilises the lone unpaired electron which conventionally may be thought as being localised to a carbon atom, hence extensive conjugation along the polymer backbone. Further consequence is that the bond lengths in the conjugated system are not of equal length as is idealised in a delocalised state. In Polyacetylene the bond lengths are  $1.44 \text{ \AA}$  ( $14.4 \text{ nm}$ ) for the  $\sigma$ -bonds and  $1.36 \text{ \AA}$  ( $13.6 \text{ nm}$ ) for the  $\pi$ -bonds (Figure 8)<sup>15,20</sup>. The  $\pi$ -bond being shorter due to the carbon atoms existing  $sp^2$  hybridized state as opposed to  $sp^3$  hybridized state, this conformational change acts to reduce the internal energy expenditure that is used to maintain the rigid and planar chain, however creating the right circumstances for the formation of band gaps, increasing the activation energy and opening the band gap of these polymers<sup>12,17</sup>.

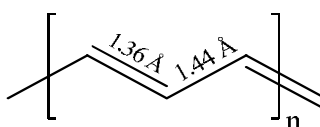
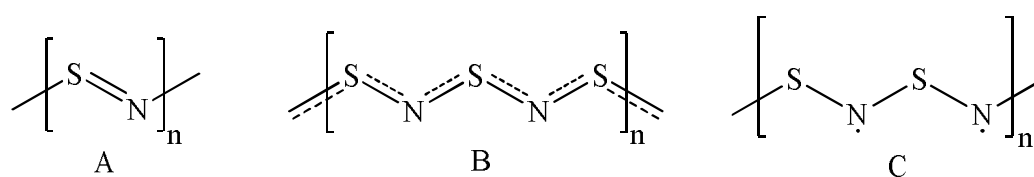


Figure 8: Bond Lengths of *trans*-Polyacetylene<sup>20</sup>.

Polysulphur nitride however remains unique amongst conjugated polymers; its distinctive properties allow certain exemptions such as exemption from the Peierls effect. The first consideration to take is that one factor influencing the conductivity of polymers in the metallic region is the presence of an unpaired electron. In the case of polysulphur nitride there is the existence of an unpaired electron localised to the repeat unit with the repeat units covalently bound to the neighbouring monomeric repeat unit (Figure 9). The NS free radical is analogous to Nitric Oxide (NO), with an unpaired electron occupying the lowest energy level of the  $\pi^*$  band (LUMO) therefore conductivity ensues.



**Figure 9: Structural representations of Poly (sulphur nitride); A, The simplified chemical structure. B, representation of the structure in terms of electron delocalisation, and C, representation of the lone unpaired electron localised to the Nitrogen atom.**

Secondly the bond lengths are not equal much like other conjugated polymers, with bond lengths of  $1.55 \text{ \AA}$  ( $155 \text{ pm}$ ) between the S-N and a bond length in the region of  $1.73 \text{ \AA}$  ( $173 \text{ pm}$ ) shared between the N-S moieties of the polymer with a bond angle of  $119^\circ$  around the Sulphur and a bond angle of  $108^\circ$  around the Nitrogen (Figure 10). This should in theory dictate that polysulphur nitride is susceptible to the Peierls effect, with the judgement based on what is seen in the case of polyacetylene. However due to the fact that polysulphur nitride possesses an unpaired electron, the ruling factor in this case is the knowledge that the unpaired electron is localised to the  $\pi^*$  band and metallic conductivity is therefore possible.

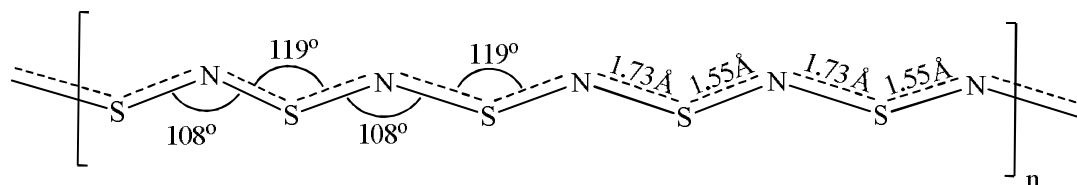


**Figure 10: Physical Structure of Polysulphur nitride<sup>26</sup>.**

#### *1.1.4.4 Manipulating the Band gaps of polymers.*

With the knowledge and better understanding that researchers now possess regarding polymers with regards to the phenomena of Band gaps and their formation it is possible to tune and manipulate conjugated polymers to produce materials with reduced band gaps and increased electrical activity. Several methods can be employed to induce and tune the polymers to the desired specifications of industry and academia via methods such as structural modifications. Polymers electro active properties are heavily influence by the physical structure, therefore by altering and modifying the structure of the polymer to an extent that the polymer becomes practical and useful has been one of the main focuses by researchers and the industry and with reports of lowered band gaps which undergone modification.

Several modifications have been postulated and implemented to lower the band gaps of the conjugated polymer, such as methods of relaxing the bonds length between the alternating  $\pi$ - $\sigma$  bonds, achievable by the insertion of aromatic rings or quinoid moieties into the polymer backbone. This also acts to increase delocalisation of electrons due to the extensive network of  $\pi$  electrons present and thus suppress the Peierls effect<sup>25</sup>.

The planarity can be modified by incorporation of aromatic systems into the backbone of the polymer this not only causing relaxation as previously described but may also go so far as to permitting the anisotropic stretching of the chain, which will subsequently allow chain alignment and stacking, allowing for the potential for charge transfer between chains. It is also reported that poly-3-hexyl thiophene which undergoes the process of stacking has a reported band gap of 2.14 eV<sup>6</sup>. Subsequently the effect of reduced torsion angles and increase in planarity has shown to reduce band gaps (generally between 1 – 4 eV), lowering the excitation energy, for example the energy supplied by a photon of visible light may be adequate to excite electrons. The net result is the increase in intrinsic semi-conductivity<sup>4,6,25</sup>.

Further suggestions have included the introduction and potential incorporation of electron donating or accepting groups into the polymer chain backbone will allow for the interactions between the HOMO of the donor and the LUMO of the acceptor reducing the effective band gap. However these methods only allow for little

manipulation of the polymer properties which may all be that as needed depending on the application of the polymer. Effectively the polymer still remains in the semi-conductive regime, however to ensure that the polymer enters a metallic regime it is suggested that doping is the possibly the only current method to achieve a state of intrinsic conductivity<sup>6,22,25,27</sup>.

### 1.1.5 Concept of Doping

The central theme and concept of the doping process is a means of changing the properties of the polymer, which initially are initially intrinsic insulators into polymers with modified properties such as superior electronic properties and advantageous characteristics over their counterpart analogues. This process has allowed for what was once a material with limited applications and a narrow window for utilisation to become a material with broadened applications and generally these polymers much more practical, serviceable and potentially more profitable.

The process of doping is a relatively new with research generally starting in the late 1970's after the chance discovery by Shirakawa and co-workers pioneering research looked at the synthetic methodologies of synthesising the simplest of conjugated polymers poly(acetylene) (abbr. PA) in both isomeric forms. Their work found that a conjugated polymer (intrinsically insulating or semiconductor), can be modified and optimised to induce conductivity within the metallic regions of conductivity along a polymer chain. After the process of doping the conductivities were identified for both isomeric forms of PA<sup>11,15</sup>.

Initial conductivities prior to doping were  $4.4 \times 10^{-5} \text{ S cm}^{-1}$  (semi-conductive) and  $1.7 \times 10^{-9} \text{ S cm}^{-1}$  (Insulating) for the *trans* and *cis*-isomers respectively (measured at 273 K (0°C)). However upon the exposure of the films for both isomers to an oxidising agent at room temperatures. The conductivities increased with great magnitude<sup>11,12</sup>, from  $4.4 \times 10^{-5} \text{ S cm}^{-1}$  to a maximum quoted at  $10^5 \text{ S cm}^{-12,17}$ . A conductivity that compares to copper, iron and silver (all  $10^6 \text{ S cm}^{-1}$ ) and an increase by  $10^{10}$  in conductivity from its neutral state to its associated charged/doped state (Figure 4).

Doping in short quite simply involves the transfer of charge to or from the  $\pi$  bonds of the conjugated polymer, whilst the  $\sigma$  bond retains the same number of electrons throughout the doping process therefore remaining unchanged and intact preserving and maintaining the structural identity of the chain. However other properties allied with the structure do change such as the electronic properties and overall the supramolecular structure is altered, giving rise to a wide range of electronic phenomena<sup>17,24</sup>. Changes with the magnetic, optical and structural aspects of the polymer are noticed and in particular there are noticeable changes in the electronic and electrical properties, increasing the conductivity over several orders of magnitude reaching potentials of a metallic regimes<sup>12</sup>. As suggested there are changes in the electrical properties during the process of doping, in context this change in the conductivities of organic polymers, which are usually within the insulating/semi-conducting regimes, increase from  $10^{-10} - 10^{-5} \text{ S cm}^{-1}$  (Insulating – Semiconducting respectively) to  $1 - 10^4 \text{ S cm}^{-1}$  (Semiconducting – Metallic regime).

The doping process of course is seen to be reversible with little to no damage or degradation to the polymer chain<sup>7</sup>, the polymer is returned back to its original upon removal of the dopant, thus the rationale for the application of dopants in the electronics industry is of significant interest and is highly advantageous in terms of the ability for recycling materials which favours environmental issues.

#### *1.1.5.1 Mechanisms and Methods of Doping Polymeric Materials.*

Doping of a material can be split into two main categories namely, Redox Doping and Non-Redox Doping. Both methods of doping each achieve the same results of increasing the conductivity and altering key electronic properties of the conjugated polymer, however these results are met. The doping species carry associated electronic states whereby their energy levels take residence within the forbidden energy of the band gap, which effectively decreases the band gap<sup>4</sup>.

##### *1.1.5.3.1 Redox Methods of Doping.*

Chemical doping was first stumbled upon by Shirakawa and co-workers<sup>11,15</sup> who as described previously, managed to obtain PA in a 'metallic' state through subjecting both isomeric films of PA to vapours of halogens, typically bromine ( $\text{Br}_2$ ) and iodine ( $\text{I}_2$ ), with later uses of arsenic pentafluoride ( $\text{AsF}_5$ ). However the procedure

for  $\text{Br}_2$  is much more difficult as upon doping, reactions remain to proceed forward, attacking the double bond and the bromine becomes covalently inserted into the polymer chain (Figure 11) producing polydibromovinylidene which intrinsically is insulating<sup>12</sup>. Likewise  $\text{AsF}_5$  acts as both an oxidising agent and a Lewis acid, with about a third acting as an oxidiser and two thirds acting as a Lewis acid. Generally whether the polymer is doped via chemical or electrochemical means, the conductivity is seen to be permanent until the material is undoped, removing the charge carriers or until the charge carriers are chemically compensated.

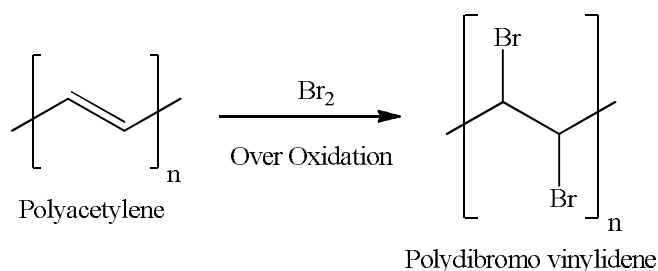


**Figure 11: The oxidation of PA in the presence of bromine vapour resulting in the undesirable saturated by product.**

In terms of whether oxidation (*p*-type) is a better method than the reduction (*N*-type) doping method or vice versa, it is reported that the conjugated polymers which have been *p*-doped show high stable conductivities, whilst in comparison to *N*-doping it is seen that conductivity is lower than what is expected and this has been attributed to the fact that the electrons injected into the  $\pi^*$  band have a tendency to be lost<sup>28</sup>.

#### 1.1.5.3.1.1 *p*-type doping.

Doping using an oxidising agents is known as *p*-type doping, they proceed by removing electrons from the  $\pi$  systems, systemically altering the number of electrons associated with the polymer chain<sup>7</sup>. Achieving this can be done through both chemical and electrochemical processes (anodic oxidation of the polymer). Both produce polycarbonium cations, whilst simultaneously inserting an anionic species (counter ion), which acts to counter balances and stabilises the charge. Due to the removal of electrons from the polymer chain results in the creation of a hole and therefore the polymer is said to be a hole conductor or in terms of the band theory is the removal of electrons from the  $\pi$  band creating an half-filled band.

The charge that is now associated with the polymer backbone shows mobility over the chain with reports suggesting that 85% of the charge is delocalised<sup>7</sup> stretching over fifteen repeat units. Such a change results in the delocalisation of the  $\pi$  system and therefore diminishing the effects of Peierls instability, where the  $\pi$  system is in dimerised conjugated state<sup>7</sup>.

Generally oxidation proceeds by initially removing an electron from the  $\pi$  system which causes formation of a radical cation, progression of oxidation promotes the removal of a further electron. The removal of a second electron produces a second radical cation, which may combine to produce a spinless dication depending on the thermodynamic favourability within the polymer system, a positive spinless charge carrier known as a soliton may be produced upon further oxidation of the polymer chain. This remains true for a simple conjugated system such as PA, however in heterocyclic or heteroatomic polymers undergo slightly different alteration. It remains similar that the removal of an electron from the  $\pi$  system proceeds to produce a radical cation (polaron), the difference in structure changes to the more favourable quinoid type bond sequence (Figure 12). The removal of a second electron leads to the formation of a second radical cation which generally combine to form a spinless dication (bipolaron), this dication separates the separate domains of the quinoid domains from the benzenoid/aromatic domains (Figure 12)<sup>12</sup>.

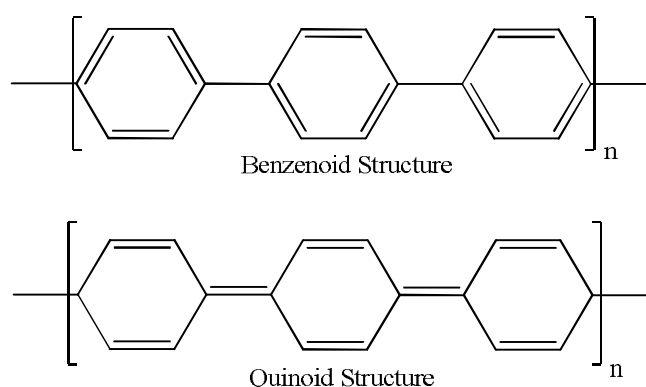


Figure 12: Structural Differences between Benzenoid and Quinoid Structure.

#### 1.1.5.3.1.1.1 Chemical Doping.

As previously described Shirakawa and co-workers showed that with suitable oxidising agents, removal of electrons from the polymers  $\pi$  system and effectively the polymer chain were achievable<sup>11,15</sup>. Initially halogens were the choice of

oxidising agents in the late seventies and research post 1970's, typically chlorine, bromine or iodine were employed to remove electrons from the polymeric material.



Equation 2: *p*-type doping of a polymer with the halogen iodine.

The conductivities for the created isomer (Figure 13) in the region of  $4.4 \times 10^{-5} \text{ S cm}^{-1}$  (Semi-conductive) and  $1.7 \times 10^{-9} \text{ S cm}^{-1}$  (Insulating) for the *trans* and *cis*-isomers respectively when measured at 273 K (0°C) prior to doping.

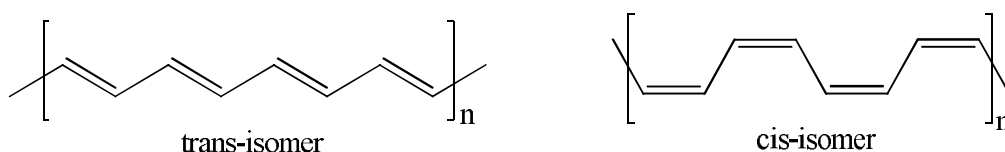


Figure 13: The isomeric forms of Poly (acetylene)

Doping with the halogen vapours saw the conductivities increase in great magnitude to a maximum of  $10^5 \text{ S cm}^{-1,24}$ , which has been attributed to the polymer existing in a stretch orientated conformation<sup>7</sup>. A conductivity that compares to Copper, Iron and Silver (all  $10^6 \text{ S cm}^{-1}$ ) and an increase by  $10^{10}$  in conductivity from its neutral state to its associated charged/doped state<sup>11,12</sup>. As a result of the oxidation, structural and electronic changes were noticed (Figure 14).

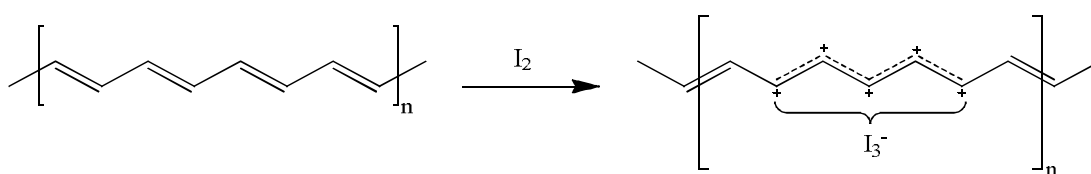


Figure 14: Doping of PA with Iodine vapour at Room temperature

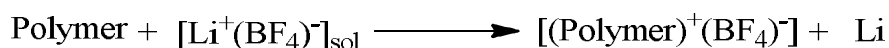
However care has to be taken when using bromine as an oxidising agent, due to its ability of further oxidise the polymeric material until the undesirable, Polydibromovinylidene is produced, which is again intrinsically insulating (Figure 11). This is the result of the bromine atoms inserting themselves covalently into the polymer chain, producing a saturated polymer chain.

Since this study other oxidising agents have been identified as suitable candidates for chemically oxidising conjugated polymers. Such as arsenic pentafluoride, which itself is a unique amongst dopants as it display both characteristics which are classic of redox dopants and properties which are similar to acid-base doping, with reports suggesting that a third of the dopant acts as an oxidising agent and the other two thirds as a Lewis acid. This can however be optimised to produce a dopant of just redox properties by the creation of nitronium salts, hexafluorophosphates, arsenates or antimonates with the cation acting as the oxidant <sup>29</sup>.

#### 1.1.5.3.1.1.2 Electrochemical Doping

Chemical oxidation of the polymer is fraught with somewhat trivial problems mainly the control over levels of doping. If exposed too much the effects may be detrimental as is seen with the over oxidation of PA when exposed to bromine vapour and in other cases where the solubility is key to the doping process. This method holds the advantage that it can be used for both soluble and insoluble polymeric material. For a soluble polymer the electrode (the anode for *p*-type doping) is dipped in the polymer solution or spin coated, whilst the insoluble polymers are electro polymerised onto the electrode or again films cast by dipping or spin coating the electrode into the colloidal solution. The method is usually carried out in non-aqueous media; acetonitrile (MeCN or ACN) and propylene carbonate, this solution usually contains LiClO<sub>4</sub>. The electrodes then supply the polymer with a redox charge of direct current causing oxidation of the polymer, the balancing of this charge is then stabilised by electrolyte, which diffuses in and out of the structure.

The levels of control for doping by methods of electrochemistry are seen to be very high as the level of doping is controlled by the voltage between the electrodes and the polymer, therefore this method is less laborious with the process just requiring the voltage to be set and waiting until the system reaches its electrochemical equilibrium. The process of *p*-type electrochemical doping can be seen below (Equation 3) where the charge on the polymer is stabilised by the anionic species of the electrolytic solution with lithium precipitating on the anode.



Equation 3: *p*-type electrochemical doping of polymer.

### 1.1.5.3.1.2 *n*-Type chemical doping.

Doping of conjugated polymers are not just restricted to oxidation or the removal of electrons from the  $\pi$  system in order to achieve conductivity but can also be achieved by the insertion of electrons into the  $\pi$  system, a reduction of the polymer chain and potentially the insertion of electrons into the  $\pi^*$  band (conduction band). As a method of doping, the reduction of the polymer is achieved by similar means as the oxidation of a polymer, via chemical or electrochemical methods.

#### 1.1.5.3.1.2.1 Chemical Reduction/Doping.

The procedure follows by the formation of a carbonium anion radical (carboanion) species, a charge carrier of negative charge which is the culmination of electrons being pumped into the  $\pi^*$  band, thus this band becomes partially populated with electrons, leading to an increase in conductivity up to  $10^3 \text{ S cm}^{-17}$ . Chemically reduction can take place using a liquid Sodium amalgam or Sodium naphthalide (Equation 4).



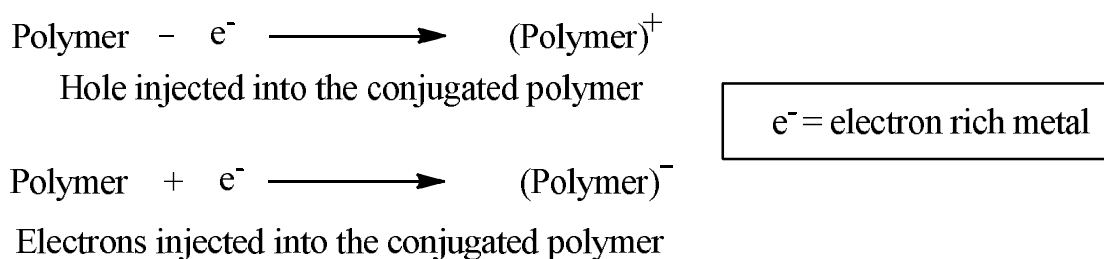
Equation 4: *n*-Type chemical doping with Sodium naphthalide.

#### 1.1.5.3.1.2.2 Electrochemical Reduction/Doping.

Reduction of the polymer via electrochemical means is achieved in the same way as the oxidation, however in this case the polymer the polymer is cast or polymerised onto the cathode and is immersed into the solution of  $\text{LiClO}_4$  or other reducing agents such as lithium boron tetrafluoride in tetrahydrofuran (THF) or MeCN and propylene carbonate. The lithium is sourced on the electrode and whilst in a solution of lithium boron tetrafluoride and is the reverse reaction of the *p*-type electrochemical doping, again the charge is stabilised by the presence of a counter ion which in this instance is lithium cation.

## 1.1.5.3.1.3 Charge Injection doping.

Charge injection doping differs from previous methods whereby electrons have been removed or inserted into the polymer chain ( $\pi$  system), resulting in a charge on the polymer which is balanced by the presence of a counter ion. But rather this method simply relies on the injection of electrons or holes onto the polymer via electron rich materials such as metals; hence no counter ions are involved. The removal of electrons as classically seen in the doping process are removed from the  $\pi$  band, whilst electrons that are injected into the polymer chain are injected directly into the  $\pi^*$  band and therefore in both situations create half-filled bands, localised structural distortions and electronic states which allow for the progression of an electrical current along the chain. This is of course providing the voltage potential is biased towards one result or the other.



Equation 5: Doping via Charge Injection.

## 1.1.5.3.1.4 Photo Induced Doping.

Unlike other methods of doping where the electrons of the  $\pi$  system are removed or electrons are added to the  $\pi$  system, photo-doping works via a different mechanism. Between the HOMO and LUMO levels or the  $\pi$  band and the  $\pi^*$  band the 'forbidden' energy gap determines whether conductivity of a current ensues, in the case of small band gaps the electrons are potentially able to migrate from one band ( $\pi$  band) and transfer into another ( $\pi^*$ band) hence conductivity is achieved, whilst larger band gaps only allow the transfer of an electron upon enough energy being supplied to the system (activation energy) and is known as excitation where the electrons transfer from their ground state to their lowest energy state. This is typical of a semi-conducting system in which conductivity is only achieved upon the energy supplied to the system being greater than the energy of the band gap; this can come from an electrical current itself or from other sources.

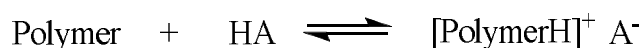
One such source that is seen to activate electrons from one band to the other in semiconductors is electromagnetic radiation, investigations have shown that the subjection of a conjugated polymer to a visible light for example is sufficient to excite and activate the electrons; therefore the light promotes electrons from one band to the other. The result of photo doping is the creation of solitons; either negatively charged or positively charged in nature, which are usually delocalised over a block of repeat units within the polymer chain. However these charges are short lived and rapidly disappear upon the positive (hole) and negative (electron) charge recombining and decaying back to ground state, trapping of charges or when the irradiation of the material with light ceases to continue. The charge separation has been reported to occur naturally, but some do report that the charge separation may be driven by external factors such as the application of a potential (voltage) to the chain causing the charges to separate and effectively conducting along the polymer chain.



**Equation 6: Photo doping of a conjugated polymer.**

#### 1.1.5.3.2 Non redox doping.

In specific and unique cases doping of a polymer can be achieved by non-redox means, such as the doping of a polymer with protonic acids or bases. This method however requires there to be basic or acid units within the polymer chain backbone. In this type of doping the number of electrons associated with the polymer chain remains unchanged during and after the doping process, although structural changes do occur as a result of doping and therefore may help to diminish the effects that the Peierls instability may hold over the polymer chain with the conductivities of treated conjugated polymers increasing with ten orders of magnitude.



**Equation 7: Non Redox Doping via a Protonic Acid**

The most common method of non-redox doping is the use of a protonic acid which is the case with examples such as polyaniline. What is more interesting is that the

protonic acid dopant species can be optimised and functionalised to counter the problems face by conjugated polymers such as solubility issues <sup>7</sup>.

### 1.1.6 Charge Transport Mechanism.

Initially several assumptions were made regarding the mechanism by which a current can be transported along a polymer chain. The conductivities of conjugated polymers were placed on the fact that the levels of conjugation of the polymer running along the backbone would be delocalised along the whole chain allowing for the transport of a current, further to this it was thought that each of the repeat unit in a conjugated system contain an unpaired electron which will be donated into a delocalised system much like a the electrons in a benzene ring. However this assumption was made on the basis that all the bond lengths were of equal distance, which is seen not to be the case of conjugated polymers with the  $\pi$ -bonds being of a shorter distance than the  $\sigma$ - bonds and so in much case the polymer retains a dimerised structure with the electrons being much more localised. This was known as the Peierls Instability/effect.

Secondly this led to the ideas of band gaps, the difference between energy levels of the  $\pi$ -bands and the  $\pi^*$ -bands which correlate to the valence band (VB) and the conduction band (CB) respectively which in the case of conjugated polymers the VB is filled with electrons and the CB being empty. The promotion of electrons from one band to the other has to have energy exceeding the forbidden energy gap, energy obtained from external factors exciting the electrons and activating the promotion from one band to the other. Hence this led to the development of doping polymeric material, with the assumption that doping created unfilled electrons bands and new energy levels within the forbidden energy gap, where electrons from the top levels of the VB or added to the bottom energy levels of the CB (Figure 15).

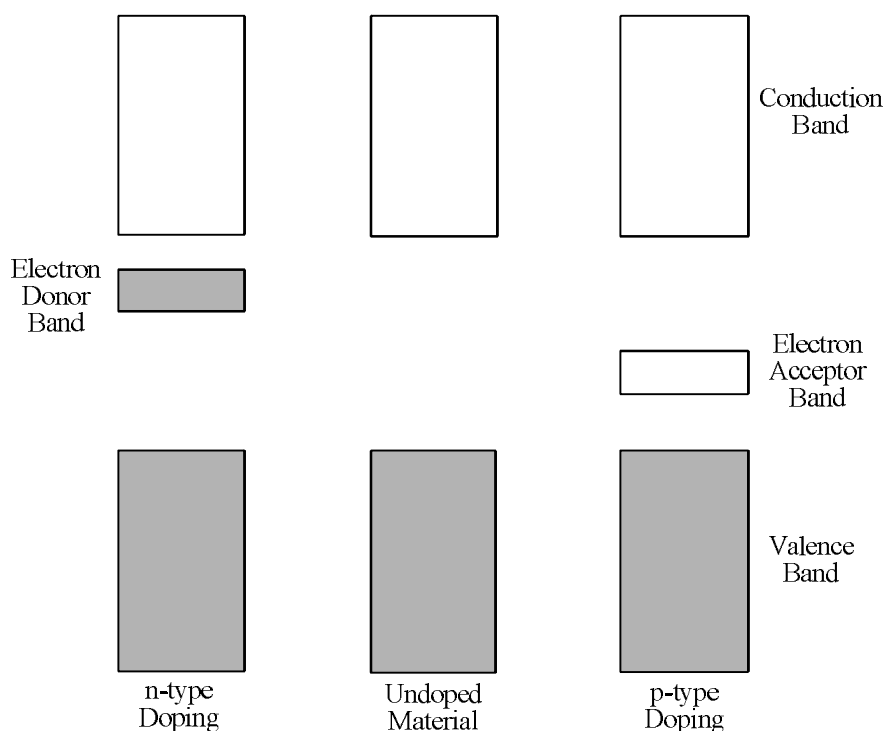


**Figure 15: Band gaps upon subjecting to *N*-type and *p*-type dopants.**

However many polymers show conductivity not by the movement of unpaired electrons per se but rather by the presence of charge carriers. The assumptions however are seen to be contributory factors in determining whether the material is insulating, semiconducting or conductive, which is evident upon the creation of the charge carriers. Structurally the polymer goes from a distorted ground state to a relaxed state (also referred to as the ionised state) that is thermodynamically favourable. Which in the case of doping the removal of electrons from the chain in *p*-type doping lowers the ionisation energy and allows the polymer to go into a relaxed state<sup>30</sup>.

For the discussion of the various charge carriers, several polymers will be used as examples to show the formation and key properties of the charges.

In the doped polymer of (PPy) polypyrrole a band gap of 3.2 eV exists, the *p*-doping of the polymer removes an electron from the chain leading to the structural relaxation of the polymer from its benzenoid analogue to the quinoid analogue. A geometric relaxation over 4 units and proceeding to form a polaron with levels found approximately 0.5 eV from the top of the VB and the bottom of the CB. The removal of a second electron results in the formation of a bipolaron which is

energetically favourable in this system due to further relaxation of the structure. The associated energy levels for the formed bipolaron are about 0.75 eV from the top and the bottom of the VB and CB respectively. Upon the situation where the polymer is highly doped, bipolaron creation is driven forward with increasing energy levels for the charge carrier being formed and eventually overlaps to form bands within the polymers band gap with a band width of around 0.4 eV for the bipolaron bands. The band gap of PPy which was originally 3.2 eV becomes wider at 3.6 eV; however this is not of detrimental effect to the conductivity of the polymer as effectively the band gap is decreasing and this is due the bipolaron. These bands overlapping with the upper energy levels of the VB and the bottom energy levels of the CB upon high levels doping. Eventually a point is reached where the levels of doping causes the bipolaron bands to widen to the point where the emergence of the bipolaron bands with the VB and CB. In the case of *p*-doping this will create a half filled VB, which is comparable to the band gaps of metals and allows the material to display high conductivities. This is also the same scenario for solitons which upon high doping levels the soliton bands start to merge with the VB and the CB<sup>17,30</sup>.

#### 1.1.6.1 Solitons

Solitons are the charge carriers formed for polymeric materials where the geometry of the polymer in its ground state is degenerate as is the case of PA (*trans* isomer) where the energy of the dimerised polymer is the same for either state (Figure 16).

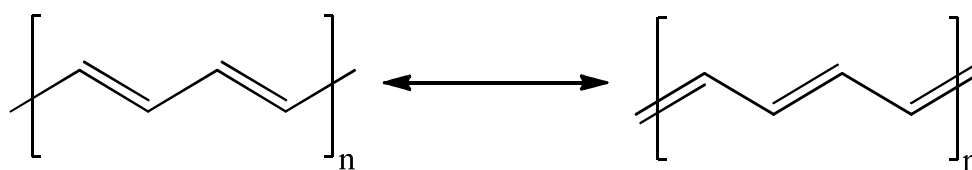


Figure 16: The dimerised degenerate ground states of *trans*-Polyacetylene.

In nature solitons are seen to be solitary, hence the term soliton, producing a solitary wave that can migrate across the whole chain without the deformation of the polymer or dissipation of the charge. A soliton is viewed as an excitation of the polymer system with little energy expenditure upon the exchanging of single bonds and double bonds between the carbons. It is produced upon the doping of the polymer causing a modification and relaxation of the conjugated polymers structure

producing two phases, phase A which the charged region and phase B which is the conjugated system.

A neutral soliton is often associated with polymers that contain an odd number of  $\pi$  bonded carbons within the polymer chain with the remaining unpaired  $\pi$  electron (radical) existing as the soliton. The neutral soliton is not localised to any one carbon in the long polymer chain but is rather idealised as being delocalised over the whole polymer chain, which at the edge/boundary of the soliton with the boundary between the distorted and the relaxed state potentially localising the charge. Structurally the double bonds get shorter and the single bonds get longer with the bond lengths equalising in the centre of the soliton. Experimentally the charge is reported to encompass 7 carbon units with the structural relaxation being over the 7 repeat units thus is thought to be delocalised. Effectively in terms of the band gap, there forms a mid-gap energy level between the valence band and the conduction band, which is half occupied by the unpaired electron in the case of a neutral soliton (Figure 17).

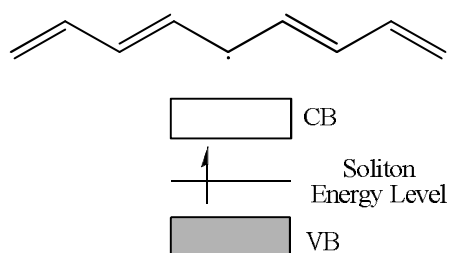


Figure 17: Neutral Soliton

In the case of negative and positive solitons (Figure 18) the energy level created is fully occupied for the negative soliton producing a spinless charge species and empty for the positive and thus creates a hole (electron hole). The charges are highly unusual as the neutral soliton (Figure 17) is half spin due to the presence of the radical and spinless in the cases of the positive and negative soliton<sup>4,17,30</sup>.

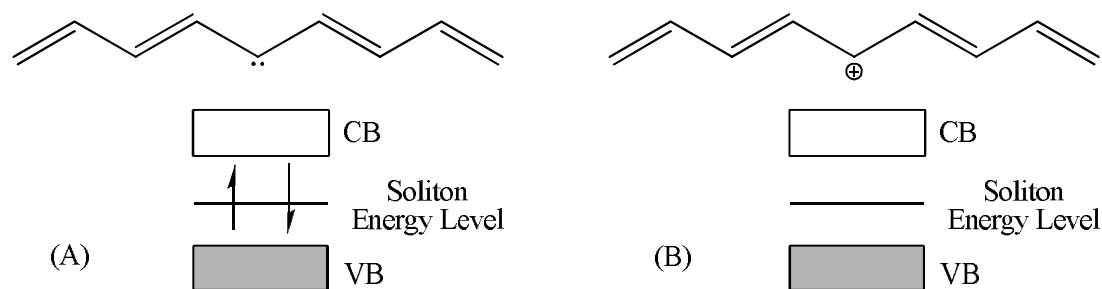


Figure 18: Solitons; A) Negative Soliton, B) Positive Soliton. Showing the mid-gap energy level between the Valence Band and the Conduction Band.

### 1.1.6.2 Polarons

A polaron is a radical ion which possesses the spin of a half and is associated with the distortion of the lattice distortion and the presence of a localised electronic state in the band gap (polaron state). It must be stressed that the formation of such a species does not correlate to the half occupancy of either the VB or CB but rather a new discrete level that is half occupied and is known as the polaron level<sup>30</sup>.

A polaron by chemical terminology is the radical ion which is created upon doping of a non-degenerate polymer, where no other electrons in the area are available for pairing and a noticeable relaxation of the polymers geometry. At higher polaron concentrations the polarons become mobile and pair up to become a bipolaron.

In degenerate polymers the pairing of these polarons become a spinless negative soliton, whilst in non-degenerate ground state polymers this pairing produces a dicationic charge transporter known as a bipolaron which has strong localised lattice relaxation both of which are responsible for the unusual electric, magnetic, and optical properties of the polymers.

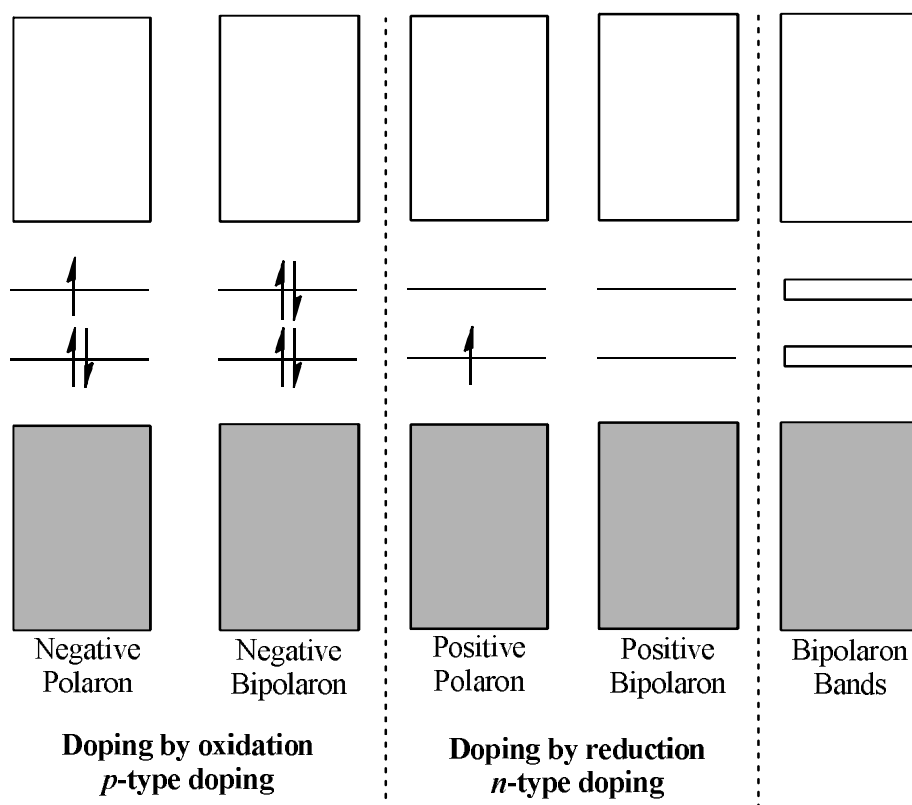


**Figure 19: Formation of Polarons, Bipolaron and Bipolaron Bands upon increasing doping levels. Most common method for obtaining these electronic species being via oxidation due to electron densities of the polymeric material.**

### 1.1.6.3 Bipolarons

It is more favourable to remove another electron from another part of the chain than from the polaron creating another polaron which results in the two polarons localising on different parts of the chain. A bipolaron is the accumulation of the two polarons both with half spin; the combination produces a di-ionic species which is spinless. The ionisation energy is further reduced post bipolaron formation, hence the species produces a more thermodynamically stable system, and is said to be more stable than the presence of two polarons, and this is despite the coulombic repulsion that would be present between the two similar charges. The presence of a bipolaron on the polymer chain causes two possible transitions in the band gap of the polymer; firstly the transition from the VB to the lower bipolaron energy level or the VB to the higher bipolaron energy level (Figure 19)<sup>30,31</sup>.

Lots of arguments have been raised as to whether the formation of a bipolaron is more favourable than the formation of two polarons. Conventionally it would be thought that the formation of two polarons would be more favourable due to the repulsion of the like charges and the coulombic effects. However one argument is

excellently presented which suggests that this is not the case. The coulombic repulsion in many cases is ineffective is due to the fact that upon the formation of the charge carrier, the structure changing from the benzenoid to quinoid uses stored elastic energy. If the bipolaron were to then separate the mechanical strain energy would cost the system more than the expenditure of the elastic energy, therefore it is more thermodynamically favourable for the like charges to remain together in the form of a bipolaron<sup>20</sup>. However in the case of PA in which its ground state is degenerate the separation of a bipolaron would be favourable as the distortion energy would not increase upon separation due to the energy either side of the charge being geometrically the same<sup>30</sup>.

#### 1.1.6.4 Charge Hopping.

Charge hopping is possible in conjugated polymers; however this is determined by several factors. Initially the polymer must show enough crystallinity and linearity in order for chain stacking to occur, this then leads onto the fact that the chains must be in close proximity to each other so that the charge is able migrate from one chain to the other. Finally the geometries of the distorted degenerate states and the relaxed charged state plays a key role, as the charge hop must be accommodated by the willingness of a chain to undergo relaxation. The energy expenditure of this process is seen to be negligible with the net energy expenditure being zero, however there is need for activation energy in order to promote the hopping of the charge in order for this to occur<sup>31</sup>. It is also reported that since most conjugated polymers are not crystalline the electrical conductivity of a finite chain requires charge hopping to occur in order for electrical conductivity<sup>20</sup> (Figure 20).

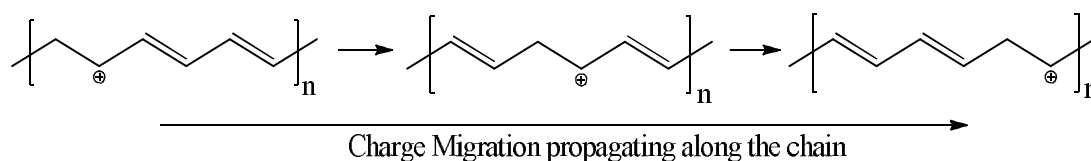


**Figure 20: Linear charge transport along the polymer chain.**

However depending on the proximity of the parallel chains (chain stacking) a charge migration to another adjacent linear chain has been postulated and can occur, this known as chain hopping (Figure 21). Largely dictated by the distance between the chains, such an event would most definitely further facilitate conductivity within the polymeric material.

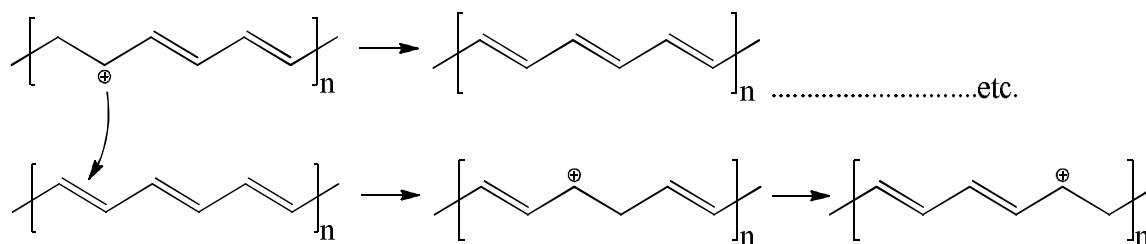


Figure 21: Charge Hopping between Parallel Chains.

Chiang et al.<sup>15</sup> provided evidence of such an interaction, in the case of polyacetylene, a proximity of 3.6 Å (36 nm), which in comparison to the carbon-carbon bond length for polyacetylene which is quoted at 1.4 Å (14 nm) (Figure 22) is relatively close and the potentially weak coupling has been inferred.

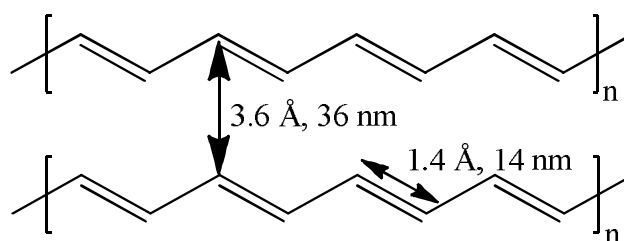


Figure 22: Intrachain carbon-carbon bond length and interchain spacing distance.

## 1.2 Polyaniline

Polyaniline (PANI, PAn) was first synthesised by H. Letherby in 1862, formed from aniline under mild conditions, a black powder is yielded resulting in being called aniline black. During this time the uses were not as significant as of present day, where it was used as the pigment within black ink and so was heavily used in the printing process, its other use of the time was in the dyeing process<sup>10</sup>. Upon further research in the early 1900's it was seen that PANI exists in four oxidation states. However research did not start to take off with regards to PANI until the 1980's<sup>32</sup>. In 1985 MacDiarmid and his research group, who with regards to the area of polymer science are well known for their research contributions within the field, they studied in depth aspects of the electric conductivity of PANI to which they found it was highly conductive under the right and optimised conditions<sup>9</sup>.

### 1.2.1 Properties of Polyaniline.

Polyaniline (PANI) and derivatives have been extensively studied as a result of their excellent physical-chemical properties, unique doping mechanisms, ease of

doping and reversibility which can be controlled by both protonation or charge transfer. The environmental stability in both undoped and doped forms make this polymer very important within the family of conductive polymers<sup>33,34</sup>, as they display different chemistry from other electro-active polymers, due to the presence of basic groups namely the amine and imine (depending on the oxidation state of the polymer). The reactive amine group (basic) at either side of the aromatic ring assists the high chemical flexibility of the system. Unlike other heteroatomic polymers the amines and imide in PANI are involved in the conduction mechanism and contribute to the  $\pi$  bonding<sup>35</sup>, with nitrogen participating in the overlapping of the  $p_z$  orbital's with the carbon, thus contributing in the formation of a conjugated system<sup>33</sup>. Another important reason for the huge interest vested into researching polyaniline is that other polymers have problems with stability and their processability, and therefore hindering the industry in terms of incorporating conductive polymers into devices and actually manufacturing such materials<sup>9</sup>. Polyaniline does not share such inherent problems that are encountered with many other common conjugated polymers, they are environmental stable in comparison to other polymers, processible, easily prepared, economically more viable over other polymers resulting from the low price of the monomer<sup>36</sup>, highly conductive and have reversible electronic properties.

Polyanilines (PANI) exists in three stable forms depending on its oxidation state; the fully reduced leucoemeraldine base (LB), half oxidised emeraldine base (EB) and the fully oxidised pernigraniline base (PB). The average oxidation states have been expressed as  $y = 0$ ,  $y = 0.5$ ,  $y = 1$ ; where  $y = 0$  is the totally reduced form of PANI,  $y = 0.5$  is the half oxidised form of PANI and  $y = 1$  is the totally oxidised form of PANI<sup>24,33,34,37</sup>. In terms of the structural and conformational changes the leucoemeraldine consists of amines attached to benzenoid rings, the emeraldine base consists of both benzenoid and quinoid rings present at ratios of 3:1 with the presence of imines and amines in equal quantities. Finally the pernigraniline form contains both benzenoid and quinoid rings at a ratio of 1:1, which are separated by imines<sup>24,33,38</sup> (Figure 23) and is interestingly analogous to *trans*-PA because it displays a non-degenerate ground state<sup>39</sup> it is found that each state can exist in a protonated salt form by treatment of base with acid e.g. emeraldine base and hydrochloric acid yields emeraldine hydrochloride or emeraldine salt. The different

forms each have different characteristic colours<sup>40</sup>. Worthy of noting is that whilst EB is seen to consist of both oxidised and reduced units, parts of the chain may be homogenous with regions which are representative of PB and other parts which are representative of LB. Both EB and LB have the ability to emit light, while it is expected for LB; electrochemical luminescence is not expected for EB since its oxidation state is not correlated with photoluminescence. However the hypothesis is that the electroluminescence is only possible if the oxidised quinoid and reduced benzenoid units are separate<sup>37</sup>.

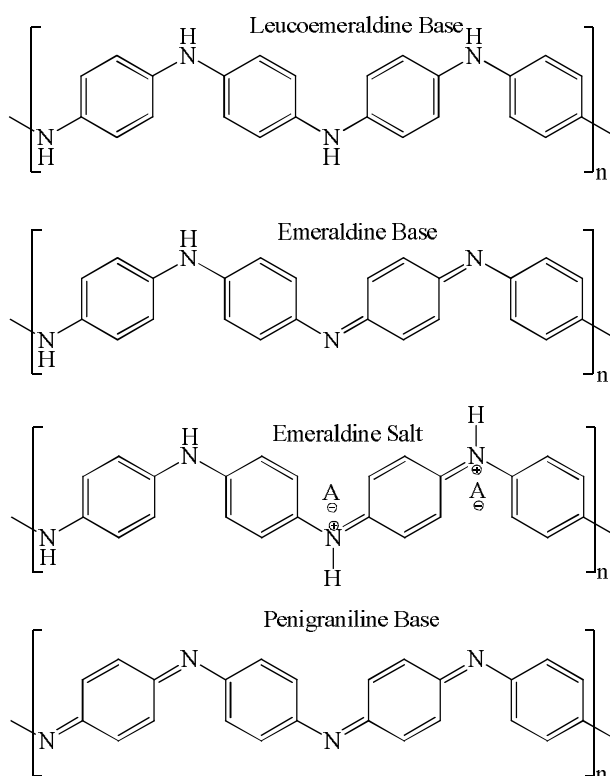


Figure 23: Oxidation States of Polyaniline<sup>3</sup>.

PANI shows insolubility in a range of solvents, thermal decomposition and immiscibility with other polymers. If it were to take liquid form it is conceivable that it would hold high conductivity analogous to mercury and redox properties. Due to its insolubility this material is difficult to disperse into solutions<sup>41</sup>. PANI is moderately soluble in polar organic solvents, such as DMF, DMA (*N,N*-dimethylacetamide), DMSO and THF<sup>34</sup>. PANI EB is insoluble in water, most mineral and organic acids and most organic solvents. However solubility is seen in concentrated sulphuric acid producing a purple-brown solution which upon the addition of water produces a green precipitant which is the ES (sulphate salt). In

solution the EB is violet blue or bright blue in cold pyridine or DMF. The EB forms a green solution in 80% cold acetic acid this presumably is in a doped state. The emeraldine salt characteristically is generally green in solution. The PB is the same as the EB, being blue in solution and forming blue salts whilst the only difference is that in 80% cold acetic acid the solution is blue as opposed to green which suggest that characteristically the salt is generally blue in solution<sup>42</sup>.

Production can be achieved directly produced by oxidative polymerisation of aniline producing the hydrochloride salt as a result of procedure. Stronger oxidation will produce the PB in protonated form which is blue and is expected to display conductivity and electro active properties. Upon the basic treatment of the penigraniline salt (PS) proceeds to a violet/dark blue PB form of PANI which is not conductive this transition occurring at a pH greater than 1. The ES variant converts to its blue non conducting counterpart with the transition when subjected to pH above 6-7. It should be noted that the PB and EB are visually distinguishable shades of blue. The reduction of PANI EB or ES results in a colourless solution of the non-conductive form LB<sup>40</sup> (Figure 24).

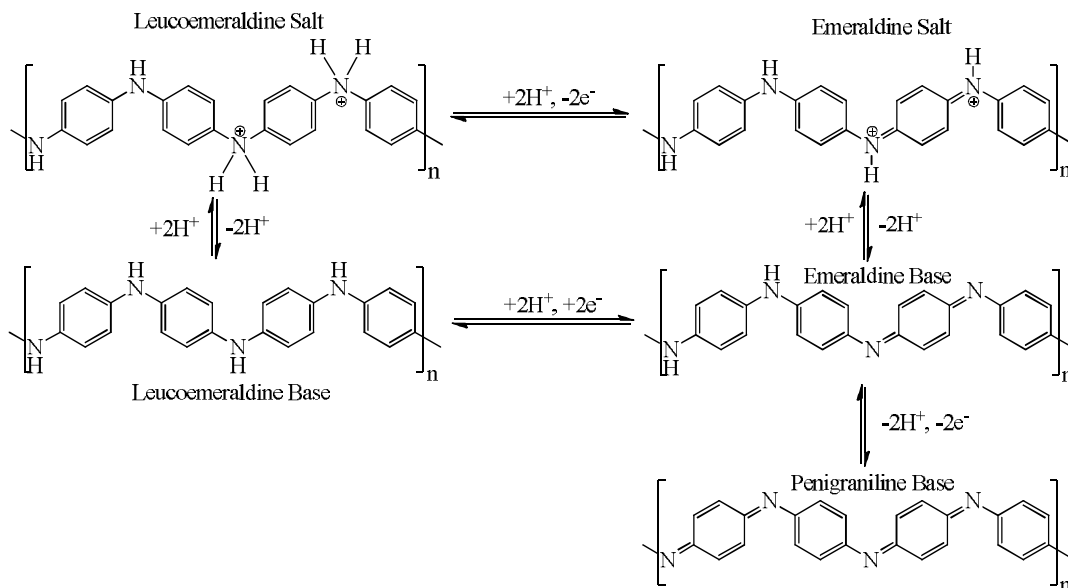


Figure 24: Electrochemical routes of obtaining PANI in different oxidation states.

This insolubility of PANI is the result of the inherent tractable properties and can be susceptibility to environmental degradation this also makes PANI unprocessable. The intractability is thought to be the result of the rigid polymer backbone, its high aromaticity and inter/intra chain hydrogen bonding. But upon the introduction of

bulky side groups and functionalised acids is seen to prevent PANI from contracting back on itself through steric hindrance with the functionalised acid counter ion inducing processibility, rendering the polymer soluble in non-polar or weakly polar solvents. It is important to notice that a bulky group alone will not necessarily render the polymer solvent into solution but the combination of a strong functionalised acid and the bulky side group. PANI-EB consists of a benzenoid diamine and a quinoid diimine repeating units. The EB form of PANI undoped is said to be only soluble in NMP regarding common solvents, selected amines and strong acids such as c. sulphuric acid<sup>43,44</sup>.

The electronic properties of PANI are controlled by changing the oxidation state of chain and by protonation of the imine nitrogen atoms, in addition it has in addition to excel/unique electrical, electrochemical and optical properties. It also exhibits good thermal and environmental stability in both base and salt forms<sup>43</sup>. EB conductivity is in the region of  $10^{-11} \text{ Scm}^{-1}$  to over  $1 \text{ Scm}^{-1}$  for the emeraldine salt<sup>34</sup>. The EB form of PANI is a semiconductor, upon its protonation of the imine nitrogen's (-N=) the conductivity increases by a factor of  $10^{10}$  going into the metallic regions of conductivities, obtaining  $10^1 \text{ Scm}^{-1}$  this despite the fact that the electron concentration remains the same contradicting previous ideas<sup>45</sup>. It has been suggested that the structure and conformation largely affects the conductivity and transport mechanisms of the polymer and PANI is no different. For example links have been connected between whether the PANI chain is in a tight coil structure or in an expanded coil and its conductivity, finding that a stretched orientated (expanded coil) film has dramatic effects on increasing the conductivity and increasing the interaction of PANI with other polymers making it suitable for blending<sup>46</sup>.

For the polaronic induced relaxation, the structure around the radical cation extends only into the middle of the phenyl rings at either side of the protonated nitrogen which is corroborated by X-ray Photoelectron Spectroscopy (XPS)<sup>45</sup>.

In the bipolaronic state the nitrogen which is protonated has a quinoid geometry with the bond lengths of the double bonds being around  $1.362 \text{ \AA}$  (136.2 pm), the single bonds ( $\sigma$  bonds) at  $1.474 \text{ \AA}$  (147.4 pm). The bond lengths around the nitrogen vary depending on the chemical environment in which they are in; double bonds of

nitrogen in the imine displaying a bond length of 1.343 Å (134.3 pm) and single bond of the nitrogen in the imine being of 1.407 Å (140.7 pm). The carbon-nitrogen bonds at either side of the nitrogen (amine) are of the length of 1.414 Å (141.4 pm). In the polaronic/bipolaronic state the C-N bonds are of equal length at 1.411 Å (141.1 pm). The benzene rings mainly adopt an aromatic geometry with the bond lengths of 1.440 Å (144.0 pm), 1.400 Å (140 pm) and 1.417 Å (141.7 pm) going away from the charged nitrogen. The torsion angles are found to be around 30° at the benzene rings with the nitrogen's being in the same plane<sup>45</sup>.

Out of all the oxidation states the LB form of PANI is the insulator with a large band gap between the  $\pi$ - $\pi^*$  bands of around 3.6 eV when measured in NMP and a band gap of 3.8 eV when the thin film is tested. The reason behind the large band gap is due to the benzene rings which are highly conjugated and connected by amine linkers, which are saturated. This affects the levels of conjugation by inhibiting the propagation of conjugation along the polymer chain, therefore localising the conjugation to the aromatic rings.

In vast contrast to this the fully oxidised PB has a much lower  $\pi$ - $\pi^*$  transition with the band gap reported to be between 1.7-2.3 eV. This is due to the allowance of conjugation to run through the entire chain due to the conjugated nature of the imine, producing a material which is semi conductive.

UV/Vis/NIR data shows that the emeraldine salt (ES) shows optical peaks at 2.8 eV and a broad peak at 1.5 eV which are interpreted as bands. The polaron bandwidth is quoted to be 1.0 eV<sup>45</sup>[43], which is attributed to the formation of low energy hole levels and the excitation of the polaron band. However some researchers suggest that the band gap for PB stands between 1.4-1.8 eV. Band gap determination of the ES is much more difficult to model due to the presence of polaron and bipolaron bands, but calculations have allowed for the prediction of the band gaps. With the excitation of the bipolaron bands being predicted between 0.4-0.65 eV and the excitation energy being predicted to be between 0.96-1.8 eV which is comparable with the experimentally obtained result of 1.5 eV<sup>47</sup>.

The band gaps for the infinite chains have been calculated by plotting the excitation energies against the inverse number of units and extrapolating to an infinite number. In LB the band gap is also determined by the levels of flexibility that

occurs between the phenyl rings and the amine linkage, thus the degree of planarity varies effectively distorting conjugation and increasing the band gap<sup>47</sup>.

### 1.2.2 Synthesis of Polyaniline.

Polyaniline is relatively cheap to obtain in its monomeric form with polymerisation occurring whilst it is in two states; either in its powder form it can be polymerised chemically, and in its thin film form it can be polymerised via electrochemical methods to produce one of the four states seen in (Figure 8)<sup>9</sup>.

The electrochemical method of synthesising PANI is the oxidative coupling of aniline and yields high quality films coating a platinum foil electrode (1 cm<sup>2</sup>), cycling the voltage from -0.2 to +0.75 V at approximately 45 cycles. This is conducted in a solution of 1 cm<sup>3</sup> aniline black and around 20 cm<sup>3</sup> 1M HCl producing a 200 nm thick film taking around 30 mins to achieve completion with the terminating voltage set to 0.4V which yields the half oxidised EB form of PANI. The film is progressively washed with 1M HCl to remove any excess aniline that may be present<sup>48,49</sup>

Several papers have outlined the synthesis of PANI, with each having slight variations, but the generally all the methods are the same. Aniline is dissolved into 1M HCl (aq) and stirred for between 30 minute and in some cases overnight at around 0°C. The polymerisation is induced upon the addition of ammonium peroxydisulphate ((NH<sub>4</sub>)<sub>2</sub>S<sub>2</sub>O<sub>8</sub>) which is 0.8 molar ratio to the amount of aniline. The product is the washed with 1M HCl (aq) and acetone successively. The mixture is then washed with 0.5M<sup>50</sup> or 5%<sup>51</sup> Ammonia solution to remove any doping effects the acid may have had, the mixture then went under further washes with water and acetone successively and the either dried under vacuum or is left remaining in the solution<sup>50-53</sup>.

### 1.2.3 Doping of Polyaniline

Like all other polymers PANI can be doped chemically, electrochemically, photo-doping and charge injection between the metal-semiconductor contact interface<sup>3</sup>. What sets it apart from other polymers is that it can be doped using oxidising species that transfer charge such as with protonic acids (Figure 24), which upon doping the number of  $\pi$ -electrons remains unchanged throughout the whole process.

So unlike other polymers which when doped have electrons removed or added to obtain unfilled bands, this is not the case with proton acid dopants<sup>3,54</sup>. The conductivity of PANI upon doping increases with a magnitude of  $10^{10} \text{ Scm}^{-1}$  to give a conductivity of  $1 \text{ Scm}^{-1}$  this being despite the number of electrons remaining the same<sup>45</sup>.

The above described method is *p*-doping; however it is possible to *n*-dope PANI using reducing agents. Hua et al. have shown that the use of strong reducing agents, namely KH and NaH will dope PANI when dissolved in DMSO, which is crucial to the process. The mechanism of doping occurs by the creation of a dimethyl salt (e.g.  $(\text{CH}_3)_2\text{SO}^- \text{Na}^+$ ), this salt is shown to remove protons away from the PANI chain, thus transferring and introducing a negative charge onto the PANI polymer backbone, which is counterbalanced with the sodium or potassium ion, whilst affording the DMSO. The hydrogen of the reducing agent and the removed proton are released as hydrogen gas which was noted during the investigation. Undoping is achieved by the addition of water, yielding a base (alkali) and a neutral PANI chain. The conductivity, when using this method occurs as a result of the reorganisation of the  $\pi$ -electrons, which produces a delocalised system of electrons<sup>54</sup>.

What is very interesting about the result of doping PANI is that it is found that a broad band is formed between the Valence Band (VB) and the Conduction Band (CB) as new energy levels are created, effectively narrowing band gap<sup>45</sup>. This again can be seen as a difference which truly puts PANI in a different class from other electro-active polymers.

However one of the major problems with the doping process of PANI is that upon doping the polymer becomes insoluble, even in organic solvents<sup>45,55</sup>. It was noticed that when PANI is doped with an acid the solubility decreased and so required the conversion to a salt to induce solubility into an aqueous medium<sup>45</sup>. The solution to this problem was quickly found, by the use of functionalised dopants such as sulphonic acids and its derivatives<sup>56</sup>; camphor sulphonic acid, tosic acid and dodecylbenzene sulphonic acid. dichloroacetic acid (DCAA) has also been promoted as another dopant that induces solubility<sup>35</sup>. Researchers have postulated that the introduction of a sulphonic acid to PANI will induce a reorganisation of

PANI's electronic structure which then forms into a polaronic metal, thus resulting in conductivity of around  $11 \text{ Scm}^{-1}$  at room temperature<sup>35</sup>.

The conductivity of PANI can be improved by doping with functionalised protonic acids such as, camphor sulphonic acid (CSA), tosic Acid (*p*-Toluene sulphonic acid, TsA), dodecylbenzene sulphonic acid (DBSA) and dichloroacetic acid (DCA or DCAA) to name but a few. The introduction of the sulphonic acids results in the reorganisation of the PANI structure to form a Polaronic metal. With direct current (DC) conductivities of PANI in the region of  $11 \text{ Scm}^{-1}$  when doped with sulphonic acids<sup>35</sup>.

The use of sulphonic acid dopants is seen to produce thermally stable forms of PANI as opposed to the case where HCl or acetic acid has been used as dopants. The conductivities for PANI doped with CSA or DBSA have been reported to be  $200 \text{ Scm}^{-1}$  and  $2 \text{ Scm}^{-1}$  respectively, suggesting a degree of self-ordering upon evaporation of solvent from cast films<sup>43</sup>.

Like other polymers PANI can be *n*-doped, utilising Potassium Hydride and Sodium Hydride in DMSO. The mechanism proceeds via the capturing of the reductants to form an active DMSO salt (e.g.  $\text{Na}^+\text{Dimsyl}$ ) with hydrogen production. The dimsyl salt is able to take the proton off of the PANI backbone, yielding DMSO. The negative charge is transferred to the polymer chain and is balanced by the counter cations (sodium or potassium). The unpaired electrons occur as a result of the reorganisation of the  $\pi$ -electrons in the benzenoid rings, the electrons are assigned to the Nitrogen atom eventually delocalising to form semi-quinoid units. The undoping of this is driven by the addition of water producing an alkaline solution such as Sodium Hydroxide, the proton of course is inserted back into the polymer chain. This method as a result show poor stability as moisture in the air may be enough to promote the undoping of the polymer<sup>54</sup> (Figure 25).

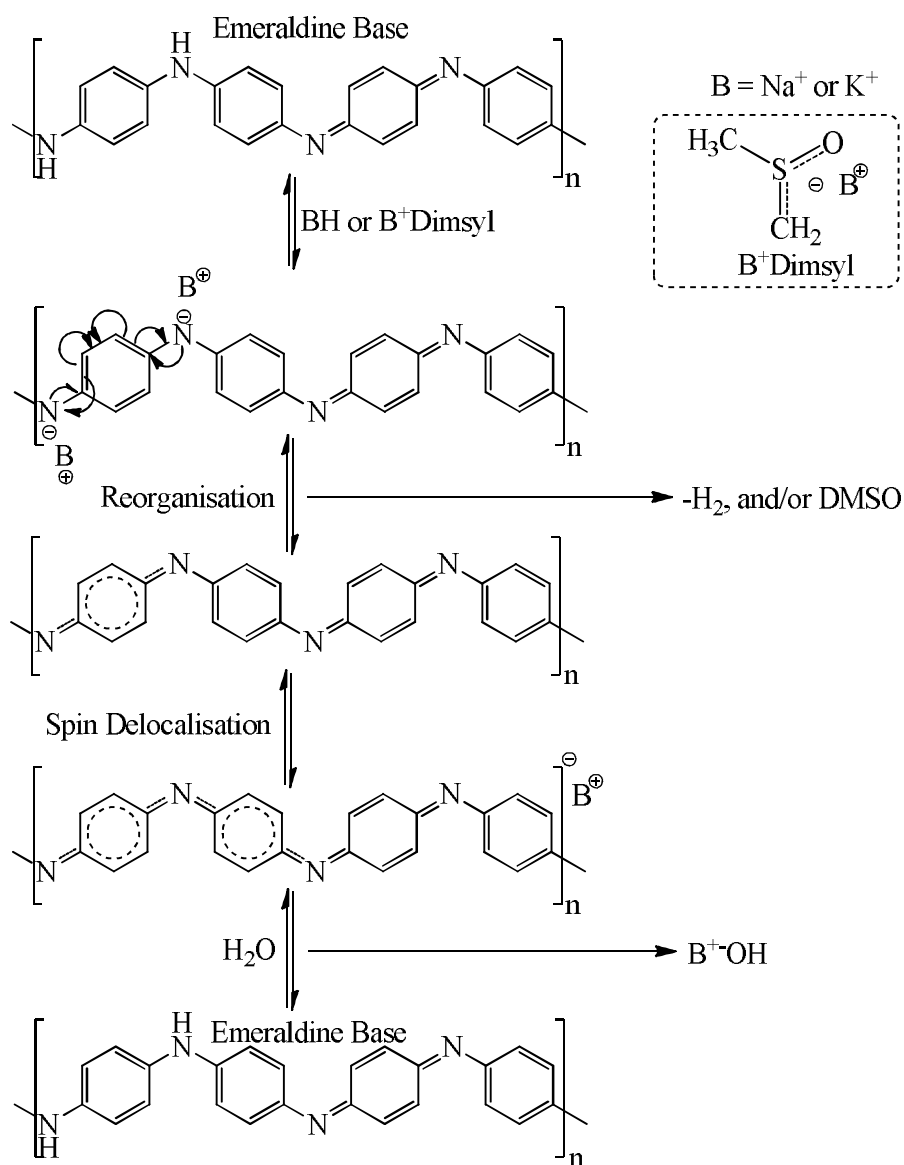


Figure 25: *n*-Doping of Polyaniline<sup>54</sup>.

Doping of LB to the ES can be achieved via oxidation (Redox methods), whilst the doping of EB to ES is conducted via the use of a protonic acid in both case the conducting salt is produced with conductivities reported as high as  $400 \text{ Scm}^{-139}$  and even  $10^4 \text{ Scm}^{-157}$ .

The conversion of the semiconducting EB to the metallic ES is achieved without any change in the number of electrons, therefore the electronic structure is converted to structure with a half filled band and metallic state where the positive charge and the unpaired electron is in the structure. The protonation of the imines converts the quinoid units into benzenoid units with an associated spin unpairing. The conductive salt blends have interestingly low percolation thresholds much

lower than the volume fractions required for activity in other classes of polymer blends with reports suggesting volume fractions typically in the region of 16% by volume are required for other conductive polymers in order for conductivity to be retained. In the case of PANI blends upon increasing the volume fraction above the percolation threshold increases the conductivity hence PANI blends can be reproducibly manufactured with the controlled levels of conductivity whilst retaining the desired mechanical properties<sup>16</sup>.

Oxidation (*p*-doping) the LB form of PANI involves the oxidation of both the  $\sigma$  bond and the  $\pi$  system in comparison to the typical mechanism characterised for other conjugated polymers which the oxidation solely occurs at the  $\pi$  system<sup>24</sup>.

The doping process of PANI principally occurs at the imine nitrogen and can be protonated throughout the whole chain or just in parts of the chain. The determining factors depend on its oxidation state, whether it is in the LB, EB or PB form and also the pH of the doping medium. The result is the formation of a polysemi-quinoid radical cations which are delocalised throughout the system<sup>7</sup>.

#### *1.2.3.1 Functionalised Dopants.*

Hydrophobic tails of DBSA strongly facilitate the solvation and dissolution of PANI into common solvents due to weak Van der Waal interactions. This is one feature that is heavily utilised due to its plasticising effects, enabling PANI to be easily incorporated into a polymer blend due to its increased processability which enables the introduction of PANI to materials such as polystyrene and polyethylene's which previously would not have been possible. This subsequently allows for PANI blends to be made more environmentally stable products with high mechanical integrity<sup>43</sup>.

Synthesis of functionalised sulphonic acids with large organic groups and side chains have allowed for an increase in solubility and processability making it possible for the production of uniform solvent cast films and allowed for the blending of PANI with other materials, with interestingly low percolation thresholds whilst retaining high conductivities<sup>46</sup>.

The uses of functionalised protonic acid dopants such as the range of sulphonic acids and phosphoric acid ester dopants have been sufficient tools to overcome the

issues of insolubility. One such researcher looking into the area of dopant engineering is Pron and his research group<sup>12,44,58,59</sup>. Looking specifically at functionalised Sulphonic acids and both aromatic and aliphatic phosphoric acid derivatives, these candidates have sufficiently plasticised the PANI into solution. One significant feature of all the dopants is that they are surfactant in nature, with a hydrophilic acid head group and a hydrophobic tail group. The result of the hydrophobic side groups of the dopant counter ion is increased interactivity with the solvent system, such as chloroform, alcohols and xylenes to name but a few. It is further noticed that upon functionalisation with large bulky side chains, the subsequent opening of the PANI chain is observed<sup>44</sup>.

#### 1.2.3.1.1 Secondary solvent doping effects

Through the process of studying dopants it is noticed that the solvents may play a part in the doping process. The solvents have been seen to facilitate the doping process and exacerbate the effects of doping; this has been identified as ‘secondary doping’. Such solvents have been shown to form a complex as is the case of m-cresol which shows a supramolecular complex between the PANI-dopant-solvent. Investigations of this effect have led to the discovery of solvents which have been identified as suitable candidates specifically for the doping process, in which the dopant and solvent form a complex, improving the mechanical and thermal properties, producing a much more metallic like polymer. This field of ‘dopant engineering’ is becoming rather large and is seen as a pinnacle process in order to obtain high conductivities in the polymer and specifically PANI<sup>29</sup>.

By definition the concept of secondary doping is upon the use of an inert substance (solvent) in combination with the dopant (primary tool for doping), causing the further changing of the electronic, optical, magnetic and structural characteristics than what would be produced by the dopant alone<sup>60</sup>.

In the case of m-cresol (MC) the interactions noticed between the PANI polymer chain, dopant and the solvent complex, promotes the opening of the tightly coiled polymer chain producing an ‘expanded/extended coil’ like chain, opening out the polymer chain with increased crystallinity and linearity. This increased linearity is shown to increase and facilitate the delocalisation of the polaron over the polymer chain. However in terms of safety, MC is thought to be carcinogenic and the result

is that many industries will not use such solvents. Therefore there is now research is placing emphasis on not only looking at dopant engineering but also looking into safer alternative solvents which will produce similar and sufficient effects on the polymer as what is produced in the case of using MC<sup>44</sup>.

By promoting the expansion of the coil like conformation, the defects exerted on the  $\pi$  system are actively reduced due to lower ring twisting. The subsequent effect of reduced conjugation defects acts to increase the conductivity with greater charge mobility<sup>60</sup>.

What is of extreme interest regarding the concept of secondary doping is that when films are cast from these solutions the polymer retains its crystallinity and associated properties post solvent removal<sup>60</sup>.

#### 1.2.4 Conduction Mechanism of Polyaniline

PANI particles when partially protonated in a suspension show polymer chain ordering upon the application of an electric field (voltage), becoming parallel to the field much like graphite and carbon black particles in suspensions forming semi-conductive chains in polarising fields<sup>40</sup>.

As a result of the mechanism of doping of PANI, in which essentially the number of electrons associated with the chain remains constant, the increase in conductivity can only be correlated to the systemic and structural modifications. The protonation of the imine produces a positive polaron and upon the doping of both imines in the oxidised segments of EB results in the formation of bipolaron, these distortions in the chain are then seen to migrate due to the chains vibrational energy and chain vibrations<sup>49</sup>.

#### 1.2.5 Uses of Polyaniline

Characteristically electro active polymers share the advantageous properties of plastics with the electronic and mechanical properties of metals upon specific scenarios, for example after doping, in which PANI is no different from the countless other conjugated and conductive polymers. These properties have been key to the development of a wide range of potential applications and has led to the introduction of the electro-active polymers in electronic devices, batteries, wiring,

selective electrodes, organic light emitting diodes (OLED's) and non-linear optics<sup>61</sup>, photo-imaging, electrochromic displays<sup>43,61</sup> and solar cells<sup>34</sup>.

Polyaniline is showing great potential for use in a wide range of applications, using both the doped (conductive) and undoped (insulating) forms<sup>50</sup>. One such application where it has a potential use of electromagnetic shield and static dissipation, due to high levels of electronic pollution caused by telecommunications, space technology, navigator technology and aircraft technology all of which may potentially cause interference. Current systems of shielding are metallic or magnetic materials possessing good mechanical properties but are cumbersome, heavy materials which can corrode and are not easily processed. Whilst in contrast PANI is lightweight, flexible, environmentally stable and resistant to corrosion and easier to process. One major advantage is the fact that not only do they reflect the electromagnetic energy but can selectively absorb at specific wavelengths, which is highly useful in military application regarding the absorption of a radar signal<sup>35</sup>.

One idea that has been postulated is the intricate use in the separation of gases such as the separation of air, in which the film of PANI produces molecular channels formed through controlling the doping of the polymer<sup>46</sup>.

Other major applications that papers have suggested and discussed is the use of PANI in lithium-PANI batteries<sup>62,63</sup>, organic light emitting diodes (OLED's) and non-linear optics (specifically the PB form)<sup>61,63</sup>, pH detector in pH sensors<sup>36</sup>, immune-assay conductometric sensors<sup>35,51,63-65</sup>, photo-imaging, electrochromic displays (specifically the use of LB)<sup>43,61</sup> and solar cells<sup>34</sup>.

### **1.3 Corrosion and the Use of Polyaniline in anti-corrosive paints.**

Corrosion is a major worldwide problem which is producing a cost of billions of dollars. The process of corrosion is defined by many papers as the unwanted chemical reaction that occurs when a material is exposed to corrosive environmental factors. This corrosion can occur with both ferrous and non-ferrous metals, although less so in non-ferrous metals. Current methods of protection rely upon the use of toxic and environmentally harming chromates and the zinc which also has its share of inherent problems. Governing bodies are placing pressure on the industry to produce much more environmentally friendly and less toxic

alternatives, and as a consequence interests and attentions have been turned to conductive polymers<sup>66-68</sup>.

### 1.3.1 Corrosion of Metallic materials.

By definition corrosion is defined as the gradual and progressive wearing of a metal or plastic materials by chemical or oxidative processes<sup>69</sup>. This event leads to a change and destruction of the materials physical and chemical properties, thus in the case of supporting structures such as buildings, in which the corrosion of metals in buildings may become unsafe, lack the strength for supporting and may be unfit for purpose, which is one of the reasons why it is costing so much as these materials need replacing upon heavy corrosion.

Atmospheric corrosion occurs when a liquid phase is adsorbed onto a metallic substrate or corrosive material, allowing the diffusion of corrosive species to diffuse through and react with the metal surface and is corroborated by the fact that the absence of water vapour pressure as in the case of low humidity, the rate at which corrosion occurs slows down to a point where no corrosion occurs at all<sup>70</sup>.

Corrosion of metals typically is heavily influenced by meteorological factors and climatic factors, such as relative humidity of the air (water vapour pressure), hours of sunlight, air temperature and the temperature of the metal surface, air velocity and movement. The relative humidity encompasses the frequency and duration of rain, fog or mists all allowing moisture to precipitate on the metal surface. However the formation of dew from fog and mist or high humidity appears to facilitate the concentration of corrosive agents on the metal surface whilst rain allows a means for corrosive agents to attack the metal surface, the surface water is constantly replenished and so has a washing effect. Subsequently the concentration of the corrosive species on the surface is reduced in comparison to water precipitation on the surface and therefore is seen as a less aggressive<sup>71</sup>. This however does not entirely take into account the fact that the rain may contain pollutants; such is the case as 'acid rain' in which the acid is in the form of sulphuric and nitric acid. Therefore rain may just be as aggressive as the formation of dew as the rain is constantly supplying the surface with corrosive agents. The rate of corrosion with regards to rain then becomes a function of the concentration of pollutants in the rain, the duration of rain and the intensity.

Adding further to this is the fact that in coastal areas there is a high chloride content as a result of sea spray, consequently as a result of this it may be postulated that the rate of corrosion is more likely to occur in tropical areas or regions where the climate is generally wet, due to high humidity in both cases and high sunlight hours and higher temperature averages in tropical regions. Such regions as the Caribbean Islands being classic examples, where the islands climate is hot, sunny, highly humid and has a high amount of coastline, elimination of any of the above factors should therefore inhibit the process with supporting evidence coming from the fact that in dry air such as the desert or the polar regions, where the relative humidity is lower than 30% corrosion does not occur<sup>69,71</sup>.

The main corrosive agents tend to be sulphur compounds, chloride ions, oxygen, water and nitrogenous compounds<sup>72</sup>. This process of corrosion is not just simply a matter of oxidation at the metal interface but rather is controlled by air pollutants such as sulphur dioxide and a range nitrogen oxides all of which are products of the industrialised world<sup>70</sup>. Layering of water acts as a 'sink' for the sulphur but of interest is that in the case of nitrogen compounds it acts as a barrier for different metallic chemical environments<sup>72</sup>. Some factors are actually synergistic, such as the corrosive agents needing water as a carrier medium which is evident when metal is immersed into deoxygenated water, no corrosion proceeds<sup>69</sup>.

The factors that affect corrosion need to be understood before dealing with prevention, it is said that many factors singularly and in collaboration induce the corrosion of materials; such as humidity, UV exposure, electrolyte concentrations, temperature, pH and chemical induced corrosion and pollutants in the air. The fact that corrosion occurs so readily is due to the thermodynamics of the process being in favour of the reactions, with a negative Gibbs free energy for the reactions of metals with water, oxygen and electrolytes, ensuring the reaction takes place. Therefore to prevent these reactions etc. is to create some method of barrier either a physical barrier or an electrochemical barrier. It is said that there are three methods of corrosion protection; a barrier method of protection, a sacrificial methods of protection (i.e. using zinc coatings) and the final method is to induce a passive layer onto the substrate which will inhibit the corrosion process. The latter two methods are seen as active methods of protection<sup>73</sup>.

### 1.3.2 Corrosion of Steel

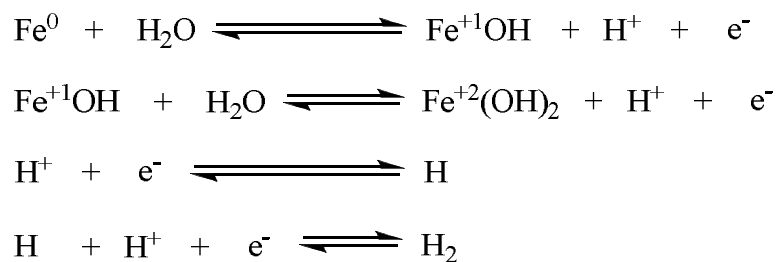
Carbon steel is one of the most important and vital metal used by man, it is of significant importance as being one of the major components of modern architecture due to its mechanical properties and structural integrity. However upon the oxidation of the material the properties are inevitably changed, with a reduction in the materials strength and integrity. The material becomes more susceptible to cracking due to its brittleness, just one of the property changes and characteristics noticed upon corrosion (oxidation) and is known as corrosion fatigue<sup>74</sup>.

The corrosion of Steel has been reported in many papers with the formation of a range of iron oxides as the end product for all corrosive agent attacks. In air, steel exposed to oxygen readily reacts and oxidises leading to the formation of a superficial oxide layer which is visually seen as rust. The oxidation due in air is a rather slow process, initially being quick with the formation of an oxide but the progression to other oxides are slow reactions with the outermost layer being iron (III) species (Equation 8).



**Equation 8: The oxidation of Steel (Iron) in Air producing an Iron (III) species (simplified)<sup>70</sup>.**

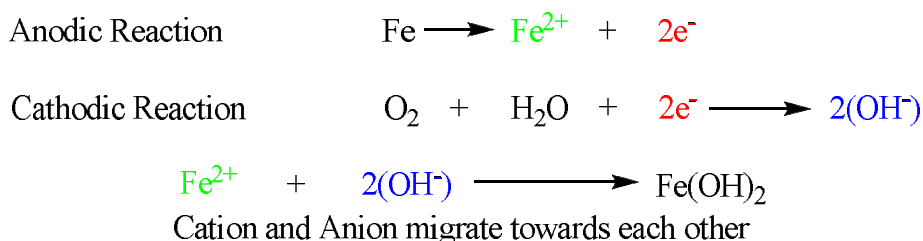
The production of hydrogen gas is also noticeable as a by-product of the oxidation of iron in the presence of water and other corrosive species (Equation 9).



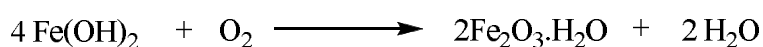
**Equation 9: Oxidation of Steel in the Presence of Water the production of hydrogen gas by-product<sup>70</sup>.**

Corrosion of steel can be seen as a electrochemical process involving the anodic reaction of the iron and the cathodic reaction of the oxygen, with the further oxidation proceeding to form hydrated ferric oxides ((Equation 10,Equation 11)<sup>69</sup>. It is later reported that for every 70mg/cm<sup>2</sup> of iron, there only needs to be 11mg/cm<sup>2</sup> of water and 30mg/cm<sup>2</sup> of oxygen. However in the presence of sulphur

compounds, Iron does not proceed to produce sulphates as is the case with copper and other metals but rather iron oxide hydroxides (FeOOH) where 1 mole of sulphur dioxide is enough to convert 60 moles of Iron to its oxidised product<sup>70</sup>.



**Equation 10: The electrochemical reaction of Steel (Iron) in the Presence of Oxygen and Water<sup>69</sup>.**



**Equation 11: Further Oxidation of Iron<sup>69</sup>**

### 1.3.3 Corrosion of Copper

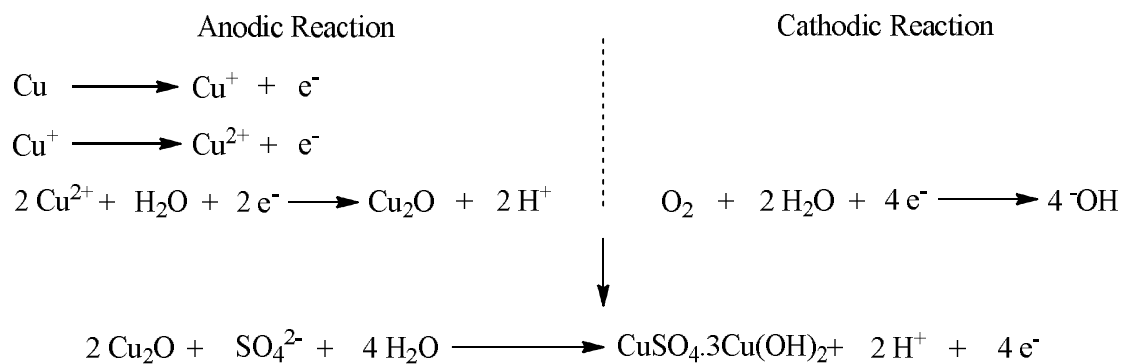
Copper much like iron has been utilised by mankind for thousands of years, for a broad range of applications and in particular for the manufacturing of tools and practical devices. In modern times and relatively recent the use of copper has expanded to uses in electrical applications for wiring, electronic components, use in communications, piping (plumbing), thermal applications such as heat conductors and heat exchangers. Uses have also been found for commercial applications such as the use in architecture and household products, and money production<sup>75</sup>.

Characteristically copper is pinkish-red and shiny in its free metal state and is noted for its very high conductivity and thermal properties. Visually copper is aesthetically pleasing to society in both pure form and in its associated corroded form, where it has been extensively used for buildings and sculptures. The corroded form, known as patina is often green-blue in colour and shows high resistivity to environmental conditions in comparison to its free form.

The corrosion of copper is quite often seen as being unique; the exposure of copper to air produces a material that gradually goes from the pinkish-red (salmon) colour to a brown which gradually darkens. Further exposure produces the green patina which is often seen to take anything from 5 to 60 years to form, but in dry environmental conditions can take a lot longer to form, to such that it is not uncommon to see roofs of houses in places such as Australia where the copper

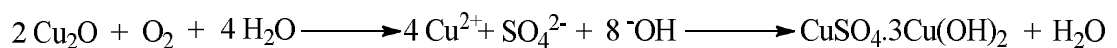
patina has not fully developed leaving the roofs dark brown<sup>76</sup>. Typically it is noticed that the patina consists of two layers; a copper oxide ( $\text{Cu}_2\text{O}$ ) layer known as cuprite, which is normally a dark brown layer around 5 -10  $\mu\text{m}$  thick at the metal interface. Secondly there is a porous external layer which resides on top of the cuprite layer. This layer is typically composed of either; basic copper sulphate,  $\text{Cu}_2\text{SO}_4(\text{OH})_6$  (bronchantite), the basic chloride form  $\text{Cu}_2\text{Cl}(\text{OH})_3$  known as actamite. Both of which form a greenish-blue layer at around 5 – 40  $\mu\text{m}$  thick, the latter is generally found mainly in marine geographic and coastal locations<sup>76</sup>.

The formation of patinas is generally observed when the copper and its oxide are constantly wet or in a humid environment producing the classic patina, whilst the dry environment forms the copper oxide. This is thought to be linked to the absorption of sulphurous air pollutants ( $\text{SO}_2$ ) (0.1 – 15 ppm) supplied to the wet surface allowing the oxidation to take place, forming an acidic surface which is rich in sulphates. As with most other types of corrosion the reaction is seen to be an electrochemical reaction with anodic and cathodic reactions taking place (Equation 12) as can be seen the copper is oxidised whilst water is reduced leading to the formation of Bronchantite<sup>76</sup>.



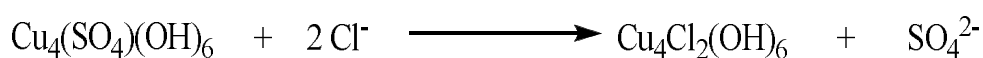
**Equation 12:** The electrochemical reaction of Copper in the presence of Sulphur containing corrosive species, initially forming the oxide and proceeding to form the patina<sup>76</sup>.

This process is corroborated by experimental findings where upon the treatment of the oxidised copper with sulphuric acid the end product remains the same as that predicted (Equation 13)<sup>76</sup>.



**Equation 13:** Formation of Sulphated patina in the presence of Sulphuric Acid.

In a marine environment the corrosion is generally a result of the presence of chlorides, present in marine aerosols. Taking Cuba for example, whose climate is classified as tropical, with annual mean temperatures of around 30°C and consisting of a high salinity coast (33% - 37%), along with the fact that the island has strong mass of air movement allows for increased sea spray and aerosols. The aerosol is noticeably sufficient to produce patinas solely of copper chlorides (Equation 14). This process is thermodynamically favourable with a Gibbs free energy of  $\Delta G^\circ -3.9 \text{ kJ mol}^{-1}$ , and also there is inference that the formation of sulphated patinas facilitates the formation of chloride patinas<sup>75</sup>.



Equation 14: Formation of Chloride Patinas.

### 1.3.4 Corrosion of Aluminium

Generally in nature aluminium is a shiny silvery grey metal that can appear dull in some instances and is relatively light weight, soft, malleable and ductile in comparison to other metals with similar properties such as copper. In its free metal state, aluminium is highly reactive chemically but in alloys and oxidised states as found in nature is relatively inert to environmental factors.

Aluminium and associated alloys like steel have found a niche in modern society, with its use in the aerospace industry as fuselages, used in nuclear reactors, surface coatings, metal/air batteries and many commercial applications such as beverage containers a results of the relative inertia and processability in specific forms making this material fit for purpose<sup>77</sup>. Aluminium also finds uses as an alternative to other metals of similar properties, when the other material is less advantageous or is not fit for the application. Such is seen with aluminium being used as an alternative to copper for transporting electricity across the country (National Grid). Copper is seen to be too heavy to be supported by structures when suspended and the likely results is the collapse of the supporting structure or more dangerously the trough of the suspended wire may be to such an extent that in may come in contact of close proximity to other structure and the electricity is likely to arc, provided there is enough potential difference (voltage) to earth via such structures.

In air the free metal readily oxidises with air to form its associated oxide (aluminium oxide), this often renders the metal inert and chemically stable, however what is of interest is that the oxide layer is an excellent protector against corrosion and is a sufficient protection barrier than the metal itself. Upon the formation of the oxide layer, this process is known as passivation (Equation 15), the rate at which oxidation continues to occur is significantly lowered.



**Equation 15: Passivation of Aluminium, leading the formation of Aluminium Oxide (Alumina).**

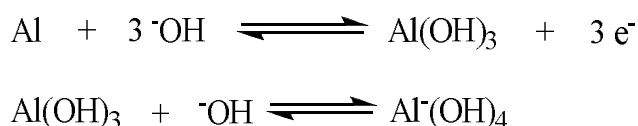
Aluminium oxide is highly stable in terms of its thermodynamics when in neutral environments and has good adherence to the metal surface. However in acidic or basic environments the aluminium is readily reactive and can be dissolved into solution depend on the pH of the solution, the end result is the existence of aluminium in several oxidised forms;  $\text{Al}^{3+}$ ,  $\text{Al}^{2+}(\text{OH})$ ,  $\text{Al}(\text{OH})_2$ .

In basic solutions the reaction is seen to be very fast, with the dissolution of the metal and the electrochemical formation of aluminium hydroxide films, further progression leads to  $\text{Al}(\text{OH})_4^-$  which terminates any further reaction and is reported to be the only stable form of aluminium in a basic solution. During the process hydrogen gas is released as a side product suggesting that the corrosion occurs via water reduction (Equation 16)<sup>77</sup>.



**Equation 16: The corrosion of Aluminium in a basic solution.**

However Zhang et al.<sup>77</sup> Make reference to reports that the formation of the aluminates occurs via intermediates (Equation 17).



**Equation 17: Corrosion of Aluminium via intermediates.**

This therefore suggests that as with the previous hypothesis, that the reaction is both partially anodic regarding the electrochemical formation and dissolution of the film and partially cathodic regarding the reduction of the water.

The oxide film also is an insufficient barrier against such attack and is also seen to dissolve in basic solutions yielding the same products as previously mentioned (Equation 18), this reaction however is far slower than the reaction of the free metal in a basic solution<sup>77</sup>.



**Equation 18: Corrosion of the Aluminium Oxide (Alumina) in a basic solution.**

The rate at which the corrosion occurs is determined by several factors ranging from pH, temperature and properties of the solution to the exposure time and the type of corrosive species, with activation energy for corrosion calculate between 12.3 – 13.7 Kcal mol<sup>-1</sup>. For example in the case of sulphurous corrosive species, in the case of these the absorption onto the surface, the production of a molecular layer reduces further corrosion caused by the sulphur species<sup>70,77</sup>.

### **1.3.5 Use of Polyaniline in anti-corrosive paints.**

Since D. DeBerry 1985 found that coatings of polyaniline (PANI) onto corrosive materials inhibited the process of corrosion, research into the applications of conductive polymers (CP) as inhibitors of corrosion has become a broad area, with many papers reporting data. PANI is seen to be at the frontier of this research due to its advantageous properties over other polymers of its class (i.e. conductive polymers), properties such as its redox properties, protonic acid doping, low cost of starting materials, low cost synthesis and its resistance to environmental degradation<sup>78</sup>. However this polymer is not without inherent problems, such as issues with the solubility of PANI into organic solvents, which leads on to the other problem of processability.

Lots of papers have been dedicated to explaining the process by which corrosion protection occurs. Commonly it is agreed that PANI possesses the ability to passivate (induction of oxide layer) a metallic substrate, which creates a protective barrier that inhibits corrosion of the material, but what is still argued is how.

Currently PANI has drawn major attention regarding its application in anti-corrosion barrier on carbonaceous steel. one such example is the coating of marine vessels metal body to prevent the fouling caused by marine organism<sup>50</sup>. The efficiencies of anti-corrosions barriers have been shown by Talo et al. who investigated the effectiveness of the emeraldine base as a protective coating, showing that acid (HCl), base (NaOH) and salt (NaCl) solutions did not induce corrosion of metal, even after damaging the barrier by drilling holes and the barrier was still effective against basic and brine solution. Analysis of the film by X-ray Photoelectron Spectroscopy showed that at the metal-polymer interface, a film (metal oxide) had developed, thus it was suggested that the emeraldine base had acted as a redox catalyst producing the metal oxide<sup>3,79</sup>. However debate is still active as to whether PANI provides the best and optimum level of protection over other available electro-active polymers<sup>3</sup>.

#### *1.3.5.1 Mechanism of protection.*

With regards to PANI the method of protection is as a result of passivation. The interaction is reported to be as a result of the electron rich metallic surface donating electrons into the LUMO (lowest unoccupied molecular orbital) of the polymer producing a 'pi-acid', producing a positively charged surface. The presence of the conductive  $\text{Fe}_3\text{O}_4$  and the semi-conductive  $\text{Fe}_2\text{O}_3$  being present results in a charge build up at the interface of these compounds. Subsequently the  $\text{Fe}_3\text{O}_4$  is electron deficient, therefore the chemical potentials change, which results in metals inability to oxidise any further and the charge build up at the interface prevents the diffusion of ions, therefore preventing corrosion<sup>80</sup>. What is very interesting is that even when scratches and patches are missing and metal is exposed to corrosive factors, the PANI layer aids in re-passivating the area and thus 'heals the metal surface'. Later the same paper describes the passivation to be cyclic, when the Emeraldine base (EB) form of PANI is presented to the surface of the metal, passivation proceeds (oxidising the surface), which reduces PANI to its Leucoemeraldine base (LB). In turn air then oxidises the PANI back to the EB, which is then available for further oxidation, therefore a metal oxide barrier should always be present and is the most likely explanation for the re-passivation of metals in exposed areas<sup>81</sup>.

Little discussion is made regarding what oxidation state PANI should be, when presented to the metal surface in anti-corrosive paints, whether as a base or as a

conducting salt. Both have supporting evidence for their use, in the case of undoped PANI (EB form), the corrosion protection is less effective, however upon a pre-treatment step using phosphoric acids or chelating agents it is seen that electrostatic interactions occur between the metal and PANI coating (Figure 26)<sup>81</sup>.

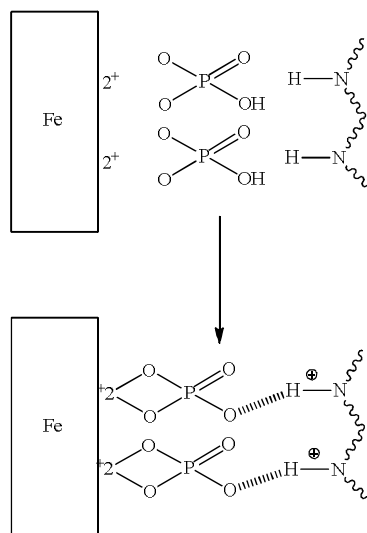


Figure 26: Electrostatic interaction at the Metal/PANI interface<sup>81</sup>.

However doped PANI is suggested to decrease the permeability of ions upon increasing the level of doping in the polymer<sup>80</sup>. Further support comes from the fact that one of the present commercially produced anti-corrosive paints utilising PANI (CORRPASSIV<sup>TM</sup>) is used in a doped form.

#### 1.3.5.2 Solubility issues and possible solutions

Solubility is one of the major issues that plagues PANI and has subsequent effects on the processibility. The two methods of applying anti-corrosive coatings are electro-deposition and solution cast (i.e. paint), however it is hindered by the fact that it is not suitable for large scale production therefore it is crucial that the solubility of the polymer is optimised<sup>78</sup>. The incorporation of functionalised dopants has been shown to induce solubility into organic solvent<sup>82</sup>. Most commonly used acids are Phosphoric acids and sulphonic acids; namely camphor-sulphonic acid (CSA) and dodecylbenzene sulphonic acid (DBSA). Cross linkable dopants will aid the dispersity, creating networks within the resin, leading to increased adhesion of the doped polymer with the substrate. However PANI has some degree of solubility with the most referenced solvent being *n*-methyl pyrrolidone (NMP), although other solvents have been mentioned such as xylene,

tetrahydrofuran (THF) and dimethylsulphoxide (DMSO) solubility is still problematic with these solvents. The blending of PANI with another polymer may offer another method of inducing solubility, and can be further progressed to polymerise the monomers within the resin matrix itself by electrochemical polymerisation<sup>78</sup>. The addition substituent's onto the polymer shows promising results, not only making PANI more soluble, but enabling PANI to solubilise in aqueous medium such a substituent have been incorporated (poly-*ortho*-ethoxyaniline), additions have been achieved in equal to the resin<sup>67,68,78,80,83</sup>.

### *1.3.5.3 Matrices, and their properties*

In terms of the resins systems, many resins are suggested, polyvinyl-pyrrolidone (PVP), epoxy resins (aqueous) would render the polymer water soluble, polyvinylchloride (PVC), alkyd, polyurethane, latex, polyvinyl acetate, nylon, polystyrene<sup>78,80,82,83</sup>. However the most discussed are epoxy resins and polymethylmethacrylate (PMMA) resins<sup>84</sup>. Epoxy resins have been described as showing excellent adhesive properties, mechanical properties and high levels of resistance to harsh environmental conditions such as humidity<sup>68</sup>. It is also interesting to see that CORRPASSIV™ uses epoxy resins as a topcoat adding a physical barrier which will protect the primer PANI coat and to ensure that the PANI coating is firmly adhered to the substrate, further to this is that pigments used within the paints actually decrease the porosity of the resin upon drying, which in itself is potentiating the resin as a physical barrier<sup>83</sup>. Many percolation thresholds have been suggested but it is interesting to see that the thresholds are all low with both conductivity and anti-corrosion seen at levels ranging from 0.007 wt% up to around 5 wt% for the resins described<sup>78,83,85,86</sup>. Dispersity within these resins is said to be good with particle sizes no bigger than 100 nm, in which ideas have been proposed to suggest that particle size should be no bigger than 100nm<sup>84</sup>, mixing by mechanical stirring or dispersion into a solvent will ensure homogeneity of the mixture<sup>83</sup>.

Other additives that are suitable to be used with PANI in paint formulations are organic waxes, cellulosic material, polyamides and synthetic polymers, these increase the malleability of the PANI-Resin mix<sup>87</sup>.

#### *1.3.5.4 Current corrosion protection paints utilising PANI.*

Current products, namely CORRPASSIV™ are available from Ormecon, it is one of a small number of paints that utilise the anti-corrosive properties of PANI. The paint is applied in two parts, the primer coat which contains the PANI and the top coat which is an epoxy resin. The PANI is present in the form of its emeraldine salts (ES), thus is doped, however the dopant is not disclosed but other components are present in the quantities of:

- PANI; should be no lower than 3% as the anti-corrosion effects are poor below this level but no higher than 49% as there is no benefit from higher percentages and the films are likely to phase separate.
- 1 -47 wt% dopants
- Resin matrix; a maximum of 86% is stated as above this the anti-corrosive properties are reduced, but proportions no lower than 40% as adhesion decreases lower than this point. Epoxy resin, polyurethanes, acrylic and cellulose acetate propionate, is indicated and that these can either be used alone or as a mixture.
- A maximum of 47 wt% additives, high amounts reduces adhesion.
- Extenders are no higher than 15 wt% but no lower than 5 wt%, with talc and clay being suggested.
- Solvents should be no more 56 wt%, with alcohols, ketones, xylene and toluene being suggested.

It is suggested that the top coat is to always be used with the primer coat as it will add protection to the primer and to 'improve the anti-corrosion effects', the proportions and constituents are as follows:

- A matrix resin similar to previously with a maximum of 89 wt%, it is stated that epoxy or polyurethane resins are used.
- A maximum of 54 wt% pigments.
- A maximum of 50 wt% additives, inc. wetting agents, anti-settling agents, defoamers and anti-decolourizing agents amongst others.

- Max of 54 wt% of solvents with the same solvents as previously stated, for the primer.

Further and full information can be obtained from <http://www.freepatentsonline.com> the patent number is 675612.

## Chapter 2 AIMS AND OBJECTIVES

### 2.1 Purpose.

In recent years demands placed on polymeric materials have become more and more prominent due to their versatility, durability, physical properties, chemical properties and the fact that such material can be used for most things. Just looking around most of the objects seen are made of or in part contain some components of a polymeric nature; clothing made from manufactured fibres of polyester and polyamide, mobile phones made from thermosetting plastics and even cars that were once bulky, heavy metallic machines are now made from polymeric carbon fibres which lighter than metal but just as strong. Just on the horizon (2013-14) OLED's (Organic Light Emitting Diodes) are about to change the home entertainment industry by the advent of OLED televisions, showing very promising results of thinner screens, higher definition of picture quality and even curved screens. Another promising field is the role of PANI (polyaniline) in the inhibition of corrosion of metals such as steel, copper and aluminium.

The discovery that conjugated polymers intrinsically possess semi-conductive qualities in their neutral ground state. Efforts have been made to develop polymers that possess greater and broader electronic properties. The conception of the principles of doping and the implications it makes have spawned a gyration in the research of conjugated polymers. Interests are now being turned from the broader nature of conjugated polymers to strictly looking into the development of polymers with higher intrinsic electro active properties showing greater potentials than their predecessors. At the centre of this drive, the core concept and central theme is placed on the research of new novel doping agents and new methodologies of doping and dopant delivery, which are seen to be crucial to progression of the next generation conductive polymers and their development. This has therefore propelled research into developing new polymers for new and broader applications by looking at the chemical engineering of existing conjugated polymers and developing new polymeric systems which can be characterised by their higher intrinsic conductivities.

### 2.1.1 Polyaniline and doping

Polyaniline, which once was thought of as being useless and uncompromising, is showing promising results. Such as how the intrinsic conductivities can be altered to make the material conductive, it is also seen to exhibit certain levels of corrosion protection when in contact with metallic material; this leads to seeing cutting-edge potential uses of these materials. Nowadays works to improve the physical and chemical properties are currently in motion that are directed at changing the processing of the material and sculpting the material to the desired needs, thus it is important to look at tweaking polyaniline and making it a more manageable material. Physically polyaniline in its native form is insoluble in common solvents, so the first hurdle and subsequently the initial focus is to render the material into a form that is soluble in common solvents, increasing the conductivity, better adhesion, increased dispersity which would lower percolation thresholds and the morphology of the material when creating thin films, creating much more uniform structures of the polymer and finally narrowing the band gap of the polymer by means of creating intermediary bands between the valence and conduction bands.

### 2.2 Proposal

For this project a collaboration and coordinated effort has been set up between the Iraqi group of the University of Sheffield and the chemical industrial giant ICI (now Akzo Nobel). The union initially set out with the aims of designing and developing electrically conducting polymers, with exploration into of their use as a matrix for silver particle filled adhesives. Incorporating the polymer into a resin with the silver particles in a bid to create an electronic component that displays enhanced electrical conductivity, with reduced levels of silver particles which will effectively reduce the expense, whilst maintaining good adhesive properties.

Currently these adhesives use non-conductive polymers as a matrix and thus the conductivity is limited and impeded, with the conductivity only achievable through the direct connectivity of the silver particles and the interfaces at either side of the adhesive.

The initial outline and mandated objectives were to develop a system with high electrical conductivities, aiming for conductivities of  $200 \text{ S cm}^{-1}$ , that are highly processible, thermally stable up to  $300^\circ\text{C}$  and finally with the incorporation of functionalised protonic acid dopants that are functionalised and have the potential

of cross linking, forming an integral part of the resin network. This would be achievable by the design and development of a range of sulphonic acid derivatives and phosphoric acid diesters with functionalised side groups capable of forming cross linkages with the resin whilst simultaneously doping PANI. The research will focus on investigating the required levels of the dopants in various proportions to PANI in order to determine; firstly, looking at optimal doping levels, whilst looking secondly at the processibility, thermal stability, adhesive properties and electrical properties of the material at the different doping levels.

However during this project ICI had been acquired by Akzo Nobel, whose company directives, objectives and aims are directed towards research and developing formulations for paints, thus the aims and objectives of this project inevitably changed direction with the core aim of designing and developing electro-active and conductive polymers for incorporation into paint formulations. The project will now explore the use of doped PANI and their use as the active ingredient of anti-corrosion paints formulations, in order to enhance current anti-corrosion paints that are currently on the market with the aim of complimenting and even replacing current paints for such jobs.

The main objectives had some cross over with the previous project objectives, so the polymer of choice remained PANI due to the amount of literature available around the discussion of PANI and its anti-corrosion properties. This encompassed looking at their processability and electro-activity and would be achieved by the preparation of processible conductive PANI and its incorporation into a resin system in order to provide a method of protection and active barrier for metallic substrates, which are susceptible to corrosion under normal atmospheric and environmental conditions. The long term objective and aim is for the integration of these materials into industrial applications, from use of coatings of marine vessels to the commercial application to architectural structures.

This was approached in three phases; **Phase one**, focusing on the development of a range of functionalised dopants, to be used subsequently for doping PANI and carried out investigations into the effects that these dopants on PANI in the terms of changes in physico-chemical properties, which were analysed by performing UV/Vis spectroscopy upon the samples to determine if the dopants create changes

in the oxidation states of the material; **Phase two**, was to perform the accelerated corrosion tests to investigate the effectiveness of the doped PANI on inhibiting the corrosion of steel and copper tablets, this will be conducted in a Heated Propagator. Finally **Phase three**, was to look at the morphology of the films produced when incorporated into resin matrices at different proportions and how it affects the surface of the metal, this will be determined by looking at the metal surface at the microscopic level by Scanning Electron Microscopy.

### 2.2.1 Phase One: The Development of Functionalised Dopants.

The aims of the first phase were to develop a range of protonic acids based on analogues of benzenesulphonic acids and phosphoric acid diesters as set out by Prón et al<sup>88-90</sup>, these have been reported to successfully dope PANI into a conductive form and broadening the use and applicability of this material. Similar approaches have been implemented by several different researchers<sup>44,91-98</sup> through numerous studies, showing that sulphonic acids and phosphoric acid diesters were sufficient agents for not only doping PANI but also for their plasticising effects they have on PANI, rendering what was previously insoluble material soluble. The investigations found that the acids were surfactants (amphiphilic) in nature with the hydrophilic head (acid) group and the hydrophobic tail group which are crucial to the function of plastification of the material. The benzene ring is shown to stabilise the polymer in solution by promoting an uncoiling of the chain, allowing for greater interactions of the PANI with the solvent.

In previous work conducted within the Iraqi group, synthesis of maleimide, epoxy, hydroxyl and acrylate functionalised side chain sulphonic acids has been successfully conducted and has shown similar observations to the reported findings in the literature<sup>88,99,100</sup>. However the hydroxyl and acrylate functionalised sulphonic acids require further investigation through dopant studies and optimisation of the synthetic methodology. The dopants synthesised were analogues of dopants created in the references above. These were namely 4-sulphophthalic acid derivatives (Figure 27)<sup>99,100</sup> and 5-sulphoisophthalic acid<sup>88,92,101</sup> derivatives (5-sulpho-i-phthalic acids, SIPA). This research will look into developing further derivatives of 5-sulphoisophthalic acid and to develop a new series of phosphoric acid diesters, including dopants already documented in literature (Figure 28).

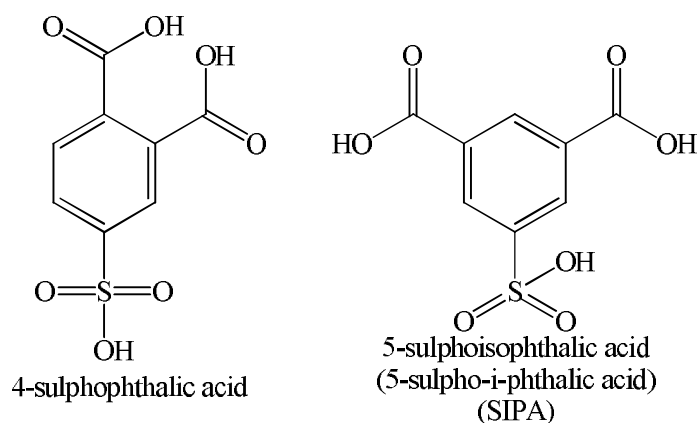


Figure 27: Structures of 4-Sulphophthalic Acid and 5-sulphoisophthalic acid.

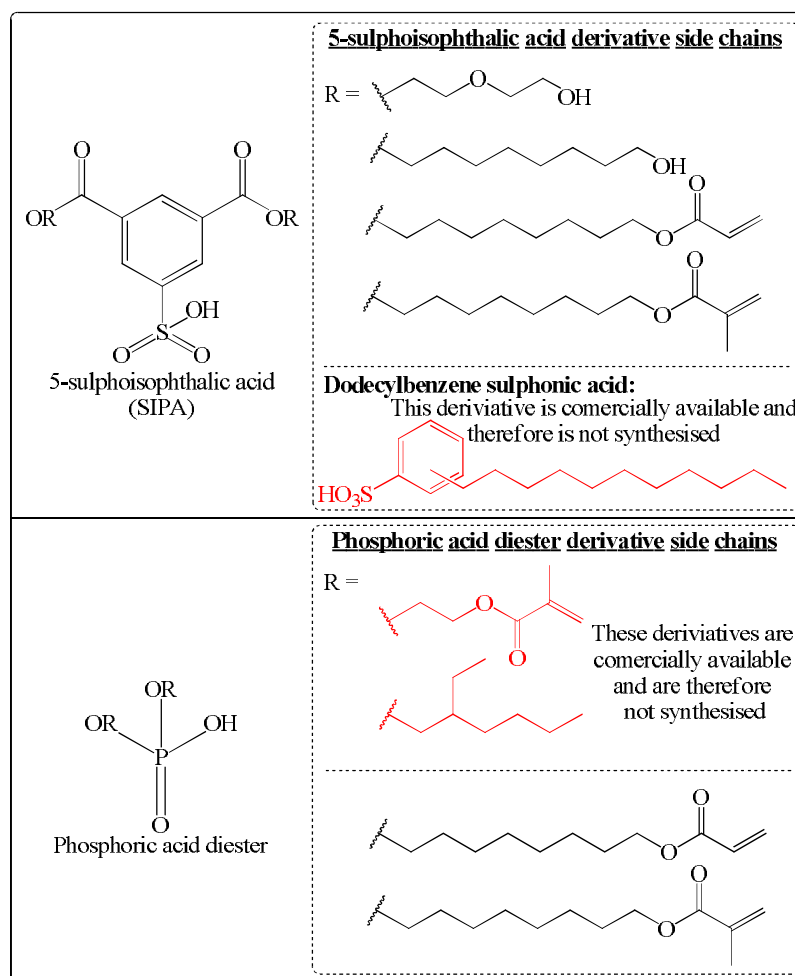


Figure 28: Proposed series of dopants to be synthesised and utilised for doping PANI, including dopants found in journal articles.

Upon the successive synthesis of the sulphonic acid derivative dopants, the aim was to successively dope PANI and cast films from solvent onto a metallic substrate. Further to this the doped polymer will also be mixed with other resins and polymers namely PVC and Epikote 828<sup>TM</sup> (Bisphenol A) (Figure 29) and acrylic resin using methyl methacrylate; with volume fractions of PANI at 50wt%, 20wt%, 10wt%,

5wt%, 2wt% and 1wt%. Again solvent cast films will be produced onto a metallic substrate from solution. The synthesis of dodecylbenzene sulphonic acid (DBSA), di(2-methoxyacryl ethyl) hydrogen phosphate (DMEHP) and di(2-ethylhexyl) hydrogen phosphate (DEHHP) doped PANI as seen in Figure 28 will be produced, all will be produced by the same conditions.

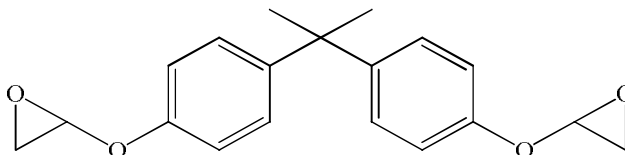
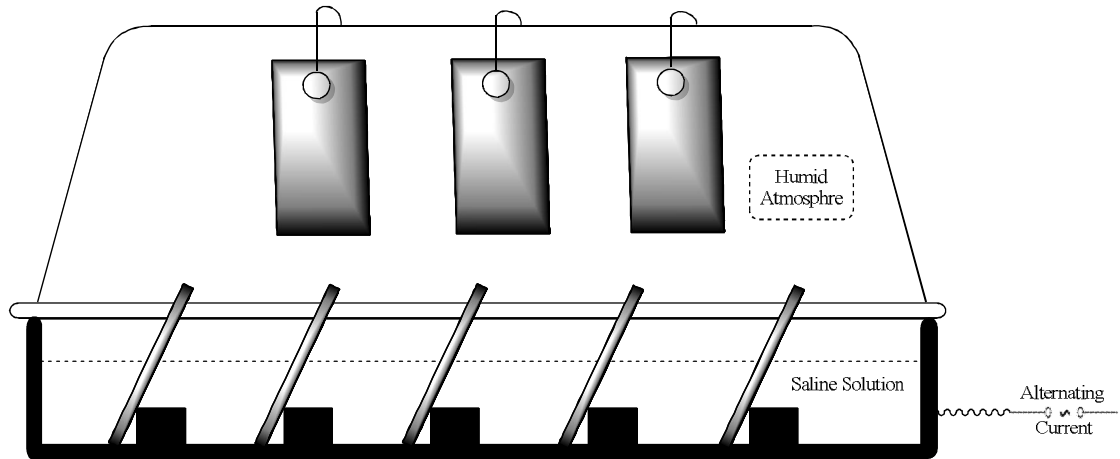


Figure 29: Bisphenol A diglycidyl ether form (Epikote 828™).

For analysis purposes the synthesised dopants will be correlated and compared to the results obtained for the DBSA, DEHHP and DMEHP doped PANI due to the previous and current research and reports that are available around the use of these compounds as a doping standard for PANI.

### 2.2.2 Phase 2/3: Corrosion testing of Metal substrates coated with various degrees of doped Polyaniline and its analysis.

The aims of the corrosion tests are to determine the minimum volume fraction of PANI required for sufficient inhibition of corrosion of the metallic samples, upon submission of the samples into a corrosive environment. Objectively this will be achieved by the incubation of the samples in an enclosed system capable of maintaining a high relative humidity. For each volume fraction film there will be two copper plates and two mild carbon steel plates, with a steel and copper sample submerged into a corrosive solution and the other two plates will be sprayed with a corrosive solution and suspended for a specified period within the highly humid environment. Thus this aspect of the investigation will be undertaken by rudimentary but effective means, by utilising a heated propagator (Figure 30) obtainable from any typical garden centre. The reasoning behind such a decision was that this equipment is used growing plant material and as such it radiates gentle heat to promote plant growth, therefore the heat will not be aggressive; we will utilise this fact and heat a saline solution within the propagator to what would be considered tropical levels, this will also be effective to create humidity that is typically found in the natural environment.



**Figure 30:** illustration of the equipment used for the accelerated corrosion testing, a rudimentary method using a heated cultivator/propagator obtainable from any general DIY or gardening establishment. As shown metal samples will be submerged and exposure to humid and harsh environment.

Similar approaches have been taken by Armelin, Wang and research by Iribarren et al <sup>66,68,83,87,102,103</sup> where samples have been subjected to corrosive environments, accelerated tests were conducted using sodium hydrogen sulphite and sodium chloride solutions (3.5wt%). However for this project using these studies as a basis, new methodologies of testing will be employed. Unlike the referenced methods, where samples were cyclically subjected to the corrosive factors. A cycle consists of immersion of the sample into the solution, retrieval of sample and allowing dripping, forced drying under incandescence and cooling to room temperature. One cycle taking 60 minutes and is conducted for a period of 30 days (720 hrs). However for this study samples will be left submerged or suspended depending on the sample with the temperature and relative humidity of the inside and the outside of the incubator (heated propagator, Figure 30) being measured throughout the sampling. Photographs were taken; before corrosion testing, then after an hour forming into the regular rhythm of every 24 hrs for 7 days, this allied with data obtained from surface analysis to obtain qualitative topographical images and film morphology data.

## Chapter 3 EXPERIMENTAL

### 3.1 General Procedures

#### 3.1.1 Materials

All the starting materials were obtained from Sigma-Aldrich, Alfa Aesar, Fisher and Acros Chemicals. All chemicals obtained were used as received unless otherwise stated. Dry solvents were used for reactions unless it is stated otherwise, with most of them being dispensed and obtained from the University of Sheffield Chemistry Departments Grubbs Solvent purification System (such as THF, DCM, Chloroform, Diethyl Ether, Hexane and Petroleum Ether 40/60). Reagent grade solvents were obtained from internal stores and were mainly used for extraction, Chromatography and for some reactions. Most of the reagents, acids, bases, salts and drying agents were obtained from the department's internal stores. All the reactions were carried out in dried glassware, under the inert atmosphere of nitrogen (unless otherwise stated) using the Schlenk line technique.

#### 3.1.2 Analysis Techniques

##### 3.1.2.1 Thin Layer Chromatography

Samples were run on silica-coated aluminium plates and utilising UV for visualisation of chromophores. In the absence of chromophores or weak response to UV light, samples were developed and visualised with developing agents and heated to produce coloured spots. *p*-anisaldehyde was mainly utilised and consisted of 3.8 ml acetic acid, 9.3 ml *p*-anisaldehyde, and 12.5 ml concentrated H<sub>2</sub>SO<sub>4</sub> and 340 ml ethanol.

##### 3.1.2.2 Elemental Analysis

Elemental analyses were carried out using a Perkin Elmer 2400 CHN Elemental Analysis instrument and the Schoniger oxygen flask combustion method for any halides or sulphur analyses. The weights submitted for analysis were around 5 mg for CHN analysis and 5 mg for the Sulphur and Halide analysis.

##### 3.1.2.3 Mass Spectroscopy (MS) and Liquid Chromatography Mass Spectroscopy (LC-MS)

Mass spectra were analysed and recorded on either the Micromass Prospector Spectrometer, with a mass range of 20 – 800 Da or on a Perkin Elmer Turbomass mass spectrometer which is equipped with autosystem LC and autosampler, capable

of operating in electrospray ionisation (ESI), Electron ionisation (EI) and chemical ionisation (CI) modes. Liquid chromatography followed pre-programmed settings, mobile phase followed a gradient starting at time = 0 minutes with 95% deionised water with 0.1% formic acid: 5% acetonitrile with 0.1% formic acid. Gradient was reversed at 2.5 minutes and then again back to the original gradient after 3.5 minutes. Flow rate through the columns were measured at 0.4 mL/minute and total run time for each sample was 5.00 minutes.

#### *3.1.2.4 Infra-Red Absorption Spectroscopy (IR)*

IR absorption spectra were recorded on the PerkinElmer Spectrum 100 FT-IR Spectrometer or on a Nicolet Model 205 FT-IR, using ATR Diamond crystal attachment for solid samples.

#### *3.1.2.5 UV-Visible Absorption Spectroscopy*

UV-Visible absorption Spectrums were measured using a Hitachi U-2010 Double Beam UV/Visible Spectrophotometer and a Specord S 600 UV-Vis Diode Array Spectrometer. The doped polymers were sampled in solutions of chloroform, methanol, ethanol, THF, NMP, m-cresol, toluene or DCAA, all at ambient temperature using rectangular quartz cuvette (light path = 10 mm) purchased from Sigma Aldrich. Thin films of the various polymers for UV-Visible absorption spectral measurements were prepared by dip coating quartz plates into the solutions at the noted concentration of doped polymer stock solution as calculated and then dried in the air and the measurements were sampled at ambient temperature.

#### *3.1.2.6 NMR Spectroscopy*

$^1\text{H}$  and  $^{13}\text{C}$  NMR Spectra were recorded on Bruker AC-250 at 250 MHz, AV1-400 at 400 MHz, AMX2-400 at 400 MHz, or DRX500 at 500 MHz NMR Spectrometers, conducted at room temperature which was controlled at 22°C. Samples were recorded in  $\text{CDCl}_3$ ,  $\text{D}_2\text{O}$ ,  $\text{DMSO-d}_6$  or methanol- $\text{d}_3$  purchased from Sigma-Aldrich or internal stores and used as received. Spectra were analysed using Bruker 1D WinNMR and Bruker TopSpin softwares.

#### *3.1.2.7 Accelerated Corrosion Testing*

Accelerated corrosion was tested using samples of copper and bright shim carbon steel. Samples were then either coated with a polymeric coating or untreated for control purposes and as an internal standard. Samples were exposed to one of two environments; either submerged in a 3.5% brine solution to simulate environmental

saline solutions such as seawater. The others were sprayed with a 3.5% saline solution and left in a humid environment. These environments were created by use of a heated propagator (available from all hardware and agricultural stores) and chosen due to its heating capabilities which is designed to support organic and biological matter and as such maintained a solution temperature of around 24°C - 25°C simulating temperatures that are found in oceans around the globe. Secondly the lid was able to maintain a humidity's that are found in the environment. Sampling was done at several and equal intervals for a total of 7 days and initial sampling included corrosion after 1 hour, then 24 hours with an interval of 24 hours for subsequent sampling. Humidity and solution temperature were measured throughout.

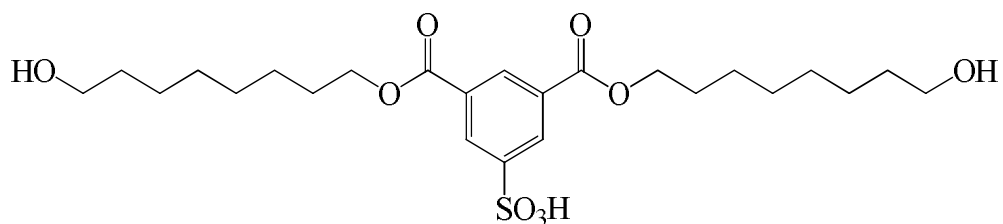
#### 3.1.2.8 Electron Microscopy

Anti-corrosion polymeric coating morphology and surface topography were recorded on a Philips XL-20 Scanning Electron Microscope (Philips, Cambridge, UK). All samples were imaged at room temperature under vacuum. Operating voltages were manually controlled and applied between 8 and 12 kV depending on the conductivity of the substrate to prevent burning of the substrate surface and to optimise the clarity of images produced. Any additional equipment required for imaging the samples were supplied by the Electron Microscopy Services of the Department of Biomedical Science, these being 1 inch diameter Pin Stubs and Leit-C conductive carbon sticky tabs (Sourced from Agar Scientific, Stanstead, England). Images processing was controlled and analysed by software designed and produced specifically for this instrument and was produced and supplied by the instruments manufacturer.

## 3.2. Dopant Synthesis

### 3.2.1. Sulphonic Acid series of Dopants.

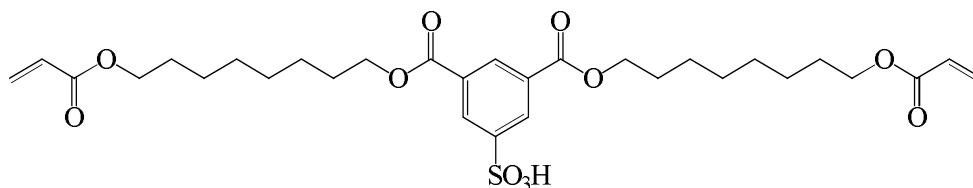
#### 3.2.1.1 Bis(8-hydroxyoctyl) 5-sulphoisophthalic acid (1) (SIPA00)



5-Sulphoisophthalic acid monosodium salt (10.19 g, 38.12 mmol) was heated to 50°C in aq. 2M aq. HCl (50 cm<sup>3</sup>) for 1 hour. 1,8-Octanediol (35.60 g, 243.5 mmol) was added to the free acid and heated at 90°C. The reaction was carried out under a stream of nitrogen until no further steam was evolved (left overnight). Water was removed in vacuo leaving a pale gold gel like waxy crude. The crude was reconstituted into an adequate amount of ethanol, producing a cream golden gel and the crude was purified via silica gel column chromatography (1:4 ethanol/chloroform), dried in vacuo to obtain a cream waxy solid product (**1**) (14.53g, 2.9 mmol, 76.2% yield). The product gave a single smear on TLC ( $R_f = 0.152$ ) in ethanol/chloroform (1:4).

**<sup>1</sup>H NMR** (400 MHz, CD<sub>3</sub>OD - d<sub>4</sub>) ppm 8.68 (dd,  $J = 3.2, 1.3$  Hz, 3H), 4.40 (t,  $J = 6.6$  Hz, 4H), 3.56 (t,  $J = 6.6$  Hz, 4H), 1.91 (quin,  $J = 7.60$  Hz, 4H), 1.52 (m, 4H), 1.37 (m, 16H). **<sup>13</sup>C NMR** (101 MHz, CD<sub>3</sub>OD - d<sub>4</sub>) ppm 166.39, 147.97, 132.57, 131.96, 128.1, 66.91, 63.01, 33.66, 30.61, 30.26, 29.76, 27.16, 26.88. **FT-IR** : (cm<sup>-1</sup>); 3411 (Brd, Stng; OH Str), 2936, 2857, 2080, 1723 (Shp, stng; C=O str), 1636 (shp; Ar-H and C=C str), 1439 – 1410, 1316, 1241, 1198, 1050, 753, 626. **LC-MS**: (m/z) 503.2 (MH<sup>+</sup>) Retention time of 1.74 minutes.

### 3.2.1.2 Bis(8-acryloxy octyl)-5- Sulphoisophthalic acid(**2**) (SIPAOA).

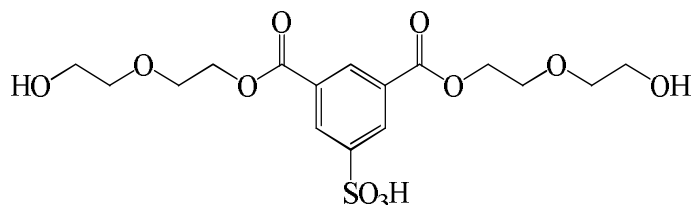


Bis(8-hydroxyoctyl) 5-sulphoisophthalic acid (**1**) (5.00 g, 9.96 mmol) was dissolved in dry THF (250 cm<sup>3</sup>) at 50°C. Acryloyl chloride (18.03 g, 16.19 cm<sup>3</sup>, 199.6 mmol) was added. TEA (20.198 g, 27.8 cm<sup>3</sup>, 199.6 mmol) in THF (100 cm<sup>3</sup>) was added drop wise to form a white suspension, which gradually turns yellow then develops to a dark golden orange. The reaction was heated at 50°C for 2.5 hours. The acrylate was stabilised with 100 ppm *p*-methoxyphenol (82 mg) and silica gel (5.00 g) was added to the solution before the THF was removed under vacuum. The crude product was purified by silica gel column chromatography (1:9 methanol/chloroform) to obtain a golden brown glass like product (**2**) (4.37 g, 7.16

mmol, 71.89% yield). The product gave a smear on TLC ( $R_f = 0.378$ ) in methanol/chloroform (1:9).

$^1\text{H NMR}$  (400 MHz,  $\text{CD}_3\text{OD}-d_4$ ) ppm 8.61 (d,  $J = 10.6$  Hz, 3H), 6.35 (dd,  $J = 15.6$ , 1.48 Hz, 2H), 6.08 (dd,  $J = 10.3$ , 6.8 Hz, 2H), 5.78 (dd,  $J = 10.4$ , 1.5 Hz, 2H), 4.28 (t,  $J = 6.7$  Hz, 4H), 4.11 (t,  $J = 6.7$  Hz, 4H), 1.72 (q,  $J = 7.1$  Hz, 4H), 1.62 (q,  $J = 6.8$  Hz, 4H), 1.34 (t,  $J = 7.3$  Hz, 16H).  $^{13}\text{C NMR}$  (101 MHz,  $\text{CD}_3\text{OD}-d_4$ ) ppm 166.37, 165.19, 145.71, 131.95, 131.15, 131.03, 130.52, 128.54, 65.64, 64.62, 29.07, 28.51, 25.81. **FT-IR:** ( $\text{cm}^{-1}$ ); 3391, 2932, 2879, 2131, 1728, 1651, 1458, 1430, 1398, 1356, 1322, 1246, 1200, 1125, 1057, 920 – 918, 751, 628. **LC-MS:** (m/z) 611.3 (MH+) Retention Time of 2.77 minutes.

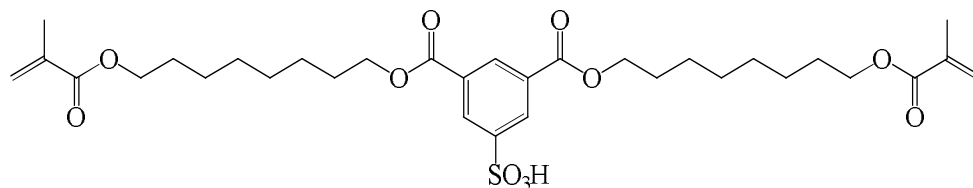
### 3.2.1.3 Bis[2-(2-hydroxy-ethoxy)-ethyl]-5-sulphoisophthalic acid (**3**).



Bis[2-(2-hydroxy-ethoxy)-ethyl]-5-sulphoisophthalic acid (**3**) was obtained using a similar method used for (**1**), using 5-sulphoisophthalic acid monosodium salt (10.00 g, 37.41 mmol) and Diethylene glycol (40.00 g, 35.8  $\text{cm}^3$ , 376.9 mmol). A golden gel like crude was purified by silica gel column chromatography (1:4 Methanol/Chloroform) to obtain a gold viscous heavy oil (**3**) (12.89 g, 30.52 mmol, 81.58% yield).

$^1\text{H NMR}$  (400 MHz,  $\text{CD}_3\text{OD}-d_4$ ) ppm 8.66 (d,  $J = 6.27$  Hz, 3H), 4.96 (s, 4H), 3.99 (s, 4H), 3.64 (m, 8H).  $^{13}\text{C NMR}$  (101 MHz,  $\text{CD}_3\text{OD}-d_4$ ) ppm 166.74, 147.89, 132.65, 132.37, 131.98, 73.48, 62.27. **FT-IR:** ( $\text{cm}^{-1}$ ); 3391, 2932, 2879, 2131, 1728, 1651, 1458, 1430, 1398, 1356, 1322, 1246, 1200, 1125, 1057, 920 - 918, 751, 628. **LC-MS:** (m/z) 423.2 (MH+) Retention Time of 0.96 minutes.

### 3.2.1.4 Bis(8-methacryloxy octyl)-5-Sulphoisophthalic acid (**4**)

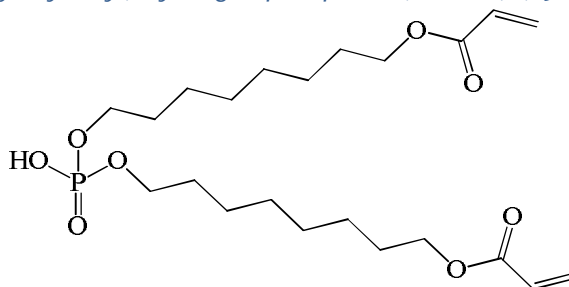


Method was as described for (2) using bis(8-hydroxyoctyl) 5-sulphoisophthalic acid (1) (5.00 g, 9.96 mmol) and methacryloyl chloride (20.86 g, 19.50 cm<sup>3</sup>, 199.6 mmol) and was base catalysed. The crude product was purified by silica gel column chromatography (1:9 methanol/chloroform) to obtain a dark gel product (4) (2.6 g, 4.08 mmol, 40.96% yield). The product gave a smear on TLC ( $R_f = 0.412$ ) in methanol/chloroform (1:9).

<sup>1</sup>H NMR (400 MHz, CDCl<sub>3</sub>) ppm 8.65 (d,  $J = 12.0$  Hz, 3H), 6.23 (d,  $J = 5.7$  Hz, 2H), 5.65 (p,  $J = 1.5$  Hz, 2H), 4.13 (t,  $J = 6.7$  Hz, 4H), 3.76 (d,  $J = 3.6$  Hz, 4H), 1.94 (s, 6H), 1.86 (q,  $J = 6.3$  Hz, 4H), 1.68 (q,  $J = 6.3$  Hz, 4H), 1.53 (m, 8H), 1.36 (m, 8H). <sup>13</sup>C NMR (101 MHz, CDCl<sub>3</sub>) ppm 167.60, 165.18, 136.46, 135.84, 131.24, 129.03, 127.38, 125.25, 67.90, 64.79, 29.11, 28.55, 25.56, 17.90. FT-IR: (cm<sup>-1</sup>); 3411, 2926, 2853, 1786, 1637, 1455, 1378, 1320, 1294, 1242, 1156, 1112, 1043, 950, 756, 627. LC-MS: (m/z) 639.3 (MH<sup>+</sup>) Retention Time of 4.04 minutes.

### 3.2.2. Hydrogen phosphate diester dopant Series.

#### 3.2.2.1 Bis(8-acryloyloxy octyl) hydrogen phosphate (DAOHP) (5)



**Method 1:** 8-hydroxyoctyl acrylate (7) (1.02 g, 5.10 mmol) was dissolved in chloroform (50 cm<sup>3</sup>). To the solution deionised water (0.045g, 0.045 cm<sup>3</sup>, 2.5 mmol) and phosphorus oxychloride (0.38 g, 0.23 cm<sup>3</sup>, 2.5 mmol) were simultaneously added drop wise to the mixture and stirred at 50°C for an hour and then allowed to cool to room temperature. The mixture was washed with water and dried over magnesium sulphate. Solvent was removed under vacuum yielding a yellow viscous residue. NMR results were not conclusive and so crude was purified via silica gel column chromatography yielding a yellow viscous oil (5) (0.012 g, 0.02 mmol, 0.8%).

<sup>1</sup>H NMR (250 MHz, CDCl<sub>3</sub>) ppm 6.37 (dd,  $J = 16.0, 1.60$  Hz, 2H), 6.09 (dd,  $J = 10.7, 6.6$  Hz, 2H), 5.79 (dd,  $J = 10.3, 1.6$  Hz, 2H), 4.12 (t,  $J = 6.7$  Hz, 4H), 3.99 (q,  $J = 6.7$  Hz, 4H), 1.64 (m, 8H), 1.31 (s, 16H). <sup>13</sup>C NMR (101 MHz, CDCl<sub>3</sub>) ppm 166.35, 130.52,

128.61, 67.66, 64.62, 30.32, 29.14, 29.05, 28.59, 25.86.  $^{31}\text{P}$  NMR (101 MHz,  $\text{CDCl}_3$ ) ppm -0.73 (s, 1P). **FT-IR:** ( $\text{cm}^{-1}$ ); 3411, 2926, 2853, 1786, 1637, 1455, 1378, 1320, 1294, 1242, 1156, 1112, 1043, 950, 756, 627.

**Method 2:** The synthetic procedure for (**5**) was a modification to the procedure laid out by Muhika et al<sup>104,105</sup>.

Pyridine (30% Solution, 5  $\text{cm}^3$ ) was added to 2-chloromethyl-4-nitrophenyl phosphorodi(octyl acrylate) (**9**) (1.0 g, 1.58 mmol) and left to stand at room temperature for 3 days and then was heated to 85°C for 2 hours. The reaction mixture was concentrated to dryness and reconstituted into Ethanol (10  $\text{cm}^3$ ). The precipitant was filtered off and the filtrate was concentrated. The yellow crude was dissolved into water (10  $\text{cm}^3$ ) and acidified with hydrochloric acid. Three extracts were taken using petroleum ether 40° - 60°, combined, dried over Magnesium Sulphate and solvent removed under vacuum to yield a yellow viscous oil (**5**) (0.2 g, 0.432 mmol, 27.34% yield).

$^1\text{H}$  NMR (250 MHz,  $\text{CDCl}_3$ ) ppm 6.41 (dd,  $J = 17.3, 1.6$  Hz, 2H), 6.13 (dd,  $J = 17.3, 10.3$  Hz, 2H), 5.83 (dd,  $J = 10.3, 1.6$  Hz, 2H), 4.16 (t,  $J = 6.7$  Hz, 4H), 4.02 (q,  $J = 6.6$  Hz, 4H), 1.68 (s, 8H), 1.35 (s, 16H).  $^{31}\text{P}$  NMR (101 MHz,  $\text{CDCl}_3$ ) ppm 1.19 (s, 1P).

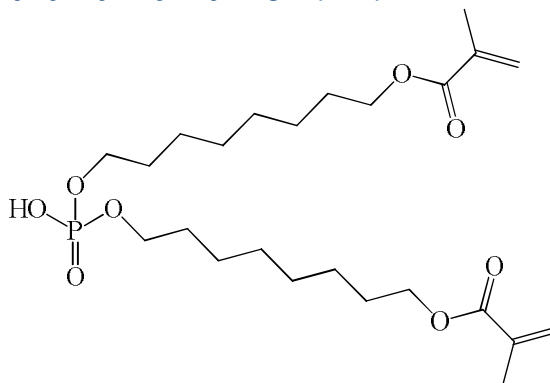
**Method 3:** Bis(8-acryloyloxy octyl) hydrogen phosphate (DAOHP) (**5**) was prepared according to a modified procedure by Jang and Jeong<sup>106</sup>.

8-hydroxyoctyl acrylate (**5**) (6.91 g, 32.15 mmol) and TEA (1.41 g, 1.95  $\text{cm}^3$ , 13.96 mmol) was dissolved in anhydrous diethyl ether (150  $\text{cm}^3$ ) at 0°C using an ice bath. A mixture of phosphorus oxychloride ( $\text{POCl}_3$ ) (2.14 g, 1.30  $\text{cm}^3$ , 13.96 mmol) in anhydrous diethyl ether (50  $\text{cm}^3$ ) was added drop wise and left to stir at room temperature for 24 hours to form a cream coloured suspension with fumes liberated. The TEA salt was removed by filtration and the filtrate was washed with 1M HCl, 10%  $\text{NaHCO}_3$  and a saturated saline solution successively. The crude extract was dried with magnesium sulphate, removing the solvent under vacuum yielding a pale yellow heavy viscous oil (**5**) (0.68g, 0.147 mmol, 10.53 %).

$^1\text{H}$  NMR (250 MHz,  $\text{CDCl}_3$ ) ppm 6.42 (dd,  $J = 17.3, 1.6$  Hz, 2H), 6.13 (dd,  $J = 17.3, 10.3$  Hz, 2H), 5.83 (dd,  $J = 10.3, 1.3$  Hz, 2H), 4.16 (t,  $J = 6.7$  Hz, 4H), 4.03 (q,  $J = 6.7$  Hz,

4H), 1.67 (m, 8H), 1.35 (s, 16H).  $^{13}\text{C}$  NMR (63 MHz,  $\text{CDCl}_3$ ) ppm 166.33, 130.43, 128.64, 64.58, 62.97, 32.71, 29.71, 29.04, 28.58, 25.82.  $^{31}\text{P}$  NMR (101 MHz,  $\text{CDCl}_3$ ) ppm 4.87 (s, 1P). FT-IR: ( $\text{cm}^{-1}$ ); 3450, 2929, 2857, 2106, 1727, 1639, 1471, 1409, 1297, 1271, 1197, 1022, 934, 814. LC-MS: (m/z) 461.23 (M<sup>-</sup>) Retention Time of 2.54 minutes.

### 3.2.2.2 Bis(8-methacryloyloxy octyl) hydrogen phosphate(**6**) (DMOHP)



**Method 1:** The synthetic procedure for (**6**) was a modification to the procedure laid out by Muhika et al<sup>104,105</sup> and was similar to the **method 2** used to obtain (**5**). NMR results showed that the product was a mixture and was purified via silica gel column chromatography to yield a yellow viscous heavy oil (**6**) (0.5 g, 1.02 mmol, 67.54% yield).

$^1\text{H}$  NMR (500 MHz,  $\text{CDCl}_3$ ) ppm 6.05 (dd,  $J = 1.7, 0.9$  Hz, 2H), 5.50 (quin,  $J = 1.6$  Hz, 2H), 4.09 (t,  $J = 6.70$  Hz, 4H), 3.98 (q,  $J = 6.74$  Hz, 4H), 1.90 (s, 6H), 1.63 (m, 8H), 1.30 (m, 16H).  $^{13}\text{C}$  NMR (126 MHz,  $\text{CDCl}_3$ ) ppm 167.43, 136.45, 125.08, 67.56, 64.64, 30.22, 29.05, 28.96, 28.50, 25.82, 18.24.  $^{31}\text{P}$  NMR (101 MHz,  $\text{CDCl}_3$ ) ppm -0.65 (s, 1P). FT-IR: ( $\text{cm}^{-1}$ ); 3446, 2932, 2855, 1720, 1637, 1456, 1320, 1298, 1170, 1061, 945, 814.

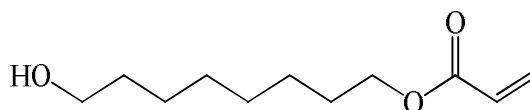
**Method 2:** Bis(8-methacryloyloxy octyl) hydrogen phosphate (DMOHP) (**6**) was prepared according to a modified procedure by Jang and Jeong<sup>106</sup>, using the same method (**method 3**) that was carried out to obtain (**5**); using 8-hydroxyoctyl methacrylate (**8**) (6.91 g, 32.15 mmol) yielding a pale yellow heavy viscous oil (**6**) (1.66g, 3.39 mmol, 21.84 %).

$^1\text{H}$  NMR (250 MHz,  $\text{CDCl}_3$ ) ppm 6.06 (dd,  $J = 1.8, 1.0$  Hz, 2H), 5.51 (quin,  $J = 1.7$  Hz, 2H), 4.09 (t,  $J = 6.64$  Hz, 4H), 4.01 (q,  $J = 6.71$  Hz, 4H), 1.90 (s, 6H), 1.61 (m, 8H), 1.30 (m, 16H).  $^{13}\text{C}$  NMR (63 MHz,  $\text{CDCl}_3$ ) ppm 167.50, 136.49, 125.08, 64.72, 62.83, 32.34,

29.77, 29.21, 28.54, 25.86, 18.22.  $^{31}\text{P}$  NMR (101 MHz,  $\text{CDCl}_3$ ) ppm 4.56 (s, 1P). **FT-IR:** ( $\text{cm}^{-1}$ ); 3457, 2966, 2861, 2115, 1715, 1640, 1465, 1398, 1298, 1189, 1058, 745, 556. **LC-MS:** (m/z) 489.26 (M-) Retention Time of 3.93 minutes.

### 3.2.3. Other Compounds and Intermediate compounds for Dopant synthesis.

#### 3.2.3.1 8-hydroxyoctyl acrylate (**7**)



**Method 1:** 1,8-Octanediol (50.01 g, 0.34 mol) was briefly dissolved in dry THF (250  $\text{cm}^3$ ) at 50°C. Acryloyl chloride (10.00 g, 8.90  $\text{cm}^3$ , 0.11 mol) was added. TEA (11.20 g, 15.45  $\text{cm}^3$ , 0.11 mol) in THF (100  $\text{cm}^3$ ) was added drop wise to form a cream coloured suspension with fumes liberated. The reaction was heated at 50°C for 2 hours before filtering off the triethylamine salt. The acrylate was stabilised with 100-200 ppm *p*-methoxyphenol before the THF was removed under vacuum. The crude product was dissolved in 2M aq. HCl (200  $\text{cm}^3$ ) and stirred for 1 hour. The product was extracted with ethyl acetate (2 x 100  $\text{cm}^3$ ), separated, dried over  $\text{MgSO}_4$ , filtered and the solvent removed under vacuum. The product is obtained as a yellow oil 3.4 g (55.2 %), which turned brown over time.

The acrylate was stabilised with 100 ppm *p*-methoxyphenol (82 mg) and silica gel (5.00 g) was added to the solution before the THF was removed under vacuum. The crude product was purified by silica gel column chromatography (1:9 methanol/chloroform) to obtain a golden brown glass like product (**7**) (4.37 g, 7.16 mmol, 71.89% yield). The product gave a smear on TLC ( $R_f = 0.378$ ) in methanol/chloroform (1:9).

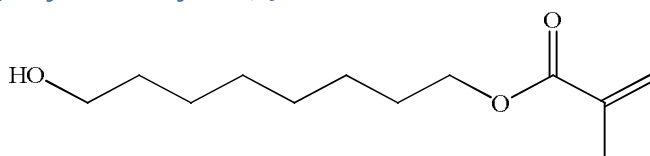
$^1\text{H}$  NMR (500 MHz,  $\text{CDCl}_3$ ) ppm 6.36 (dd,  $J = 17.4, 1.5$  Hz, 1H), 6.09 (dd,  $J = 17.3, 10.4$  Hz, 1H), 5.78 (dd,  $J = 10.4, 1.5$  Hz, 1H), 4.12 (t,  $J = 6.7$  Hz, 2H), 3.60 (t,  $J = 6.6$  Hz, 2H), 1.63 (m, 2H), 1.53 (m, 2H), 1.31 (s, 8H).  $^{13}\text{C}$  NMR (126 MHz,  $\text{CDCl}_3$ ) ppm 166.34, 130.43, 128.56, 64.62, 62.86, 32.64, 29.21, 29.12, 28.52, 25.79, 25.59. **ESI-ToF** m/z: 201.3 (100% Molecular Ion).

**Method 2:** 1,8-Octanediol (50.01 g, 0.34 mol) was briefly dissolved in dry THF (250 cm<sup>3</sup>) at 50°C. Acryloyl chloride (10.00 g, 8.90 cm<sup>3</sup>, 0.11 mol) was added. TEA (11.20 g, 15.45 cm<sup>3</sup>, 0.11 mol) in THF (100 cm<sup>3</sup>) was added drop wise to form a cream coloured suspension with fumes liberated. The reaction was heated at 50°C for 2 hours. Crude was dried in vacuo and was purified via silica gel column chromatography (1:4 ethyl acetate/petroleum ether 40° - 60°) to obtain a very pale golden heavy oil† (**7**) (22.84 g, 0.1142 mmol, 33.59% yield). The product gave a single spot on TLC (R<sub>f</sub> = 0.32) in Ethyl Acetate/Petroleum Ether 40° - 60° (1:4).

<sup>1</sup>H NMR (400 MHz, CDCl<sub>3</sub>) ppm 6.38 (dd, *J* = 17.33, 1.43 Hz, 1H), 6.10 (dd, *J* = 17.33, 10.42 Hz, 1H), 5.80 (dd, *J* = 10.42, 1.43 Hz, 1H), 4.13 (t, *J* = 6.74 Hz, 2H), 3.60 (t, *J* = 6.65 Hz, 2H), 1.64 (m, 2H), 1.53 (m, 2H), 1.34 (s, 8H). <sup>13</sup>C NMR (101 MHz, CDCl<sub>3</sub>) ppm 166.38, 130.49, 128.57, 64.66, 62.80, 32.66, 29.25, 29.16, 28.54, 25.82, 25.64. FT-IR: (cm<sup>-1</sup>); 3418, 2932, 2857, 1725, 1637, 1619, 1467, 1407, 1297, 1269, 1196, 1059, 1050, 982, 812. Elemental Analysis (%) calculated for C<sub>11</sub>H<sub>20</sub>O<sub>3</sub>: C, 65.97; H, 10.07. Found: C, 59.89; H, 9.32. LC-MS: (m/z) 201.149 (MH<sup>+</sup>) Retention Time = 1.84 minutes.

† Product was not stabilised with *p*-methoxyphenol due to its much more favourable reactivity with phosphorus oxychloride in comparison to the product, thus resulting in undesired by-products that are difficult to separate from the desired phosphodiester.

### 3.2.3.2. 8-hydroxyoctyl methacrylate (**8**)



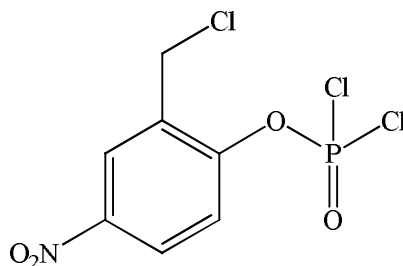
**Method 1:** 8-hydroxyoctyl methacrylate was obtained using the same method as those used to obtain (**7**) using methyl methacrylate (11.55 g, 10.8 cm<sup>3</sup>, 0.11 mol) giving a very pale golden heavy oil (**8**) (43.8 g, 0.204 mol, 60.2% yield). The product gave a single spot on TLC (R<sub>f</sub> = 0.39) in ethyl acetate/petroleum ether 40° - 60° (1:4).

<sup>1</sup>H NMR (500 MHz, CDCl<sub>3</sub>) ppm 6.04 (dd, *J* = 1.7, 1.0 Hz, 1H), 5.49 (quin, *J* = 1.6 Hz, 1H), 4.08 (t, *J* = 6.70 Hz, 2H), 3.57 (t, *J* = 6.68 Hz, 2H), 1.88 (dd, *J* = 1.56, 1.07 Hz, 3H), 1.62 (q, *J* = 6.71 Hz, 2H), 1.50 (q, *J* = 6.80 Hz, 2H), 1.28 (s, 8H). <sup>13</sup>C NMR (126 MHz, CDCl<sub>3</sub>) ppm 167.50 (s,1C), 136.37 (s,1C), 125.11 (s,1C), 64.70 (s,1C), 62.69 (s,1C), 32.54 (s,1C), 29.16 (s,1C), 29.07 (s,1C), 28.45 (s,1C), 25.78 (s,1C), 25.55 (s,1C), 18.17 (s,1C).

**Method 2:** Method is as described for **method 2 (7)** yielding a very pale golden heavy oil<sup>†</sup> (**8**) (44.06 g, 0.206 mol, 60.55% yield).

**<sup>1</sup>H NMR** (400 MHz, *CDCl*<sub>3</sub>) ppm 6.02 (dd, *J* = 1.49, 0.88 Hz, 1H), 5.48 (quin, *J* = 1.53 Hz, 1H), 4.06 (t, *J* = 6.67 Hz, 2H), 3.60 (q, *J* = 7.04 Hz, 2H), 1.87 (s, 3H), 1.59 (m, 2H), 1.46 (m, 2H), 1.26 (s, 8H). **<sup>13</sup>C NMR** (101 MHz, *CDCl*<sub>3</sub>) ppm 167.66 (s,1C), 136.36 (s,1C), 125.24 (s,1C), 64.79 (s,1C), 62.43 (s,1C), 32.51 (s,1C), 29.22 (s,1C), 29.11 (s,1C), 28.47 (s,1C), 25.82 (s,1C), 25.60 (s,1C), 18.06 (s,1C). **FT-IR:** (cm<sup>-1</sup>); 3437, 2932, 2851, 1713, 1632, 1454, 1322, 1297, 1170, 1021, 932, 815. **LC-MS:** (m/z) 215.165 (MH<sup>+</sup>) Retention Time = 2.04 minutes.

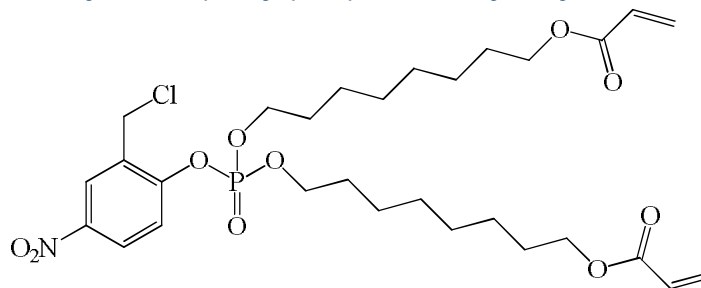
### 3.2.3.3 2-Chloromethyl-4-nitrophenyl phosphorodichloridate (**9**)



The synthesis of 2-chloromethyl-4-nitrophenyl dichlorophosphoridate (**9**) was performed according to a modified procedure by Hata, Mushika and Mukaiyama<sup>105</sup>.

2-Chloromethyl-4-nitrophenol (5g, 26.66 mmol) and phosphorus oxychloride (10.22g, 66.64 mmol) were refluxed for 6 hours in the presence of potassium chloride (1g) until fuming ceased. Excess phosphorus oxychloride was removed in vacuo and the concentrate was distilled under high vacuum via a kugelrohr oven at 170°C (bp 165<sup>-1</sup>67°C at 0.2mmHg). Collecting a pale yellow viscous oil (**9**) (0.89g, 2.92 mmol, 10.95% yield).

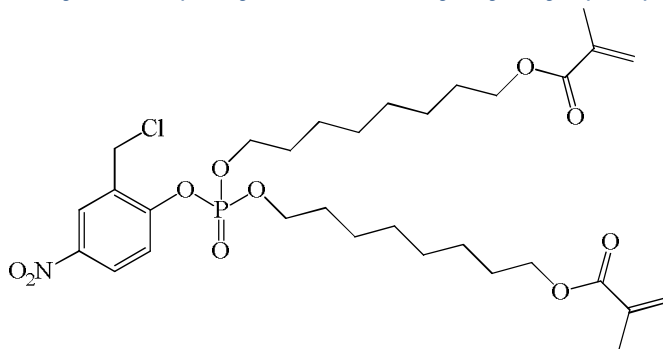
**<sup>1</sup>H NMR** (400 MHz, *CDCl*<sub>3</sub>) ppm 8.48 (s, 1H), 8.31 (dd, *J* = 9.08, 2.78 Hz, 1H), 7.71 (dd, *J* = 9.03, 1.68 Hz, 1H), 4.72 (s, 2H). **<sup>31</sup>P NMR** (162 MHz, *CDCl*<sub>3</sub>) ppm 3.57 (s,1P). **LC-MS:** (m/z) 302.01 (MH<sup>+</sup>) Retention Time of 1.64 minutes, 326.04 (MNa<sup>+</sup>) Retention Time of 3.03 minutes.

3.2.3.4 2-Chloromethyl-4-nitrophenyl phosphorodi(octyl acrylate) (**10**)

The synthetic procedure of 2-chloromethyl-4-nitrophenyl phosphorodi(octyl acrylate) (**10**) was performed according to a modified procedure by Hata, Mushika and Mukaiyama<sup>105</sup>.

8-Hydroxyoctyl acrylate (**7**) (4.24 g, 21.2 mmol) was dissolved into THF (100 cm<sup>3</sup>) and was cooled to 10°C using a brine ice bath. 2-chloromethyl-4-nitrophenyl phosphorodichloridate (**9**) (2.38 g, 7.82 mmol) was dissolved into THF (50 cm<sup>3</sup>) added drop wise and stirred for 24 hours in the presence of TEA (0.73g, 1.01 cm<sup>3</sup>, 7.82 mmol). The mixture was evaporated to dryness in vacuo and purified by silica gel column chromatography (1:4 Ethyl Acetate/Petroleum Ether 40° - 60°) to yield 2-chloromethyl-4-nitrophenyl phosphorodi(octyl acrylate) (**10**) (2.0 g, 3.16 mmol, 40.4 % yield).

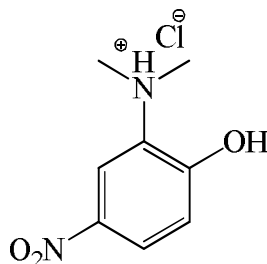
**<sup>1</sup>H NMR** (500 MHz, CDCl<sub>3</sub>) ppm 8.33 (dd, *J* = 2.9, 1.1 Hz, 1H), 8.18 (dd, *J* = 9.0, 2.8 Hz, 1H), 7.57 (d, *J* = 9.1 Hz, 1H), 6.35 (dd, *J* = 17.34, 1.45 Hz, 2H), 6.08 (dd, *J* = 17.34, 10.43 Hz, 2H), 5.78 (dd, *J* = 10.44, 1.43 Hz, 2H), 4.65 (s, 2H), 4.16 (m, 4H), 4.10 (m, 4H), 1.67 (m, 4H), 1.61 (m, 4H), 1.29 (s, 16H). **<sup>13</sup>C NMR** (126 MHz, CDCl<sub>3</sub>) ppm 166.28 (s,1C), 153.48 (s,1C), 153.43 (s,1C), 144.37 (s,1C), 130.46 (s,1C), 128.52 (s,1C), 126.25 (s,1C), 125.43 (s,1C), 120.30 (s,1C), 69.38 (s,1C), 64.49 (s,1C), 39.71 (s,1C), 30.10 (s,1C), 28.99 (s,1C), 28.85 (s,1C), 28.48 (s,1C), 25.73 (s,1C), 25.21 (s,1C). **<sup>31</sup>P NMR** (101 MHz, CDCl<sub>3</sub>) ppm -7.12 (s,1P). **FT-IR:** (cm<sup>-1</sup>); 3396, 2929, 2861, 1728, 1638 - 1619, 1467, 1409, 1295, 1274, 1198, 1056, 985, 813. **LC-MS:** (m/z) 632.23 (MH<sup>+</sup>) Retention Time of 3.03 minutes.

3.2.3.5 2-Chloromethyl-4-nitrophenyl bis(8-methacryloxy octyl) phosphoridate (**11**)

The synthetic procedure of 2-chloromethyl-4-nitrophenyl phosphorodi(octyl methacrylate) (**11**) was performed according to a modified procedure by Hata, Mushika and Mukaiyama<sup>104,105</sup> using the same methodology as used for 2-chloromethyl-4-nitrophenyl phosphorodi(octyl acrylate) (**10**) to yield 2-chloromethyl-4-nitrophenyl phosphorodi(octyl acrylate) (**11**) (2.0 g, 3.16 mmol, 40.4 % yield).

**<sup>1</sup>H NMR** (500 MHz,  $CDCl_3$ ) ppm 8.37 (d,  $J = 2.5$  Hz, 1H), 8.22 (dd,  $J = 9.0, 2.8$  Hz, 1H), 8.02 (d,  $J = 2.5$  Hz, 1H), 6.08 (dd,  $J = 1.7, 0.9$  Hz, 2H), 5.78 (quin,  $J = 1.7$  Hz, 2H), 4.65 (s, 2H) 4.16 (t,  $J = 6.7$ , 4H), 4.10 (q,  $J = 6.74$  Hz, 4H), 2.01 (s, 6H), 1.67 (m, 4H), 1.61 (m, 4H), 1.29 (s, 16H). **<sup>13</sup>C NMR** (126 MHz,  $CDCl_3$ ) ppm 166.28 (s,1C), 153.48 (s,1C), 153.43 (s,1C), 144.37 (s,1C), 130.46 (s,1C), 128.52 (s,1C), 126.25 (s,1C), 125.43 (s,1C), 120.30 (s,1C), 69.38 (s,1C), 64.49 (s,1C), 39.71 (s,1C), 30.10 (s,1C), 28.99 (s,1C), 28.85 (s,1C), 28.48 (s,1C), 25.73 (s,1C), 25.21 (s,1C). **<sup>31</sup>P NMR** (101 MHz,  $CDCl_3$ ) ppm -7.12 (s,1P). **FT-IR:** ( $cm^{-1}$ ); 3396, 2929, 2861, 1728, 1638 - 1619, 1467, 1409, 1295, 1274, 1198, 1056, 985, 813. **LC-MS:** (m/z) 661.1 (MNa<sup>+</sup>) Retention Time of 2.89 minutes.

## 3.2.4 Other Synthesis

3.2.4.1 2-(*N,N*-Dimethylamino)-4-nitrophenol hydrochloride (**12**).

The synthetic procedure of 2-(*N,N*-dimethylamino)-4-nitrophenol hydrochloride (**12**) was performed according to a modified procedure by Taguchi and Mushika<sup>107</sup>

2-amino-4-nitrophenol (15.4 g, 0.1 mol) and Triethylamine (TEA) (15.1 g, 20.80 ml, 0.15 mol) was added to acetone (100 ml). Methyl Iodide (35.6 g, 15.61 ml, 0.25 mol) was added dropwise to the mixture and stirred at room temperature for 30 minutes. The mixture was then refluxed for 4 hours, upon completion reaction mixture was evaporated to dryness under vacuum and crude was dissolved into Sodium Acetate (100ml, 2M) and extracted with ethyl acetate (3 x 50 ml), combined and dried over sodium sulphate. Filtrate was evaporated to dryness and the crude was successively dissolved into Hydrochloric acid (100 ml, 1M) and preceded to filtering mixture through activated charcoal (~2 g). The filtered mixture was evaporated to dryness under reduced pressure and crystallised with ethanol (50 ml) to yield a pale yellow crystalline needles (**12**) (6.51 g, 2.9%). Analysis showed that the product was not the hydrochloride salt but rather its free base.

<sup>1</sup>H NMR (400 MHz, CD<sub>3</sub>OD-*d*<sub>6</sub>) ppm 8.65 (d, *J* = 2.60 Hz, 1H), 8.35 (dd, *J* = 9.09, 2.63 Hz, 1H), 7.26 (d, *J* = 9.12 Hz, 1H), 3.37 (s, 6H), 4.92 (s, 1H). ESI-ToF (MeOH) m/z: 183.1 (100%, Molecular Ion).

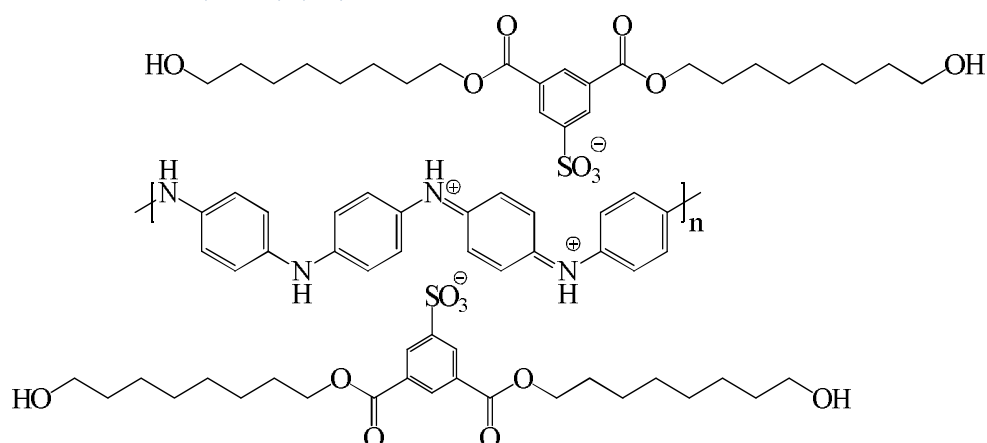
### 3.3 Polymer Doping

#### 3.3.1 Procedure for doping PANI with dopants.

Polyaniline was added to the synthesised dopants (**1** – **4**), (**6**) and for comparative purposes and analytical purposes, PANI was doped with several literature standard dopants namely; dodecylbenzene sulphonic acid (**14**), bis(2-methacryloxy ethyl) hydrogen phosphate (BMEHP) (**15**) and bis(2-ethyl hexyl) hydrogen phosphate (BEHP) (**16**).

Dopant (**1** – **4**), (**6**) (5.5 mmol) was added to polyaniline (1g, 10.99 mmol) and mechanically mixed using a pestle and mortar, dichloroacetic acid was added drop wise during the mixing process until a solution was formed (50 cm<sup>3</sup>). The mixtures was transferred to a round bottom flask and stirred at 50°C for 24 hours to ensure full dissolution. DCM (100 cm<sup>3</sup>) was added to the solution and the resulting mixture was washed with water until aqueous extracts were neutral. The solution was dried over magnesium sulphate and filtered several times through glass wool.

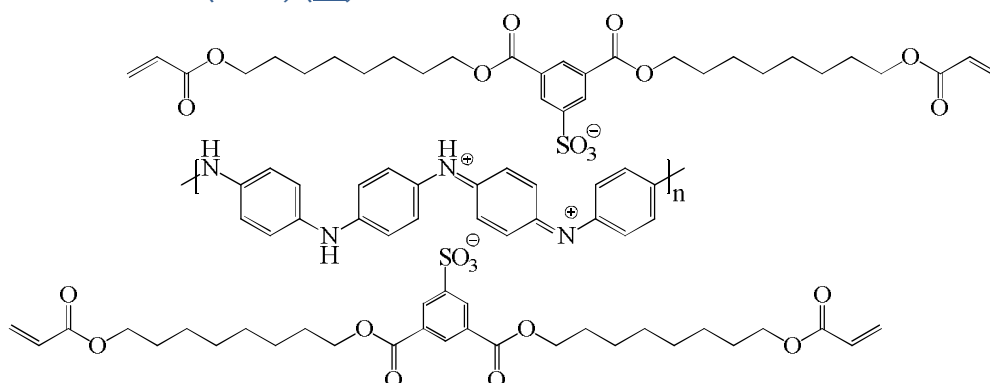
3.3.1.1 Doping of PANI with bis(8-hydroxy octyl)-5-sulphoisophthalic acid (**1**) in dichloroacetic Acid (DCAA) (17).



Bis(8-hydroxy octyl)-5-sulphoisophthalic acid (**1**) (2.75 g, 5.5 mmol) was added to polyaniline (1g, 10.99 mmol).

**FT-IR:** ( $\text{cm}^{-1}$ ); 3472, 3232, 2914, 2851, 2101, 1851, 1707, 1570, 1464, 1290, 1222, 1138, 1094, 1037.

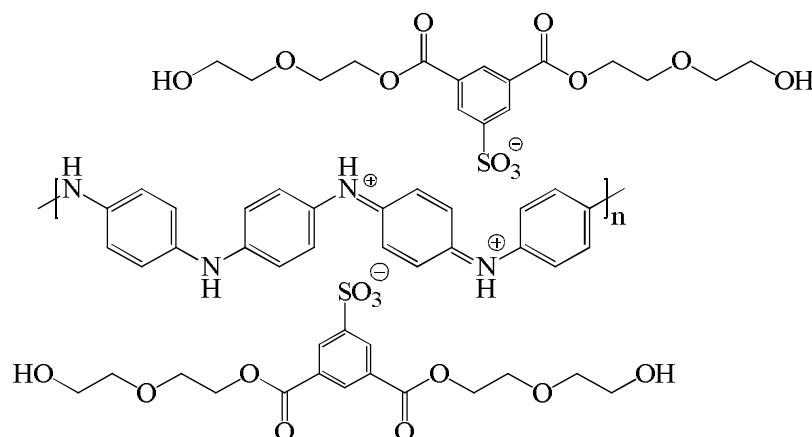
3.3.1.2 Doping of PANI with bis(8-acryloxy octyl)-5-sulphoisophthalic acid (**2**) in dichloroacetic Acid (DCAA) (18).



Bis(8-acryloxy octyl)-5-sulphoisophthalic acid (**2**) (3.35 g, 5.5 mmol) was added to polyaniline (1g, 10.99 mmol).

**FT-IR:** ( $\text{cm}^{-1}$ ); (3603 – 1829), 3384, 3224, 1664, 1463, 1288, 1211, 1073.

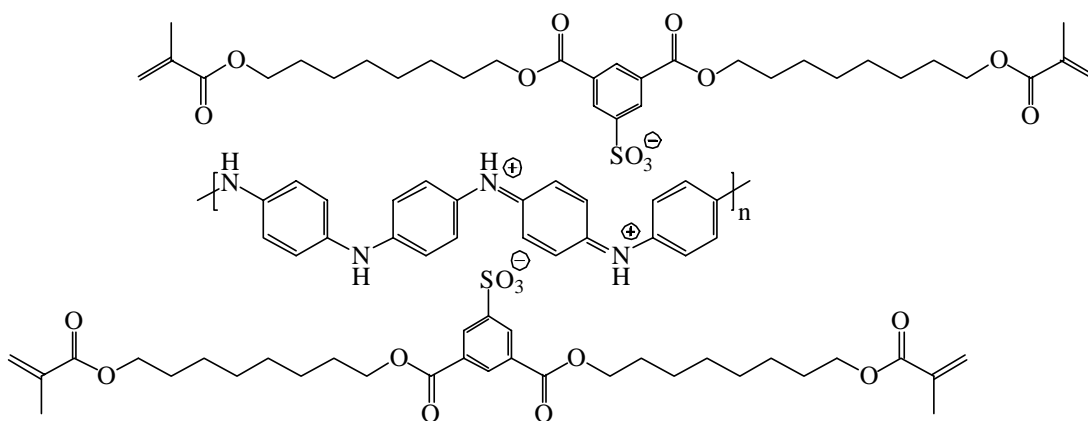
3.3.1.3 Doping of PANI bis[2-(2-hydroxy-ethoxy)-ethyl]-5-sulphoisophthalic acid (**3**) in dichloroacetic Acid (DCAA) (**19**).



bis[2-(2-hydroxy-ethoxy)-ethyl]-5-sulphoisophthalic acid (**3**) (2.31 g, 5.5 mmol) was added to polyaniline (1g, 10.99 mmol).

**<sup>1</sup>H NMR** (400 MHz, *DMSO-d6*) ppm 8.44 (d,  $J = 7.04$  Hz, 1H), 8.39 (d,  $J = 13.74$  Hz, 2H), 7.02 (d,  $J = 7.50$  Hz, 4H), 6.57 (t,  $J = 11.07$  Hz, 4H), 4.67 (s, 2H), 4.46 (d,  $J = 5.04$  Hz, 4H), 3.78 (d,  $J = 4.08$  Hz, 4H), 3.51 (s, 6H), 3.37 (s, 46H). **FT-IR**( $\text{cm}^{-1}$ ): 2957, 2085, 1752, 1715, 1648, 1601, 1557, 1441, 1394, 1296, 1254, 1217, 1160, 1088, 1011, 911, 862, 788.

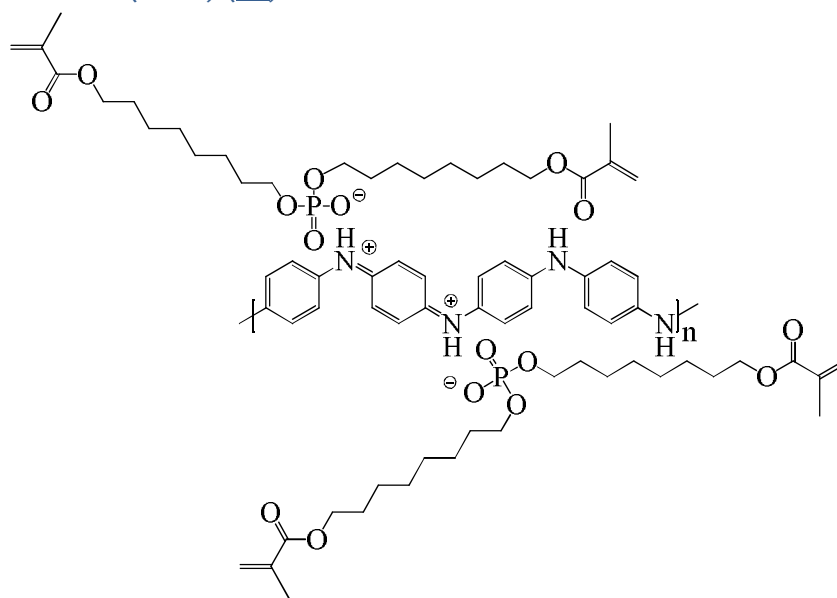
3.3.1.4 Doping of PANI with bis(8-methacryloxy octyl)-5-sulphoisophthalic acid (**4**) in dichloroacetic Acid (DCAA) (**20**).



Bis(8-methacryloxy octyl)-5-sulphoisophthalic acid (**4**) (3.51 g, 5.5 mmol) was added to polyaniline (1g, 10.99 mmol).

**FT-IR:** ( $\text{cm}^{-1}$ ); 3475, 3203, 2961 - 2845, 2107, 1851, 1714, 1568, 1427, 1254, 1059, 1001.

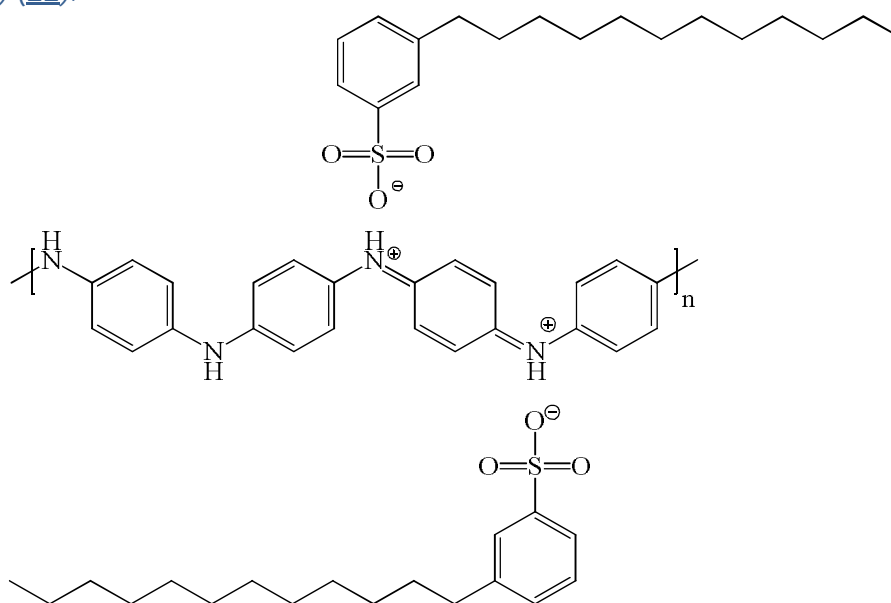
3.3.1.5 Doping of PANI with bis(8-methacryloxy octyl) hydrogen phosphate (**6**) in dichloroacetic acid (DCAA) (**21**).



Bis(8-methacryloxy octyl) hydrogen phosphate (**6**) (2.70 g, 5.5 mmol) was added to polyaniline (1g, 10.99 mmol).

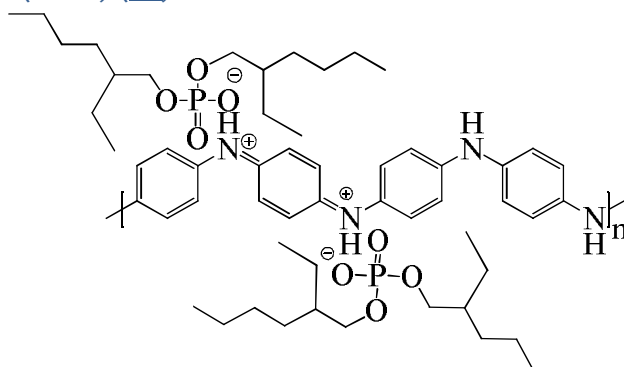
**FT-IR:** ( $\text{cm}^{-1}$ ); 3238, 2915, 2855, 2301, 1716, 1635, 1443, 1300, 1066.

3.3.1.6 Doping of PANI with dodecylbenzene sulphonic acid (**14**) in dichloroacetic Acid (DCAA) (**22**).



Dodecylbenzene sulphonic acid (**14**) (1.99 g, 5.5 mmol) was added to polyaniline (1g, 10.99 mmol).

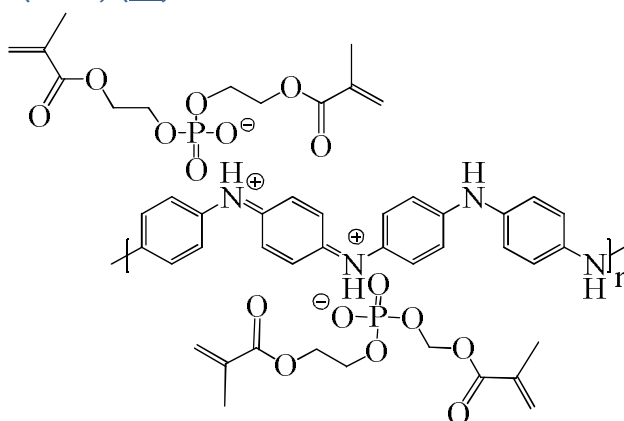
3.3.1.7 Doping of PANI with bis(2-ethyl hexyl) hydrogen phosphate (**15**) in dichloroacetic Acid (DCAA) (**23**).



Bis(2-ethylhexyl) hydrogen phosphate (**15**) (1.69 g, 5.5 mmol) was added to polyaniline (1g, 10.99 mmol).

**FT-IR:** ( $\text{cm}^{-1}$ ); 3448, 3225, 3052, 2917, 2849, 2664, 2335, 2086, 1993, 1861, 1716, 1559, 1455, 1287, 1219, 1121, 985, 872.

3.3.1.8 Doping of PANI with bis(2-methacryloxy ethyl) hydrogen phosphate (**16**) in dichloroacetic Acid (DCAA) (**24**).



Bis(2-methacryloxy ethyl) hydrogen phosphate (**16**) (1.69 g, 5.5 mmol) was added to polyaniline (1g, 10.99 mmol).

**FT-IR:** ( $\text{cm}^{-1}$ ); (3628 – 2408), 3307, 2964, 2161, 2031, 1974, 1730, 1635, 1452, 1380, 1296, 1036.

### 3.4 Preparation of polymer coating solutions.

#### 3.4.1 Preparation of polyaniline composites.

##### 3.4.1.1 General preparation of PANI/PVC composite Solutions.

Polyvinyl chloride (PVC) (43,000  $M_w$ ) was added to a solution of Doped Polyaniline (**17** - **24**). The different doped polymers were at different

concentrations, therefore for ease and practicality, aliquots were taken from the stock solutions and concentrated to  $6 \text{ mg ml}^{-1}$  (100ml). The PVC was added to the Doped PANI (**17** - **24**) ( $6 \text{ mg ml}^{-1}$ , 100 mL) in varied amounts to produce a series of weight percent solutions; 80, 20, 10, 5, 1 for doped PANI (**15**), 20, 10, 5, 2, 1 wt% for DBSA doped PANI (**22**) and 5, 2, 1 wt% for the remaining doped PANI samples. PVC was added in the amounts of; 150 mg (80 wt%), 2.4 g (20 wt%), 5.4 g (10 wt%), 11.4 g (5 wt%), 29.4 g (2 wt%) and 59.4 g (1 wt%). The composite mixture was sonicated until all the PVC had dissolved (2 hrs). Solution was left to stir at ambient temperature up to the casting of films onto the metallic substrates.

**Sigma-Aldrich PVC: FT-IR:** ( $\text{cm}^{-1}$ ); 2963, 2908, 2158, 2025, 1974, 1426, 1326, 1240, 1092, 955.

3.4.1.1.1 Doped PANI (**17**)/PVC 1 wt% film.

**FT-IR:** ( $\text{cm}^{-1}$ ); 3329, 2904, 2843, 2163, 1985, 1726, 1426, 1315, 1242 - 1171, 1088, 1037, 951.

3.4.1.1.2 Doped PANI (**18**)/PVC 1 wt% film.

**FT-IR:** ( $\text{cm}^{-1}$ ); 3290, 2971, 2911, 2155, 2033, 1629, 1426, 1329, 1242, 1085, 1032, 951.

3.4.1.1.3 Doped PANI (**20**)/PVC 1 wt% film.

**FT-IR:** ( $\text{cm}^{-1}$ ); 3318, 2949, 2905, 2155, 2032, 1655, 1426, 1318, 1240, 1192, 1098, 1045, 959.

3.4.1.1.4 Doped PANI (**21**)/PVC 1 wt% film.

**FT-IR:** ( $\text{cm}^{-1}$ ); 3314, 2902, 2160, 1987, 1623, 1425, 1327, 1233, 1103, 967.

3.4.1.1.5 Doped PANI (**22**)/PVC 1 wt% film.

**FT-IR:** ( $\text{cm}^{-1}$ ); 3395, 2930, 2911, 2161, 2027, 1427, 1316, 1232, 1102, 957.

3.4.1.1.6 Doped PANI (**23**)/PVC 1 wt% film.

**FT-IR:** ( $\text{cm}^{-1}$ ); 3317, 2949, 2906, 2155, 2036, 1636, 1426, 1325, 1236, 1189, 1085, 960.

### 3.4.3 General preparation of PANI/epoxy resin composite solutions.

Aliquots of doped PANI (**15**) ( $1.97 \text{ mg ml}^{-1}$ , 75 mL) were taken and Epikote 828 (Bisphenol A epoxy resin) was added to produce a series of weight percent's; 592.13 mg (20 wt%), 1.332 g (10 wt%), 2.813 g (5 wt%), 7.239 g (2 wt%) and 14.627 g (1wt%). Solutions were sonicated (2 hrs) and left to stir at ambient temperature until production of thin film coatings. However the epoxy resin crashed

out of solution and aggregated to the bottom producing two different layers. Samples were therefore discarded.

#### 3.4.4 General preparation of epoxy resin composite solutions.

Epikote 828 and polypropylene glycol bis(2-amino propyl ether) were added into DCM (100mL) at a ratio of 2:1 mole equivalent respectively. In order to produce the different weight percent's, individual solutions for each weight percent was created, this was based on the stock solution of the doped PANI (**15**) being  $1.1 \text{ mg ml}^{-1}$ .

**FT-IR:** ( $\text{cm}^{-1}$ ); 3365, 2966, 2932, 2867, 2164, 2022, 1973, 1721, 1607, 1579, 1508 1451, 1383 - 1363, 1299, 1231, 1181, 1102, 1036, 1009, 919, 826.

##### 3.4.4.1 Preparation of Epikote 828 for a 20wt%.

Epikote 828 (440 mg) was made up to  $4.4 \text{ mg ml}^{-1}$  and polypropylene glycol bis(2-amino propyl ether) (220 mg) was made up to  $2.2 \text{ mg ml}^{-1}$  into DCM (100 ml) and was stirred in a sealed flask and then transferred to a spray apparatus for thin film casting.

##### 3.4.4.2 Preparation of Epikote 828 for a 10wt%.

Epikote 828 (990 mg) was made up to  $9.9 \text{ mg ml}^{-1}$  and polypropylene glycol bis(2-amino propyl ether) (495 mg) was made up to  $4.95 \text{ mg ml}^{-1}$  into DCM (100 ml) and was stirred in a sealed flask and then transferred to a spray apparatus for thin film casting.

##### 3.4.4.3 Preparation of Epikote 828 for a 5wt%.

Epikote 828 (2.09 g) was made up to  $20.9 \text{ mg ml}^{-1}$  and polypropylene glycol bis(2-amino propyl ether) (1.045 g) was made up to  $10.45 \text{ mg ml}^{-1}$  into DCM (100 ml) and was stirred in a sealed flask and then transferred to a spray apparatus for thin film casting.

##### 3.4.4.4 Preparation of Epikote 828 for a 2wt%.

Epikote 828 (5.39 g) was made up to  $53.9 \text{ mg ml}^{-1}$  and polypropylene glycol bis(2-amino propyl ether) (2.7 g) was made up to  $27.0 \text{ mg ml}^{-1}$  into DCM (100 ml) and was stirred in a sealed flask and then transferred to a spray apparatus for thin film casting.

#### 3.4.4.5 Preparation of Epikote 828 for a 1wt%.

Epikote 828 (10.89 g) was made up to 108.9 mg ml<sup>-1</sup> and polypropylene glycol bis(2-amino propyl ether) (5.45 mg) was made up to 54.5mg ml<sup>-1</sup> into DCM (100 ml) and was stirred in a sealed flask and then transferred to a spray apparatus for thin film casting.

#### 3.4.5 General preparation of acrylic resin/PANI composite solutions.

Methyl methacrylate (MMA) (180 g, 168.48 ml), methyl acrylate (15 g, 14.34 ml), ethylene glycol dimethacrylate (EGDMA) (18g, 18.918 ml), azobisisobutyronitrile (AIBN) (9 g), benzophenone (5.94 g) were added together and stirred for 1 hr. To the resin mixture doped PANI (**16** – **23**) (2 mg ml<sup>-1</sup>) (150 ml) the resin mixture was added in the following amounts; 5.7 g (5.02 ml) (5 wt%), 14.7 g (12.96 ml) (2 wt%) and 29.7 g (26.14 ml) (1 wt%).

**Acrylic resin: FT-IR:** (cm<sup>-1</sup>); 2950, 2149, 1718, 1415, 1388, 1238, 1122, 1047, 941, 875, 812.

##### 3.4.5.1 Doped PANI (**18**)/acrylate resin film 1 wt%

**FT-IR:** (cm<sup>-1</sup>); 3304, 2508, 2156, 2027, 1973, 1710, 1105, 700.

##### 3.4.5.2 Doped PANI (**20**)/acrylic resin film 1 wt%

**FT-IR:** (cm<sup>-1</sup>); 3437, 2930, 2166, 1967, 1716, 1454, 1379, 1277, 1126, 1046, 938, 886, 817, 754.

##### 3.4.5.3 Doped PANI (**21**)/acrylic resin film 1 wt%

**FT-IR:** (cm<sup>-1</sup>); 3351, 2914, 2498, 2158, 2032, 1975, 1719, 1628, 1456, 1365, 1291, 1148, 1036.

##### 3.4.5.4 Doped PANI (**23**)/acrylic resin film 1 wt%

**FT-IR:** (cm<sup>-1</sup>); (3659 – 2418), 3281, 2991, 2963, 2161, 1991, 1725, 1635, 1453, 1365, 1295, 1122, 1036, 958.

### 3.5 Preparation of Metal Plates.

#### 3.5.1 Preparation of mild carbon steel plates.

A single mild carbon steel plate was added to a concentrated HCl (35-37%) solution and was acid pickled until the acid was spent, releasing hydrogen during the process. A yellow solution was produced and producing a dull grey rough surface on the metal interfaces. Sample was then washed with deionised water until washings were clear. The sample was then washed with acetone to remove excess

surface water and to aid the production on an anhydrous surface. Subsequently the plate was store desiccated under vacuum until casting a polymer film.

### 3.5.2 Preparation of pure copper plates.

A single copper plate was added to a nitric acid (25%) solution and was acid pickled for 10 minutes, releasing gases during the process. A blue solution was yielded and a dull salmon pink-red rough copper surface remained. Samples were then washed with deionised water until washings were clear, followed by acetone washes to remove excess surface water and to aid the production on an anhydrous surface. Subsequently the plate was store desiccated under atmospheric pressure until casting a polymer film.

## 3.6 Preparation of Solvent Cast Films.

### 3.6.1 Preparation of polyaniline films.

The acid pickled metal was dipped into the polyaniline stock solutions (6 mg ml<sup>-1</sup>) (**15** – **23**) solution and allowed the solvent to evaporate under heat. There was a total of 20 successive cycles per plate producing dark green rough films which became darker upon successive casting. A successive cycle included the submersion of the metal plate into the polyaniline solution, the solvent was evaporated leaving a polyaniline coating.

### 3.6.2 Preparation of PVC films.

The acid pickled metal was dipped into a PVC solution (6 mg ml<sup>-1</sup>) and allowed the solvent to evaporate under gentle heat. There was a total of 20 successive cycles per plate producing clear-white smooth shiny films which became less transparent upon successive casting.

### 3.6.3 Preparation of polyaniline/PVC composite films.

The acid pickled metal was dipped into the composite solution of the various weight percent's and allowed the solvent to evaporate under heat. There was a total of 20 successive cycles per plate producing dark green smooth shiny films which became darker upon successive casting. The films got lighter as lower volume fraction polyaniline composition were used.

### 3.6.4 Preparation of polyaniline/epoxy resin composites

Polyaniline (1.1 mg ml<sup>-1</sup>) was sprayed onto the acid pickled metal plate mildly heating with a heat gun for 20 successive cycles. The plates were left to stand and

dry for 10 minutes. The resin/cure mixture was sprayed on to the plates under mild heating for 20 successive cycles producing a purple-blue sticky gel film at various percent weights (20, 10, 5, 2 and 1 wt%). The plates were left in the oven for 24 hr, yielding a solid clear shiny purple-blue coating.

#### *3.6.4.1 Preparation of polyaniline – epoxy resin composite (20wt%).*

Composite was made using polyaniline ( $1.1 \text{ mg ml}^{-1}$ ) and a resin/cure mixture of  $4.4 \text{ mg ml}^{-1}/2.2 \text{ mg ml}^{-1}$ .

#### *3.6.4.2 Preparation of polyaniline – epoxy resin composite (10wt%).*

Composite was made using polyaniline ( $1.1 \text{ mg ml}^{-1}$ ) and a resin/cure mixture of  $9.9 \text{ mg ml}^{-1}/4.95 \text{ mg ml}^{-1}$ .

#### *3.6.4.3 Preparation of polyaniline – epoxy resin composite (5wt%).*

Composite was made using polyaniline ( $1.1 \text{ mg ml}^{-1}$ ) and a resin/cure mixture of  $20.9 \text{ mg ml}^{-1}/10.45 \text{ mg ml}^{-1}$ .

#### *3.6.4.4 Preparation of polyaniline – epoxy resin composite (2wt%).*

Composite was made using polyaniline ( $1.1 \text{ mg ml}^{-1}$ ) and a resin/cure mixture of  $53.9 \text{ mg ml}^{-1}/27.0 \text{ mg ml}^{-1}$ .

#### *3.6.4.5 Preparation of polyaniline – epoxy resin composite (1wt%).*

Composite was made using polyaniline ( $1.1 \text{ mg ml}^{-1}$ ) and a resin/cure mixture of  $108.9 \text{ mg ml}^{-1}/54.5 \text{ mg ml}^{-1}$ .

**FT-IR:** ( $\text{cm}^{-1}$ ); 3391, 2965, 2929, 2870, 1608, 1507, 1456, 1373, 1292, 1245, 1179, 1079, 1027, 928.

### **3.6.5 Preparation of polyaniline – acrylic resin composites.**

Doped PANI/acrylic resin composites were added dropwise to the surface of one side of the metal until the metal surface was completely covered. The samples were left in the oven until the solvent evaporated off before placing another successive coat. A total of 20 successive cycles were conducted and the samples were left for a period of 24 hrs in the oven before turning over and the same was done on the opposite side. This practice was conducted for all the different weight percent composites.

### **3.7 Corrosion inhibition testing.**

A saline solution (3.5%) was sprayed on to the surface of a coated plates and control plates of both steel and copper. The plates were then suspended in an

enclosed heated propagator. To a saline solution (3.5%) in the heated propagator; a copper plate and a steel plate were submerged controls were also conducted on bare surface metals in the same manner. The relative humidity and air temperature inside and outside the propagator, the solution temperature was also obtained averaging around 23 °C for internal air temperature, solutions temperature was maintained at 25 °C and the relative humidity ranging from 70 – 90 %. Photographs were taken at time points; an hour after the initiation accelerated corrosion testing, 24 hrs, 48 hrs, 72 hrs, 96 hrs, 120 hrs, 144 hrs and 168 hrs. Plates were then desiccated under vacuum and stored until further analysis was conducted on the plates. This remained standard procedure for all samples produced.

## Chapter 4 RESULTS AND DISCUSSION:

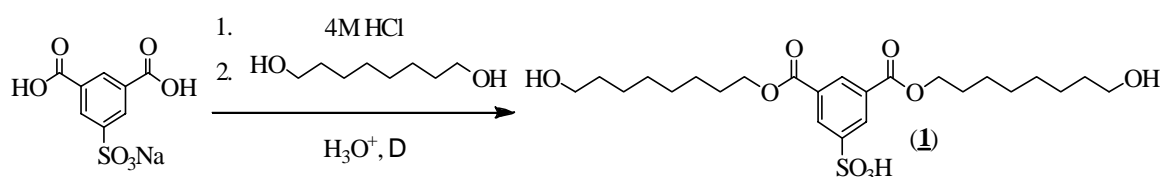
### DOPANTS SYNTHESIS AND DOPING STUDIES

#### 4.1 Synthesis of sulphonic acid series of dopants.

##### 4.1.1 The synthesis of bis(8-hydroxyoctyl) 5-sulphoisophthalic acid (**1**) (SIPAOH).

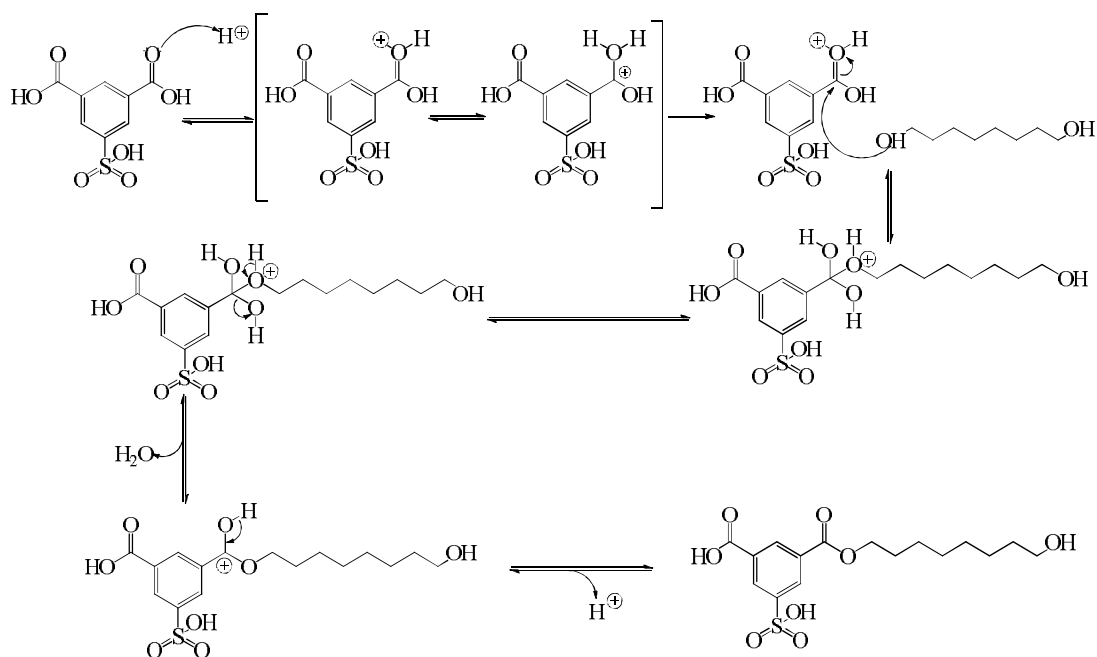
Synthesis of bis(8-hydroxyoctyl) 5-sulphoisophthalic acid (**1**) was performed according to a modified procedure by Kulszewicz-Bajer *et al.*<sup>88,92,101</sup> It was obtained via esterification of 5-sulphoisophthalic acid. Hydrochloric acid acts as a reaction catalyst, initiating the esterification between 1,8-octandiol and the 5-sulphoisophthalic acid moiety and generating the acidic proton (

Scheme 1: Synthesis of bis(8-hydroxyoctyl) 5-sulphoisophthalic acid (**1**).



Scheme 1: Synthesis of bis(8-hydroxyoctyl) 5-sulphoisophthalic acid (**1**).

The alcohol was supplied in large excess. The free acid of 5-sulphoisophthalic acid was formed upon heating the sodium salt in 4M HCl<sub>(aq)</sub> until there was total dissolution, cooling allowed for the acid to precipitate out of the acidic solution. The solution was heated and the alcohol was added, producing a white milky solution which eventually turned into a clear gold gel. Nitrogen was bubbled through the mixture until no more steam was liberated; this also allowed excess HCl to be liberated from the solution, whilst maintaining catalytic amounts to push the esterification forward (Mechanism 1). The viscous crude was then distilled under vacuum at 120°C and the excess alcohol was removed from the crude.



**Mechanism 1: The mechanism of esterification of 1,8-octanediol with 5-sulphoisophthalic acids leading to the eventual formation of bis(8-hydroxyoctyl) 5-sulphoisophthalic acid (1).**

The mechanism follows a typical acid catalysed esterification with the acid activating the carbon centre of the carboxylic acid, forming a positive charge on the double bonded oxygen creating the unstable intermediate. The electron density moved from the central carbon to the charged oxygen adding some stability to the system and allows the hydroxyl oxygen (nucleophile) to attack. Further similar rearrangements occurred until the condensation reaction releases water as the thermodynamically stable leaving group and eventually the acid catalyst is regenerated.

Distillation was successful occurring under heat and high vacuum (<0.1 mmHg), however with the successive removal of 1,8-octanediol, the viscosity of the crude increased making further removal of the alcohol starting material very difficult. Upon completion of the distillation, the crude product remained heavily contaminated with excess alcohol as shown by  $^1H$ -NMR, which also identified the appearance of a by-product (Figure 31).

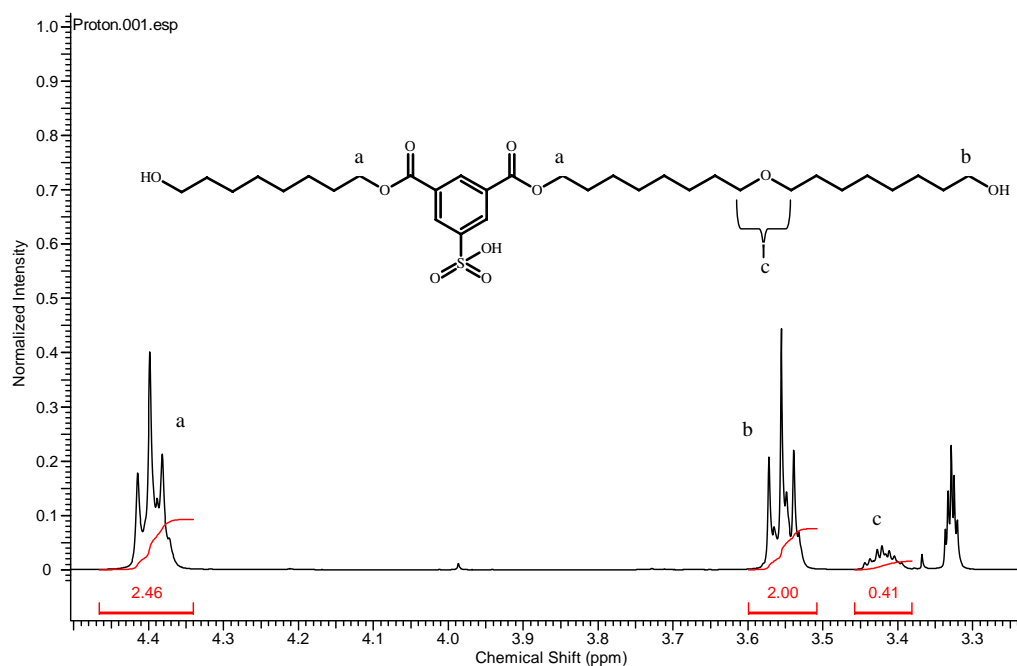


Figure 31:  $^1\text{H-NMR}$  portion representing the labelled areas; a, b and c. Integrations included for calculating the levels of alcohol dehydration to produce an ether linkage (c).

During the early stages of method development, many problems associated with the separation and purification of (**1**) were encountered. These problems arose due to the surfactant nature of (**1**); an initial problem that was encountered, was during the work up with ethyl acetate in order to remove excess 1,8-octanediol. The product prior to this was turned to its salt using different bases (sodium hydrogen carbonate or sodium hydroxide) in order to increase hydrophilicity and to keep it in water while extracting the excess 1,8-octanediol. This had no effect due to the surfactant nature of the product as its salt was as soluble in organic and aqueous phases. Subsequent processing with *n*-butanol (*n*-BuOH) post desalination also proved extremely difficult. Butanol shows slight miscibility in water, however when presented with the acidified dopant in an aqueous solution, the *n*-BuOH and water created an emulsion that did not separate upon leaving to stand and showed only little separation. Filtering the emulsion through celite, (known for its ability to disperse emulsions), proved ineffective. Drying of the solvent with  $\text{MgSO}_4$  was very difficult due to the hygroscopic properties of *n*-BuOH. In this instance the solvent was heavily saturated with water which solubilised the added  $\text{MgSO}_4$  as was evident upon solvent evaporation. Attempts at removing *n*-BuOH at reduced pressure at low temperature (30 - 40°C), to prevent hydrolysis or *trans*-esterification from occurring was difficult due to the viscosity and low volatility of

*n*-BuOH. Several other methods were employed to try to separate the starting materials from (**1**) but none showed any success.

Ion exchange chromatography is in theory a method that should have been a successful tool to separate 1,8-octanediol from the product but this proved difficult. Elution with 20% and 50% w/w acetic acid, 0.5M and 2M NH<sub>4</sub>OH and 2M sodium hydroxide all failed to displace the product from the column. No product was found in any of the fractions collected before elution. A solution of 8% w/v NaOH was recommended by the manufacturers Dowex, to regenerate the Ion Exchange resin which had no effect on elution.

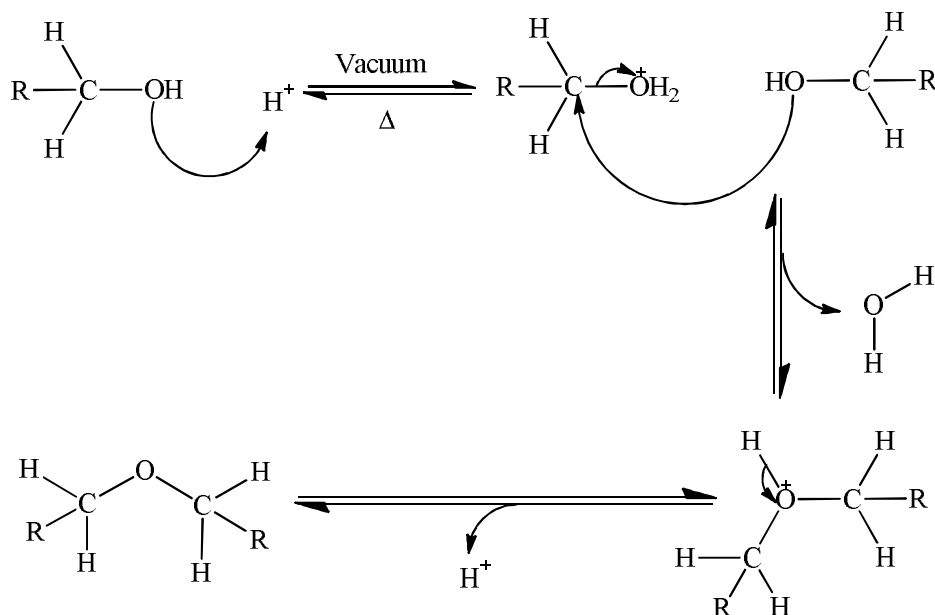
Bis(8-hydroxyoctyl) 5-sulphoisophthalic acid (**1**) showed very low mobility on silica with the exception when methanol was used as an eluent solvent, 1,8-octanediol on the other hand was readily mobile on silica gel with several solvents. Column chromatography was initially believed to be impractical due to the strong sulphonic acid interactions with the silica which accounted for the poor mobility, whilst the alcohol was easily eluted using polar solvents. This observation was exploited for the separation of the product. The product was trapped on the silica and the excess 1,8-octanediol was eluted-off using solvents that are less polar than methanol, the product was eventually washed off the silica using methanol. This method of purification proved to be highly effective and when compared with the process of vacuum distillation and solvent extractions, the yield increased to above 90%.

The purity of the compound and the structure was confirmed by NMR, Liquid chromatography mass spectrometry, elemental analysis and FT-IR. The <sup>1</sup>H-NMR spectra showed a double doublet at 8.68 ppm correlating to the protons attached to the aromatic ring, peaks corresponding to the alcohol protons occur at 4.40 and 3.56 ppm and finally the number of protons shown in the aliphatic region were in agreement with those in the proposed structure of (**1**). The FT-IR of the product displayed a broad band at 3411 cm<sup>-1</sup> which belongs to an OH vibrational stretch, two bands at 2936 and 2857 cm<sup>-1</sup> correspond to C-H stretching, with the vibration bending occurring at 1439 and 1410 cm<sup>-1</sup>. Bands at; 1723cm<sup>-1</sup> belong to the stretching of the carbonyl, a stretching vibration at 1636 cm<sup>-1</sup> relates to the aromatic ring. Weak bands at 1198, 1241, 1316 and 1322 cm<sup>-1</sup> were due to the vibrational

stretches of S=O. The liquid chromatography mass spectrometry showed a peak at 503.2 which corresponds to the positive molecular ion eluted from the column at 1.74 minutes.

*4.1.1.1 The alcohol dehydration of bis(8-hydroxyoctyl) 5-sulphoisophthalic acid (1) with excess 1,8 - octanediol in hot, dry low pressure conditions.*

As described briefly previously, there were significant problems found with the distillation and the subsequent side reaction which formed an ether product. The formation of the impurity was the result of alcohol dehydration. Such a process should have been unlikely to occur, however in view of the highly acidic environment and the high temperature during the esterification reaction, ether formation via alcohol dehydration was able to take place as a side reaction (Mechanism 2).



**Mechanism 2: Mechanism to demonstrate the formation of an ether product via alcohol dehydration.**

The reaction was initiated by the protonation of the alcohol which was driven by high temperatures and the reduced pressure. The positive moiety created was highly unstable with entropy favouring the removal of the hydronium species in the form of water. Electron density will be towards the oxygen ( $\delta^-$ ), inducing electron deficiency ( $\delta^+$ ) around the carbon centre, therefore the carbon was attacked by the nucleophilic hydroxyl group of a 1,8-octanediol chain to stabilise the highly reactive carbon intermediate and follows a typical S<sub>N</sub>1 substitution reaction. The

positive charge was then placed on the newly formed ether linked oxygen and the acidic proton catalyst was therefore liberated and regenerated.

Upon a reduction of the temperature during distillation to below 100°C, it was evident there was a correlated reduction in the production of the by-product reinforcing the link between the experimental conditions and the production of the ether.

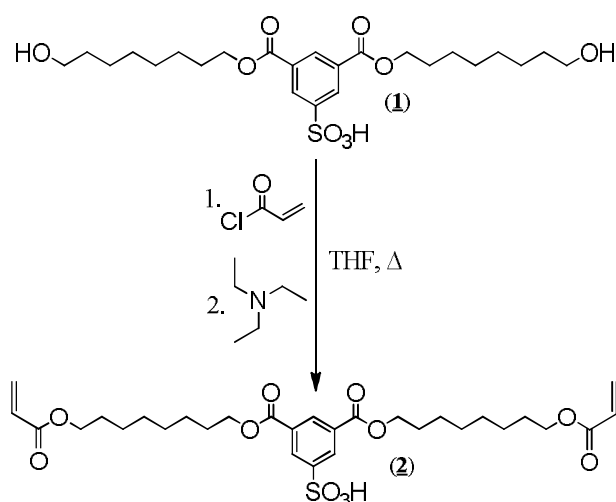
The  $^1\text{H-NMR}$  (Figure 31) showed an anomalous multiplet peak at around 3.42 ppm, this was attributed to protons adjacent to an ether linkage. Bis(8-hydroxyoctyl)-5-sulphoisophthalic acid (**1**) was contaminated at levels around 10% based on integration intensities of the  $^1\text{H-NMR}$  and this was confirmed by mass spectrometry, with a peak at 501 m/z for the molecular ion and another at 629 m/z for the contaminant. The increase of 128 amu correlated to a hydroxyl octyl unit of 128 amu, and confirmed the two moieties were connected via an ether linkage. The percentage of contamination was confirmed by comparing the integrals of the protons (**b**) adjacent to the hydroxyl group ( $\text{CH}_2\text{OH}$ ) with the protons (**c**) either side of the ether ( $\text{CH}_2\text{-O-CH}_2$ ). The integration of the impurity was 0.41 which correlated to four protons surrounding an ether oxygen link; therefore for one proton an integration of 0.1125 would be expected. The percentage of impurities was calculated using Equation 19 to determine the levels of contamination at 10%.

$$\frac{0.1125}{(0.1125 + 1.00)} \times 100 = 10.11 \%$$

Equation 19: Calculation of the impurities using the integrations obtained from the  $^1\text{H-NMR}$ .

#### 4.1.2 The synthesis of bis(8-acryloxy octyl)-5-sulphoisophthalic acid (**2**) (SIPAOA) and bis(8-methacryloxy octyl) 5-sulphoisophthalic acid (**4**) (SIPAOA).

Bis(8-acryloxy octyl)-5-sulphoisophthalic acid (**2**) and bis(8-methacryloxy octyl)-5-sulphoisophthalic acid (**4**) were prepared by esterification of bis(8-hydroxyl-octyl)-5-sulphoisophthalic acid (**1**) with acryloyl chloride and methacryloyl chloride respectively in the presence of stoichiometric amounts of triethylamine as shown in Scheme 2.

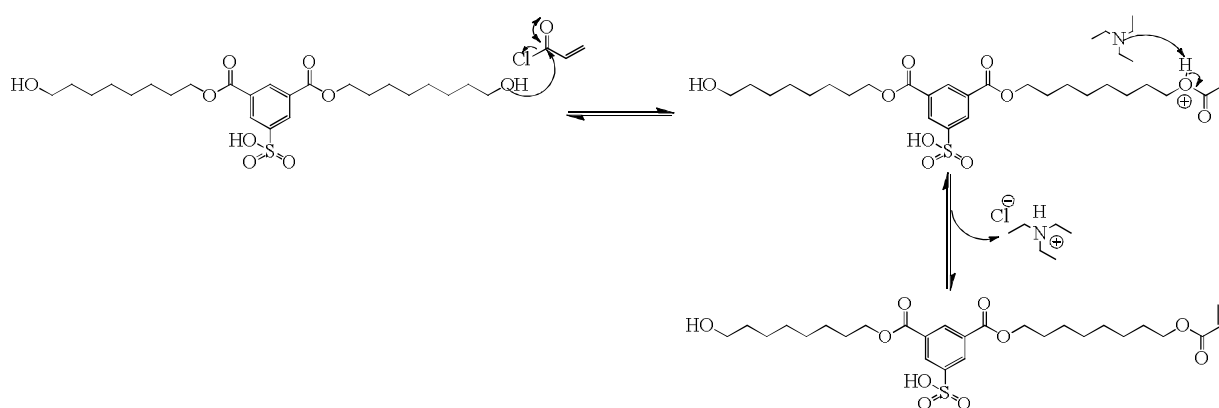


Scheme 2: The synthesis of bis(8-acryloxy octyl) 5-Sulphoisophthalic acid (**2**).

The synthesis of both (**2**) and (**4**) were carried out in a dry and purged atmosphere ( $\text{N}_2$ ) with dry THF at  $50^\circ\text{C}$  for 1 hour, it was crucial to carry out the reactions in the absence of light due to the reactivity and sensitive nature of the acrylic acid chlorides. Triethylamine was added to the solution prior to the addition of the acrylic material, these were added dropwise. Initially milky cream precipitants were formed which upon completion turned dark orange to golden brown and were filtered resulting in a substantial loss of product. The quenching agent and antioxidant (*p*-methoxyphenol) was incorporated into both systems at around 200 ppm, it was noticed that the methacrylic product was less reactive and more stable than the acrylic component, with reduced sensitivity to light, heat or acid treatment. The products were acid washed and extracted with ethyl acetate. Several attempts were made to develop an optimised methodology, removing the filtration step and the main source of yield loss. The products showed better mobility on silica gel than

the starting material and were able to be eluted using a mix of chloroform/methanol at a ratio of 9:1.

The mechanism (Mechanism 3) for this esterification process occurs via an  $S_N2$  type reaction in multiple steps; The initial step was the nucleophilic attack on the acid chloride carbon centre, with the elimination of the chloride ion, the second stage was the removal of the acidic proton by triethylamine from the newly formed ester, with the formation of ammonium chloride inevitably which precipitates out of solution.



**Mechanism 3:** Example showing part of the esterification leading to the eventual formation of bis(8-acryloxy octyl) 5-Sulphoisophthalic acid (2).

The syntheses of these products were problematic due to the inherent nature of the dopant and their readiness to form crosslinks; the dry products (2) and (4) showed limited solubility in aqueous acidic medium and required the presence of organic solvents to induce some degree of solubility. Toluene, methanol and other such solvents enabled solubility however proved to be detrimental during extraction. The use of chloroform was difficult and 3 layers were noticed with the emulsion becoming inseparable. A yellow crude product of around 50% was obtained upon removal of the solvent which darkened, turning brown over time. The products were subsequently stored in sealed containers in the freezer preventing cross-linking. A range of dry solvents were used for the reaction to maximise the solubility of the starting bis(8-hydroxyl octyl) 5-sulphoisophthalic acid (1). The yields were not vastly increased; DMF, DMSO and NMP were all utilised, however the reactions do not produce clean products when compared to THF as the solvent

system. In the case of DMF there were slight increases in solubility but more particulates were found than seen when THF was used as the solvent. DMSO totally solubilised the starting material, but no reaction occurred, a result of the reactivity of DMSO when presented with acryloyl chloride which produced the strong oxidising activated DMSO compound similar to the oxidiser seen in the Swern reaction. Solvent systems such as NMP were much like DMSO, resulting in the total solubility of the starting sulphonic acid (**1**), but were hygroscopic and were extremely difficult to remove even under high vacuum.

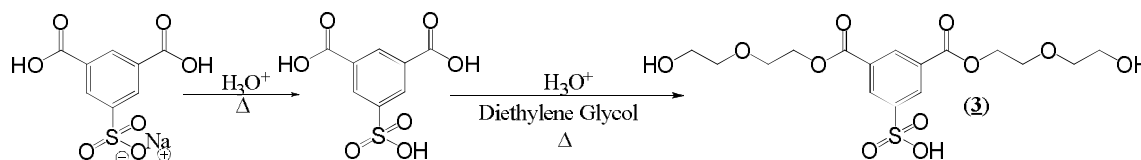
The products (**2** and **4**) were characterised by NMR, mass spectroscopy, FT-IR. Early NMR results showed that there were impurities from both cross-linked and ether products of (**1**) along with the desired product. Mass spectrometry showed the molecular ions for both (**2**) at 609 and the liquid chromatography mass spectrometry of (**4**) confirmed a peak at 4.04 minute corresponding to the positive molecular ion at 639.3.

The  $^1\text{H-NMR}$  of (**2**) showed a doublet at 8.61 ppm with a more deshielded shift to 8.65 ppm for (**4**) corresponding to the three protons on the aromatic ring. Three peaks of double doublet between 6.35 – 5.78 ppm were characteristic of the acrylic group found in (**2**), whilst peaks at 6.23 and 5.65 ppm correspond to the methacrylate group's protons. The protons involved in the esters were identified at 4.28 and 4.11 ppm for (**2**) and 4.13 and 3.76 ppm for (**4**). Finally, the peaks at 1.94 ppm were the protons of the methyl group attached to the acrylic group. There were no signs of contamination in the aliphatic region and all protons correlate to the product.

The FT-IR of the products displayed a band at  $1728\text{ cm}^{-1}$  and  $1786\text{ cm}^{-1}$  belonging to the stretching vibration of the carbonyls for (**2**) and (**4**) respectively. A stretching vibration at  $1651\text{ cm}^{-1}$  (**2**) and  $1637\text{ cm}^{-1}$  (**4**) and a weaker band at  $1463\text{ cm}^{-1}$  (**2**) related to the aromatic ring. Weak bands at  $1356$ ,  $1322$  (**2**) and  $1320\text{ cm}^{-1}$  (**4**) were due to the vibrational stretch of S=O. Peaks at  $1288\text{ cm}^{-1}$  and at  $1073\text{ cm}^{-1}$  in (**2**) both belong to the stretching of the sulphur centre of the acid. Other bands at  $3391\text{ cm}^{-1}$  (**2**) and  $3411\text{ cm}^{-1}$  (**4**) correlated to the vibrational stretch of an OH of the acid group.

### 4.1.3 The synthesis of bis[2-(2-hydroxy-ethoxy)-ethyl]-5-sulphoisophthalic acid (**3**) (SIPADEG).

The synthesis of bis[2-(2-hydroxy-ethoxy)-ethyl] 5-sulphoisophthalic acid was conducted via the esterification of diethylene glycol with the 5-sulphoisophthalic acid and the product was purified via silica gel column chromatography and obtained as a golden gel in 81.58% yield (Scheme 3).



**Scheme 3: Synthesis of 5-Sulphoisophthalic acid bis [2-(2-hydroxy-ethoxy)-ethyl] ester (**3**) (SIPADEG).**

The reaction was carried out using the same method carried out to obtain (**1**) and was purified via silica gel column chromatography using methanol/chloroform 1:4 which was sufficient to elute the product.

The process of distillation of excess ethylene glycol was much easier and quicker than the distillation of bis(8-hydroxyl octyl) 5-sulphoisophthalic acid (**1**) under very high vacuum (<0.1 mmHg) giving a golden brown gel, however transfer of product from the reaction vessel was much more difficult. The flask was first submerged into liquid nitrogen which turns the gel into a glass like solid, which could be chipped without too much effort, allowing for a clean transfer to another vessel. Bis[2-(2-hydroxy-ethoxy)-ethyl] 5-sulphoisophthalic acid (**3**) held one major advantage over its predecessor, namely its increased solubility over a range of solvents including water. This was beneficial for the purification of the dopant by column chromatography (MeOH: CHCl<sub>3</sub> 1:4), and the mobility of this dopant on the column does not appear to cause any problems.

The purity of the compound and the structure was confirmed by NMR, liquid chromatography mass spectrometry and FT-IR. The <sup>1</sup>H-NMR spectra showed a doublet at 8.66 ppm correlating to the protons attached to the aromatic ring, peaks corresponding to the alcohol protons occur at 3.99 ppm, the double triplet at 3.64 correlates to the protons around the ether centre and the protons adjacent to the hydroxyl group are found at 3.37 ppm. The FT-IR of the product displayed a broad band at 3391 cm<sup>-1</sup> which belongs to the OH vibrational stretch, two bands at 2932 and 2879 cm<sup>-1</sup> correspond to C-H stretching, with the vibration bending occurring

at 1458 and 1398  $\text{cm}^{-1}$ . Bands at 1728  $\text{cm}^{-1}$  belong to the stretching vibration of the carbonyls, a stretching vibration at 1651  $\text{cm}^{-1}$  relates to the aromatic ring. Weak band at 1322  $\text{cm}^{-1}$  was due to the vibrational stretch of S=O also 1356, 1288 and 1200  $\text{cm}^{-1}$ . The ester and ether peaks are at 1125, 1057 and 920  $\text{cm}^{-1}$ . Liquid chromatography mass spectrometry showed a peak at  $m/z = 423.2$  for the positive molecular ion after 0.96 minutes elution time.

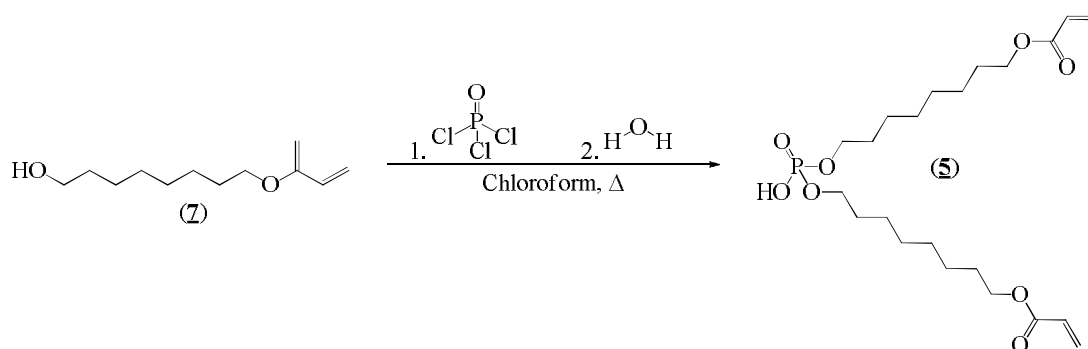
## 4.2 Synthesis of Phosphoric Acid Diesters Series of Dopants.

### 4.2.1 The synthesis of bis(8-acryloxy octyl) hydrogen phosphate (DAOHP) (**5**) and the synthesis of bis(8-methacryloxy octyl) hydrogen phosphate (DMOHP) (**6**).

Bis(8-acryloxy octyl) hydrogen phosphate (**5**) and bis(8-methacryloxy octyl) hydrogen phosphate (**6**) were prepared according to modified methods by Muhika et al.<sup>104,105</sup> and Jang and Jeong<sup>106</sup>. Several methods were employed to obtain (**5**) and (**6**) in order to determine the optimised synthetic route. Phosphodiester (**5**) was obtained by 3 methods as described below with the methacrylated version (**6**) being obtained by the latter 2 methods. The crudes were processed and purified by either silica gel column chromatography or by solvent extraction depending on the method used, to afford a slight yellow clear heavy oil in yields of; 0.8% for methodology one; 27.34% (**5**) and 67.54% (**6**) for methodology two; 10.53% (**5**) and 21.84% (**6**) for methodology three.

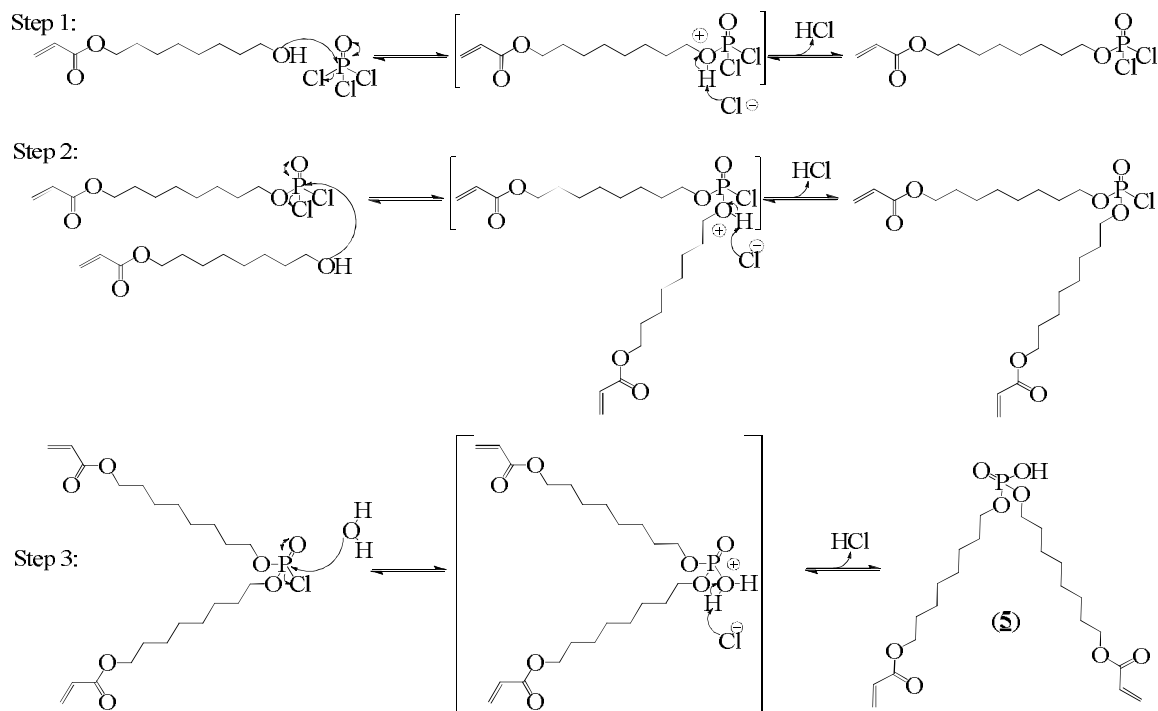
#### 4.2.1.1 The synthesis of bis(8-acryloxy octyl) hydrogen phosphate (**5**) via original developed methods (Method 1).

Bis(8-acryloxy octyl) hydrogen phosphate (**5**) was prepared according to an original developed procedure. The crude was purified via silica gel column chromatography to obtain a pale yellow heavy oil in 0.8% yield (Scheme 4).



Scheme 4: The Synthesis of bis(8-acryloxy octyl) hydrogen phosphate (**5**) by Method 1.

The reaction was carried out at 50°C for an hour in chloroform containing the alcohol, 8-hydroxyoctyl acrylate (**7**). Phosphorus oxychloride and water were added to the heated mixture dropwise and were used at 0.5 equivalents to drive the successful synthesis of the diester product.



**Mechanism 4: The Synthesis of Bis(8-acryloxy octyl) Hydrogen Phosphate (**5**) in the presence of water (Method 1).**

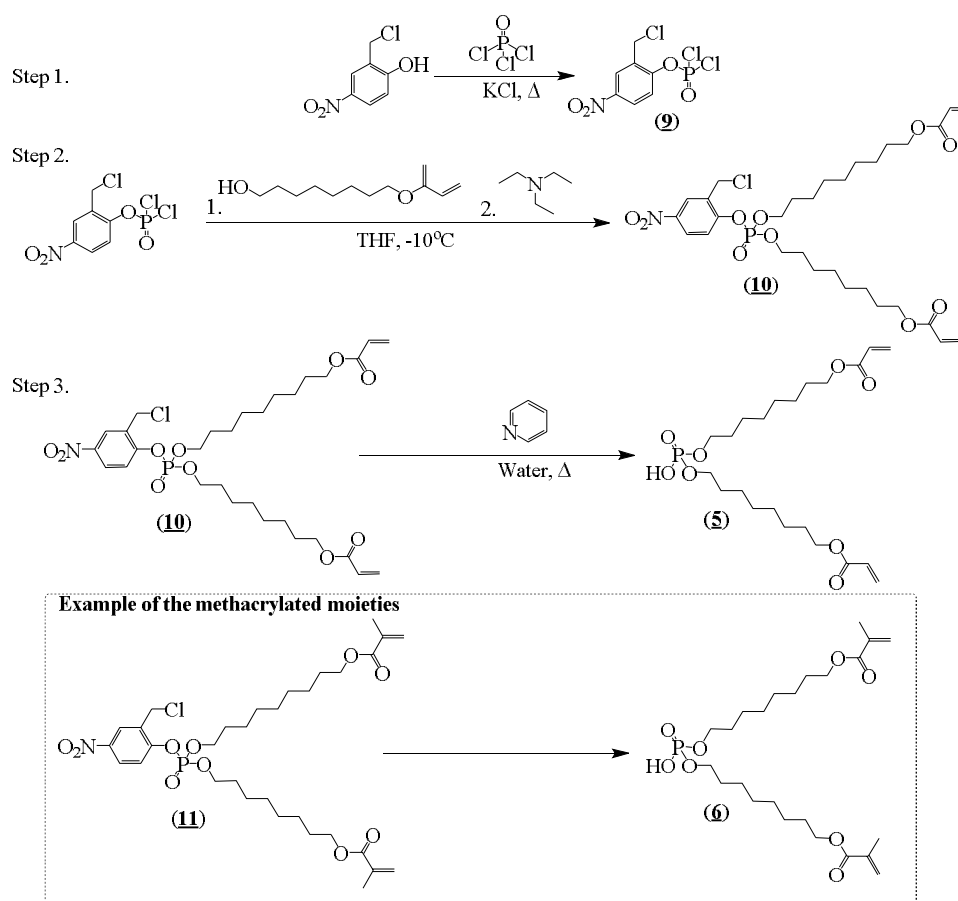
The procedure follows an  $\text{S}_{\text{N}}2$  type nucleophilic substitution with the initial attack of the acrylated alcohol onto the phosphorus centre to substitute a chloride, this formed a positively charged intermediate. The chloride subsequently acted as a Lewis base and attacked the acidic proton, leading to the release of hydrogen chloride. The final step utilised the water which at that point was the strongest nucleophile present, substituting the final chloride. The chloride in turn acted as a Lewis base stripping the acidic proton from the positively charged oxygen and stabilised the system releasing hydrogen chloride (Mechanism 4).

Product (**5**) was characterised and its purity determined by  $^1\text{H}$ -NMR,  $^{13}\text{C}$ -NMR,  $^{31}\text{P}$ -NMR and FT-IR. The  $^1\text{H}$ -NMR showed three double doublets in the region of 6.37 – 5.79 ppm which correspond to the acrylic protons, peaks at 4.12 ppm and 3.99 ppm relate to the protons adjacent to the esters. The  $^{31}\text{P}$ -NMR showed a single peak at -0.73 ppm which belongs to the phosphoric acid diester. The FT-IR of the

product displays a strong broad peak at  $3411\text{ cm}^{-1}$  due to OH stretch vibration of the acid. Strong absorption at  $2926\text{ cm}^{-1}$  and  $2853\text{ cm}^{-1}$  are due to C-H vibrational stretching of the aliphatic chains, with further peaks at  $1455$  and  $1378\text{ cm}^{-1}$  corresponding to C-H vibration bending of the aliphatic chains. The esters are represented by a peak at  $1786\text{ cm}^{-1}$  which relates to C=O vibration stretching. Peaks at  $1294$  and  $1242\text{ cm}^{-1}$  correspond to P=O stretching and the bands at  $1043$  and  $950\text{ cm}^{-1}$  belong to P-O-C aliphatic asymmetric stretching.

*4.2.1.2 The synthesis of bis(8-acryloxy octyl) hydrogen phosphate (5) and bis(8-methacryloxy octyl) hydrogen phosphate (6) via a modified method of Muhika et al<sup>104,105</sup>(Method 2).*

Bis(8-acryloxy octyl) hydrogen phosphate (5) and bis(8-methacryloxy octyl) hydrogen phosphate (6) were obtained by first protecting the phosphorus oxychloride with 2-chloromethyl-4-nitrophenol. This allowed for the selective esterification of one of the chlorides first, followed by reaction with the acrylated alcohol producing the desired diesters. The protecting group was then selectively cleaved leaving the phosphoric acid diester as a clear light yellow heavy oil in 27.34% yield (5), 67.54% (6). A scheme for the synthetic route is shown below and uses (5) to demonstrate the procedure (Scheme 5).



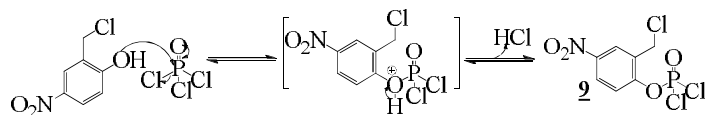
**Scheme 5: The synthesis of bis(8-acryloxy octyl) hydrogen phosphate (5) via Method 2.**

The products were obtained by similar mechanisms previously described; the procedure started with the protection of one of the ester sites, this was achieved by selectively substituting one of the chlorides and a protecting group was attached. This selective substitution was controlled by stoichiometry and ensured that only one chloride was displaced at a time due to the different and increased energy of substituting the other chlorides in succession. The remaining chlorides were subsequently substituted by the acrylated alcohol and the protecting group was cleaved.

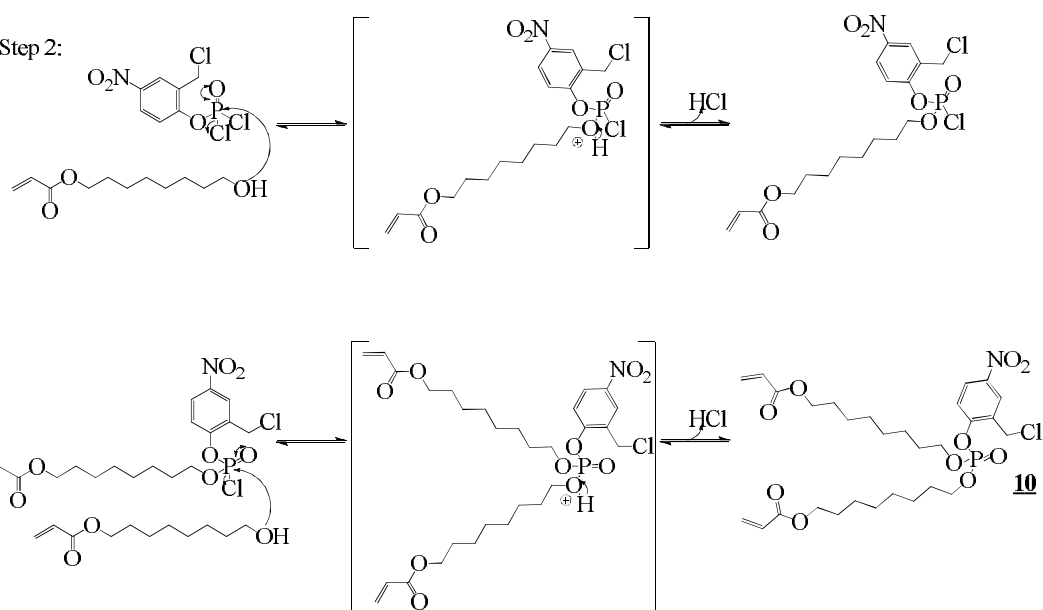
Initially the reaction was carried out with the phosphoryl chloride acting as both the solvent and the reagent in hot, dry conditions during the reaction. The crudes were distilled under high vacuum via a Kugelrohr oven at 170°C (bp 165-167°C at 0.2 mmHg) to obtain 2-chloromethyl-4-nitrophenyl phosphorodichloridate (**9**) (Scheme 5). The product was placed into dry THF and added dropwise to the acrylic alcohol in the presence of triethylamine at -10°C, this ensured the rate of esterification was controlled. The crudes were filtered removing the ammonium salt and evaporated to

dryness, yielding 2-chloromethyl-4-nitrophenyl phosphorodi(octyl acrylate) (**10**) and 2-chloromethyl-4-nitrophenyl phosphorodi(octyl methacrylate) (**11**). In the final step the products were placed into aqueous pyridine for several days before being mixed and heated to 85°C for 2 hours, the pyridine activated at this stage the protecting group towards cleavage by hydrolysis, yielding the desired phosphodiesters.

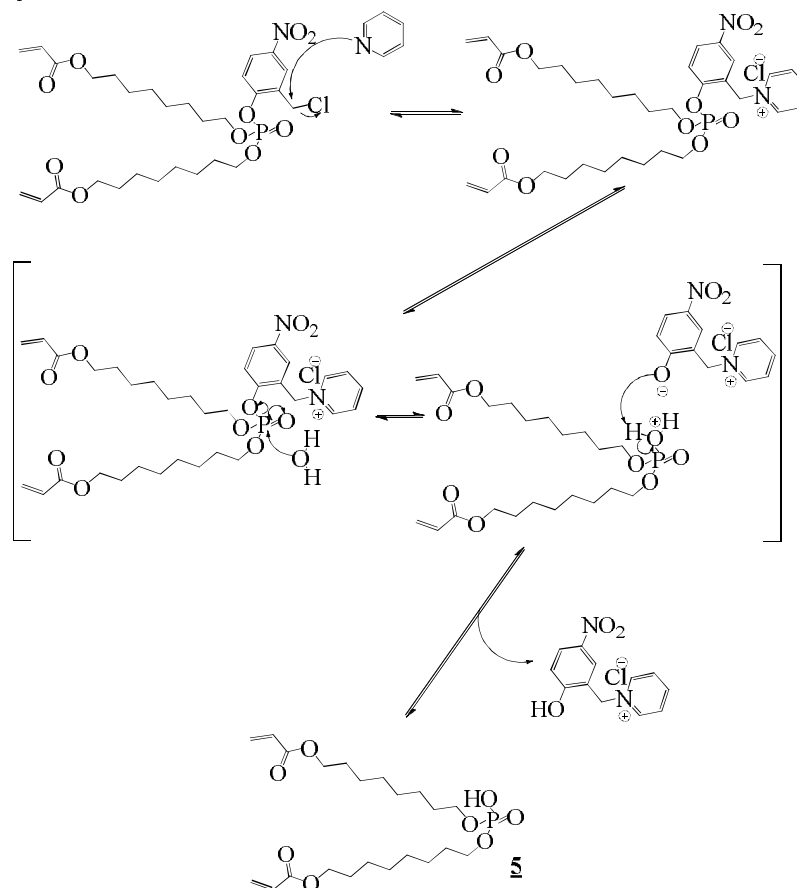
Step 1:



Step 2:



Step 3:



**Mechanism 5: The mechanism of Synthesis of bis(8-acryloxy octyl) hydrogen phosphate (5) via ester protection.**

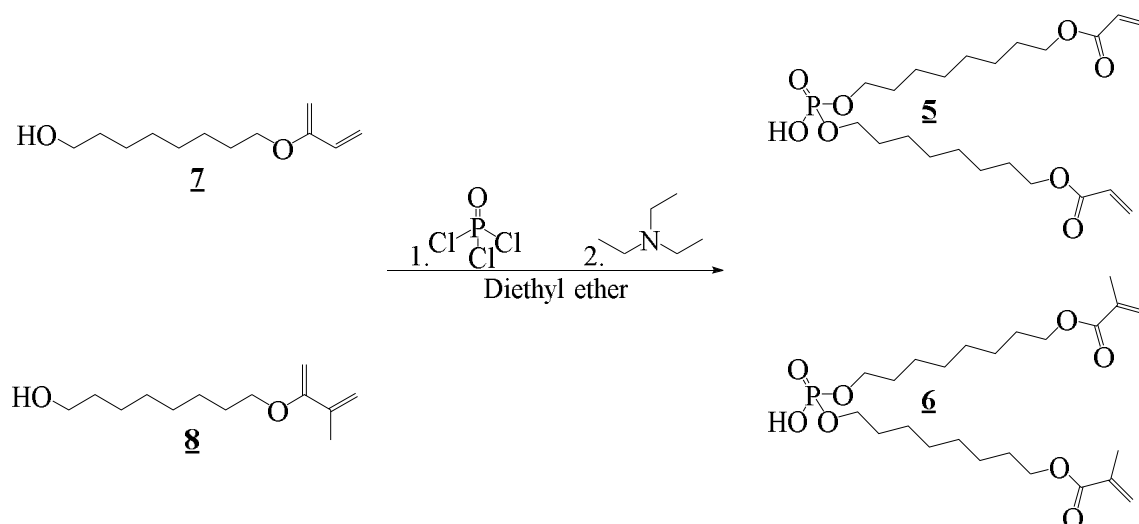
The mechanism (Mechanism 5) by which the phosphodiester was produced proceeded via similar steps to those discussed and shown in Mechanism 4. The stability of the protecting group was such that any efforts made hydrolysing the protecting group would result in the cleavage of the newly formed esters. To address this, the protecting group was ‘activated’ ensuring this was the more favourable leaving group. The term ‘activated’ referred to the quaternisation of pyridine with the chloromethylene of the protecting group, this made the group bulky, strained and electron withdrawing with the electron density shifted to the aromatic system for stability. A momentarily induced dipole was formed and resulted in the hydrolysis of this group in the aqueous environment. After hydrolysis the positive charged phosphodiester was deprotonated by the now negative charged (2-methylpyridinium-4-nitrophenoxide) protecting group which produced 2-methylpyridinium-4-nitrophenol as the by-product.

The purity and the products was confirmed by  $^1\text{H-NMR}$  and  $^{31}\text{P-NMR}$ . The  $^1\text{H-NMR}$  spectrum showed three double doublets at between 6.41 – 5.83 ppm that correlated to the acrylic protons of (**5**) and two singlets between 6.05 - 5.50 ppm for the methacrylic protons. Two peaks were seen for the ester at 4.16 and 4.02 ppm (**5**) and 4.09 and 3.98 ppm (**6**). Finally the aliphatic region showed a prominent singlet at 1.90 ppm for the methyl groups of the methacrylate (**6**). The  $^{31}\text{P-NMR}$  spectra showed a single peak at 1.19 ppm (**5**) and 0.65 ppm (**6**) which alluded to the presence of one chemical environment for the phosphorus centre.

The FT-IR results displayed a broad band at  $3446\text{ cm}^{-1}$  which belonged to the acidic OH vibrational stretching, C-H stretching was found at  $2932$  and  $2855\text{ cm}^{-1}$  with C-H vibrational bending at  $1456$ , strong bands at  $1720$  and  $1637\text{ cm}^{-1}$  were associated with the C=O vibrational stretch and the C=C. The product showed bands at  $1320$ ,  $1298\text{ cm}^{-1}$  which were shoulder peaks correlating to P=O vibrational stretching, a broad weak peak at  $2106\text{ cm}^{-1}$  was seen for phosphorus acid and ester O–H stretching. The peaks at  $1061$ ,  $945$ ,  $814\text{ cm}^{-1}$  correlated to the aliphatic asymmetric P–O–C, P–OH and aliphatic symmetric P–O–C vibrational stretching respectively.

#### *4.2.1.3 The synthesis of bis(8-acryloxy octyl) hydrogen phosphate (**5**) via a modified method of Jang and Jeong<sup>106</sup> (Method 3).*

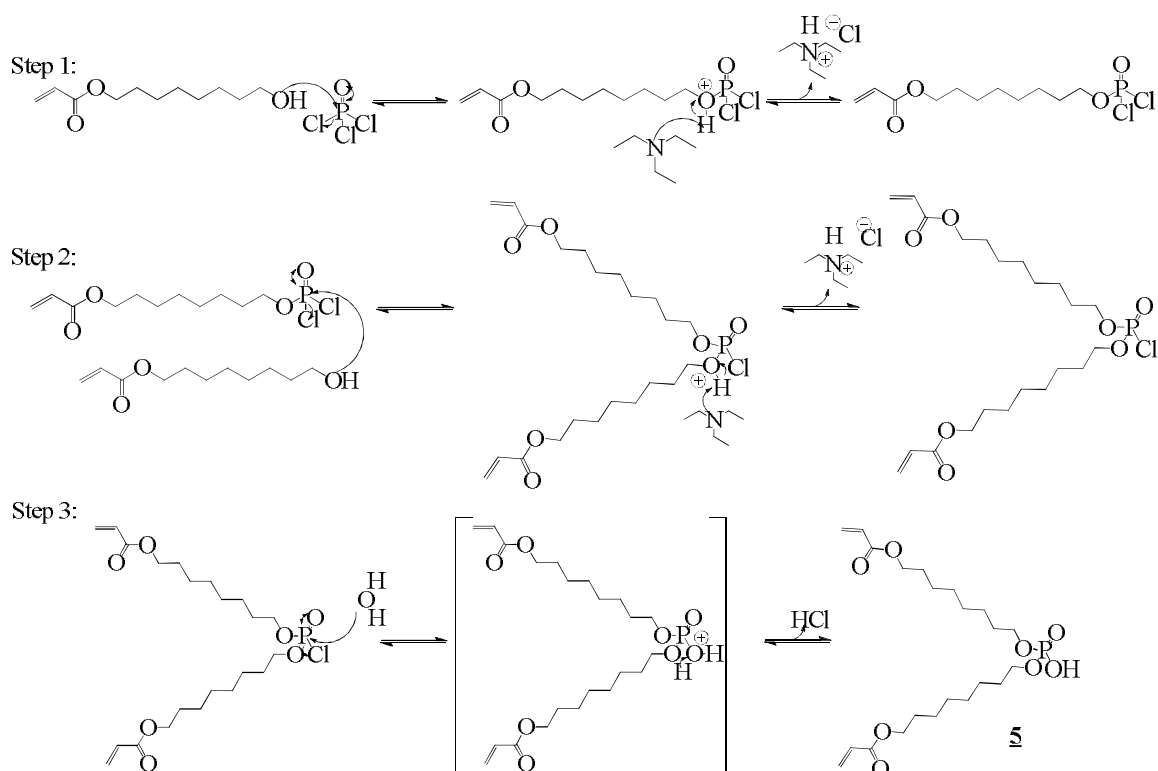
Bis(8-acryloxy octyl) hydrogen phosphate (**5**) and bis(8-methacryloxy octyl) hydrogen phosphate (**6**) were also prepared according to a modified method described by Jang and Jeong<sup>106</sup>. Like the previous methods employed, the reaction was carried out via the nucleophilic substitution of the chlorides with (**7**) and (**8**), after completion the products were obtained by solvent extraction into diethyl ether giving as pale yellow clear heavy oils in 10.53% yield for both (**5**) and (**6**) (Scheme 6).



**Scheme 6: The Synthesis of bis(8-acryloxy octyl) hydrogen phosphate (5) and bis(8-acryloxy octyl) hydrogen phosphate (6) via a modified method of Jang and Jeong<sup>106</sup>. [Method 3](#).**

The esterification was carried out in the presence of triethylamine which was in 0.5 molar equivalents to the alcohol and was equimolar to phosphorus oxychloride. The reaction was cooled in an ice bath and left over a 24 hr period and produced a creamy white milk like solution with a white effervescent released.

The mechanism for the reaction proceeded in three steps as shown in Mechanism 6 and followed the pattern of events as previously described in the previous methods. This approach was driven by the presence of the amine, removing the acidic protons that were produced during the esterification of the first step. The amine and the phosphate were present in stoichiometric amounts and prevented the formation of the triester. Upon completion the crude was treated with 1M HCl solution to yield the phosphodiester. The purity and the products was confirmed by NMR, mass spectrometry and FT-IR.



**Mechanism 6: The esterification of phosphorus oxychloride according to a modified method of Jang and Jeong<sup>106</sup>**

#### 4.2.1.4 Problems encountered during the synthesis of the phosphodiester.

During the synthesis of bis(8-methacryloxy octyl) hydrogen phosphate (**6**), it was noticed that the presence of the anti-oxidant *p*-methoxy phenol produced a side reaction and competed with the functionalised alcohol during the esterification. The products that were produced by this side reaction were extremely difficult to separate from the desired product. The <sup>1</sup>H-NMR confirmed the side reaction as shown in Figure 32, showing the spectra of contaminated bis(8-methacryloxy octyl) hydrogen phosphate (**6**) as an example. The percentage of contamination was calculated by comparing the integrals of the protons (**A** - **B**) of the aromatic system of *p*-methoxyphenol, with the protons (**C**) of the methacrylic protons (-C(CH<sub>3</sub>)=CH<sub>2</sub>).

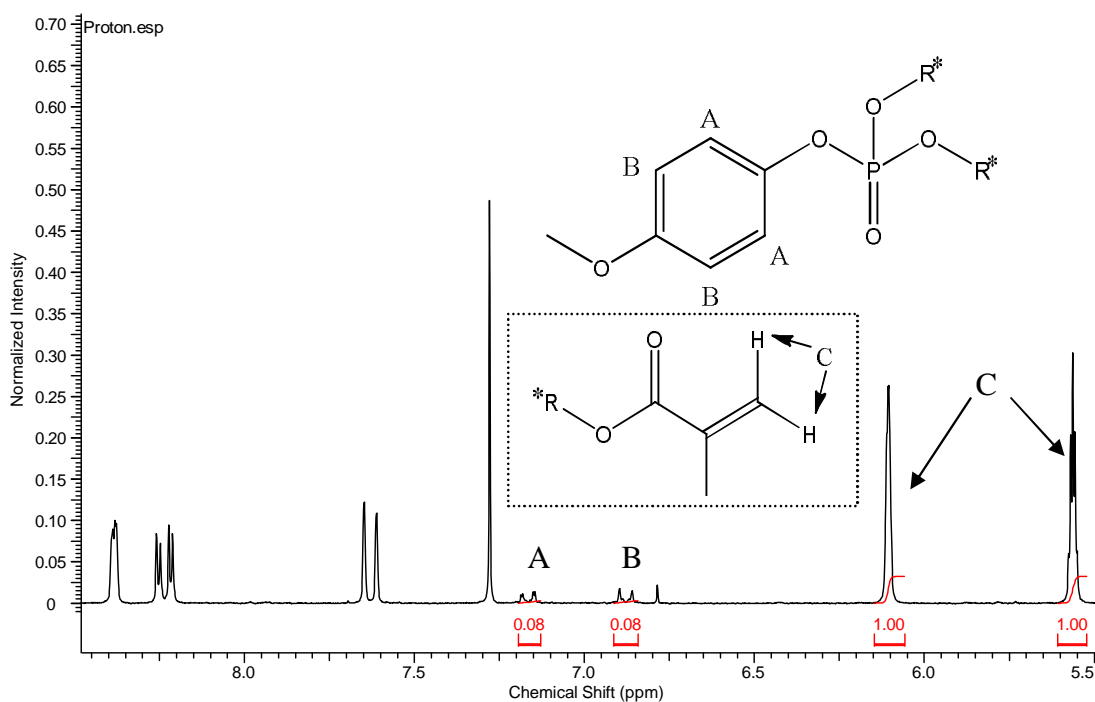


Figure 32:  $^1\text{H-NMR}$  displaying side products produced in the presence of *p*-methoxyphenol.

The integration of the impurity was 0.08 for the two protons, therefore for one proton an integration of 0.04 would be expected. Thus the percentage of impurities was calculated to be around 4% using the calculation demonstrated in Equation 20.

$$\frac{0.04}{(0.04 + 1.00)} \times 100 = 3.85 \%$$

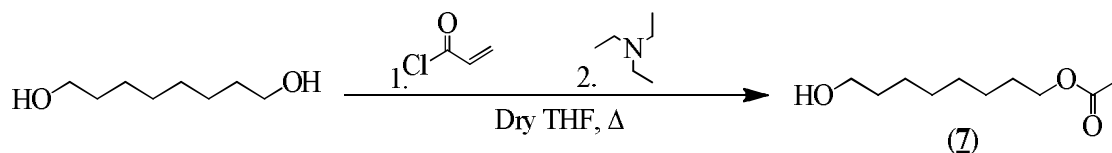
Equation 20: Calculation of the impurities using the proton integrations obtained from the  $^1\text{H-NMR}$  displaying the side product.

The subsequent reactions were therefore performed without the presence of the anti-oxidant and needed much more care during synthesis to prevent the cross-linking of the acrylates.

### 4.3 Synthesis of additional and auxiliary compounds.

#### 4.3.1 The synthesis of 8-hydroxyoctyl acrylate (**7**) and the 8-hydroxyoctyl methacrylate (**8**).

8-Hydroxyoctylacrylate (**7**) and 8-hydroxyoctyl methacrylate (**8**) were prepared by simple esterification of 1,8-octanediol with acryloyl chloride or methacryloyl chloride respectively, as seen in Scheme 7 using the formation of (**7**) as an example, giving a clear pale yellow heavy oil of 71.89% yield (**7**) and 60.55% yield (**8**).



**Scheme 7: The Synthesis of 8-hydroxyoctyl acrylate (7).**

The reactions were carried out in dry THF at 50°C for 2 hours which upon completion the crudes were passed through a silica gel column; the products were eluted with ethyl acetate and chloroform in a ratio of 1:4.

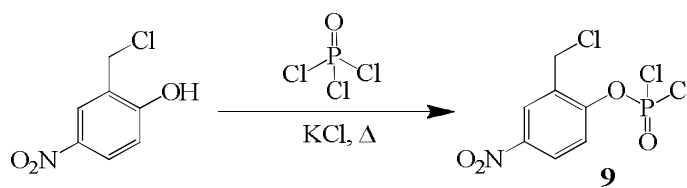
Addition of the *p*-methoxyphenol stabiliser into the reaction mixtures to produce (7) and (8) was dependant on their subsequent use. The synthesis of the phosphodiesteres required 8-hydroxyoctylacrylate (7) and 8-hydroxyoctylmethacrylate (8) without the presence of *p*-methoxyphenol due to the reasons previously discussed.

The purity of the products was confirmed by NMR, mass spectrometry and FT-IR. The <sup>1</sup>H-NMR shows three double doublet peaks due to the acrylic protons of (7) in the regions between 6.38 – 5.78 ppm and two double doublet peaks for the methacrylic protons of (8) between 6.04 and 5.48 ppm, a triplet at 3.60 ppm corresponding to the methylene protons adjacent to the alcohol. Methylene protons adjacent to the ester groups were identified by a triplet peaks at 4.12 ppm for (7) and at 4.08 ppm for (8). The aliphatic region showed the correct number of protons for the product. A mass spectrometry peak at *m/z* = 201.3 was observed for the molecular ion of (7) whilst the methacrylic product (8) showed a positive molecular ion at *m/z* = 215.165. The FT-IR results displays broad bands around 3418 cm<sup>-1</sup> belonging to the acidic OH vibrational stretching, C-H stretching was found around 2932 and 2857 cm<sup>-1</sup> with C-H vibrational bending at 1467 and 1407 cm<sup>-1</sup>. Strong bands at 1725 and 1637 cm<sup>-1</sup> were associated with the C=O vibrational stretch and the aromatic C-H respectively and showed second peaks at 1196 cm<sup>-1</sup> for a C-C-O stretch in the ester.

#### 4.3.3 2-Chloromethyl-4-nitrophenyl phosphorodichloridate (9).

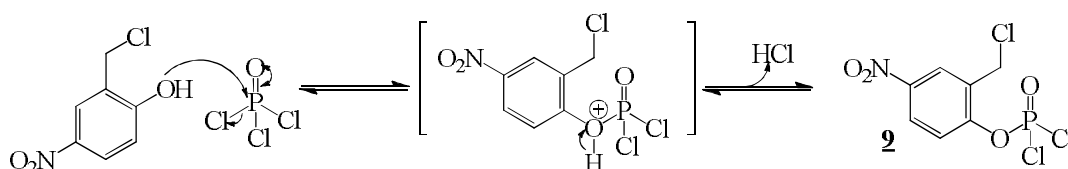
The synthesis of 2-chloromethyl-4-nitrophenyl dichlorophosphoridate (9) was performed according to a modified procedure by Hata, Mushika and Mukaiyama<sup>105</sup>.

The product was obtained by high vacuum distillation at 170°C to afford a clear pale yellow viscous oil in 10.95% yield.



**Scheme 8: The synthesis of 2-chloromethyl-4-nitrophenyl phosphorodichloridate (9).**

The reaction was carried out by refluxing 2-chloromethyl-4-nitrophenol in phosphorus oxychloride for 6 hours, the 2-chloromethyl-4-nitrophenol was used in 0.3 equivalents and phosphorus oxychloride was used in excess to drive the reaction to produce monoesters only. The crude was then concentrated and distilled under high vacuum via Kuglerohr distillation apparatus (Scheme 8).



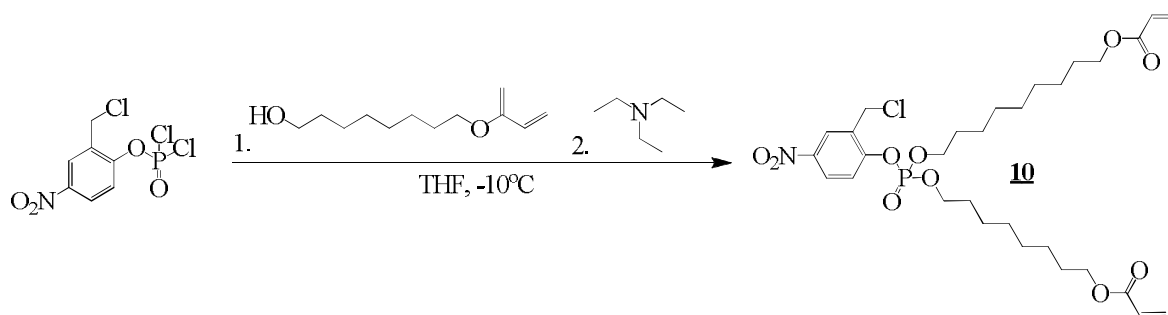
**Mechanism 7: The esterification of 2-chloromethyl-4-nitrophenol with phosphorus oxychloride.**

The mechanism (Mechanism 7) of the esterification occurs via an  $S_N2$  type reaction, the protecting group (2-chloromethyl-4-nitrophenol) being a strong nucleophile attacked the phosphorus centre, releasing a chloride. The charged intermediate now proceeded to release the acidic proton to stabilise the compound and was released as hydrogen chloride gas.

The purity of the product was confirmed by NMR and liquid chromatography mass spectrometry. The  $^1\text{H}$ -NMR spectra showed a singlet at 8.48 ppm correlating to the aromatic proton situated between the nitro group and the chloromethyl group. A double doublet peak at 8.31 ppm corresponds to the aromatic proton in the *meta* position to the phosphorodichloridate and another double doublet peak at 7.71 ppm relating to the aromatic proton *ortho* to the phosphorodichloridate and *meta* to the nitro group. The final singlet peak at 4.72 ppm corresponds to protons of the chloromethyl group. The  $^{31}\text{P}$ -NMR showed a peak at 3.57 ppm correlating to the phosphorus present as a phosphorodichloridate. The LC-MS produced a peak at  $m/z = 302.01$  for the positive molecular ion.

#### 4.3.4 The synthesis of 2-chloromethyl-4-nitrophenyl phosphorodi(octyl acrylate) (**10**) and 2-chloromethyl-4-nitrophenyl bis(8-methacryloxy octyl) phosphoridate (**11**).

The synthetic procedure of 2-chloromethyl-4-nitrophenyl phosphorodi(octyl acrylate) (**10**) (Scheme 9) and 2-chloromethyl-4-nitrophenyl phosphorodi(octyl methacrylate) (**11**) were performed according to a modified procedure by Hata, Mushika and Mukaiyama<sup>105</sup>. The products were purified by silica gel column chromatography in 40% yield for both.



**Scheme 9: The synthesis of 2-Chloromethyl-4-nitrophenyl phosphorodi(octyl acrylate) (**10**).**

The reaction was carried out by adding 2-chloromethyl-4-nitrophenyl phosphorodichloridate (**2**) to 8-hydroxyoctyl acrylate (**7**) or 8-hydroxyoctyl methacrylate (**8**) in THF dropwise at -10°C. The mixture was stirred for 24 hours in the presence of triethylamine. The crude was concentrated and purified by silica gel column chromatography using a mixture of ethyl acetate/petroleum ether 40° - 60° in a ratio of 1:4 yielding a pale yellow heavy oil. The reaction mechanism is similar to that described Mechanism 5 which occurs via an S<sub>N</sub>2 type reaction to produce the triester (**10**).

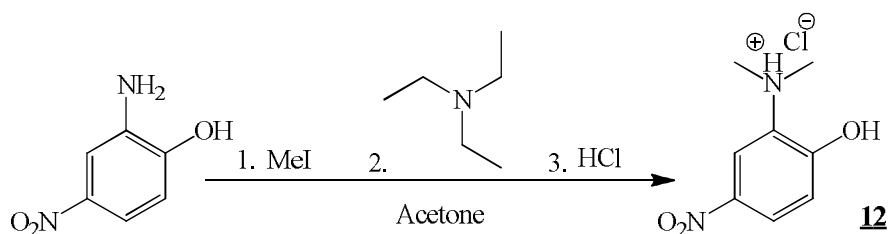
The structure and purity of the product was determined by NMR, FT-IR and liquid chromatography mass spectrometry. The <sup>1</sup>H-NMR showed peaks at 8.33, 8.18 and 7.57 ppm corresponding to the aromatic protons, three double doublets at 6.35, 6.08 and 5.78 all corresponded to the acrylate protons and two double doublets at 6.05 and 5.50 all corresponded to the methacrylate protons. The singlet at 4.65 ppm correlated to the chloromethyl group, the peaks related to protons of the methylene esters were found at 4.16 and 4.10 ppm. The aliphatic region contained the correct amounts of protons for the desired product. The <sup>31</sup>P-NMR showed a peak at -7.12 ppm and correlated to the phosphotriester. FT-IR displayed broad bands at 3396 cm<sup>-1</sup> which belong to the vibrational stretch of the acidic OH, C-H stretching was

found at 2929 and 2861  $\text{cm}^{-1}$  with C-H vibrational bending at 1467 and 1409  $\text{cm}^{-1}$  and strong bands at 1728 and 1638  $\text{cm}^{-1}$  were associated with the C=O vibrational stretch and the aromatic C-H respectively. There was a second peak for the ester at 1198  $\text{cm}^{-1}$  which correspond to the C-C-O stretching. The phosphate group produced bands at; 1295  $\text{cm}^{-1}$  correlating to the P=O vibrational stretching, broad peaks with shoulders at 1056, 985, 813  $\text{cm}^{-1}$  were attributed to the aliphatic asymmetric P-O-C vibrational stretching, phosphorus ester P-OH vibrational stretching and the aliphatic symmetric P-O-C stretching respectively. The LC-MS produced a peak at 632.23 for the positive molecular ion with a retention time of 3.03 minutes for (**10**) and a peak at 661.1 for the positive sodium adduct of the molecular ion with a retention time of 2.89 minutes (**11**).

#### 4.3.6 2-(*N,N*-Dimethylamino)-4-nitrophenol protecting group (**12**).

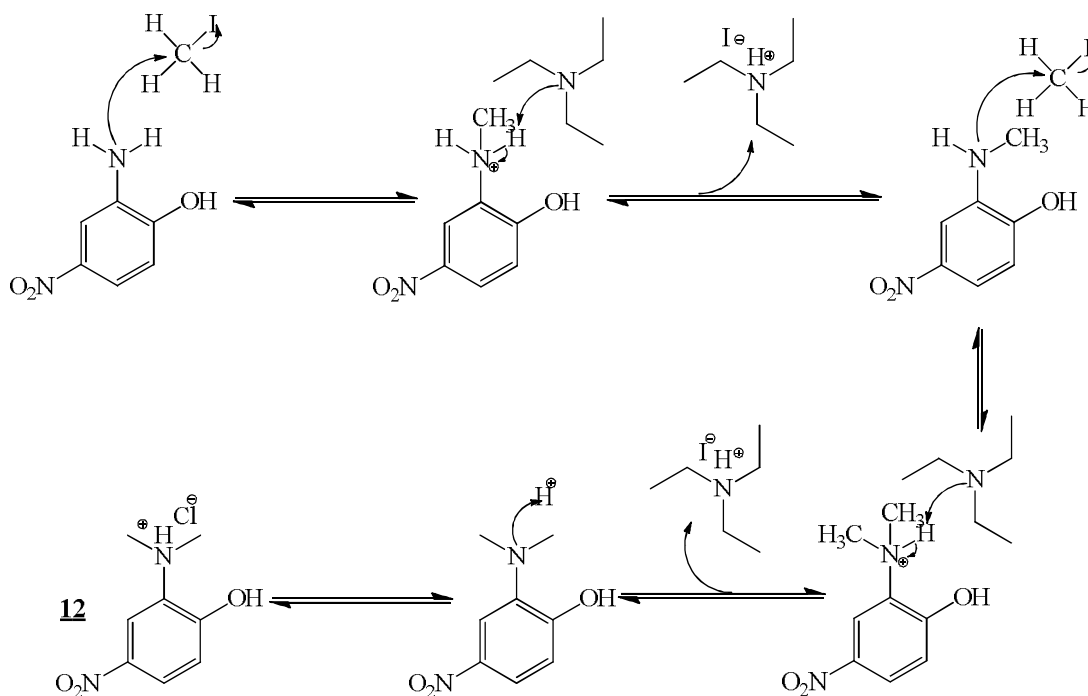
2-(*N,N*-Dimethylamino)-4-nitrophenol protecting group (**12**) was prepared according to the procedure by Taguchi and Mushika<sup>107</sup>. The product was obtained via recrystallisation from ethanol as yellow crystal needles in 2.9% yield (

Scheme 10). The compound was however not used in the synthesis of the phosphodiester.



**Scheme 10:** The synthesis of 2-(*N,N*-dimethylamino)-4-nitrophenol protecting group (**12**).

The reaction was performed in basic conditions in the presence triethylamine. It proceeded through a nucleophilic substitution (Mechanism 8), with the amino group attacking the halogenated compound and releasing the iodide ion. The resulting positive ammonium group then released the proton to triethylamine, liberating triethylamino iodide. The process of methylation occurred a second time and the reaction mixture was washed removing the triethylammonium iodide. The mixture was then exposed to acid producing the less soluble salt before the crude was recrystallised from ethanol.



**Mechanism 8: Methylation mechanism of 2-amino-4-nitrophenol.**

The product structure and purity was characterised and confirmed by H-NMR and mass spectrometry. The  $^1\text{H-NMR}$  shows peaks in the aromatic region (8.65 – 7.26 ppm), the two methyl groups attached to the nitrogen produce a singlet at 3.37 ppm. Mass spectrometry analysis showed a peak at  $m/z = 183.1$  which correlates with the molecular ion.

#### 4.4 Polymer Doping

The doped PANI systems (**17** - **25**) were prepared via a modified method as described by Proń et al.<sup>44,88,92,94</sup>. The target polymers were obtained by mechanically mixing the polymer in DCAA, adding the polymer/DCAA mixture to DCM and finally washing the DCM solution, extracting the DCAA from the DCM solution yielding the doped polymer in a solution (Scheme 11).



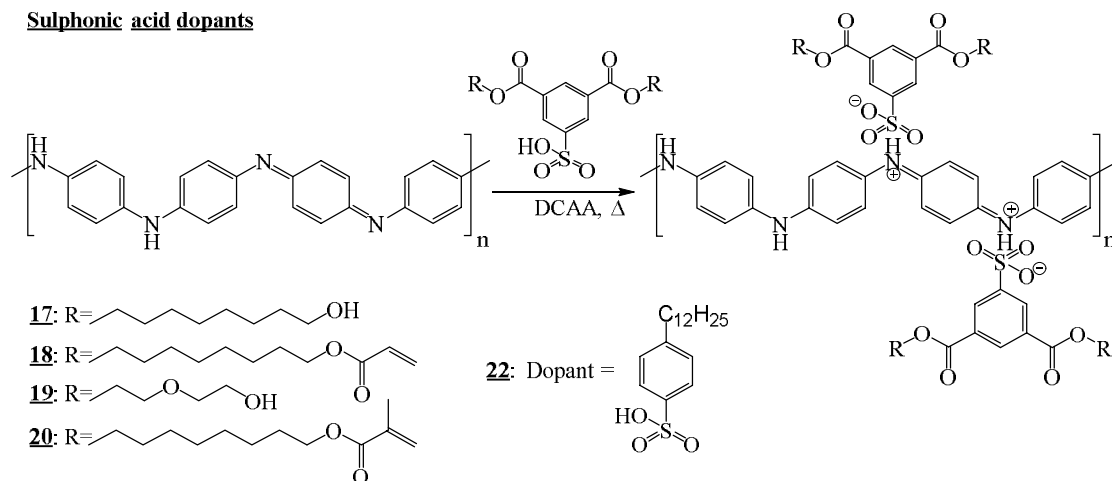
**Scheme 11: The doping of polyaniline in the presence of a protonic acid.**

#### 4.4.1 The doping of PANI with the sulphonic acid and phosphoric acid diesters (17 – 25).

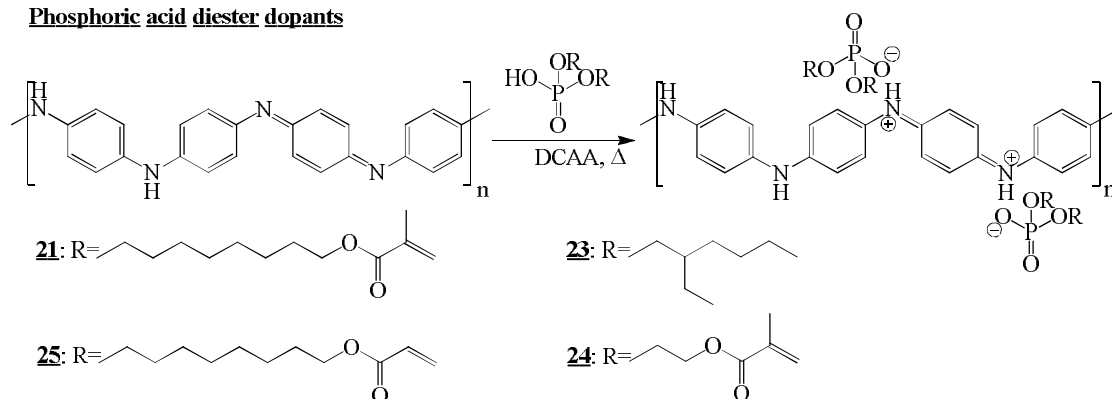
The doping process was carried out by mechanical mixing both polyaniline and the doping agent using a mortar and pestle at room temperature. The dopant was mixed at a molar ratio of 0.5/1 with respect to the polymer (repeat unit =Ph-N), with DCAA added progressively dropwise. The addition of DCAA produced aggregated polymer in solution, the mortar and pestle was therefore used to break up the lumps of PANI into the solution. DCM was then added to the solution and the mixture was subjected to sonication to further disperse and break-up any aggregates not sufficiently mixed, after this the solution was then heated and stirred at 50°C for approximately 72 hours until homogeneity was reached.

The sulphonic and phosphoric acid doped PANI complexes were obtained by the removal of DCAA from the solution through successive washing and extraction of the DCM solutions with water to yield the doped PANI in DCM at around 2 mg ml<sup>-1</sup> (Scheme 12).

##### Sulphonic acid dopants

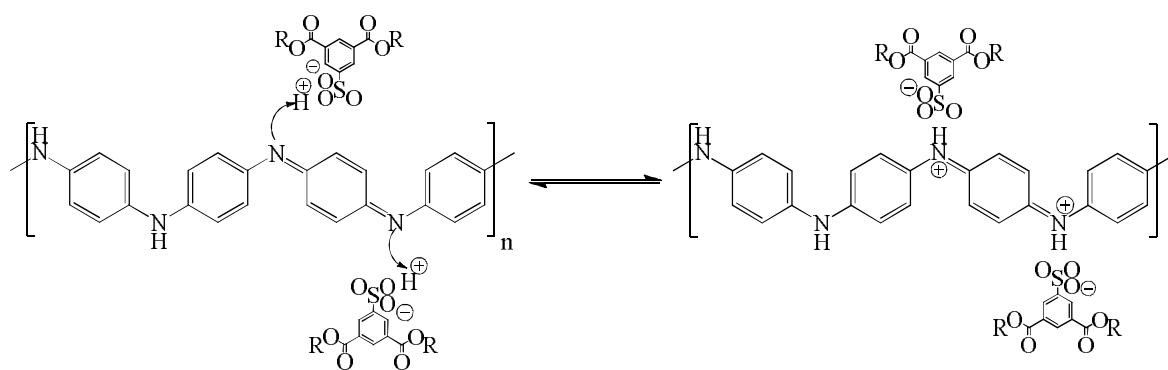


##### Phosphoric acid diester dopants



Scheme 12: Doping of PANI with the sulphonic acid and phosphoric acid diester series of dopants.

The solutions were successfully washed with brine until the aqueous layer showed no signs of acidity when tested by litmus. The mechanism of doping (Mechanism 9) was by the acid attack of the amine or imine groups, resulting in the protonation of the amines or imines, changing the electronic configuration at the doping site.



**Mechanism 9: The mechanism of protonic acid doping, example using sulphonic series of dopants.**

The doped PANI systems were characterised by FT-IR to determine the structures and to determine the successful doping of the material. The FT-IR for the sulphonic acid doped series of PANI showed similar peaks around; 3470  $\text{cm}^{-1}$  corresponding to asymmetric and symmetric stretching vibration of non-hydrogen bonded aromatic amines (-NH), though this was not found in the spectra for doped PANI (**19**), it also correlated to the OH vibration stretching of the dopant in doped PANI system (**17**). The band at 3384  $\text{cm}^{-1}$  correlating to the vibration stretching of benzoid (B) attached amines (-B-NH-B-), within this region there were bands around 3200  $\text{cm}^{-1}$  relating to the C-H aromatic stretching, with further C-H vibration stretching out of plane at 862  $\text{cm}^{-1}$ . Peaks at 1601  $\text{cm}^{-1}$  were characteristic of the deformation of the benzoid rings and benzoid C-C vibration stretching. Bands at 1570, 1557 and 1568  $\text{cm}^{-1}$  correspond to quinoid ring stretching (-N=Q=N-) which in comparison to un-doped PANI (emeraldine base), showed the quinoid ring stretching band at 1583  $\text{cm}^{-1}$ , a distinct move down field to a lower frequency. The peaks around 1464  $\text{cm}^{-1}$  belong to C-N (-NH-B-NH-), C-C vibration stretching and C-H bending. The bands at 1138  $\text{cm}^{-1}$  illustrate N=Q vibration stretching, aromatic C-H out of plane bending and in plane bending but even more importantly were their relevance to the presence of B-<sup>+</sup>NH=Q and B-<sup>+</sup>NH<sub>2</sub>-B. In terms of determining the doping of PANI, the bands at 1278 - 1211  $\text{cm}^{-1}$  and 1073

– 1059  $\text{cm}^{-1}$  all correspond to the sulphur centre of the dopants (S=O) and (S-OH) respectively. Finally the peaks at 2961 – 2914  $\text{cm}^{-1}$  correlates to the aliphatic C-H stretching of the dopant.

The FT-IR for the phosphoric acid doped series of PANI showed peaks around; 3448  $\text{cm}^{-1}$  corresponding to non-hydrogen bonded aromatic amines (-NH); asymmetric and symmetric stretching and vibration stretching of benzoid (B) attached amines (-B-NH-B). Within this region there were bands around 3238 - 3225  $\text{cm}^{-1}$  relating to C-H aromatic stretching, with further C-H vibration stretching out of plane at 872  $\text{cm}^{-1}$ . The peaks at 1601  $\text{cm}^{-1}$  were characteristic of benzoid ring deformation and benzoid C-C vibration stretch. Bands at 1559  $\text{cm}^{-1}$  corresponds to quinoid ring stretching (-N=Q=N-) which in comparison to un-doped PANI (emeraldine base) which showed the quinoid ring stretching band at 1583  $\text{cm}^{-1}$ . The peaks around 1455 - 1443  $\text{cm}^{-1}$  belong to C-N (-NH-B-NH-) and C-C vibration stretching and C-H bending. The band at 1121  $\text{cm}^{-1}$  illustrated an N=Q vibration stretch, aromatic C-H out of plane bending and in plane bending and also B-<sup>+</sup>NH=Q and B-<sup>+</sup>NH<sub>2</sub>-B with bands at 1300 – 1287  $\text{cm}^{-1}$  corresponding to C-N stretching. Bands for the dopant were also found in the spectrum; determining the doping of PANI, peaks at 2161 - 2086  $\text{cm}^{-1}$  for the phosphorus acid group and ester O-H stretching and bands at; 1219  $\text{cm}^{-1}$  band correlating to P=O vibrational stretching, broad peak with shoulders around 1073 - 1036  $\text{cm}^{-1}$ , 985 and 872  $\text{cm}^{-1}$  are the aliphatic asymmetric P-O-C vibrational stretching, phosphorus ester P-OH vibrational stretching and aliphatic symmetric P-O-C stretching respectively. Finally the peaks at 2964 – 2849  $\text{cm}^{-1}$  correlates to the aliphatic C-H stretching of the dopant.

#### 4.4.2 The preparation of doped PANI composites with PVC.

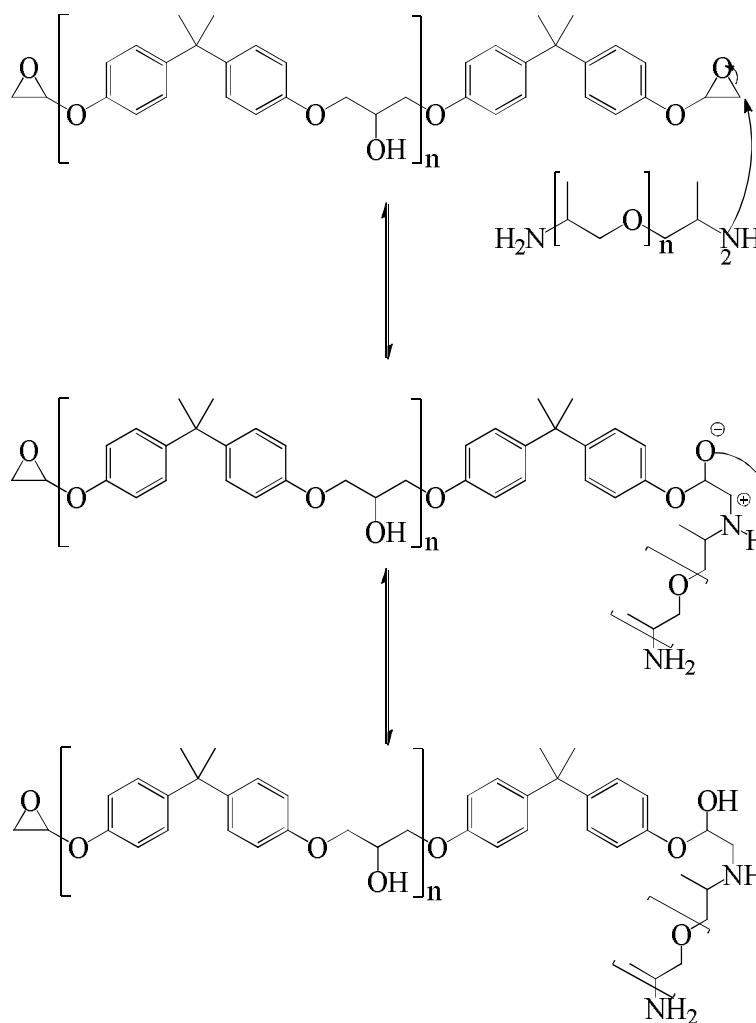
Polyvinyl chloride (PVC) (43,000  $M_w$ ) was added to solutions of doped polyaniline (**17** - **25**) in different proportions to produce a range of composites with different weight percentages. The solutions had to be slightly heated and sonicated in order to obtain homogeneity. They were extremely viscous and gelation occurred even at low volume fractions. Films were cast by the ‘dip-dry’ method, the substrates were submerged into the composite solutions and left to dry. The adhesion of the films was quite strong which allowed for this method of casting films to be ideal to use. The DCM allowed for quick drying with the solvent evaporating quickly which set

the films in place quickly. The PVC/PANI films were malleable, producing soft and pliable rubbery films and with the progression of time cracks formed in the films, the result of continual solvent release from the films. Doped PANI remained intact throughout the whole process producing smooth green coloured films.

The films were characterised by FT-IR; Bands in the region of  $3400 - 3300 \text{ cm}^{-1}$  correlated to the OH and NH stretching of the polymer backbone and acid groups of the dopants. The bands at  $2949 - 2930 \text{ cm}^{-1}$  correspond to the vibration stretch of C-H of both the matrix polymer and the doped PANI. It was noticed that in all the spectra correlating to the PVC films, distinct characteristic bands at  $2160$  and  $2032 \text{ cm}^{-1}$  were found which were not found in any of the other IR spectra. The band at  $1426 \text{ cm}^{-1}$  belong to C-H vibration bending,  $1329 \text{ cm}^{-1}$  corresponds to the presence of C-H twisting and CH-Cl vibration bending. The peaks at  $1240 \text{ cm}^{-1}$  were characteristic of C-H wagging, ( $-\underline{\text{C}}-\underline{\text{C}}\text{H}-\text{Cl}$ ) bend and wagging, with further C-H rocking and deformation and C-C stretch around  $967 \text{ cm}^{-1}$ . Very strong peaks between  $700 - 600 \text{ cm}^{-1}$  correspond to the  $-\text{C}-\text{Cl}$  stretching. Peaks for the doped polymers are mostly hidden within the PVC peaks due to the strength of the signals.

#### 4.4.3 The preparation of doped PANI composites with epoxide resin.

The composite of doped PANI (**17**) and Epikote 828™ (bisphenol A) epoxy resin was successfully created. Unfortunately the composite had to be made up at the point of casting the films; the problems encountered were the result of the presence of the curing agent (Jeffamine®D230, CAS# 9046-10-0). Being a strong base the curing agent attacked the protonated PANI chain, stripping the proton off the polymer (undoping the polymer). This was evident upon casting the films and mixing all of the constituents together, the polymer solution went from a dark green solution to a navy blue solution. The emeraldine base (un-doped) was characteristically blue colour in solution whilst the emeraldine salt were characteristically dark green clearly indicating the polymer going from one state to the other. The films were spray cast and the sample was mixed with the resin at the spraying stage, with the epoxy resin and curing agent in one spray bottle and the doped polymer was contained in the other. The application of all constituents were sprayed simultaneously producing thick gel like films that were then placed into the oven for 24 hours allowing full curing of the film. The films produced were hard, rigid and extremely smooth, creating a watertight barrier.



**Mechanism 10: The mechanism for the curing of the epoxy resin by the curing agent Jeffamine D230.**

The mechanism for the curing of the epoxy resin is shown in Mechanism 10. The curing process proceeds with the nucleophilic attack of the strained epoxide group with the amine of the curing agent; this opens the ring, creating a charged intermediate which contained a newly formed bond between the nitrogen and carbon. The unstable intermediate quickly rearranges with the charged oxygen accepting the proton from the charged amine, resulting in the new cross-linked compound, this cross linking was in a ratio of 2:1 (epoxide : amine), therefore for each molecule of the curing agent, up to four chains can be crossed linked as shown in Figure 33. The resin contained huge amount sites for potential hydrogen bond formation, this being just one of the characteristics which made this ideal for the hydroxyl functionalised dopants to integrate. Further still the hydroxyl groups of the dopant can also participate in the attack onto the epoxy groups of the resin, opening the epoxide and therefore crosslinking with the resin. This acts to promote extensive interactions between the doped PANI and the resin matrix increasing the

dispersity of the polymer and making for a better dispersion into the resin. The overall crosslinking of the material produced a strong, durable, vast and extensive network of polymer/dopant and resin.

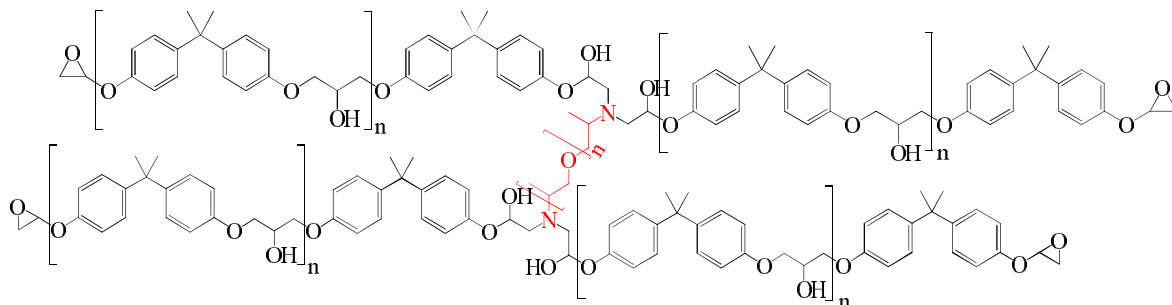


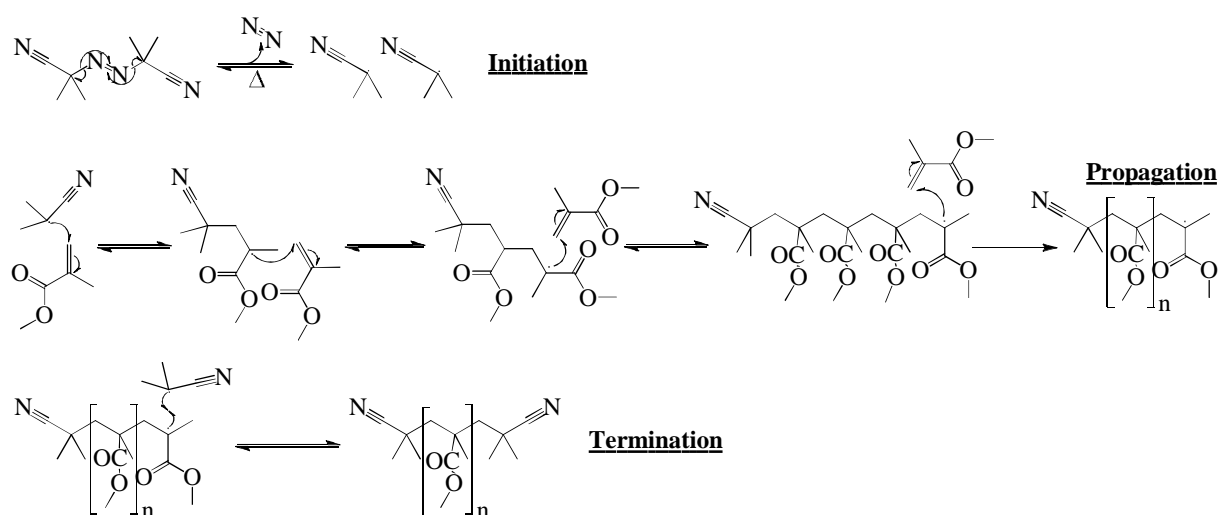
**Figure 33:** Example of a cross linked segment of the composite with the curing agent (Jeffamine ®D230), shown in red.

The film was characterised by FT-IR and showed a broad band at  $3365\text{ cm}^{-1}$  corresponding to the OH vibration stretching, bands at  $2966$ ,  $2932$  and  $2867\text{ cm}^{-1}$  belong to the aliphatic C-H stretching with further bands at  $826\text{ cm}^{-1}$  correlating to C-H vibration wag. Peaks at  $1607\text{ cm}^{-1}$  correlated to the epoxy ring vibration stretching, further absorption at  $1231\text{ cm}^{-1}$  and  $1181\text{ cm}^{-1}$  belonged to C-O symmetric vibration stretching and at  $826$  for the C-O asymmetrical vibration stretch. Finally the bands at  $1102 - 1009\text{ cm}^{-1}$  are characteristic of C-O-C ether stretching.

#### 4.4.5 The preparation of doped PANI composites with acrylic resin.

Composites of doped PANI (**18**, **20**, **21**, **23** - **25**) with an acrylic resin were also successfully created. The composition of the acrylic resin consisted of methyl methacrylate (MMA), methyl acetate, ethylene glycol dimethacrylate (EGDMA), azobisisobutyronitrile (AIBN) and benzophenone in ratios of around; **20:1.6:2:1:0.8** respectively. The mixture was stirred together for 1 hour and then added to solutions of the doped PANI (**18**, **20**, **21**, **23** - **25**) at volume fractions of; 5 wt%, 2 wt% and 1 wt% to the doped PANI ( $2\text{ mg ml}^{-1}$ , 150 ml). The solutions were stable and were refrigerated or stored in the freezer. The films were cast by drop coating; with the composite solutions being spotted on the surface of the substrate and then left to cure in the oven at temperatures above  $80^{\circ}\text{C}$ . Curing typically occurred within 1 hour, this was the point at which the solvent was removed and the films were touch dry, though caution and care was taken in order to limit the damage to the films. The process was continued on the opposite side of the substrate, the films

were then left in the oven to fully cure taking several days producing hard brittle cracked films which showed signs of extremely poor adhesion to the substrate surface. Many problems were noticed with the films regarding defects, aside from the poor adhesion, the films contained many bubbles which formed during the curing process and large cracks within the films causing peeling and delamination. The morphology of the films was really poor with many peaks and troughs in the film, the result of aggregation and concentration of the resin mixture during the curing process. The doped PANI samples all remained intact and showed no signs of degradation or redox reactions between the polymer and the other resin constituents present.

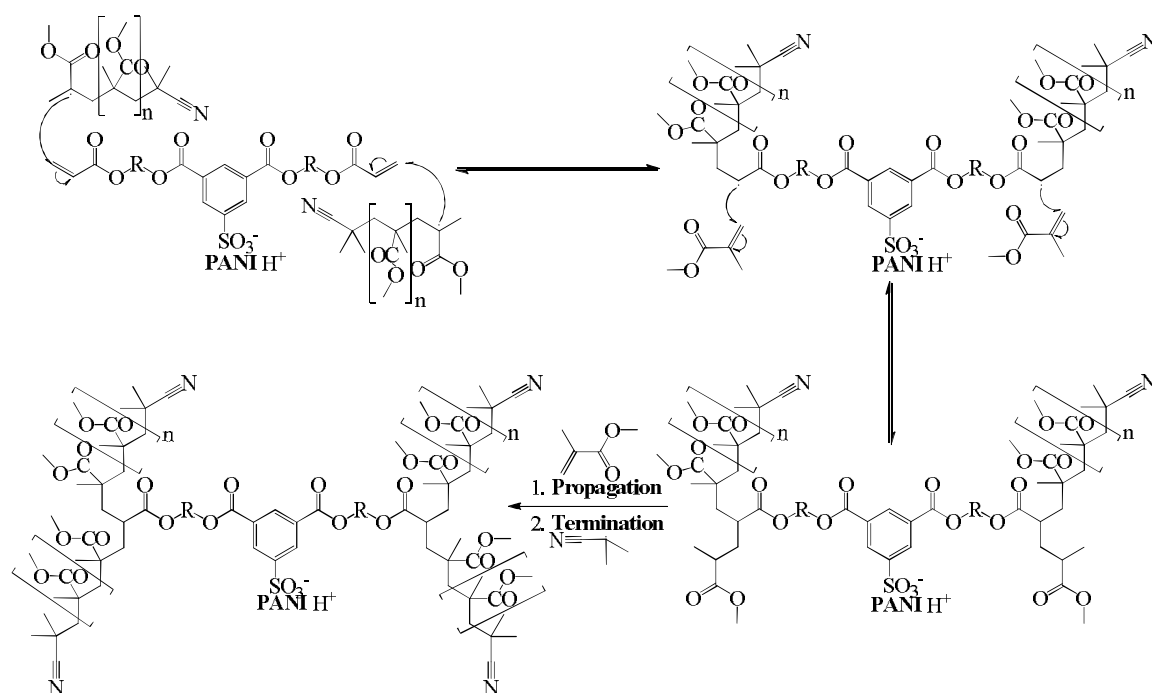


**Mechanism 11: Free radical polymerisation of methyl methacrylate in the presence of AIBN.**

The mechanism for the curing the acrylic resin can be seen in Mechanism 11. The curing process proceeded via free radical polymerisation, which required an initiator that self-perpetuated the reaction. The free radical initiator used was 2,2-azobis(2-methylpropionitrile) (Azobisisobutyronitrile, **AIBN**), under conditions such as heat or exposure to UV light, a rearrangement was able to take place with the movement of the electrons shared between the carbon and nitrogen of the central imine of the initiator. One of the shared electrons moves into the imine moiety and the others onto the central carbon adjacent to the nitrile. This releases  $N_2$  gas and two nitrile containing moieties which now exist as 'activated' radical initiators. The radical then attacks the double bond of the methyl methacrylate creating a new  $\sigma$  bond between these two groups forming a new carbon radical which also ensues to attack another molecule of methyl methacrylate, the process

continues with the growth of the newly formed polymeric chain with the methyl methacrylate repeat unit, this process is known as the propagation step.

Methyl methacrylate is not the only molecule present in the acrylate resin formulation that participates in the radical polymerisation, ethylene glycol dimethacrylate is also added on to the propagating chain during the radical polymerisation and also the dopant with its own acrylic group is able to integrate into the growing network of the PANI/cross-linked resin.



**Mechanism 12: The mechanism of dopant crosslinking with the acrylic resin.**

This was key to the specific development of a series of acrylic functionalised dopant; the idea and rationale was to increase processability and one key element to increasing processability was to increase interaction with the resin matrix. The dopant achieves this by incorporation of an acrylic group from its side chain into the resin and is also able to participate in cross linking (Mechanism 12) to add to the growing polymer chain. It can also act as a bridge between the different chains of poly(methyl methacrylate) formed.

**Figure 34: Generalised structures of the potential crosslinking of the methacrylate and acrylate functionalised dopants.**

Figure 34 illustrates the potential interaction of the methacrylate and acrylate functionalised dopants, demonstrating the bridging of the different acrylate resin chains.

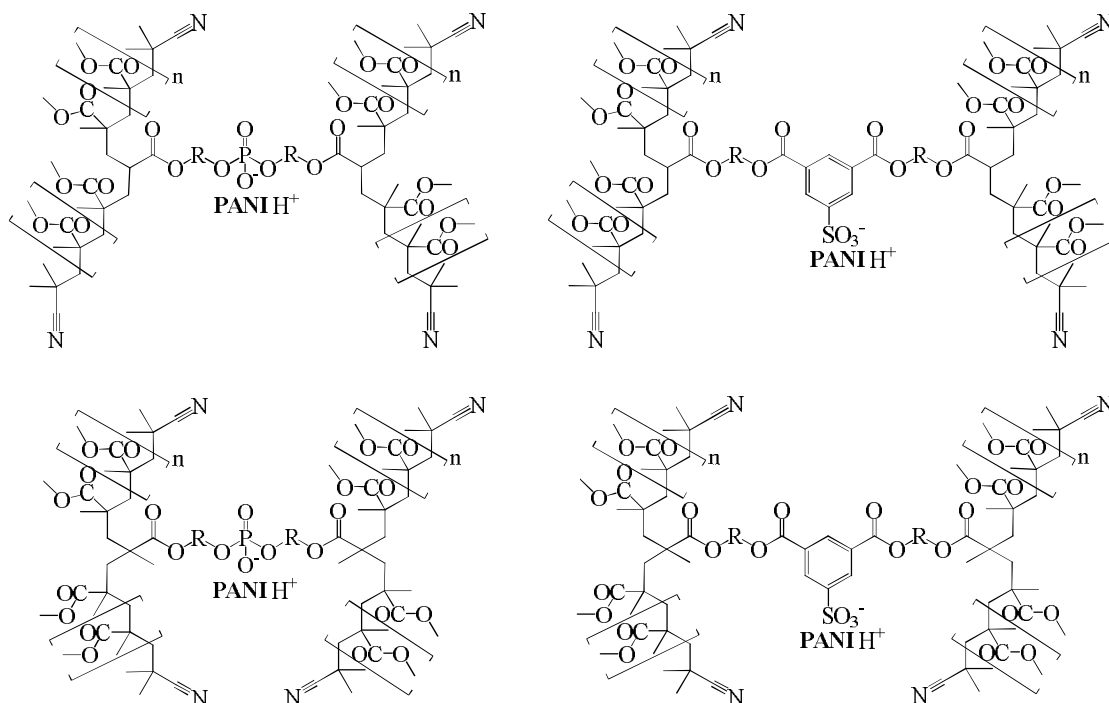
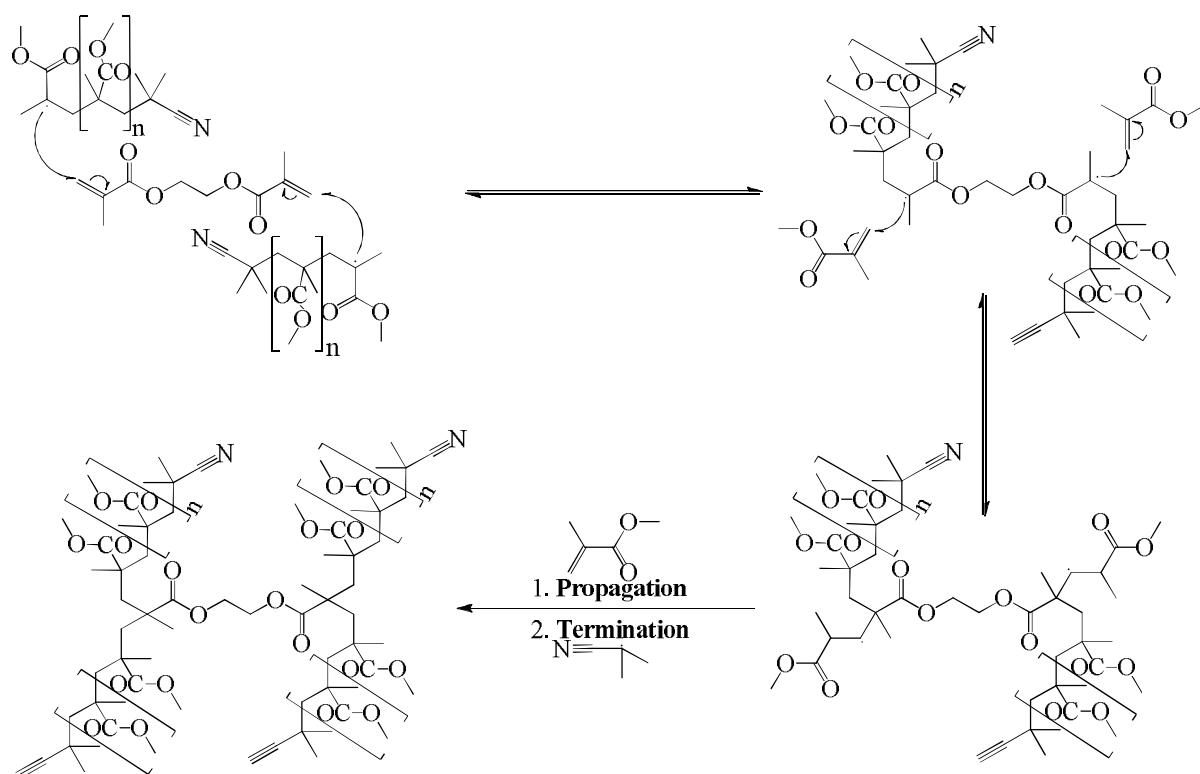


**Figure 34: Generalised structures of the potential crosslinking of the methacrylate and acrylate functionalised dopants.**

As seen the interaction and bridging effect propagated within the resin matrix which acted to increase the dispersion of the doped polymer complex within the resin and potentially allow for lower percolation thresholds as the chains crosslink.

It was important from the beginning to bridge the polymer chains in the resin. In these systems the dopants acted as an anchor, fixing the chains in place. Subsequently the physical properties of the material inevitably change; with the soft and extremely flexible materials being sensitive to damage, and having poor adhesion and extremely rigid, hard materials being prone to cracking and breaking which would be problematic. Therefore it was important to consider these factors when developing the doped systems, ensuring a balance of properties. Cross linking played an integral part in the development of the coating, producing rigid, hard but flexible films which were resistant to physical damage. The rationale behind this

was similar to the vulcanisation process of rubber, turning a soft flexible material into a harder, durable material by adding cross linkages in the form of sulphur bridges. For this reason ethylene glycol dimethacrylate was incorporated into the composite mixture which ensured that there was some degree of cross linking between polymers chains, Mechanism 13 shows the process of cross linking with PMMA.



**Mechanism 13: The crosslinking and bridging of poly(methyl methacrylate) with ethylene glycol dimethacrylate (EGDMA).**

The films were characterised by FT-IR and showed broad bands around 3400 - 3300  $\text{cm}^{-1}$  corresponding to the OH and NH vibrational stretching, bands around 2900  $\text{cm}^{-1}$  were characteristic of aliphatic C-H stretching. Peaks in the region of 1720  $\text{cm}^{-1}$  correlated to the C=O vibration stretching, 1450  $\text{cm}^{-1}$  correlated to C-H vibration bending and C-CH<sub>3</sub> planar deformation. The weak peaks found around 1365 - 1370  $\text{cm}^{-1}$  belonged to C-H twisting and wagging. Absorption at 1295 - 1270  $\text{cm}^{-1}$  corresponded to C-O asymmetric stretch vibrations with further absorption around 1120  $\text{cm}^{-1}$  for the C-O symmetric vibration stretching. The bands between 950 - 930  $\text{cm}^{-1}$  corresponded to C-O-CH<sub>3</sub> and C-H rocking. Peaks for the S=O and P=O of the dopants were found in the spectra's at around 1380 - 1300  $\text{cm}^{-1}$ .

<sup>1</sup> and further peaks at around 1047 – 1036 cm<sup>-1</sup> corresponded to the P-O-C vibrational stretch.

#### 4.5 UV/Vis spectroscopy of doped polyaniline.

Analysis was conducted on all the prepared doped polyaniline samples that were successfully produced (**17** – **25**). The samples were all investigated in a solution of DCM, which were further processed into thin films on quartz plates for analysis and comparative purposes. However films were not produced for all of the samples; Doped PANI samples showed very low adhesion properties on quartz glass plates and proved difficult to produce due to poor film properties. Analysis was therefore conducted mainly on solutions of the doped polymer instead of the films. Arguments exist which suggest the electronic properties of doped polymers require analysis of the polymer in a solid state (cast as a film), where the polymers are fixed into position in the resins or in blends with PVC, thus the band gap and other electronic properties can be accurately determined. The main reason for this is due to the mobility of the polymer in a solution, this leads onto a second issue that in solution the chains have freedom of movement; in some instances the chains may adopt a coil like structure and in other instances the chains may be more linear. Therefore when the solutions and films were analysed, the films showed shifted absorbance towards the higher wavelengths of the spectrum. Un-doped polyaniline were found to be coiled in both solution and as cast films, judging by the results obtained.

These pieces of evidence were crucial in proving that the levels of doping, the crystallinity of the polymer and the electronic properties were interlinked. In explanation to what was happening; firstly upon doping the material became more linear, reducing the amount of kinks and reducing the Peierls effect. In terms of the electronic properties, new intermediary energy levels (polarons) formed within the band gap of the polymer, effectively reducing energy for electronic transition. These polarons upon higher levels of doping have the potential to become delocalised along the polymer chains.

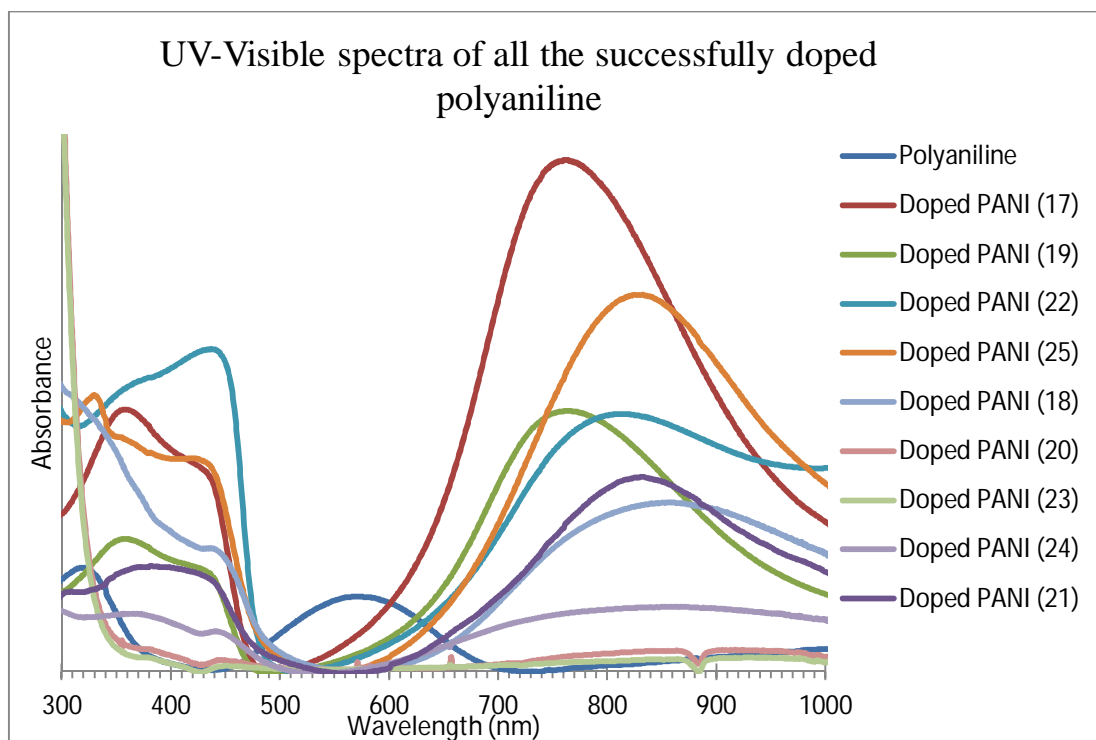


Figure 35: UV-Visible spectra of all the successfully doped polyaniline

The spectral overlay (Figure 35) shows the complete UV-Visible spectra of all the doped polyaniline (17 – 25).

The spectra all showed strong absorption bands into the near infra-red and the infra-red region, suggesting that all the dopants had effected the conformation of the polyaniline and increased the planarity of polymers. It was previously seen, the dopants structure and functionalities were crucial factors in their efficiency and ability to cause such conformational changes. The increased steric hindrance and higher steric effects showed the greatest results and highest levels of doping for these systems. Therefore a certain level of importance was placed on tuning the dopants and their respective side chains, not only focussing on the functional groups attached to them but also looking at branched chains for their higher steric effects. This promoted optimal doping of the polymer and increased crystallinity, not only at a localised level but also the net conformational effects to give the maximum potential electronic properties.

#### 4.5.1 Electronic and optical properties of the sulphonic acid and phosphoric acid doped series of PANI in solution and cast films.

The first conceptualised series of dopants were functionalised with hydroxyl terminal groups on the side chain such as those seen in doped PANI (17) and (19),

the aliphatic chain were positioned around a sulphonic acid aromatic ring at a *meta*-configuration in relation to the sulphonic acid. This position was thought to be the optimal configuration for creating a dopant that would at least exert steric hindrance on the polymer chain, opening the structure of the polymeric material. The reasons for placing consideration onto the structure and functionality comes from the fact that the sulphonic acid needed to be distant enough and extended in such a fashion from the aromatic ring that the sulphonate groups are able to fit into the spaces between the quinoid and benzoid rings, allowing closer ionic interactions between the protonated amine or imine and the sulphonate. It was important to recognize that in order for the polymer to be rendered a processable material, the dopant (sulphonate) needed to insert into the spaces created by the aromatic centres of the polymer backbone. This not only ensures a strong interaction between the ionic species but also allows the dopant to get to such a proximity that the other parts of the dopant played their roles in making the polymer processable. This led on to the discussions such as; how the rest of the dopant could be modified and the role of functionalised side chains. The investigations were therefore directed towards looking at the factors that influenced the structure of PANI and how it could be objectively addressed. As a result it was subsequent to look at how the dopant could be tuned to increase interaction not only with the solvent but also with the other materials that are vital in the formulation of a coating, such as the resins.

The sulphonic acid and phosphoric acid dopants all shared common features and relative structures as shown in Figure 36.

The characteristics of the sulphonic acids featured the side chains and a sulphonyl hydroxide group both placed around an aromatic ring, which the aromatic ring itself played some part in increasing the doping effect through their interactions with the aromatic rings of the polymer chain. The phosphoric acids contained similar features to the sulphonic series, such as ester linked functional side chains and a protonic acid (doping agent) around a central structure/atom which in this case was the phosphorus centre.

It was important to consider during the design of the dopants that the processability of the doped PANI is linked with both the crystallinity of the polymer and the functionality of the dopants. Therefore the side chains were designed to perform

two tasks; opening the polymer structure and increasing the processability of the doped material. The dopants themselves need to be highly soluble in common solvents which should aid to plasticise the doped PANI complexes at later stages. It was vital that the side chains are of a length that promotes the uncoiling of the structure around the doping site through steric effects and are structures that are known for their solubility in common solvents. The design also includes an increase of the interaction of the doped polymer complex with not only the solvent but also the polymeric resin matrices that are used.

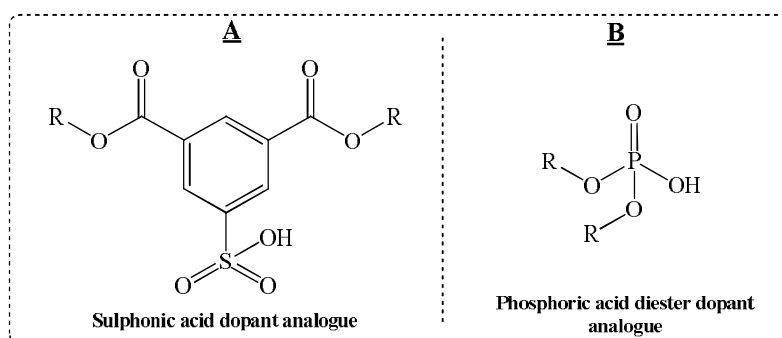


Figure 36: Precursor and general analogue for; A) sulphonic acid and B) phosphoric acid range of dopants

#### 4.5.1.1 Analysis of the sulphonic acid doped PANI series in solutions of DCM.

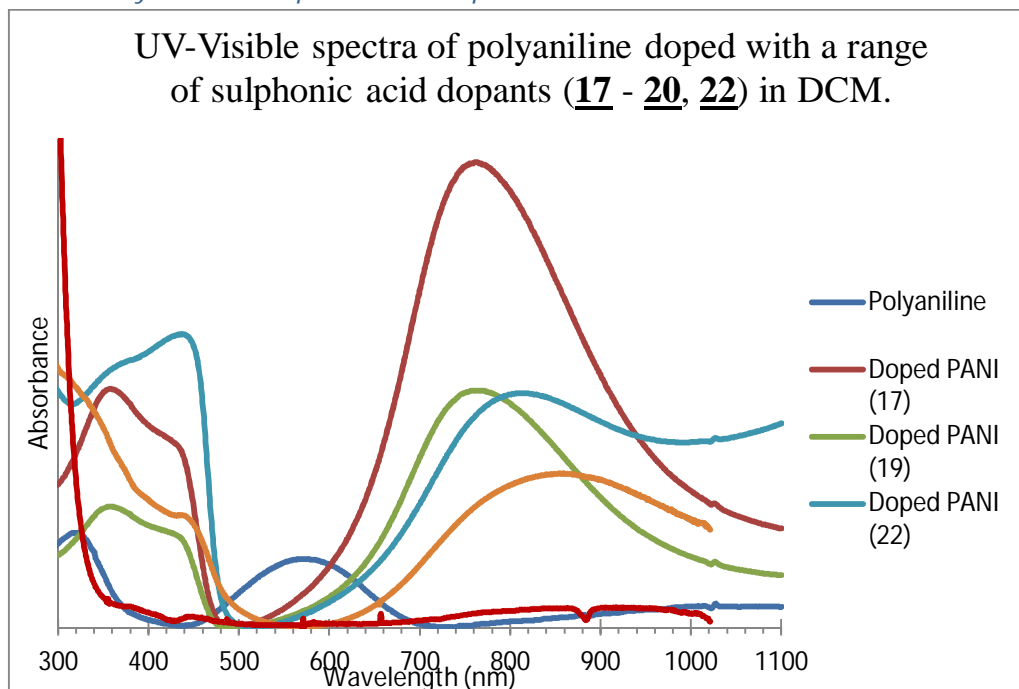


Figure 37: Spectral overlays of polyaniline doped with a variety of dopants belonging to the sulphonic acid series, measured in a solutions of DCM.

Illustrated in Figure 37 are the spectral overlays obtained for the sulphonic acid doped series of PANI (see appendix for individual spectra). The absorption spectra

display broad bands in the regions between 650 nm and 1100 nm in dichloromethane solution, weaker bands with smaller shoulders were within the UVA region of the spectrum (Near UV, 300 - 400 nm, 4.11 – 3.10 eV) and up to the blue end of the visible light spectrum (440 – 500 nm, 2.82 – 2.48 eV) which is a common feature in all of these spectra and is due to the aromatic components of the doped systems. The fact that there are two shoulders within the band suggested that one correspond to quinoid and the other to benzoid rings of repeat units on the polymer chains.

The data collected clearly suggests that there are relationship between; the functionality of the dopant, the functional groups present and the plasticising effects of the dopants. For comparative purposes polyaniline in the un-doped state was included to demonstrate the red shift from the un-doped emeraldine base to the doped emeraldine salt. The emeraldine base inherently was insulating, having a wide band gap and requiring lots of energy to promote electrons from the valence band to the conduction band which in this case requires energy in the region towards the UV end of the spectrum and the un-doped polymer displays a  $\lambda_{\max}$  of 572 nm in a solution of DCM. Taking doped PANI (**17**) as an example; the broad band for this system gives a  $\lambda_{\max}$  of 762 nm which corresponds to radiation in the near IR region, this was a clear red shift from its native un-doped form to the doped version of the polymer.

Doped PANI	$\lambda_{\max}$ (nm) Solution		
	1	2	3
<b>17</b>	354	430	<b>762</b>
<b>18</b>	448	-	<b>865</b>
<b>19</b>	356	435	<b>764</b>
<b>20</b>	-	443	<b>917</b>
<b>22</b>	364	439	<b>831</b>
Polyaniline	327	-	<b>572</b>

**Table 1: Summary of absorption data from UV-Visible spectroscopy of polyaniline doped with various sulphonic acid dopants.**

Table 1 summarises the spectral analysis of all the sulphonic acid doped PANI series. Doped PANI (**17**) and (**19**), both of which were functionalised with hydroxyl end groups in preparation for their incorporation into an epoxy resin, displayed sharp and intense bands at around 762 – 764 nm (

Table 1). Doped PANI (**18**) and (**20**) contrary to this, displayed much broader bands and less intense peaks, with absorption around 865 and 917 nm respectively. These two polymers contained dopants functionalised with acrylic groups, however it can be seen that doped PANI (**20**) is much more red shifted than doped PANI (**18**). This red shift is the result of the additional methyl group on the acrylate; it appears that the methylacrylate groups have a greater plasticising effect than their acrylate counterparts. Whether this effect was the result of the methyl groups promoting a higher order of crystallinity or the fact that the addition of methyl groups to the acrylate, rendered the whole unit more soluble in DCM is open to interpretation.

#### 4.5.1.1.1 Electronic properties of bis(8-hydroxy octyl) 5-sulphoisophthalic acid doped PANI (**17**) (PANI-SIPAOH).

Comparing the spectrum of doped PANI (**17**) with un-doped polyaniline (Figure 37), there is a significant shift in the electronic properties that is seen, shifting from the blue-green region to the near infra-red. The changes are assigned to conformational changes of polymer chains, which in the un-doped state are highly coiled structures in solution and cast as a film. This coiling reduces upon doping and the subsequent casting of films produces more crystalline structures. This coiling gives rise to the Peierls distortion effect<sup>1</sup>, which explains why the conjugated system of polyaniline is semi-conducting at best. Peierls effect explains how the geometry of the polymer and the bond lengths variations (short  $\pi$ -bonds and longer  $\sigma$ -bond) increases the energy difference between the LUMO and HOMO bands.

Dopant (**1**) was the first of the sulphonic acid series to be synthesised and produced, with the aim to produce a functionalised dopant that has the ability for potential reactions with the resin such as an epoxy resin (bisphenol A, Figure 38) during curing.

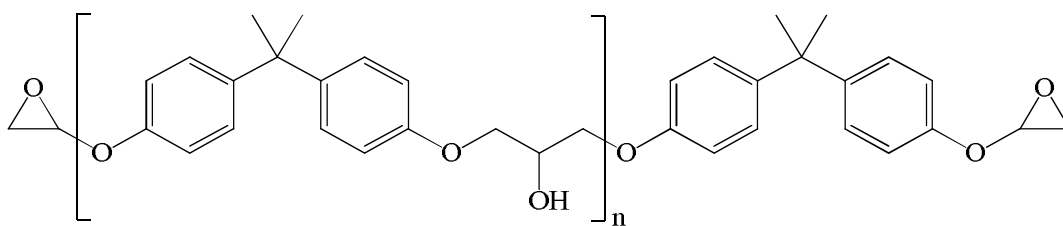


Figure 38: Structure of bisphenol A epoxide resin.

As with all epoxy resins the main common feature is the epoxide end group which are key sites for the hydroxyl group of the functionalised dopant to interact, through simple forces like hydrogen bonding or potentially creation of new covalent linkages that lock the doped polymer in place, this ensured high levels of distribution through the resin and is a method of controlling the rheology. Previously one of the major issues preventing the processing and production of emeraldine base polyaniline is that the polymer displays very little interaction with other chemicals other than itself. This results in areas where the polymer is phase separated and is unevenly distributed. Therefore a great deal of control is gained by functionalising the dopant side chains to be good hydrogen bonding groups and/or have reactive ends with the resin matrix, addressing the issue of the polymers processability.

The structure of the side chain can be seen in Figure 39 showing a hydroxyl terminated aliphatic chain of around eight bond lengths. After researching literature it was clear that the most effective dopants had an aliphatic carbon side chains greater than 10 bond lengths<sup>96</sup>, however these were not functionalised and were simple. Hence for this research chains in the region of around 8 carbons were sufficient in size to address the highlighted problems. Functionalising the dopant with hydroxyl groups at the terminals ensured that there would be sufficient interaction with the epoxide resin to effectively plasticise the polymer into the resin giving even distributed cast film/coatings.

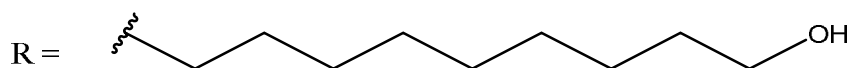


Figure 39: Structure of the aliphatic side chain for the Dopant used in doped PANI (17)

Looking at the UV-Vis spectroscopy of doped PANI (**17**), a peak with a  $\lambda_{\text{max}}$  of 769 nm in solution was seen, which in comparison with the  $\lambda_{\text{max}}$  of un-doped PANI (emeraldine base) in solution ( $\lambda_{\text{max}}$  of 572 nm) showed it had prominently shifted of

around 197 nm. This suggested that the doping of the PANI was successful but also further confirmed that the polymer was in a much higher ordered state and that the polymer existed in a much more conductive regime by the formation of polaronic bands.

#### 4.5.1.1.2 Electronic properties of bis(8-acryloxy octyl) 5-sulphoisophthalic acid doped PANI (**18**) (PANI-SIPAOA).

When designing the dopant for this system, the idea at the beginning of its development was to create products that are able to interact with acrylic resins through functionalising the side chains of the dopant with acrylic groups. Upon curing with the resin, the acrylate groups should cross link producing physical bridges in the form of covalent bonds. Similar to the previous dopant, the physical interaction of the doped polymer with the resin should increase the dispersity through the resin matrix and prevent the phase separation of the doped-PANI into concentrated areas in the films of blends.

The UV/Vis profile (for a closer look see Appendix 2) of this doped system showed strong absorption in the near infra-red region of the spectrum at a  $\lambda_{\text{max}}$  of 865 nm in solution. This demonstrates that doping into the emeraldine salt does take place with this dopant and also that this dopant is more efficient than the previous dopant (PANI **17**) at altering the conformation and electronic state of the resulting polymer. Doped PANI (**18**) complex showed an absorption at  $\lambda_{\text{max}}$  865 nm in solution, a prominent shift further into the near infra-red of nearly 100 nm and a clear red shift in the electronic properties of this polymer, as such doped PANI (**18**) complex exists in a more crystalline conformation than the prior case of (**17**). This provided strong evidence that the changes in conformation and electronic properties were the result of the variable which in these investigations was the functionalised groups. Interestingly it's clear to notice that the acrylic groups had more impact on the electronic properties of the polymer compared to the hydroxyl groups, most likely due to higher steric effects exerted from the acrylate than hydroxyl group. Further inspection of the spectrum (Figure 37) showed the presence of a carrier free tail, a tailing off of the spectrum into the infra-red region. This was indicative of a very high crystalline structure with a degree of delocalisation of the polarons, similar to systems where PANI is highly doped in *m*-cresol

#### 4.5.1.1.3 Electronic properties of bis[2-(2-hydroxy-ethoxy)-ethyl]-5-sulphoisophthalic acid doped PANI (**19**) (PANI- SIPADEG).

Prepared in parallel to bis(8-acryloxy octyl) 5-sulphoisophthalic acid (**18**), bis[2-(2-hydroxy-ethoxy)-ethyl]-5-sulphoisophthalic acid (**19**) was produced as another dopant in the series of the hydroxyl functionalised dopants. The main difference between this dopant and the prior hydroxyl functionalised dopant was the side chain length and the presence of a central oxygen in the side-chains of the dopant. The decision to incorporate the ether functionality on the side chain of the dopant was taken as a measure to increase the ability of hydrogen bonding between the dopant and the matrix of the doped PANI, whether this was the solvent or the resin. Therefore in the case of this dopant the chains had further potential to interact with the epoxide resin in comparison to the other hydroxyl functionalised dopant (**17**). The side chain in comparison to the other hydroxyl functionalised dopant was comparably shorter from 8 bond lengths to 6 bond lengths. The absorption  $\lambda_{\max}$  of 764 nm in comparison to 762 nm of the other hydroxyl functionalised doped PANI (**17**), this suggested that the chain length had no direct relationship on the crystallinity of the polymer. This led to the hypothesis that the valence electrons of the ether oxygen in some way had some steric effect on the polymer backbone and explains why the shorter chain is able to promote similar levels of crystallinity as doped PANI (**17**).

The evidence obtained here suggested that doped PANI (**17**) and (**19**) induced the same levels of crystallinity and subsequently that the dopants functionalisation had played more of a key part in the efficacy of doping. It also suggested that dopants with shorter chains lengths were just as efficient at doping as those with longer chain lengths and emphasis should be placed more on the functionalization and increasing the steric effects exerted by the dopants side chains.

#### 4.5.1.1.4 Electronic properties of bis(8-methacryloxy octyl)-5-sulphoisophthalic acid doped PANI (**20**) (PANI-SIPAOMA).

Upon investigating the relationship between the levels of PANI-doping of the various functionalised dopants, it became clearer that the dopants with acrylate functional groups, were more effective at altering the electronic properties of polyaniline than the hydroxyl functionalised variants. The absorbance readings measured were in the near infra-red region and beyond when tested in solution.

Looking particularly at doped PANI (**20**), the absorption of PANI when doped with bis(8-methacryloxy octyl)-5-sulphoisophthalic acid (**4**) in solution is around  $\lambda_{\max}$  of 917 nm and in comparison to the other acrylic functionalised doped PANI (**18**) of  $\lambda_{\max}$  of 865 nm shows a red shift in its absorption. PANI (**20**) and PANI (**18**) were found to have some of the highest absorbance readings recorded during this investigation. This raised the question as to why the acrylic functionalised dopants had higher efficiency of doping. The answer could be related to the structure of the functionalised side chains of the dopants and their steric effects. Interestingly the methacrylic functionalised dopants produced some of the highest absorbances in the electronic spectra of all the doped polymer samples tested and it was clear to that they were most effective dopants.

The increased steric hindrance was as a result of the rigidity and bulky nature of the double bond a result of an overlap of the  $\pi$  orbitals. This overlap produced a rigid structure whereby rotation was reduced around the double bond/ $\pi$  orbital overlap; this rigidity therefore prevents movement at the carbons of the side chain unlike the aliphatic side chains. This freedom of rotation in the aliphatic systems, whilst still having some effects on the crystallinity of doped-PANI, allowed the movement of the polymer backbone to bend and kink which reduced the efficiency of chain opening. The addition of the methyl group in the acrylate meant that the steric hindrance was further increased through branching and was evident in the recorded electronic properties for doped PANI (**20**).

#### 4.5.1.1.5 Electronic properties of dodecylbenzene sulphonic acid doped PANI (**22**) (PANI-DBSA).

As a method of benchmarking and standardising control, polyaniline was also doped with dodecylbenzene sulphonic acid (DBSA). This dopant is well documented for its doping characteristics and efficiency.

UV-Visible spectroscopy results (Figure 37) in solution showed there was a shift in absorbance from the emeraldine base of PANI to the doped state (emeraldine salt) of PANI, moving from a  $\lambda_{\max}$  of 572 nm to  $\lambda_{\max}$  831 nm. In comparison to the rest of the sulphonic acid dopants, this system was highly efficient at doping and showed similar levels of doping to the acrylate functionalised dopants which have a  $\lambda_{\max}$  865 nm and 917 nm for doped PANI (**18**) and (**20**) respectively. These readings suggested that upon doping, the dopant promoted the conformational changes in the

polymer into a more elongated and open structure. Following the pattern of previously analysed systems, the optical properties also indicated that there was an increase in the wavelength of absorption, something that was seen previously in other systems; it would be safe to assume that upon re-analysing the solution sample in an instrument that has a much wider detection limit up to 2000 nm, further peaks or even a tailing off of the peak would have been witnessed. This characteristic was linked to the formation of bipolaron states, which with increasing levels of doping would have resulted in a fully delocalised system and an observable tailing off of the absorption bands in spectra.

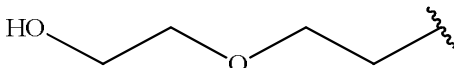
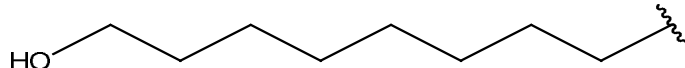
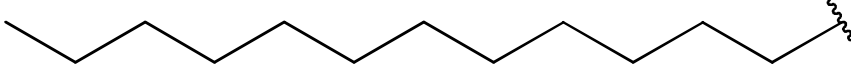
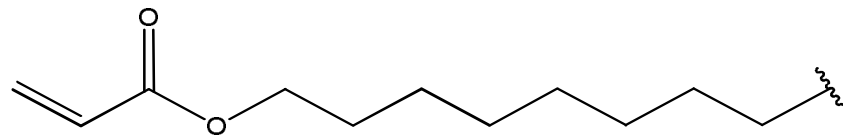
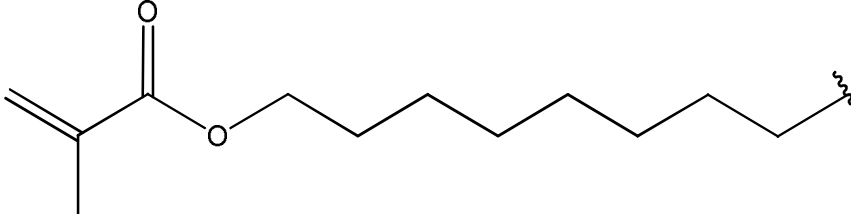
DBSA shared relatively common features when used for doping PANI in comparison with the rest of the sulphonic acid dopant series. It contained the protonic acid (doping constituent) as well as a plasticising constituent in view of its long aliphatic substituent. As discussed earlier, the absorption bands suggest two things which are in direct correlation with each other; firstly that the bands correlated to the formation of polarons and suggested doping and secondly that the conformation of the polymer is such that the structure is less coiled, as previously mentioned due to lower incidence of kinking which acts to reduce the energy (band gap) in the system (reduces the Peierls distortion). The uncoiling was the consequence of the steric effects exerted by the long dopant side chain preventing the doped polymer to coil back again.

What was also interesting is that up to this point the amount of side chains were not considered and as a result of using DBSA, it was shown that the number of side chains is irrelevant. Based on the results obtained it was evident that there was a correlation between the chain length, the steric effects and the efficiency of doping, with longer chains or shorter branched chains promoting the highest levels of crystallinity.

In

Table 2 the variable side chains are illustrated to show the length of the chain and branching in some case. The constituents are arranged in ascending order based on the length and branching. It was of interest to notice that; firstly, increasing length of the chain correlated to an increase in the  $\lambda_{\max}$ . Secondly, the introduction of branched chains further increased linearity of the polymer extending the  $\lambda_{\max}$  into

the infra-red region, more efficient doping was identified by the intensity of the peaks and was a good indicator to the level of doping.

Functionalised dopant side chain (sulphonic acid series) (functionalised constituent)	Doped PANI System	$\lambda_{\max}$ (nm) Solution
	<b>19</b>	764
	<b>17</b>	762
	<b>22</b>	831
	<b>18</b>	865
	<b>20</b>	917

**Table 2:** Table to illustrate the various lengths of the dopant side chains in ascending order of length, correlating the length of the chains to the optical properties observed and recorded.

#### 4.5.1.2 Analysis of the phosphoric acid diester doped PANI series in solutions of DCM.

Running parallel to the doping studies of the sulphonic acid doped systems, a series of phosphoric acid based dopants were produced. Based on the outcomes and results of the sulphonic acid series of doped systems, the phosphates shared many similarities in terms of functionalisation and the end uses such as resin incorporation were considered. Previously the acrylate functionalised dopants showed the most efficiency in terms of the doping, the effects elicited and the subsequent advantages acrylics offered in terms of the formulation potential.

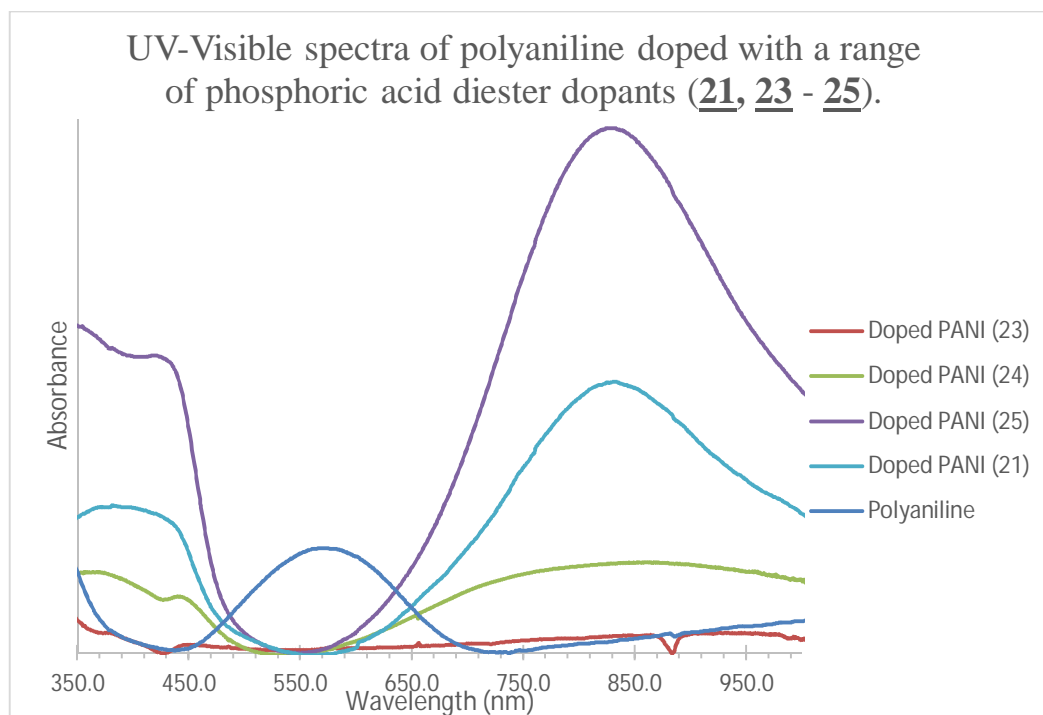


**Figure 40: Spectral overlays of polyaniline doped with a variety of dopants belonging to the phosphoric acid diester series.**

Looking closely at Figure 40, the spectra followed similar trends and patterns with the other spectra recorded; red shifted electronic properties from the un-doped state to the emeraldine salt of PANI (doped PANI) (

Table 3). Doped PANI (21, 24 and 25) are all functionalised with acrylic end groups; (21) and (24) being methacrylates and (25) being an acrylate. In the cases of (21) and (25) unlike the sulphonic acid doped polyaniline the absorption remained the same for both the acrylate (25) system and methacrylate (21) system with bands situated at 831 and 833 nm respectively. Doped PANI system (24) which was also functionalised with a methacrylic end groups, showed a broader band at a higher  $\lambda_{\text{max}}$  as shown in

Table 3. As a theory it may be possible for more localised steric effects around the site of doping affecting the aromatic ring of the polymer repeating unit, which evidently may be possible in the phosphoric acid diester dopants as opposed to the sulphonic acid dopants.

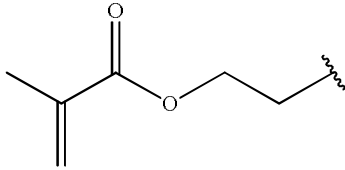
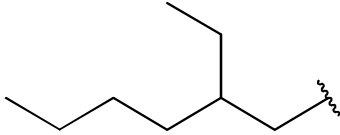
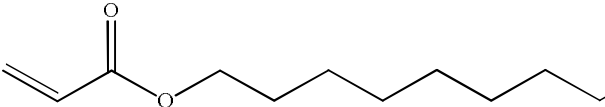
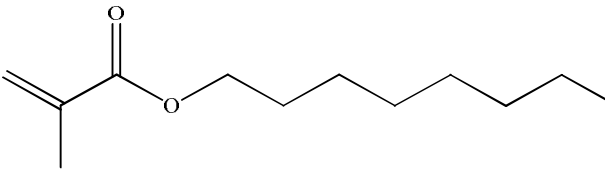
Doped PANI	$\lambda_{\max}$ (nm) Solution		
	1	2	3
<b>21</b>	398	-	<b>833</b>
<b>23</b>	380	445	<b>944</b>
<b>24</b>	376	442	<b>863</b>
<b>25</b>	326	427	<b>831</b>
Polyaniline	327	-	<b>572</b>

**Table 3: Summary of absorption data from UV-Visible Spectroscopy of Polyaniline doped with various phosphoric acid diester dopants.**

Our previous results have so far shown that the chain length had significant effects on the efficacy of doping, the ability to affect conformational changes of the polymer and the ability to plasticise the material. Therefore it was expected that dopants with shorter functionalised chains would have blue shifted electronic properties. Also the fact that the phosphates possess no aromatic group, would in theory reduce the levels of interaction with the polymer chain due to the absence of aromatic ring stacking. By this evidence it would have been expected that doped PANI systems (**22**) and (**24**) would be weak doping agents, producing less significant changes but this was not the case.

This presented contradictory and counter intuitive evidence and therefore original hypotheses were not entirely accurate, other factors were involved in the doping process. It still remained a fact that the functionality of the dopant side chains and the size of the side chains were significant to the outcome, which was evident from the data already gathered.

Table 4 tabulates the structure of the side chains used in the phosphoric acid diesters and their respective maximal absorption.

Functionalised dopant side chain of phosphoric acid series.	Doped PANI System	$\lambda_{\max}$ (nm) Solution
	<u>24</u>	863
	<u>22</u>	944
	<u>25</u>	831
	<u>21</u>	833

**Table 4:** Table to illustrate the various lengths of the dopant side chains of the phosphoric acid dopants in ascending order of length, correlating the length of the chains to the optical properties observed and recorded.

In

Table 4 it can be seen the emergence of a pattern. The table has been tabulated in ascending order of chain size of chain, showing that the smaller side chains produced better electronic properties and were likely to produce higher levels of crystallinity, ideally it would have been thought that the longer the side chains would have given greater steric effects. Based on the latter idea, dopants with a side chain of just 2 to 4 carbons in length would have been expected to display inferior doping properties, be disadvantageous and promote minimal conformational changes in the polymer; the phosphates however proved otherwise with regards to this matter.

From these findings it was rationalised that there were other factors affecting the observed optical properties. When comparing the phosphate dopants with the sulphonic acid dopants the size and shape was an important variable to consider, with the latter dopants being larger and bulkier molecules. Focussing on the subject

of size, it could be suggested that the phosphate dopants were able to reach a closer proximity to the site of doping compared with the bulky sulphonic acid dopants. Evidence has been stated that the aromatic rings play a role in the process of doping. Working with this fact it then becomes apparent that the larger sulphonates had an impact further away from the site of doping due to the steric effects being further down the polymer chain, whilst the phosphates being smaller fitted into the cleft of the amine between the aromatic rings of the polymer chain. The side chains of these phosphates would have their effects at the site of doping and due to their smaller size, there is the potential for doping at each amine/imine site, giving rise to higher levels of crystallinity. Adding to this the idea of branching the side chains gives the potential for greater degrees of conformational changes, further increasing the steric effects on the polymer chain as seen in the case of doped PANI (**23**). Looking at the spectral reading for doped PANI (**23**) the absorption is very weak which suggests that the level of doping may have been low but it can be seen that there is maximum peak absorption at 944 nm which displays the highest  $\lambda_{\max}$  of all the phosphodiester dopants and in fact all the dopants.

#### 4.5.1.2.1 Electronic properties of bis(8-methacryloyloxy octyl) hydrogen phosphate doped PANI (**21**) (PANI-DMOHP).

Doped PANI (**21**) in DCM solution produced a broad peak of absorption  $\lambda_{\max}$  at 836 nm, which was considerably more prominent in comparison to that obtained from its sulphonic acid counterpart (**20**) at  $\lambda_{\max} = 917$  nm (Figure 41). This blue shift in absorption suggested that these phosphate dopants are less efficient doping agents in comparison to their sulphonic acid counterparts. One reason for this could be due to the presence of the aromatic ring in the sulphonic acid, participating in  $\pi$ -bond overlapping of the aromatic systems in the dopant and the polymer. However the levels of doping seen in doped PANI (**21**) was much higher than that of (**20**) (Figure 41) and so it is not as straightforward as was previously thought.

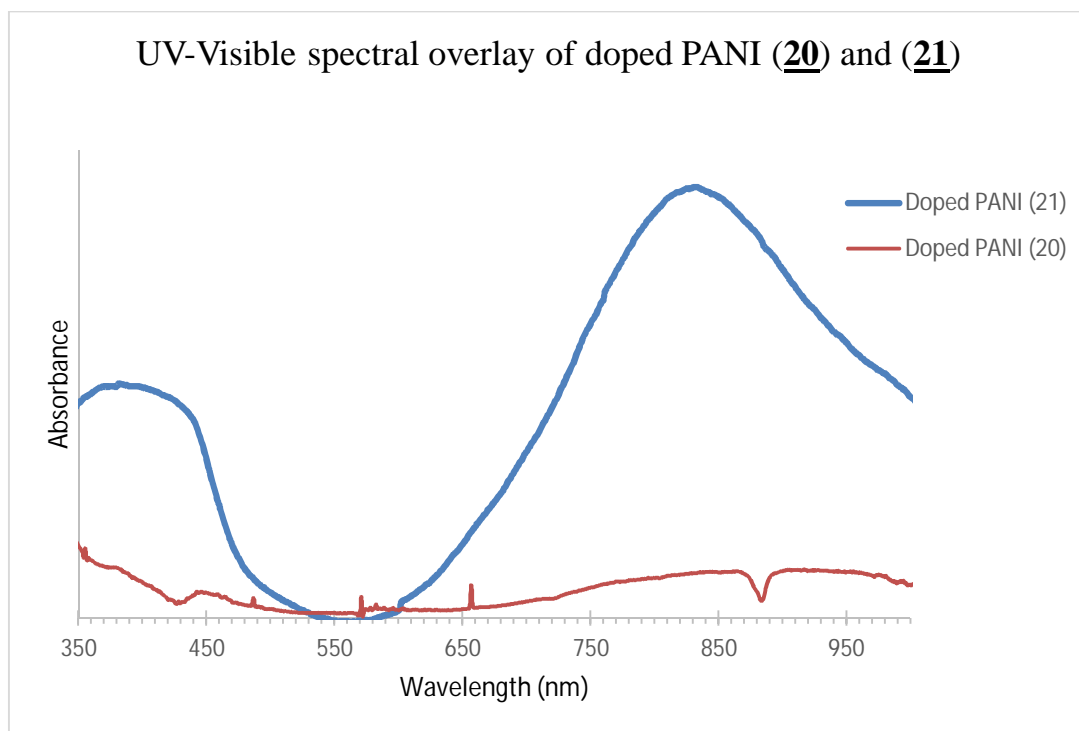


Figure 41: Spectral overlays of the phosphoric and sulphonic acid (functionalised with methacryloyloxy octyl chains) doped PANI (21) and (20) respectively.

Looking closely at doped PANI (21), when compared with other dopants of the sulphonic acid series (17) and (19), the prior showed higher doping efficacy and higher efficiency of causing changes to the structure and the electronic properties. The absorption bands had red shifted from;  $\lambda_{\text{max}}$  of 762 nm (17) and  $\lambda_{\text{max}}$  of 764 nm (19) to  $\lambda_{\text{max}}$  of 833 nm to (21). These values are similar to those obtained for doped PANI (22), a system doped with DBSA. It can therefore be concluded that these systems produced similar levels of uncoiling in the doped polymer. The evidence gathered so far suggested that the ideal dopant would be; aromatic which would enable and increase the interactions between the dopant and polymer and contain branched side chains to increase the steric hindrance and promote conformational changes, with doped PANI (22) and (21) fitting into at least one of these categories. As both have at least one of these characters, it explains why they remain midrange in terms of the  $\lambda_{\text{max}}$  absorption values observed, suggesting that both factors are really important regarding optimising the dopants.

Therefore looking at the individual characteristics of the dopants, factors such as the lengths of the chains might not be as important as previously thought. The functionality of the side chains by this reckoning remained important not only for their interactions with the resin matrices but also to the levels of doping achieved.

In comparison to the other phosphoric acids in the series, doped PANI (**21**) displayed a band at  $\lambda_{\text{max}} = 833$  nm which was not the highest level of absorbance recorded but was characteristic of the absorbance region at which the phosphoric acid doped series of PANI produced good results. When comparing doped PANI (**21**) in which the dopant has the methacrylate functionalised phosphate substituent with the acrylate functionalised phosphate system (doped PANI (**25**)) there was very little difference between the two (bands at  $\lambda_{\text{max}}$  of 833 nm for doped PANI (**21**) and 831 nm for doped PANI (**25**)). This small difference did not correlate to the wide red shifts observed on comparing doped PANI (**18**) (acrylate functionalised sulphonic acid dopant) and doped PANI (**20**) (methacrylate functionalised sulphonic acid dopant), These sulphonates seemed to give a wider range of absorption for the doped polymer.

#### 4.5.1.2.2 Electronic properties of bis(2-ethylhexyl) hydrogen phosphate doped PANI (**23**) (PANI-DEHHP).

As was the case with DBSA doped PANI (**22**), where it was included as a benchmark due to its prevalence in literature, it was similarly important to include an equivalent phosphate doping agent. Therefore both bis(2-ethylhexyl) hydrogen phosphate (DEHHP) and bis(2-methacryloyloxy ethyl) hydrogen phosphate (DMEHP) were used to produce doped PANI (**23**) and (**24**) respectively.

In this investigation it was seen that doped PANI (**23**) produced the highest observable  $\lambda_{\text{max}}$  of all the doped PANI systems tested, giving rise to a band at 944 nm in the infra-red region demonstrating a high level of planarity and crystallinity. Figure 35 displays the optical properties of this doped polymer system with a shape that is similar to the spectrum seen for doped PANI (**20**). The shape is somewhat uneven with a tailing off of the absorption reaching its maximum at 944 nm and then dropping off, this may suggest that the electronic properties were verging towards delocalisation whilst all of the other spectra showed and suggested localised electronic properties with concise bands of absorption (Figure 35).

The structure of the dopant and the functionality gave a clearer indication and proved imperative in its efficacy as a doping material; the dopant used in doped PANI (**23**) contained side chains that were branched much more significantly than the other dopants used. The readings and observations for this serve as key evidence which denoted that the branching of the side chain was one of the most

important factors of all the considerations that needed to be taken into account when designing the optimal dopant.

#### 4.5.1.2.3 Electronic properties of bis(2-methacryloyloxy ethyl) hydrogen phosphate doped PANI (24) (PANI-DMEHP).

The doping of PANI with bis(2-methacryloyloxy ethyl) hydrogen phosphate was very important for this investigation as it not only one of the dopants discussed in the literature, but also because it has a methacrylic functionalised side chains, similar to doped PANI (21), therefore allowed firm conclusions to be made and acted to reinforce the observations seen for doped PANI (21) system.

The optical properties of doped PANI (24) in solution in DCM, showed a distinct and noticeable broad band of absorption at around  $\lambda_{\text{max}} = 863$  nm. In comparison to the other methacrylate functionalised doped PANI (21) system where  $\lambda_{\text{max}} = 833$  nm there is a slight red shift of around 30 nm.

In order to consider the tuning a dopant for optimum and maximum effect, the length of the side chain takes lesser precedence than the structure and geometry of the side chain (branching) as previously mentioned.

The central and bridging component of the dopant in some way account for these differences; looking at the sulphonic acid dopants firstly the aromatic ring are proposed to participate in  $\pi$ -bond stacking between the aromatic rings of both dopant and polymer. This allowed for close proximity of the acid and the conjugate sulphonate to the amine in the polymer chain, the side chains extended away from the doping site causing steric effects and uncoiling much further down the chain. Taking that into consideration, when looking at the phosphate dopants the central component (phosphorus) was relatively smaller than the aromatic ring thus the size of these phosphate dopants allowed its insertion into the site of the amine. As a result the side chain of the phosphate dopants increased crystallinity from the site of doping as opposed further down the chain as may be the case of the sulphonic acid dopants (Figure 42).

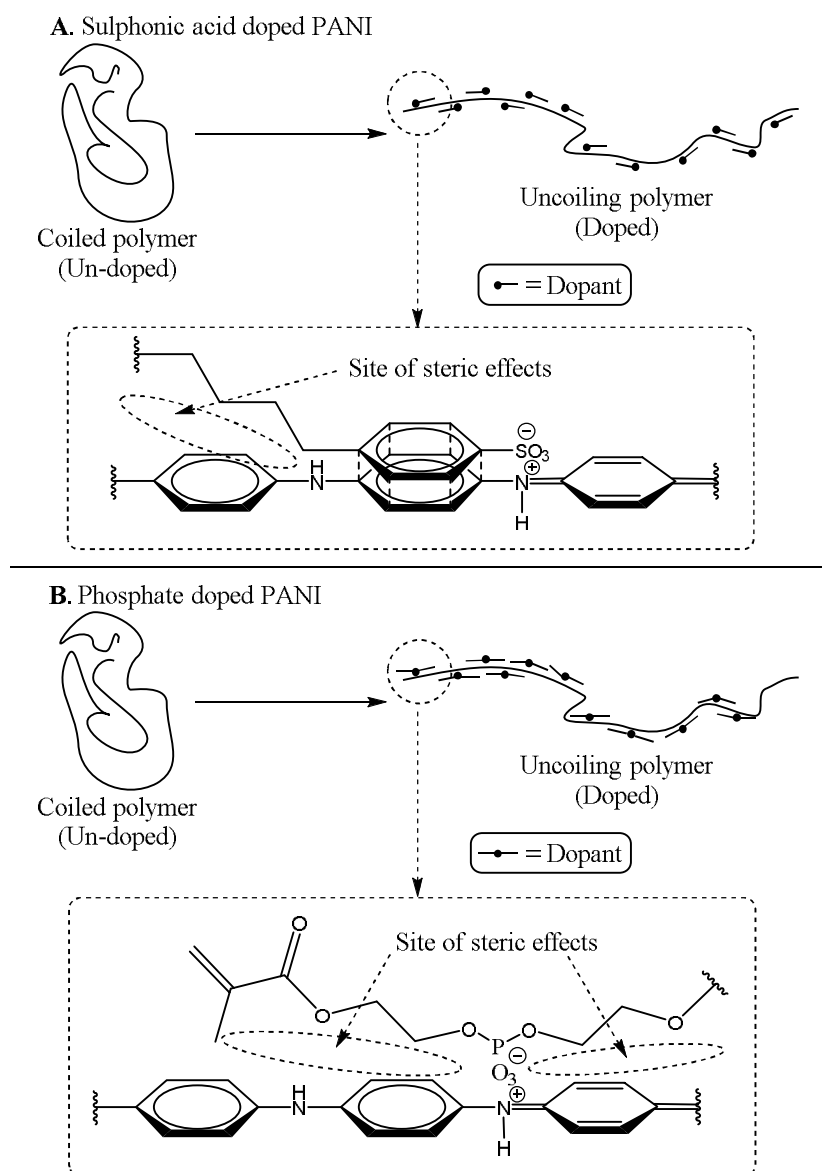


**Figure 42:** Simple illustration to show the sites of steric effects between the dopant and the polymer chain (PANI). A) displays the effects seen when PANI is doped with a sulphonic acid dopant (in this case DBSA) and B) is the same as previous but demonstrating the sites of steric effects when a phosphoric acid doping systems is utilised, in this case bis(2-methacryloyloxy ethyl) hydrogen phosphate (DMEHP).

#### 4.5.1.2.4 Electronic properties of bis(8-acryloyloxy octyl) hydrogen phosphate doped PANI (**25**) (PANI-DAOHP).

Bis(8-acryloyloxy octyl) hydrogen phosphate was synthesised alongside bis(8-methacryloyloxy octyl) hydrogen phosphate, during the production of the phosphoric acid dopant series, with the optical properties displayed in Figure 40.

Doped PANI (**25**) gave a distinct band of absorption around  $\lambda_{\text{max}}$  831 nm, however when compared with the other phosphoric acid doped PANI systems of the series it showed a slight blue shifted absorption which was similar to that of the acrylic functionalised sulphonic acids.

Doped PANI (**25**) (with the acrylate functionalised phosphoric acid dopant) and doped PANI (**21**), (the methacrylated functionalised phosphoric acid dopant) share similar spectral characteristics (Figure 43), such as broad bands of absorption and produced bands in similar regions;  $\lambda_{\text{max}}$  of 833 nm for doped PANI (**21**) and  $\lambda_{\text{max}}$  of 831 nm for doped PANI (**25**). However (**25**) is seen to produce higher levels of doping as evident from the intensity of the absorption. This doped PANI system showed the same trend as the previous doped systems of the series, showing a high order of electronic delocalisation and thus higher order of linearity (Figure 43).

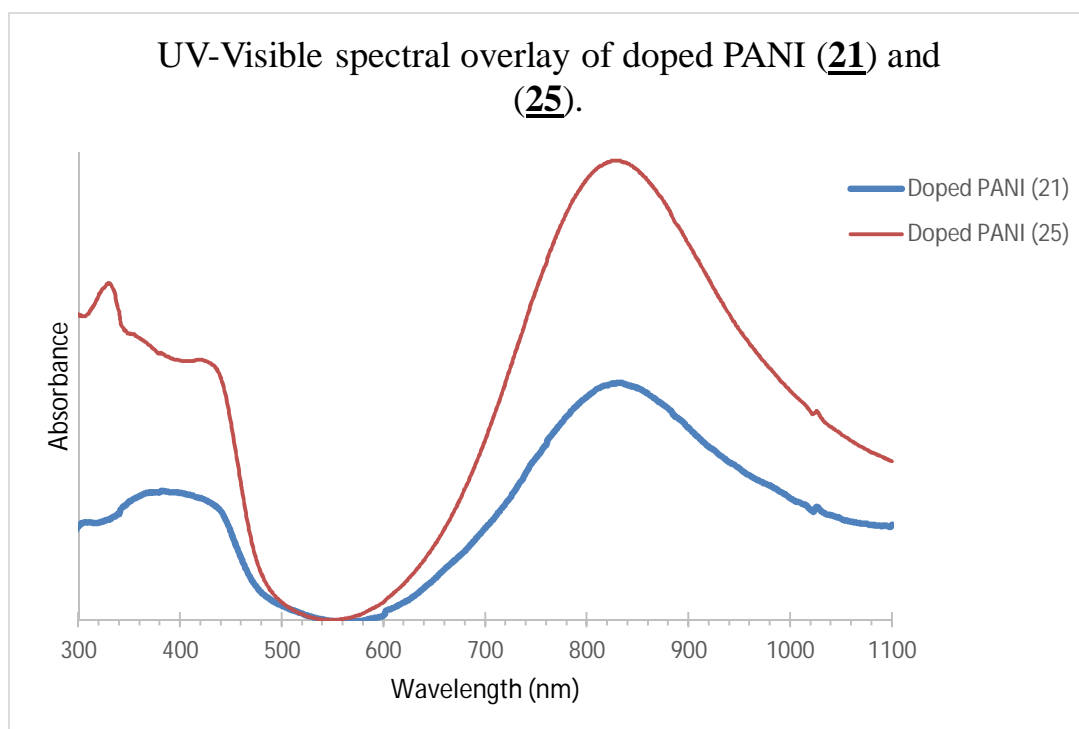


**Figure 43:** Spectral overlays of the phosphoric acid (functionalised with methacryloyloxy octyl (**21**) and acryloyloxy octyl (**25**) chains) doped PANI (**21**) and (**25**) respectively.

#### 4.5.1.3 Analysis of the phosphoric acid diester doped PANI series cast films from DCM solutions.

Films were used to demonstrate the changes in electronic properties between the polymer systems in solution and in the solid state. In solution the polymer chains are more mobile, increasing the likelihood of kinks and bends that gave rise to blue shifted absorption spectra. In cast films, the polymers become more ordered and have a higher degree of linearity which is seen as red shifted bands in their optical spectra.

The films were cast from the stock solutions ( $2 \text{ mg ml}^{-1}$ , DCM) of doped PANI (**21** and **25**) by dipping quartz plates. The films were created by dipping the plate

several times into the solutions of doped PANI and allowing the plates to dry at intervals producing several successive layers of the doped polymer on the surface of the plate. The solutions that the films were cast from were the same solutions used to determine the optical properties of the doped polymer in solution. The film thickness was not controlled which in this case was not essential as the information needed was of a qualitative nature to determine the optical properties.

#### 4.5.1.3.1 Optical properties of bis(8-methacryloyloxy octyl) hydrogen phosphate doped PANI (21) (PANI-DMOHP) Films.

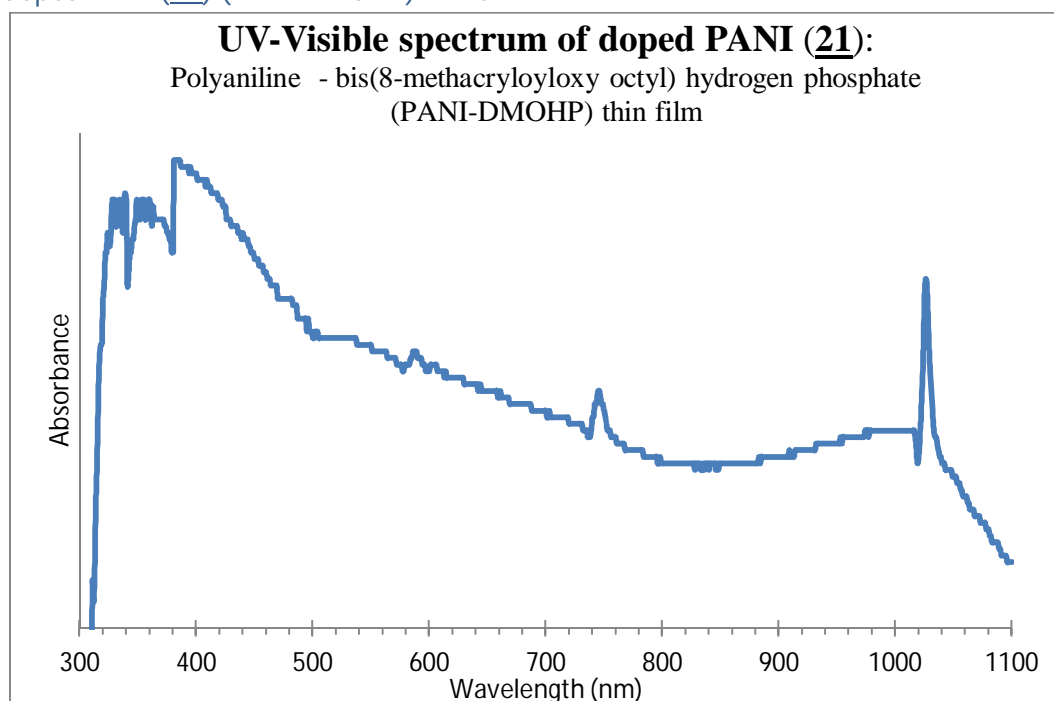


Figure 44: UV/Vis spectroscopy displaying the electronic properties of polyaniline doped with bis(8-methacryloyloxy octyl) hydrogen phosphate (PANI-DMOHP) (21) cast as a thin film from a solution of DCM onto a quartz plate.

The spectrum showed that the film thickness was low and as such produced a poor spectrum, this however was not detrimental as the  $\lambda_{\max}$  could still be identified at around  $\lambda_{\max}$  1027 nm, this showed the electronic properties were well into the infra-red region with the onset of this absorption being beyond the detectable region of the instrument.

From the optical properties observed in Figure 44, the optical band gap for this doped PANI (21) system can be calculated and determined using the equation illustrated in Equation 21. The optical band gap in this case was calculated to be  $E_g = 1.21$  eV.

$$eV = \frac{\left(\frac{hc}{\lambda}\right)}{\text{energy per } eV} = \frac{\left(\frac{1.99 \times 10^{-25} \text{ J.m}}{\lambda_{\max \text{ of Doped PANI } (\times 10^{-9} \text{ m})}\right)}{1.602 \times 10^{-19} \text{ J.eV}} = eV$$

Equation 21: Equation used for the calculation of the optical band gaps from the  $\lambda_{\max}$  absorption for the doped polymers ( $hc$ ) is a factor of plank's constant ( $6.626 \times 10^{-34}$  J.s) multiplied by the speed of light in a vacuum ( $c = 2.998 \times 10^8$  m.s).

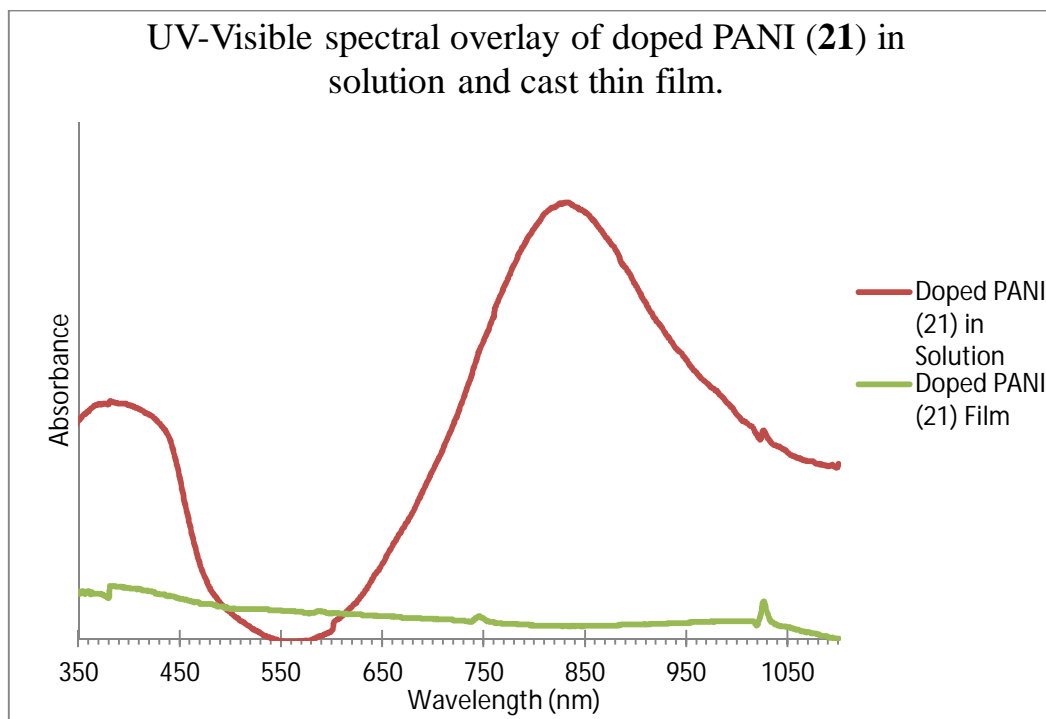


Figure 45: The spectral overlay of doped PANI (21) in a solution of DCM and its correlating thin film cast from a solution of DCM.

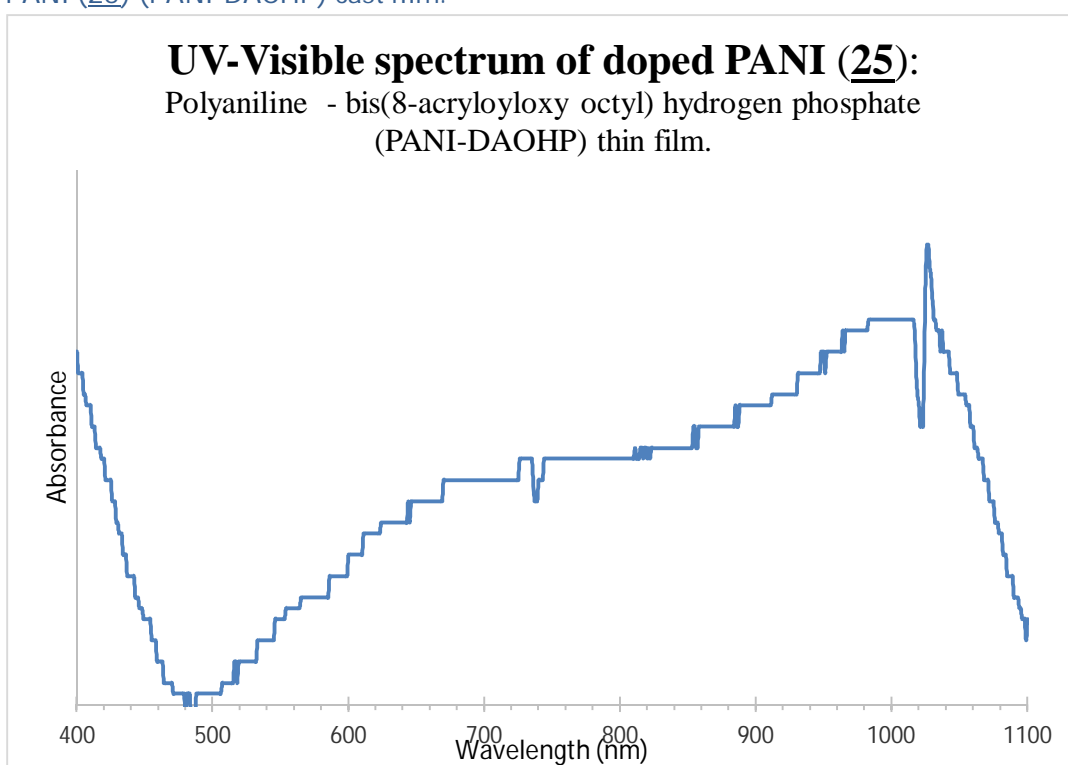
Figure 45 shows the spectral overlays for doped PANI (**21**) in both solution of DCM and solid state (thin film). Noticeable is the distinct red shift from the maximal absorption of the solution in comparison to the film, with the  $\lambda_{\max}$  of 833 nm for the solution and  $\lambda_{\max}$  of 1027 nm in solid state, a red shift of around 194 nm. This red shift was accounted for by the fact that in the solution the doped polymer has freedom of movement and although the dopants clearly is efficacious at promoting higher levels of crystallinity, the fact remained that it can still move allowing for kinks and bends to form. Upon casting the film from solution, the polymer movement is prevented and the polymer becomes locked in its position which in the case of doped PANI (**21**) showed a high degree of linearity and crystallinity. This therefore decreased the optical band gap of the polymer as displayed in

Table 5.

Solvent	Doped PANI in solution		Doped PANI cast Film	$\lambda$ Onset Absorbance (nm)	$E_g$ Optical (Band Gap) (eV)
	$\lambda_{\max}$ (nm) Solution		$\lambda_{\max}$ (nm) Film		
	1	2	1		
DCM	398	<b>833</b>	<b>1027</b>	Beyond recordable detection	<b>1.21</b>

**Table 5: Summary of the recorded optical properties of doped PANI (21) in a solution of DCM and solid state cast from a solution of DCM.**

4.5.1.3.2 Optical properties of bis(8-acryloyloxy octyl) hydrogen phosphate doped PANI (25) (PANI-DAOHP) cast film.



**Figure 46: UV/Vis spectroscopy displaying the electronic properties of polyaniline doped with bis(8-acryloyloxy octyl) hydrogen phosphate (PANI-DMOHP) (25) cast as a thin film from a solution of DCM onto a quartz plate.**

As in the previous case of doped PANI (21), the optical properties for both the solution and thin films of doped PANI (25) were recorded. Looking at Figure 46 this system produced a band at around a  $\lambda_{\max}$  of 1028 nm for the solid state and was in the same region as doped PANI (21), both showing optical properties within the

infra-red region of the spectrum. Much like the previous case the optical onset of absorption is just beyond the detection limit, but upon using a broader spectrum detector this could be determined. The optical band gap for doped PANI (**25**) has been calculated to be around  $E_g = 1.21$  eV similar to doped PANI (**21**).

Figure 47 shows the spectral overlays for doped PANI (**25**) in both a solution of DCM and solid state (thin film), the intensity of the spectrum for the film showed that the film thickness was rather thin as previously seen, however the  $\lambda_{\max}$  was determined from this plot for comparison with the more intense spectrum for the polymer complex in solution. The spectrum exhibited very noticeable red shifts from the maximal absorption of the solution to that of the film, with the  $\lambda_{\max}$  of 831 nm for the solution and  $\lambda_{\max}$  of 1028 nm in solid state. The red shift again suggested that the polymer in its solid state was highly crystalline. There appeared to be very little differences between the optical properties of doped PANI (**21**) and doped PANI (**25**) which are summarised in

Table 6.

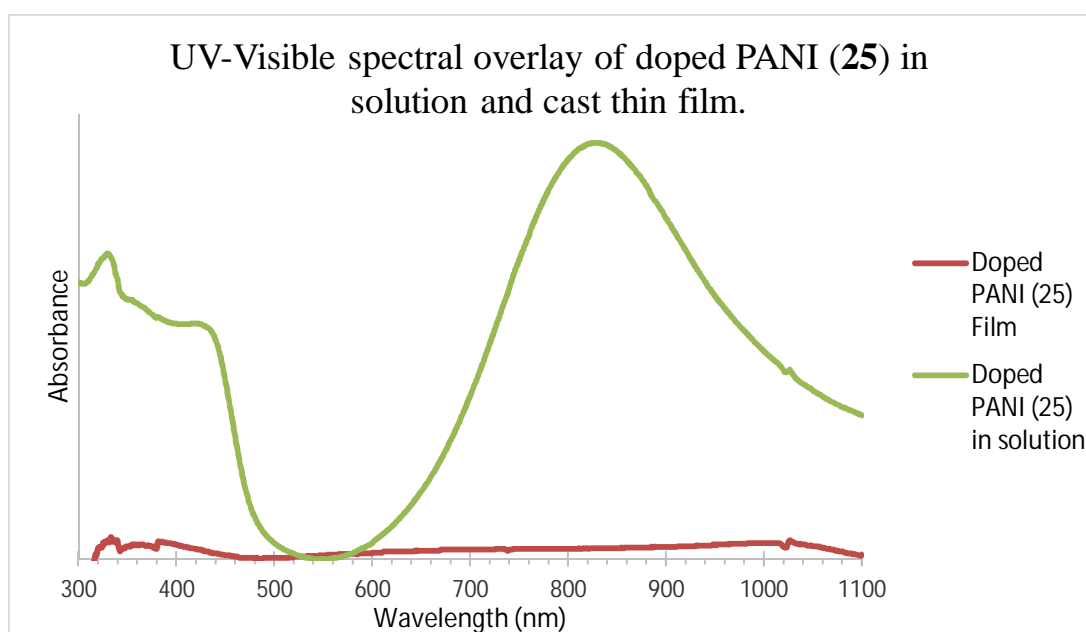


Figure 47: The spectral overlay of doped PANI (**25**) in a solution of DCM and its correlating thin film cast from a solution of DCM.

Solvent	Doped PANI in solution			Doped PANI cast Film	$\lambda$ Onset Absorbance (nm)	$E_g$ Optical (Band Gap) (eV)
	$\lambda_{\max}$ (nm) Solution			$\lambda_{\max}$ (nm) Film		
	1	2	3	1		
DCM	326	427	<b>831</b>	<b>1028</b>	Beyond recordable detection	<b>1.21</b>
Doped PANI System	Doped PANI cast Film			$\lambda_{\max}$ (nm) Film	$\lambda$ Onset Absorbance (nm)	$E_g$ Optical (Band Gap) (eV)
<u>21</u>						
<u>25</u>				<b>1028</b>	Beyond recordable detection	

**Table 6: Summary of the recorded optical properties of doped PANI (25) in a solution of DCM and solid state cast from a solution of DCM; includes the summary of the optical properties of the thin films for both doped PANI (21) and (25).**

## 4.5.2 Electronic and optical properties of doped PANI series PVC films

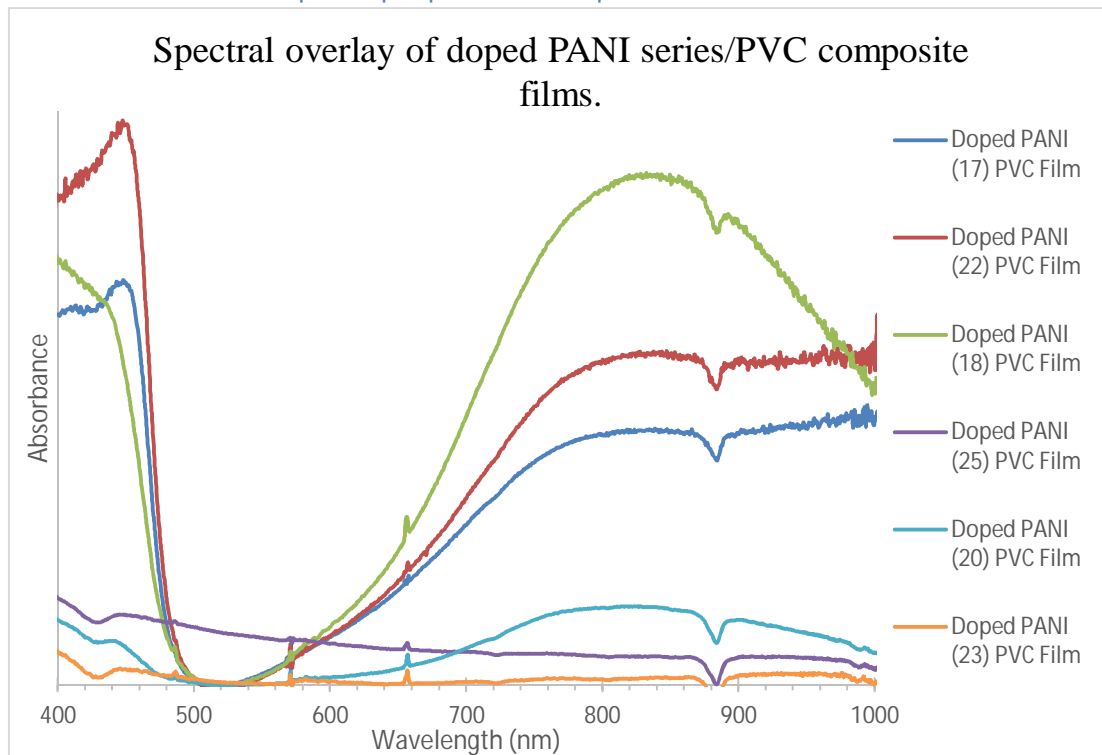


Figure 48: Spectral overlay of the optical properties of doped PANI (17 – 18, 20, 22 - 23, 25) incorporated into a PVC matrix and cast as a film onto quartz glass.

During the production of doped PANI composites and the casting of films onto the metal substrate, several thin films were cast onto quartz plates to investigate the optical properties of the composite looking for any changes in optical properties. Several of the doped PANI systems are not included due to detector problems.

Figure 48 gives clear indication to certain patterns that have previously been noticed; such as the doped PANI (23) system producing the highest  $\lambda_{\max}$  of series and is closely followed by doped PANI (25) system which suggest that these blends are well mixed and these doped polymer systems show high dispersity when mixed with PVC. One explanation is that the side chains of the dopants that have been functionalised to increase plasticisation, do increase processability and aid blending with other polymeric resins. This indicated that the higher the dispersity of the doped polymer and the more efficient the dopant side chains are at having plasticising effects, the higher the detectable absorption will be for the polymer system. The bands of absorption for doped PANI (23) and doped PANI (25) are around a  $\lambda_{\max}$  of 977 nm and 970 nm respectively.

In terms of the other systems, the bands of absorption appeared to occur in similar regions of the spectrum with doped PANI (**18**) producing an intense and broad band at around  $\lambda_{\max}$  of 839 nm. Doped PANI (**17**) and (**22**) systems appeared to produce identical optical spectra which appear to tail off beyond the detection limit representing high polaronic states in these composites with absorption for these two systems around  $\lambda_{\max}$  of 821 nm and 828 nm but these bands continue to tail off into the far infra-red region. The lowest band of absorption is around  $\lambda_{\max}$  of 813 nm for doped PANI (**20**) system which could be different due to rheological reasons.

Looking at

Table 7 both red shifts and blue shifts are seen in the films of the different doped PANI systems composites with PVC depending on which system is used to make the composite blends. In particular doped PANI (**17**), (**23**) and (**25**) showed a red shift in the optical spectra of their composite films, while the other doped PANI systems, (doped PANI (**18**), (**20**) and (**22**)) show a blue shift in their electronic spectra. When comparing the optical spectra of doped PANI in solution to those in composite films, one explanation for a shift in their optical properties could be due to aggregation of doped PANI and its phase separation in PVC composites. It could also be an indicator that there is some compatibility issues in the PVC matrix that maybe causing the polymer to coil, bend and kink.

Questions are raised as to why doped PANI systems which produced extended electronic delocalisation in solution are blue shifted when presented in a PVC composite. For example (**18**) shows a blue shift of around 26 nm, which previously showed one of the highest levels of electronic delocalisation in solution whilst doped PANI (**25**), again a doped system with high levels of doping shows a red shift of around 139 nm. So when comparing these two acrylated dopants; (**18**) being the sulphonic acid dopant and (**25**) being a phosphodiester, the difference is noticeable. However it may not solely be due to the side chains which in the cases of these two systems are functionalised with acrylates but rather what they are attached to, as the blue shift in doped PANI (**18**) is very small. It is clear that the dopant side chains are crucial to the processability of the overall doped polymer system and it is further clear to see that certain doped PANI systems have a specific level of processability into the PVC. This hypothesis is supported by the fact that

the doped PANI systems that have red shifted are the phosphate doped PANI systems. This is with the exception of doped PANI (**17**), which is a sulphonic acid dopant but produced red shifted optical spectra in composite films.

Doped PANI system	Doped PANI Cast Film in PVC	$E_g$ Optical (Band Gap) (eV)	Doped PANI in Solution
	$\lambda_{\max}$ (nm)		$\lambda_{\max}$ (nm)
<b>17</b>	821	1.51	762
<b>18</b>	839	1.48	865
<b>20</b>	813	1.53	917
<b>22</b>	828	1.50	831
<b>23</b>	977	1.27	944
<b>25</b>	970	1.28	831

**Table 7: Optical properties for the thin films of Doped PANI systems in PVC composite blends and their respective optical properties in solution.**

#### 4.5.3 Solvent effects on doping and electronic properties of PANI.

UV-Visible spectroscopy was conducted on both doped and un-doped PANI in different solvents and investigated to show the potential effects that different systems had on the electronic properties of the polymer. The solvents that were investigated were; *m*-cresol, DCAA and NMP, all of which have been well discussed significantly in articles for their effects on the properties and characteristics of polymers.

DCAA was used as the solvent medium of choice during the doping process for numerous reasons; mainly due to the solubility of PANI in this solvent. All the three listed solvents mentioned prior had serious health implications and were quite high boiling solvents (low volatility) therefore these solvents were not the solvents of choice and were superseded by solvents such as the halogenated solvents that were highly volatile and enabled the casting of polymeric films onto surfaces. PANI in the un-doped form was not readily soluble in these common solvents and the doped version required intricate processing into solution such as dissolving in one solution and transferring to another which raised its own issues. *m*-Cresol or NMP

were almost impossible to remove from a solvent mixture and so could not be used as processing solvents. DCAA however is readily soluble in both water and in most common organic solvents including DCM. This gave great advantage as the polymer was processed into the DCAA and mixed with another solvent (DCM) and finally the solvent (DCAA) was removed by successive washings of the solution until neutral pH was achieved. The doped polymer remained contained intact in the DCM solution.

#### 4.5.3.1 Electronic and optical properties induced by DCAA.

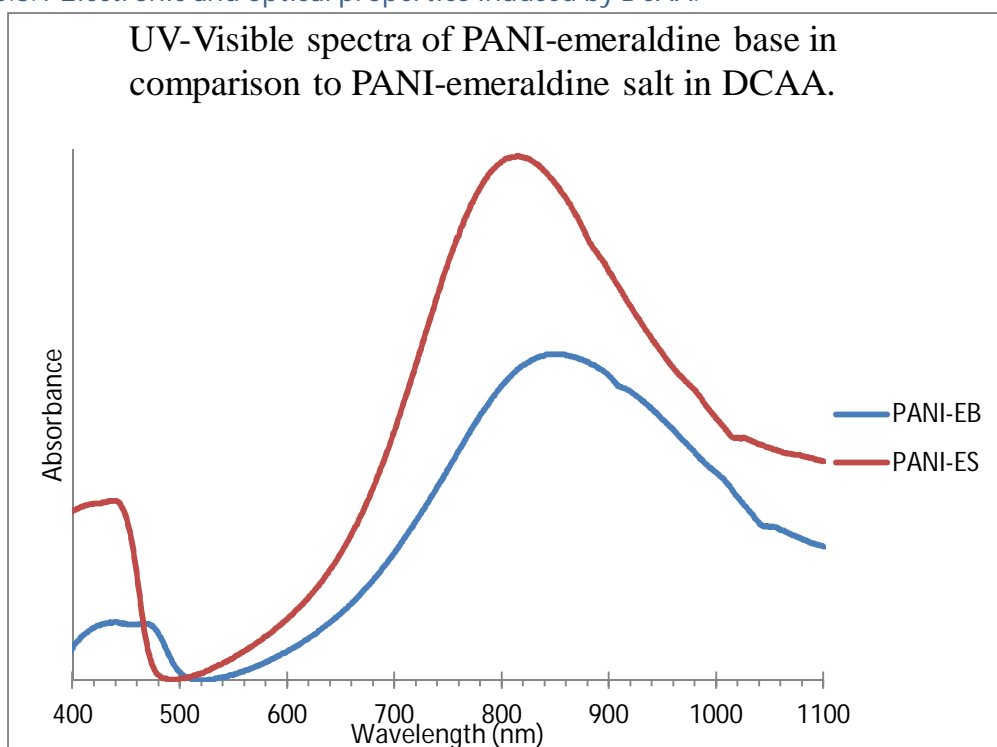


**Figure 49: Spectral overlays of doped PANI (PANI-ES) and un-doped PANI (PANI-EB) in DCAA to demonstrate any potential effects that may be exhibited in DCAA.**

Figure 49 shows the spectral overlay for doped PANI (**19**) (PANI-ES) with a  $\lambda_{\max}$  of 824 nm and un-doped PANI (PANI-EB) with a  $\lambda_{\max}$  of 815 nm are observed. In comparison to previous results where PANI-ES produced a  $\lambda_{\max}$  of 764 nm in a solution of DCM, this suggested that the DCAA was also acting as a dopant agent in this system, which is logical as DCAA is a protonic acid. The fact that this occurred suggested that DCAA acts both as a solvent and a competing dopant. Several explanations were concluded; Firstly the solvent (DCAA) enhanced the effects of the doping agent, increasing the electronic properties of the material. The fact that the polymer was not readily soluble in DCM initially, and only upon doping becomes marginally soluble, suggested that the polymer had more coil-like

structure in DCM solutions than in DCAA. Therefore the DCAA acts to increase the uncoiling that then enabled the polymer to have greater interaction with the DCM, hence the increased solubility. Second explanation proposed was that the solvent itself competitively doped the polymer and upon the successive washes was substituted with the doping agent that remained.

#### 4.5.3.2 Electronic and optical properties induced by *m*-cresol.

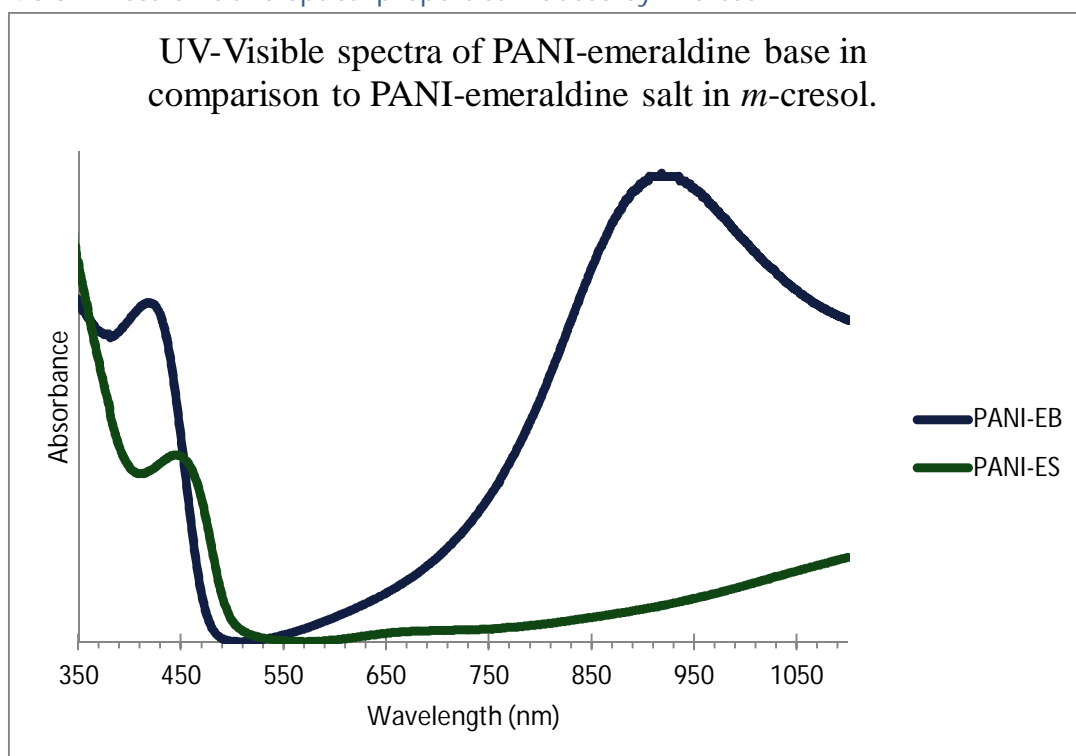


**Figure 50:** Spectral overlays of doped PANI (PANI-ES) and un-doped PANI (PANI-EB) in *m*-cresol to demonstrate any potential effects that may be exhibited by the solvent.

Figure 50 shows the spectral overlay of both doped (ES) and un-doped (EB) PANI as contained in a solution of *m*-cresol. Evidently it was clear to see that the *m*-cresol not only acted as the solvent which showed full dissolution of both forms of PANI but also displayed the ability to act as the dopant. Peaks were seen at 420 nm and 918 nm correlating to polaron- $\pi^*$  band and  $\pi$ -polaron band respectively for PANI-EB, there seems to be a peak in the UV region beyond 350 nm for the  $\pi$ - $\pi^*$  transition. Whilst the doped polymers (PANI-ES) saw a red shift at 451 nm correlating to polaron- $\pi^*$  transition and a tailing off into the IR region, which suggested that the polaron band was half filled and was a delocalised broad intra-band transition (Figure 51).

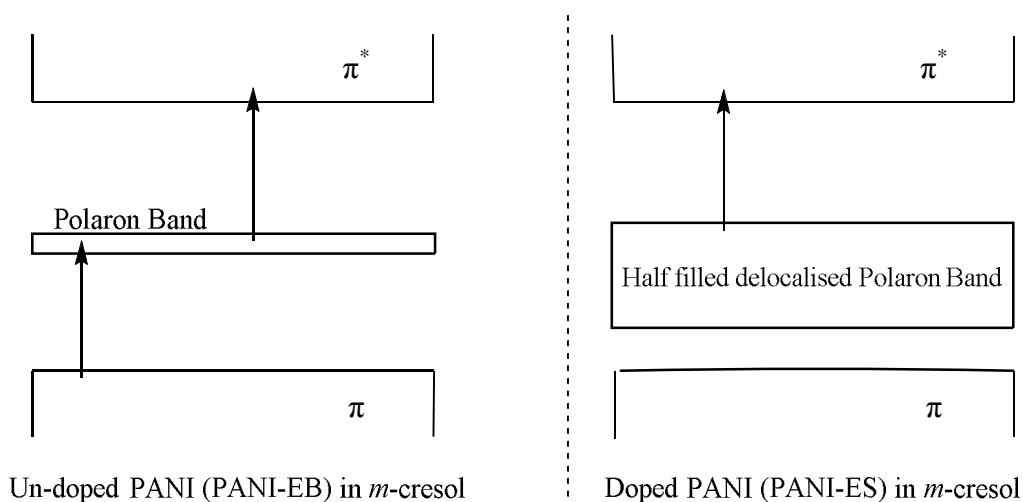


Figure 51: Illustration of band gaps in the case of *m*-cresol.

In terms of the electronic spectra; PANI-EB showed a distinct localised polaron  $\pi$ -transition band which had formed with the polarons being localized to segments of the polymer backbone. It is assumed that there is formation of a supramolecular complex between the PANI/Solvent. In the case of doped PANI systems, (PANI-ES) it is possible that a complex is formed between PANI and both the dopant as well as the solvent. In this case the polarons are delocalised along the polymer chain giving the tailing off of absorption bands into the infra-red region<sup>29</sup>.

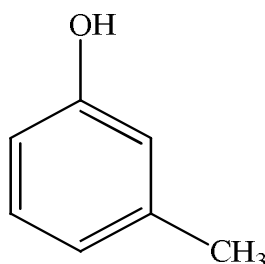
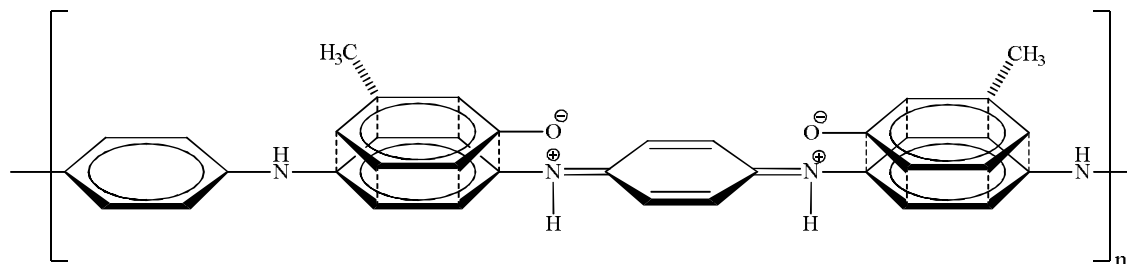


Figure 52: Structure of *m*-cresol.

This gave deeper understanding of the role that the doping agents played and gave more understanding to the conformation of PANI in both oxidation states. The conclusion was that *m*-cresol being mildly acidic (Figure 52) with a  $pK_a$  of around 10, was sufficient to participate in doping PANI by protonation of the amines. Second conclusion reached was that the increased electronic properties seen were due to the interactions between the aromatic rings of the polymer and *m*-cresol. The result was the  $\pi$ -bond stacking (Figure 53) which promoted the uncoiling and increased the conformational change, giving the higher  $\lambda_{max}$  than those systems doped with the synthesised dopants. In Figure 53 it is shown the possible

mechanism by which the solvent is interacting with the polymer and acting as the dopant, reducing the twists and kinks to further increase conjugation.



**Figure 53:** Aromatic  $\pi$  stacking of the polyaniline backbone in a solution of *m*-cresol, illustrating secondary doping effects.

This could be explained by the similar size of *m*-cresol to that of the dopants and the fact that the *m*-cresol is analogous to the sulphonic acids and that all amine sites may have been doped. Unlike the dopants however, *m*-cresol had no substantial side chains attached to the aromatic ring, which previously were proved important in preventing the coiling of the polymer through steric hindrance. Instead the electronic properties in this case can only be due to a vast array of aromatic ring stacking propagating along the chain, such an opening of the polymer chain is responsible for the observed electronic properties.

Examination of the optical spectrum of the doped PANI in *m*-cresol, more assumptions were deduced to explain why the absorption bands seem to tail off into the infra-red region. One explanation to be considered was that the dopants open the polymer chains from a coiled structure to one which is somewhat crystalline and elongated, however twist, kinks and conjugation defects remained leading to defects in the  $\pi$ -conjugation<sup>29,60</sup> limiting the red shift in the doped polymers' electronic spectra. However the addition of *m*-cresol to the doped PANI system saw the  $\pi$ -stacking of not only the polymer but all three components. The PANI/dopant/solvent (*m*-cresol) complex displayed a higher order of crystallinity and elongation to a much greater extent than either the solvent alone or the dopant alone. This diminished the incidence of defects in  $\pi$ -conjugation allowing a delocalisation, thus the absorption was far into the infra-red region. The vast array of  $\pi$ -stacking and reduced conformational defects produced a system where the polymer was 'locked' in an elongated and uncoiled position by the aromatic ring

interactions of both solvent, dopant and PANI, this being known as secondary doping.

Steric matching or otherwise known as molecular recognition crucially dictates the outcome of secondary doping. It is stated that the solvating solution had to possess certain criteria or functionality, such as hydrogen bond donors/acceptor, acidic groups and aromatic groups where the  $\pi$  bonds of different molecules can interact through weak Van der Waal forces. These however rely on the rings being within close proximity of each other in order to interact. Well documented is the secondary doping of PANI doped with camphor sulphonic acid; in this case the molecular recognition occurred through hydrogen bonds between the acidic proton of *m*-cresol and the carbonyl present in camphor sulphonic acid (Figure 54), second interaction was the mutual interaction of the phenyl rings of the solvent and the phenyl rings of the PANI backbone. This interaction occurred through weak Van der Waal forces which result in the stacking of the aromatic rings<sup>95,108,109</sup>.

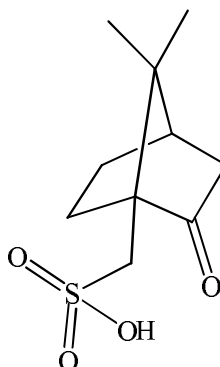
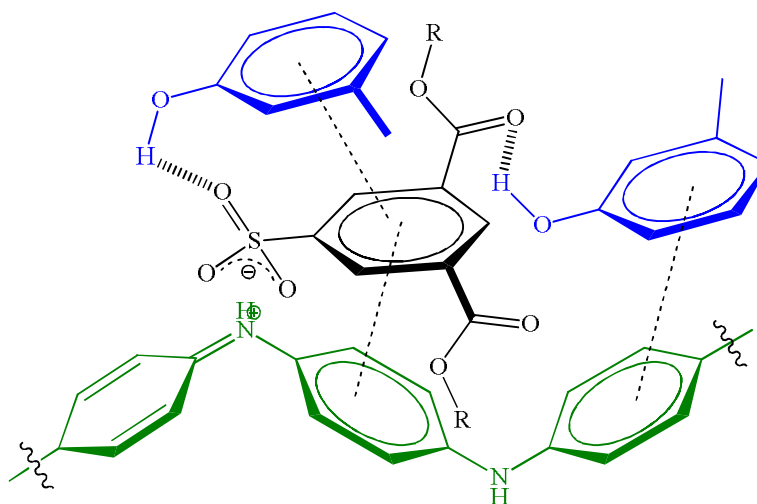


Figure 54: Structure of camphor sulphonic acid.

The distances involved between the components was extremely crucial and also a further factor affecting the levels of secondary doping possible. In the case of the camphor based dopant that is widely documented, such a complex is possible due to the distances involved; the size and length of the *m*-cresol molecule from the hydrogen bond donor to the phenyl ring matches the hydrogen bond site of the dopant (the carbonyl) and the phenyl ring of the polymer, allowing for the close proximity of aromatic rings of the polymer and the solvent therefore phenyl-phenyl interaction is close enough to be held by Van der Waals forces. It must be noted that upon the hydrogen bonding of the solvent-dopant, the orientating effects and

conformation as a result of the bonding means that phenyl-phenyl interaction becomes possible<sup>108</sup>.

It is therefore postulated that such interactions were possible in the case where the dopants successfully synthesised had been used to dope PANI and then presented in *m*-cresol, as evident by the spectra of PANI in *m*-cresol (Figure 50). Figure 55 illustrates the process of secondary doping and the interactions when the dopants synthesised have been used to dope PANI. Here it can be seen that there are several sites where hydrogen bonding can occur, and also it shows some possible instances where the interaction between the aromatic rings of both solvent and polymer take place. Therefore creating an extended uncoiled structure within the solution and therefore reduce the  $\pi$ -defects in the polymer.



**Figure 55: Molecular recognition (steric matching) doped PANI in *m*-cresol. Demonstrating the examples of forces involved in the development of the supramolecular complex (PANI = Green, dopant = Black and *m*-cresol = Blue).**

#### 4.5.3.3 Electronic and Spectroscopic effects induced by NMP.

As seen above, solvents have the potential to increase the electronic delocalisation of doped polymers, enabling further elongation of the polymer from a coiled twisted structure to a highly ordered crystalline structure. However the solvent utilised can also have the opposite and detrimental effect of the conformation of the polymer and more so on the electronic properties that are exhibited by the polymer.

NMP (*N*-methyl-2-pyrrolidone or *N*-methypyrrolidone) (Figure 56) a five membered lactam ring, a slight yellow dipolar aprotic solvent which is miscible in a range of solvents including water has been well documented as one of only a few solvents for its ability to dissolve intractable polymers, such as PANI. However

NMP is inherently basic and therefore inhibit or even remove any dopant from doped PANI.

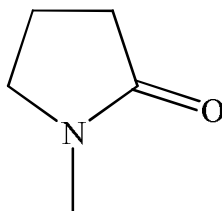


Figure 56: Structure of *N*-methyl-2-pyrrolidone (NMP)

Looking at Figure 57 it can be seen that the  $\lambda_{\max}$  is around 543 nm for the doped PANI (**21**) in NMP which when compared to the same doped polymer in a different solvent such as DCM presents a clear blue shift, shifting from a  $\lambda_{\max}$  of around 833 nm. The peak at 325 nm in NMP and 398 nm in DCM correlates to a  $\pi$ - $\pi^*$  band transition whilst the peaks at 543 nm and 833 nm are associated with polaron- $\pi^*$  bands. The recorded spectrum is not too dissimilar from the recorded spectrum of un-doped PANI (Polyaniline emeraldine base) in DCM with readings of 327 nm and 572 nm, which leads assumptions to the fact that in an NMP solvent system the doped polymer sample actually exists in an un-doped form in this solution, raising the question of why and how un-doping takes place.

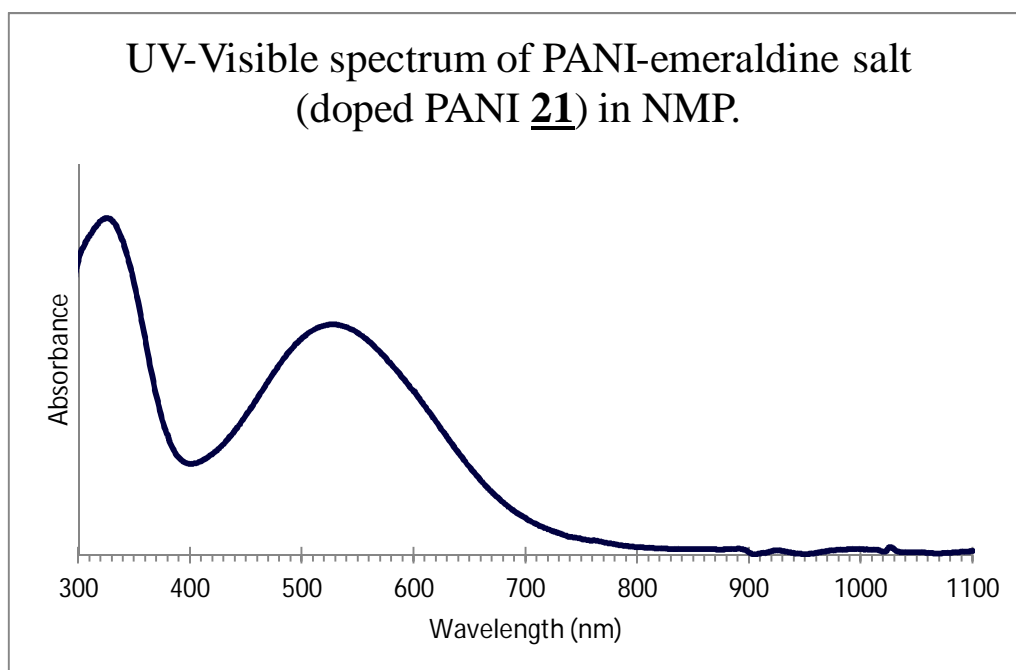


Figure 57: Spectrum of doped PANI (**21**) in NMP.

So looking at the results it can be said with a certain confidence that the polymer appears to exist in an un-doped form when presented in NMP. In order to

understand what is happening in this solvent system it should be noted that three factors need to be considered regarding any effect of the doping of PANI; Firstly investigations into electrostatic interactions ranging from very weak forces like Van der Waals to much stronger interactions like hydrogen bonding, second factor to be considered is the polarity of the solvent which will no doubt determine how the solvent interacts with not only the dopant but also the polymer and finally the entropy of solvation, which in the case of explaining how NMP affects doping is the least important of the three. Therefore it may be assumed that there exists a complex between PANI/dopant/solvent, this complex is formed by the electrostatic interaction (factor one) between the carbonyl (C=O) of the solvent as seen in Figure 56 and the acid proton of the dopant whether this be a carboxylic (-COOH), sulphonic (-SO<sub>3</sub>H) or a phosphoric acid diester (P(OR)<sub>2</sub>OH), thus this hydrogen bonding of the acidic proton (H<sup>+</sup>) will inhibit and prevent the doping of PANI<sup>110</sup>. Therefore two systems may result; these being PANI-H<sup>+</sup> + Dopant<sup>-</sup> + NMP = NMP-Dopant + PANI<sup>111</sup>. In terms of the entropy, PANI can interact with NMP and in doing so increases entropy of solvation, this leads to the eventual decrease in planarity and conjugation within the polymer chains and goes so far as to explain why a blue shift may occur and why the band gap is likely to be increased<sup>110</sup>.

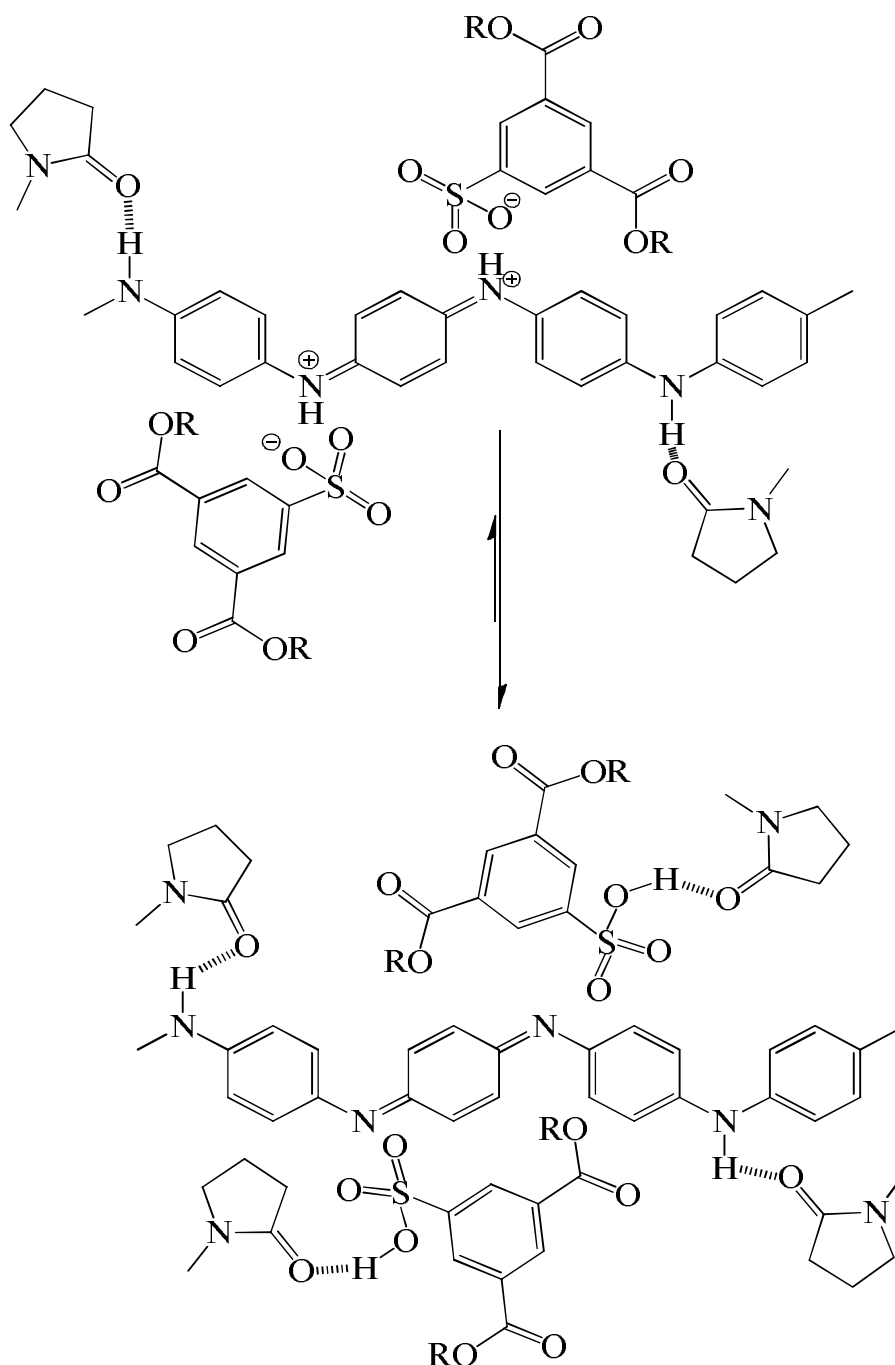


Figure 58: Illustration of the NMP/PANI/Dopant complex.

#### 4.5.3.4 Electronic and optical properties of doped PANI (21) films cast from different Solvents.

In theory, upon the casting of electro-active polymeric films it was expected that there be a significant and a noticeable effect on the electronic properties of the polymer, such as the band gap, increased absorption to a higher wavelength and a more structured and crystalline regime. The spectral overlays of doped PANI (21) cast films can be seen in Figure 59.

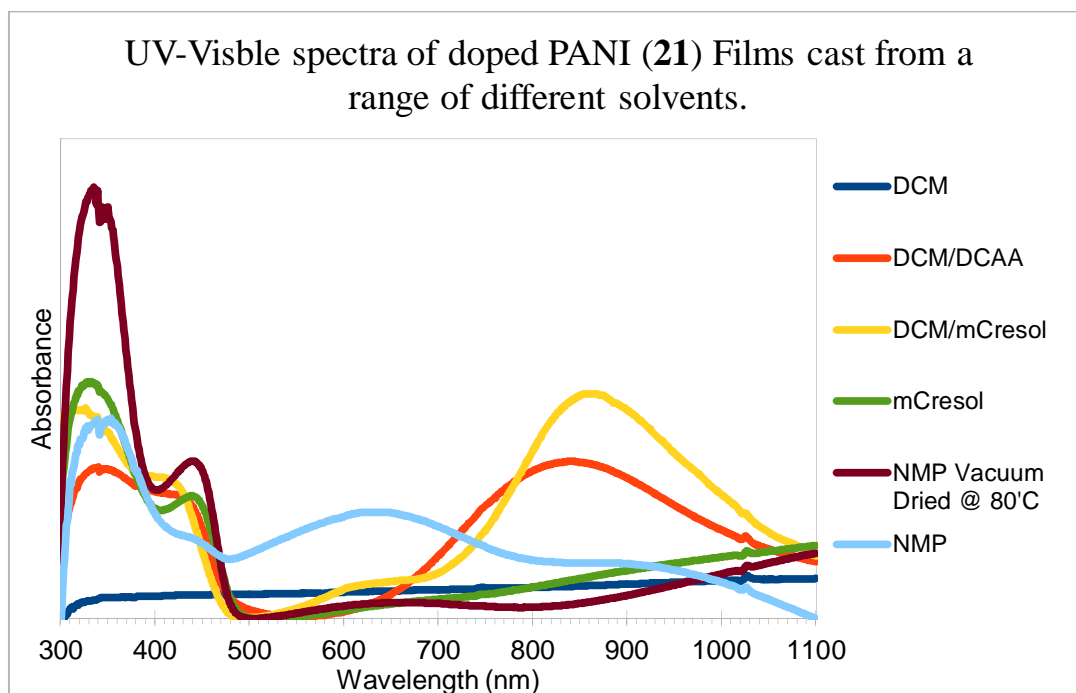


Figure 59: Spectral overlays of doped PANI (**21**) films cast from a variety of solvents illustrating red shifts in absorption from solutions to thin films.

Figure 59 summarises the  $\lambda_{\max}$  for doped PANI (**21**) cast from several solvents used previously to determine the optical properties in solution. In the case of *m*-cresol and DCAA, the data collected correlated to doped PANI (**19**) in their respective solvents for comparative reason. Although these samples were doped with different doping agents, the effects should be the same across all the doped PANI samples.

As illustrated by Figure 59 distinct changes in the electronic properties were noticed between the films and the solutions, with cast films displaying smaller band gaps than those observed in solution. The reasons for the red shifts were due to conformational and structural changes caused by the reduction in coiling of the polymer upon the removal of solvent, giving the chains increased crystallinity upon casting.

Mobility of the polymer chains was one of the main reasons for the noticed optical shift between the films and solutions, given that in the solution the polymer chains were mobile and free to bend, kink and coil. The kinks and twist of the polymers determine the levels of  $\pi$ -conjugation defects and directly affect the band gap of polymers, translating to blue shifted optical absorptions in solution in comparison to those in cast films. Upon casting of the films it is assumed that the polymer chains stretches and open up to a highly ordered or crystalline state, becoming

locked in position during the process of solvent removal and evaporation. Second point to be made regarding the levels of crystallinity, that whilst in solution the conformational properties of the polymers in solution act as a determining factor for the crystallinity of the films produced. In Figure 59, this statement can be justified by what was seen when different solvents were used; polyaniline showed different crystallinities in various solvents which determined the crystallinity of the film produced, this was in part mainly due to the levels of interaction between the solvent and polymer and the polymers respective solubility.

Solvent	Doped PANI Cast Film					Doped PANI in Solution	
	$\lambda_{\max}$ (nm) Film				Band gap	$\lambda_{\max}$ (nm) Solution	
	1	2	3	4		1	2
DCM	-	-	942-NIR		$\leq 1.32$	398	833
DCM/ DCAA	341	434	856		1.45	419	824 <sup>NB1</sup>
DCM/ <i>m</i> - cresol	357	446	868	1026	1.21	-	-
<i>m</i> -Cresol	331	435	Carrier Tail into NIR		-	451	Carrier Tail into NIR <sup>NB2</sup>
NMP*	341	452	667	NIR	-	-	-
NMP	344	436	645	927	1.34	325	543

**Table 8:** Table summarising the absorption bands of doped PANI (21) cast films in comparison to doped PANI (21) in solution. (\*= NMP sample film cast under vacuum at 80°C.NB1; Sample is doped PANI (19) in DCAA, NB2; Sample is doped PANI (19) in *m*-cresol).

In solution, doped PANI samples in NMP display the lowest  $\lambda_{\max}$  and widest band gap of all the doped PANI's, in comparison to doped PANI in *m*-cresol. Looking at the registered absorption bands for films cast, *m*-cresol still displayed the lowest band gap/highest  $\lambda_{\max}$  with those of NMP following closely. Samples cast from DCM displayed high orders of crystallinity suggesting that the polymer in solution displayed some uncoil like properties. In the cases of *m*-cresol and NMP, films cast from these solvents would be expected to have shown similar results due to the solubility and interactions of both doped and un-doped PANI in these solutions. DCM also displayed absorption bands that tailed into the IR region which suggested that cast films of the polymer became more crystalline as it was set in

place during solvent evaporation. However samples cast from DCAA showed the lowest red shift and actually the lowest  $\lambda_{\max}$  of all the films, it was suggested that this was due to the fact that DCAA showed little volatility and so residual solvent remained. NMP sample similarly proved difficult to dry, it was thought that whilst in solution the PANI existed in an un-doped form due to NMP interactions with the polymer, removal of NMP allowed for some doping to reoccur. This was further illustrated when films cast from NMP samples were compared with films cast from NMP under vacuum at 80°C. The removal of *m*-cresol, another high boiling solvent, was also difficult and it has been reported that when using such solvents up to 18 wt% remains within the film when the solvent has a high boiling point<sup>110</sup>, however in this case there is no detriment to the films properties as in the case of *m*-cresol, the absorption bands reach far within to the IR region regardless.

## Chapter 5 RESULTS AND DISCUSSION: ACCELERATED CORROSION STUDIES.

### 5.1 Accelerated Corrosion Testing

Accelerated corrosion testing was carried out using a heated propagator (Figure 60), meeting all the criteria needed to perform the tests; gentle heating (30-35°C) an enclosed controllable system providing humidity and robust design for cultivation of biological material. The humidity during testing averaged around 70% with air temperatures around 22-23°C internally. The internal solution temperature was maintained from the start to the end of the study at around 25°C. The effects of humidity and submersion into a 3.5% saline solution (representative of sea water) were both tested.

The sampling time for the tests were set to last 7 days in length which was far less than those reported in literature<sup>68,83,87,112-115</sup>; photographs were taken at specified time points: 1 hour then 24 hours and every 24 hours after this for a maximum of 7 days (168 hours). Images for both sides of the plates were obtained.



Figure 60: A typical heated propagator used for the Accelerated corrosion testing. Images obtained from:[http://www.britcropshydroponics.co.uk/components/com\\_virtuemart/shop\\_image/product/Stewart\\_propagat\\_4cdd2f3a96c1c.jpg](http://www.britcropshydroponics.co.uk/components/com_virtuemart/shop_image/product/Stewart_propagat_4cdd2f3a96c1c.jpg) and [http://www.bostockshomeandgarden.co.uk/WebRoot/BT/Shops/Store\\_002E\\_Shop910/470B/772C/D366/14C2/F3C3/AC10/3D2A/EC93/Large\\_Electric\\_Propagator.jpg](http://www.bostockshomeandgarden.co.uk/WebRoot/BT/Shops/Store_002E_Shop910/470B/772C/D366/14C2/F3C3/AC10/3D2A/EC93/Large_Electric_Propagator.jpg)

#### 5.1.1 Scanning Electron Microscope (SEM)

Scanning Electron Microscopy was used to image the surface of all the samples, post accelerated corrosion testing; the model used was a Philips XL20 SEM (Figure 61). This was accompanied by a fully integrated high vacuum oil pump, creating a vacuum pressure of around 1mmHg. The microscope was connected to a computer processor that housed specialist software created by in-house by Philips.



**Figure 61: Philips XL20 Scanning Electron Microscope. Operating voltages between 8 and 12 kV, resolution to 4nm and a maximum magnification of x50,000.**

A conductive layer was not applied to the surface of the samples due to their integral conductivities of the metal and the conductive polymeric coating dissipating any charge build up on the surface. The coating with gold or graphite was an irreversible process and so the samples would have limited use post microscopy, and eliminating the pre-coating reduced the costs and sampling time. During the microscopy some of the resins used such as PVC saw some build up of charge which was alleviated by using a lower voltage.

### **5.1.2 Accelerated corrosion of the experiment standards for benchmarking.**

Samples were assessed at specified time points as previously described and sampling included the air temperature measurements and humidity measurements both internally and externally using an hygrometer multi-meter. The brine solution temperature was measured using a mercury thermometer. Images were collected at each time point with a digital camera, gathering images for both sides of the plates.

Prior to the investigation the metals were acid pickled using either a concentrated solution of hydrochloric acid (37%) for the cleaning mild steel samples and a nitric acid (25%) solution for cleaning of the copper samples. Pickling was carried out

until no visual signs of corrosion, grease or any other debris were present on the plates.

For the purpose of control and standardisation both uncoated copper and mild steel samples were subjected to the same conditions as plates with polymeric coatings, for benchmarking purposes. Benchmarking was also performed on samples coated with PVC, acrylates and the epoxy resins without the presence of the doped polyaniline complexes.

#### *5.1.2.1 Accelerated corrosion of uncoated metal and morphology results.*

Figure 62 showing the uncoated plates after 7 days of submersion in brine solution gave clear indication that corrosion had occurred being more noticeable on the samples of steel. The copper samples appear to be more resistant to corrosion showing only traces of patina formation.



**Figure 62: Photograph of mild steel and copper post submersion in a (3.5%) saline solution for 7 days.**

Electron Microscopy was conducted on the steel and copper samples post acid pickling, identifying any changes that had taken place during the accelerated corrosion tests, benchmarking corrosion levels on uncoated samples of steel and copper plates.

Images captured at high magnification showed that some areas remained free of rust on the steel samples. Firstly, looking at the image captured of the rust free zone, it shows a surface that is jagged which would aid the adhesion of the coatings to the surface, contrasting episodic smoother zones between rougher areas on the surface. The smooth planes were very similar to tectonic plates in appearance as seen in Figure 63. The images showing the rusted areas were visually

distinguishable from rust free areas. The rust appeared to be furry globular structures, with hidden patches of rust free metal that were approximately 25-30  $\mu\text{m}$ .

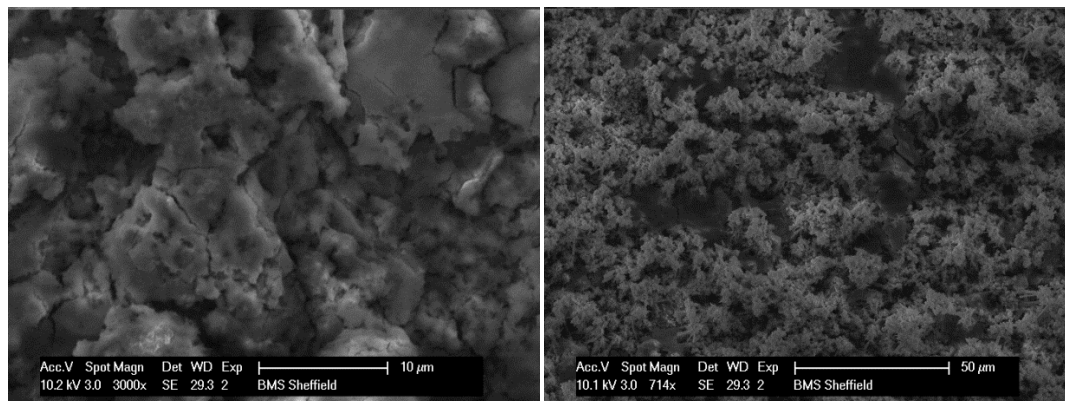


**Figure 63: A) Magnified un-corroded area (left), magnified to x3000 and B) Rusted area magnified to over 700 times.**

The bare copper samples, in contrast to the steel samples, showed smoother surfaces; however protrusions were noticed in a most areas of the sample when magnified. Contrary to logic, the adhesion was not favourable towards the rougher textured surface and in fact the polymeric material favoured the steel surface which suggested that there was a reaction or some form of interaction between the polymeric materials or doped polymer and the steel plates interface.

#### *5.1.2.2 PVC Alone Accelerated corrosion tests and morphology of the coating.*

PVC was chosen as a benchmarking coating due to its commercial use and popularity as an industrial coating. This determined two key aspects of the coating: the barrier properties and the barrier potential in contrast to the other benchmarkers (epoxide and acrylic coatings). Figure 64 shows the levels of corrosion after 7 days of accelerated corrosion testing. The corrosion appeared to be rather episodic, indicating that the coating had porosity issues and obvious corrosion at the edges was expected due to these areas being naturally weaker areas of the films. The copper samples showed that lower levels of corrosion and adhesion of PVC on both metals was good, with little delamination at this stage.

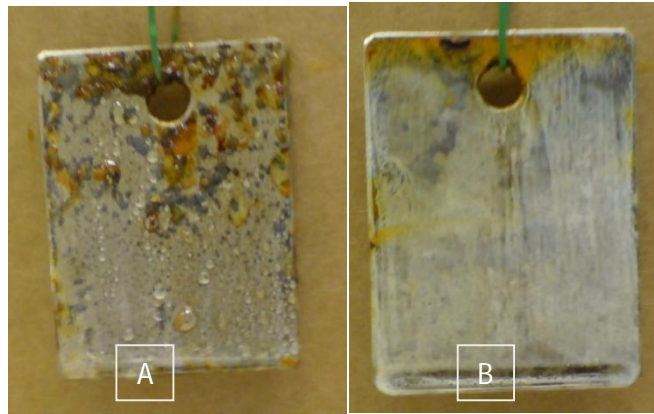


**Figure 64:** Photographs of PVC cast film onto mild steel; sampling A) 7 days after being sprayed with a 3.5% saline solution and B) 7 days after being submerged into a 3.5% saline solution.

One of the main barrier properties highlighted during the testing of the coated samples was that these films were highly porous, allowing the corrosive species to migrate through the film to the metal surface. The scanning electron microscopy of the films confirmed the porous morphology PVC coatings: the pores within the films appeared to interlink with other pores, creating a network of channels capable of allowing the migration of a corrosive medium. Figure 65 shows the morphology of PVC at 2760x magnification, the pores sizes and diameters were estimated and appeared to range from a few microns to hundreds of nanometres. Further inspection of Figure 65 confirmed that the pores existed at the micron level as collective network of interlinking pores, allowing water to travel through to the metal surface giving their suggested short shelf lives of such industrial coatings.

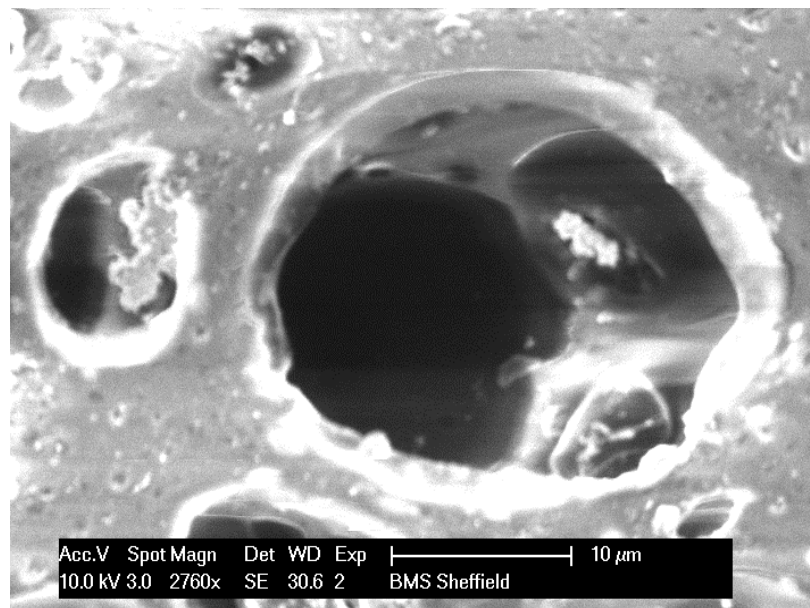


**Figure 65:** PVC cast onto pre-treated copper, illustrating internal structure of a pore on a cast film.

### 5.1.2.3 Accelerated corrosion tests and morphology of the Epikote 828™ films

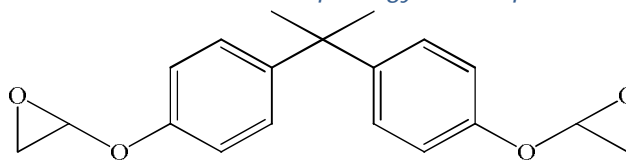


Figure 66: Structure of bisphenol A diglycidyl ether form (Epikote 828™) used for this research.

Epikote 828™ (Figure 66), the epoxide chosen for this investigation, was renowned for its adhesive properties: long lasting coatings and like other epoxides, it gives excellent barrier properties which have been the reason how it has found use in the manufacturing of industrial coatings.

The images captured showed a well adhered coating that had no obvious signs of corrosion on the metal surface with the exception at the metal plate's edge; this was anticipated as this was the weakest point on the film. The coating itself was extremely smooth with a clear brown colouration and it appeared to be very rigid, hard and brittle. At the edges of the steel samples, oxidation was minimal and this was due to penetration of water and the diffusion of oxygen through the film whilst the passage of other corrosive species was prevented (Figure 67).

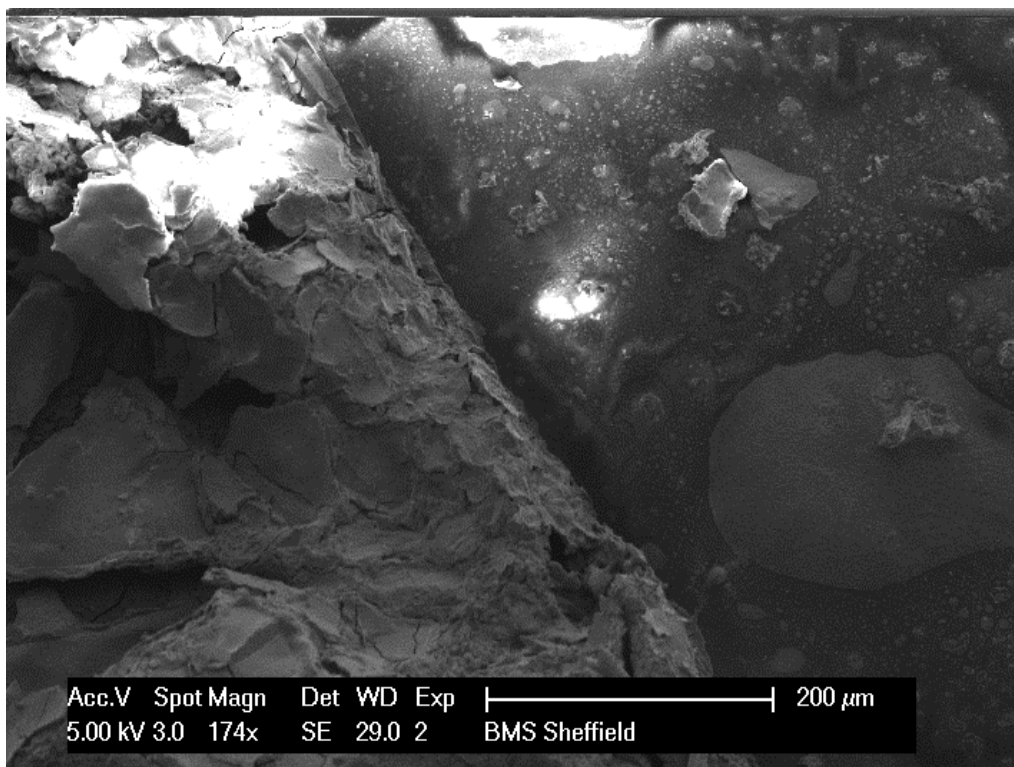


Figure 67: Close up of showing rust/metal interface under the epoxide film.

The copper samples showed patina formation at the edges where they were most likely hydrated cupric chloride ( $\text{CuCl}_2$ ) and cuprous oxide (Cuprite) ( $\text{Cu}_2\text{O}$ ). Figure 68 shows a close up of the patina/copper interface under the epoxy resin. Here the patina is smooth and uniform with little pitting present and it is represented by the lighter area in the image. It's worthy to note that there did not appear to be any form of delamination taking place, justifying their commercial use as an industrial coating.

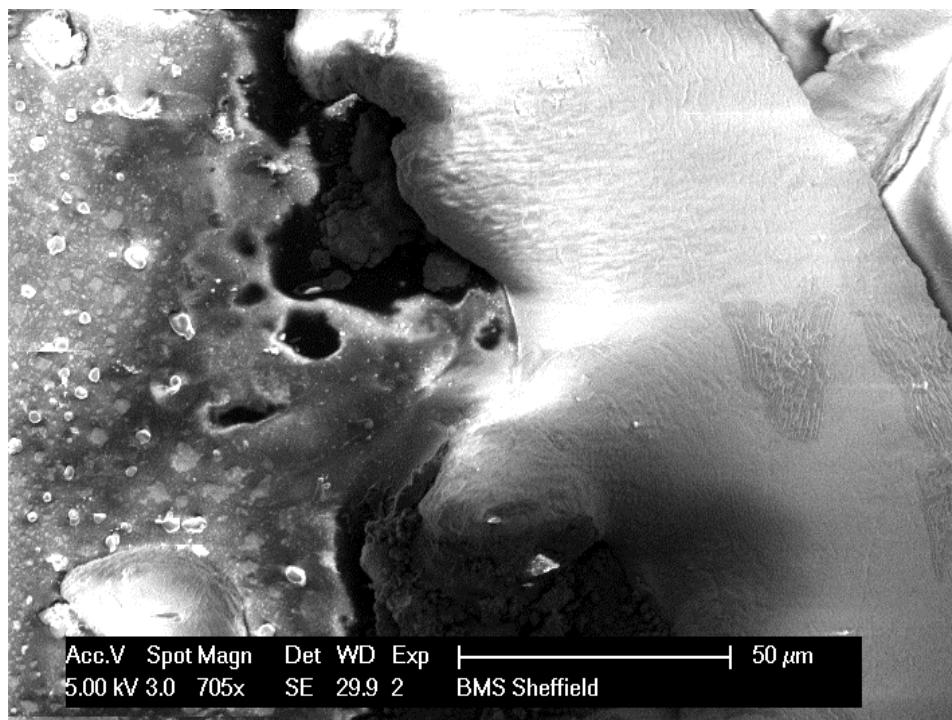


Figure 68: Close up patina/copper interface.

#### 5.1.2.4 Accelerated corrosion tests using acrylic resin alone films.

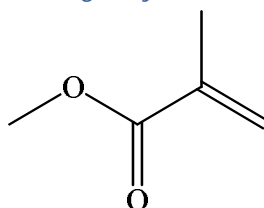


Figure 69: Structure of methyl methacrylate, upon the crosslinking and free radical polymerisation forms a vast network which results in a thin film (coating).

The final film of interest was the acrylic resins; these were of interest as some of the dopants were functionalised for the purpose of being formulated into an acrylic resin mixture.

Prior to the accelerated corrosion tests, the films appeared glass like and shiny, similar to the epoxide resins; however it was apparent that unlike the epoxide films, these films were extremely brittle. The morphology of the films was very poor and it proved to be an unacceptable coating due to these films showing high levels of breakdown (excessive cracking) and inadequate adhesion. The conditions of the accelerated corrosion tests proved too aggressive and these coatings subsequently failed. After 7 days (168 hrs) (Figure 70), it was clear to see that the films integrities were compromised from the excessive cracking.

The process of coating the metal samples with the acrylic resins proved the most difficult to produce. The adhesion was poor therefore the films had to be cast by spot coating followed by curing in an oven before the opposite side could be coated. The brittleness of the coatings was addressed by incorporating other acrylic species into the mixture which lowered the ( $T_g$ ) thermal glass transition temperature. Nevertheless, this did little to solve the brittleness or the adhesion properties of the coatings which are well renowned<sup>116</sup>. The two steel samples which were dark rust brown (Figure 70) showed extensive corrosion, causing the film to disbond and delaminate. The coatings appeared to enhance the effects during the accelerated corrosion tests; it may be possible that the coatings were trapping and concentrating the corrosive medium under the film.



**Figure 70: Metal plates coated in acrylic resin alone after 7days (168 hrs) of accelerated corrosion testing. From left to right; steel submerged in brine and copper submerged in brine, steel sprayed with saline and copper sprayed with saline.**

### **5.1.3 Accelerated corrosion of metal coated with doped PANI.**

After investigating the potential effects of the resin matrices, their potential protective effects and their ability to promote healing of metals post contact with corrosive agents<sup>117</sup>, it was then crucial to determine the effects of the doped polymer and the effect they could have on the surface of the metal. Ideally a

synergistic system was aimed for, whereby one aspect was for the coating to be a physical barrier and taking a sacrificial role and the second aspect to be considered would be to prevent corrosion by inhibiting the movement of corrosive species from reaching the surface or even diminishing the electrochemical reactions at the metal interface.

### 5.1.3.1 Films cast with Sulphonic acid series doped PANI.

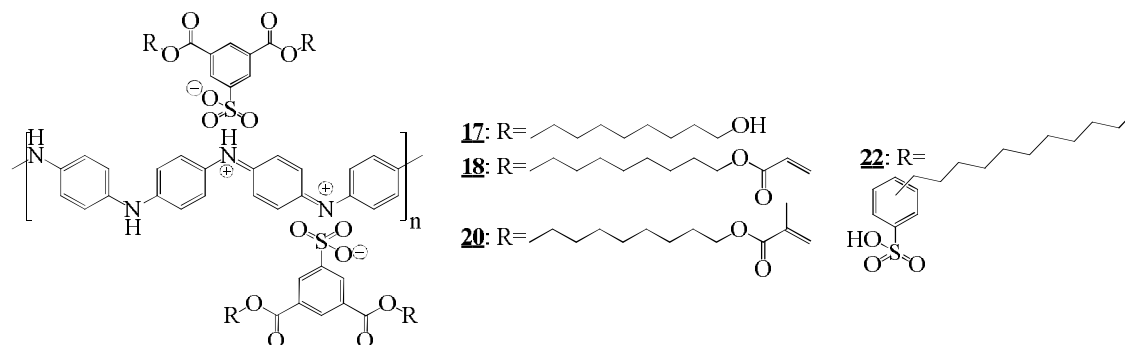


Figure 71: Structures of the sulphonic acid series of dopants used to dope PANI.

Films of doped PANI (**17**, **18**, **20** and **22**) were successfully cast onto steel and copper and were subjected to accelerated corrosion tests. The films produced were dark green and felt at the touch very grainy. The grain texture was fine and it felt slightly coarser than the feel of talc. Visually from a distance the films appeared to cover the metal but after closer inspection the films contained lots of pin holes. The adhesion of all the doped PANI films where the dopants are sulphonic acids, seemed to present very weak adherence<sup>118</sup> to the metal surface: physical contact was enough to break the integrity of the film and overcome the adhesion. Consequently, the plates were not touched during the tests as the lightest application of pressure was enough to dislodge the film. In order to avoid such result, the plates were hooked through the eyelets.

#### 5.1.3.1.1 Films cast with hydroxyl functionalised sulphonic acid doped PANI.

The hydroxyl functionalised dopants were successfully synthesised and subsequently used to dope PANI; however, only one of the dopants was taken forward for the accelerated corrosion testing.

The films created using doped PANI (**17**) showed that, after 1 hr the steel samples that were sprayed with brine showed extensive levels of corrosion. The samples that

were submerged showed corrosion to a less extent than those sprayed. Taking 24 hrs before, any signs of corrosion were seen. The submerged sample also showed some interesting characteristics: it appeared that a line (tide line) at the solution air interface had extensive corrosion but very little below this line. One explanation proposed was that the submerged samples were rested in grooves of the propagator's tray which created an area where the corrosive species mobility was low and were concentrated. The copper samples also evidently corroded, but with these samples the corrosion was not noticeable until after 48hrs for samples submerged. Again, corrosion was seen after 1 hr for the sample that was sprayed with the saline solution. The corrosion of both metals appeared to be worse in the case of the saline sprayed samples, this was due to a layer of sodium chloride remaining on the surface upon drying and then the humidity acted to drive the ions through to the metal surface. The submerged samples were not subject to this as the ionic species were free to move around the samples whilst in the solution.

#### 5.1.3.1.1.1 The morphology of hydroxyl functionalised sulphonic acid dopants.

Upon magnification it could be seen that there was a distinct interface with dark areas representing polymeric material and the lighter areas being corroded areas. Within the polymer coating there was the presence of rust which was the result of pockets and holes within the coating, the polymer surface can be seen in Figure 72 which was captured at the highest magnification before there was a drop off in resolution. The image shows that the polymer was smooth but it contained lots of crack which as previously explained was the likely cause for rust occurring the same area. The coating was well adhered to the surface and it was noticed that the morphology of film was interesting. On the edge of the film it is clearly seen that the polymer was crystalline in structure and the rod like spike structures that appeared to percolate and radiate outwards. In fact, the edge of the film is spiked reinforcing the fact that the latticed network was the result of layering crystalline PANI.

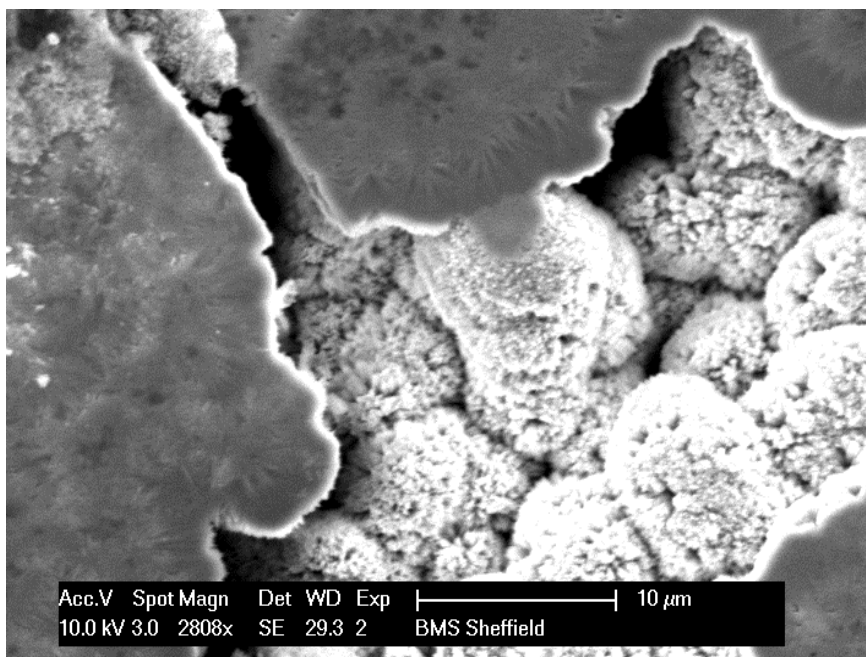


Figure 72: Polymeric film sitting on the edge of a patch of rust. An illustration of potential crystallinity of the doped PANI.

Similar results were seen with the copper samples, the polymer film was smooth with lots of cracks and holes in the coating. On the surface it appeared to be some kind of debris or contaminant, suspected to be dried sodium chloride from the accelerated corrosion tests. It was evident that the occurrence of the debris was on the surface of smooth polymer regions and so it could not be correlated to patina formation as this would be expected to appear at the sights of the cracks.

#### 5.1.3.1.2 Films cast with acrylic functionalise sulphonic acid doped PANI.

The acrylate functionalised dopants showed - as previously with the metal substrates coated in doped PANI (17) - that corrosion occurred from after 24 hr of exposure to the aggressive environment suggesting a poorly adhered and porous coating. It was clear to see the dried salt on the surface of the sprayed plates which was not present on the submerged samples; firm evidence that upon spraying, the salt remains on the surface and the reaction is driven by humidity. This was not a feature noticed on submerged samples and as previously discussed, led to a belief that the ionic species were free moving in the solution. So the concentration of ionic compounds in contact with the surface at any one time was lower in submerged samples than the concentration on the samples sprayed. Therefore it is conclusive that the sprayed samples will have much higher rates of corrosion than the submerged samples.



Figure 73: Photograph of A) Mild steel after 24 hrs submersion in 3.5% saline solution and B) mild steel after 1 hr post saline spray, coated with doped PANI (17).

The samples coated with doped PANI (18) saw higher levels of corrosion than the samples coated in doped PANI (20). This could be due to many reasons such as film thickness which acted to reduce the chance of ionic species to the metal surface and polymer concentration as it was apparent that the films in doped PANI (18) were much darker than those of doped PANI (20).

The hydroxyl functionalised appeared to give a better film morphology and rheological properties. Consequently it was deduced that during the casting of films interactions formed between the polymer chains, and these interactions differed greatly between the hydroxyl and acrylate functionalised system. The hydroxyl groups participated in hydrogen bonds with each other upon solvent evaporation, due to the decreasing proximities between the chains. The acrylates differed and the acrylic components were physically cross linked with the resin matrix (covalently bound) giving some degree of inflexibility to the network. The hydrogen bonds were weak in comparison, so the inter-chain links were constantly changing. It should be noted that the difference in surface tension of the metal and the coating solutions resulted in what is known as dewetting (pinholes) which with further formulation would be negated by the addition of dewetting agents which reduce the surface tension of the coating solution.

#### 5.1.3.1.2.1 The morphology of acrylic functionalised sulphonic acid dopants.

Acrylic analogues of doped PANI (18, 20) were created and tested in the exact same conditions. Figure 74 shows the acrylic functionalised sulphonic acid doped PANI coating and as it can be seen; they did not produce a smooth film in a similar manner to the hydroxyl functionalised dopants. Although the film was smooth to an extent, it was more block angular and rough in patches. It appeared as though the

polymer was layered as opposed to being uniform as in the case of the hydroxyl polymer (doped PANI 17). One explanation for the layering may be down to the very nature of the acrylates; upon doping the polymer it was assumed that the polymer, in this case PANI, became more crystalline and rigid in contrast to the undoped moiety. Secondly, the acrylate groups are highly sensitive to temperature, light and even mechanical stress/pressure which are enough to initiate cross linking and polymerisation. Subsequently the effects upon the morphology were exacerbated when the dopant in question was acrylic; the result in the production of layers.

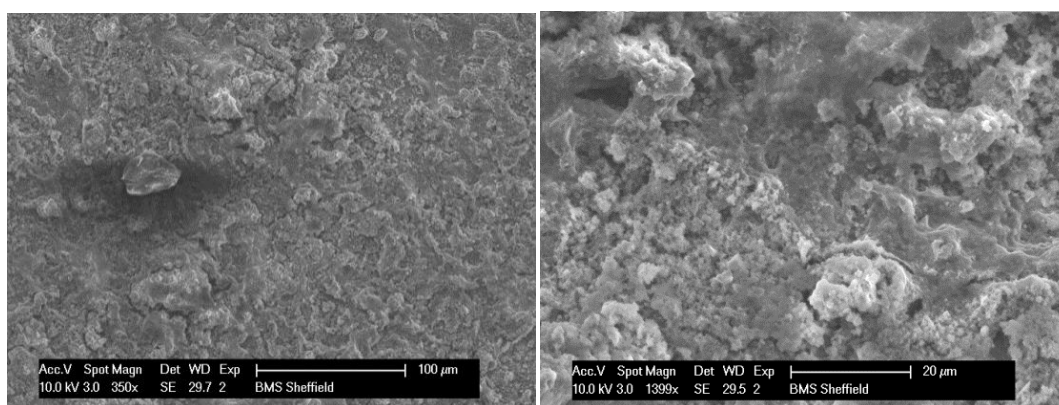


Figure 74: Morphology of doped PANI (18); a) 350x mag., b) 1339x mag.

#### 5.1.3.1.3

#### Films cast with dodecylbenzene sulphonic acid doped PANI.

As with all the experiments, standards and controls were used for comparative measures, for the sulphonic series DBSA (dodecylbenzene sulphonic acid) was used as the choice of dopant... The films produced by this doped system were very dark and thick with no noticeable pin holes or defects in the films integrity. With these samples (Figure 75) corrosion inhibition seemed to last almost until the end of the investigation and corrosion was not noticed until close to the 7<sup>th</sup> day of sampling. Exactly as the other cases, the samples which were sprayed showed much more aggressive levels of corrosion than those submerged and further still no corrosion was identified at all with the submerged copper sample. In the figure the sprayed plate contained lots of pits and wells which were formed by the corrosion products; however there was no noticeable sign of film delamination suggesting that the adhesion was strong or stronger than what was normally seen with PANI films.

In the literature, dopants such as DBSA produced much more crystalline polymeric chain by means of opening the globular polymer<sup>35,43,56</sup>. Therefore with the increased crystallinity and increased processability it would be safe to put forward that the percolation threshold will be lower for these films coating formation will be more uniform.



**Figure 75:** Photograph of both steel and copper submerged for 7 days in (3.5%) saline solution (left and middle image) and effects 7 days after being sprayed with (3.5%) saline solution, coated with doped PANI (22).

#### 5.1.3.1.3.1 Morphology of dodecylbenzene sulphonic acid films.

In literature a cases are made for the use of DBSA and CSA (camphorsulphonic acid) as doping agents and for this reason it was decided to use DBSA as a standard<sup>119,120</sup>. Figure 76 shows the polymer surface of a steel sample coated with the doped PANI (22). As with doped PANI (17) the surface looks to be smooth and uniform. The crystallinity of this doped polymer system was significantly noticed in the higher magnified images and appeared to be far higher than what was seen in the sample for doped PANI (17). The needle like structures appeared to be integral to the structure of the coating a result of the polymers conformational changes once doped. It was also much clearer to see that the film was actually a lattice of overlapping structures of varying size and orientation.

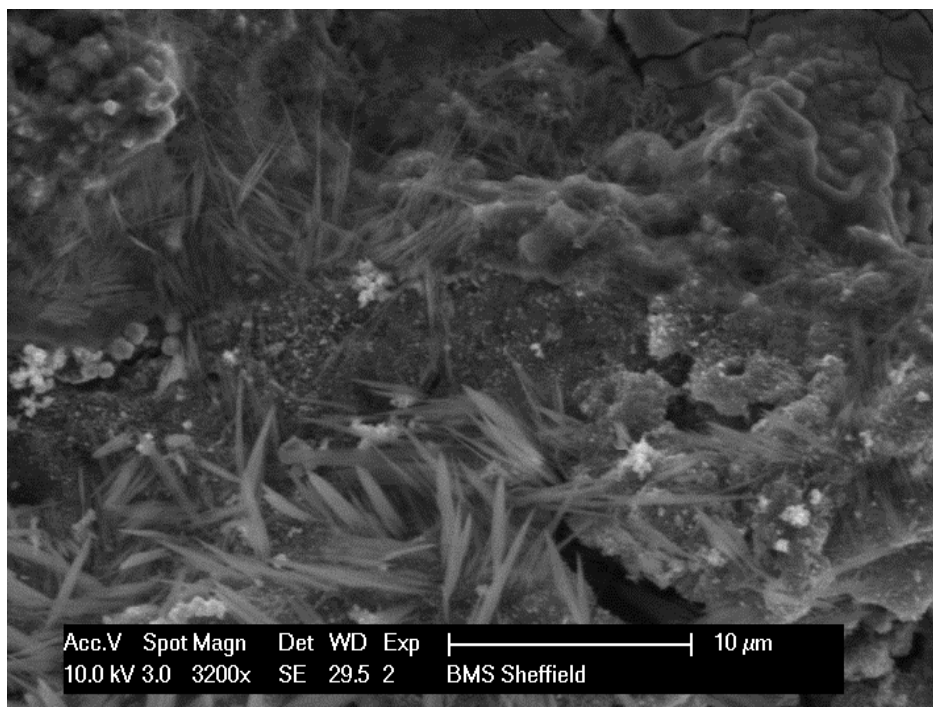


Figure 76: Polyaniline doped with literature standard DBSA.

#### 5.1.3.2 Films cast with Phosphoric acid diester series of doped PANI.

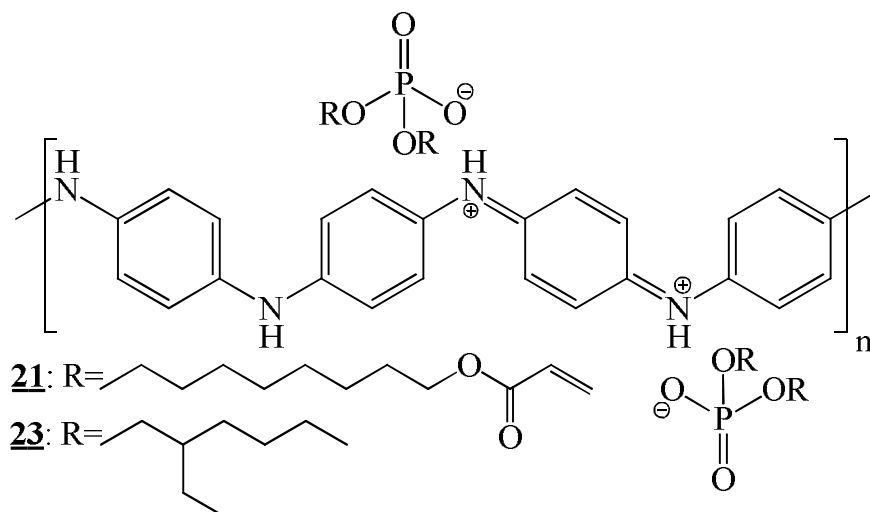


Figure 77: Structures of dopants used in doped PANI (**21**) and (**23**).

Films of doped PANI (**21** and **23**) were successfully cast onto steel and copper and were subjected to accelerated corrosion tests. The films were light green and almost unnoticeable on the surface in stark contrast with the sulphonic acid series. There was no texture that could be felt by the film and mechanical stress easily disrupted the coating. To avoid this issue, the samples were hooked through their eyelets in order to pick up the plates. The adhesion of all phosphate series doped PANI films was very weak, however it was expected that the presence of

phosphates would have increased the interaction between the polymer and the metal surface, almost idealised as a sort of linker.



**Figure 78:** Photograph of both steel and copper 24 hrs of testing (top image) and corrosion noticed after 7 days; from left to right steel submerged, copper submerged, steel sprayed and copper sprayed with (3.5%) saline solution and coated doped PANI (21).

In Figure 78 it is shown that the levels of corrosion were amongst the most severe seen in all the samples. It appeared as though there were some chemical reactions taking place on the surface of the metal when presented with the saline solution. This image gave the impression that instead of impeding corrosion it had potentiated the rate of corrosion. The films produced using acrylic monomers were poor and these reactions may not have occurred if the films had been wholly integral. In such case, the reactions would have been different if the film had been water tight. By looking at the steel sample that was submerged it was obvious that below water line was highly corroded even after just 24 hrs whilst on the same sample above the water line it seemed to be untouched, suggesting that some sort of unknown and other reaction was taking place. The submerged copper sample was a similar, but in this case it appeared that the reaction had cleaned the surface of the copper whilst above the water line there was evidence of patina formation and corrosion which raised questions of: what was happening in the saline solution between the metal and the doped polymer? Why was this happening? After

extensively searching through literature, the answers to this still remained unclear. Regarding the sprayed samples, these also underwent extensive corrosion. The steel samples showed a multitude of pits and the film itself was delaminated. The copper sprayed samples remained covered with the film. However patinas were present on the surface more than the submerged samples.



**Figure 79:** Photograph of both steel and copper 24 hrs of testing (top image) and corrosion noticed after 7 days; from left to right steel submerged, copper submerged, steel sprayed and copper sprayed with (3.5%) saline solution and coated doped PANI (23).

### 5.1.3.2.1 *Morphology of films phosphoric acid diester series.*

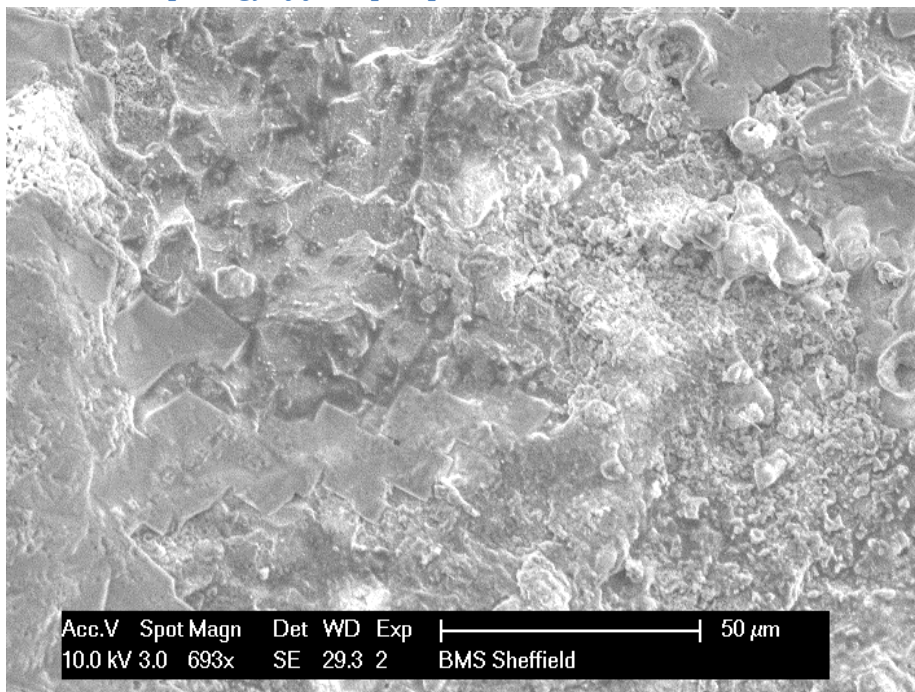


**Figure 80: Morphology of doped PANI (21) film on steel.**

By creating a series of phosphoric acid dopants it was hoped that, aside from doping the polymer, it may promote adhesion of organic coatings and prime the surface ready for any barrier. At the interface any unreacted phosphate dopant may participate in reacting with the surface of the metal to create a metal phosphate species that would extend from the surface outwards. It will act as a point where the organic coating can anchor itself to and thus may result in a much more strongly adhered film<sup>121-124</sup>. The films appeared to be layered (Figure 80), the layers appeared to be block angular which was attributed to the increased crystallinity of the polymer upon doping. The results were no different from the sulphonic acid analogues: with both being functionalised with acrylates it was expected that they would display similar results. Nonetheless what was expected to be different was the adhesion of the polymer to the surface and therefore in this case the phosphate was more favourable. In comparison to the acrylate functionalised sulphonic acid looking at Figure 74b it was noticed that the film was much more disordered, rough and uneven. This was less prominent in the case of the phosphate and further backed up the fact that the phosphate has higher adhering properties. The sulphonic analogue was percolated from sites where polymer managed to adhere to the surface, producing areas of thick coatings and areas of thin coatings.

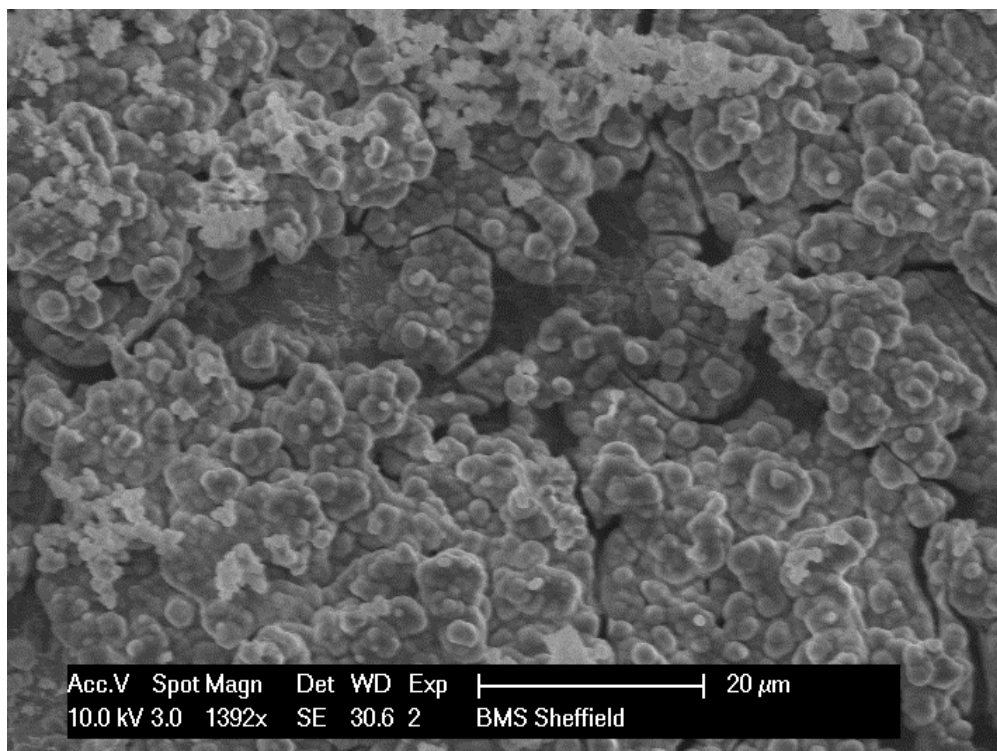


**Figure 81: Copper sample coated with doped PANI (21).**

In the case of the copper samples Figure 81 shows a different picture. The film was rough and globular, the porosity may be an issue due to the visible cracks and ravines. In the image it is clear that there were several pores ranging from, 2 μm to the biggest about 8-9 μm which was more than enough for ionic species, water and other oxidising agents to permeate through. In the lower layers cracks appeared to be prevalent and appeared to be no bigger than a couple of micrometres. As previously stated the film appeared to be globular and uneven, a characteristic of lower adhesion to the copper surface.

As a result of the polymer proliferating from the sites on the metal surface, where the material had adhered; it is logical to think that it is easier for the polymer to adhere to sites where it has formed connections/adhesion to the metal surface. As such it the film proliferated and spread from these sites and the adhered polymer hence acted as an anchor. It could be suggested that these were seeding sites; sites where the polymer was able to proliferate from and grew. However this does not say that the film was not totally covering the surface of the sample, but that the coating was thinner in some areas than in other areas. This becomes problematic for any coating that is designed to place protection onto the metal surface as the thinner

parts are likely to be weaker points (a sort of Achilles heel for the organic coating), similar cases have been seen in other research published<sup>125</sup>. Therefore in comparison to its steel covering counterpart, which showed smoother, even films, the adhesion in the case of steel was due to potential chemical reactions of the phosphate with the steel surface whereas in the case of copper, it was much more a physical attractions such as Van der Waals, hydrogen bonding and electrostatic interactions which would result in poorly adhered films. The second point to note is the globular nature may represent bubbling at the surface and delamination. The process of delamination is reliant on several determining elements; firstly considerations to the adhesion properties and considering how strong the polymer is bound to the surface of the metal. Second factor to concede is how permeable the film is and how accessible the metal surface is to the corrosive agents, basically how easy it is for them to permeate and diffuse through the film and finally the inter-metal species created as a result passive diffusion of such reactive species. Considering these three things, delamination occurs when oxygen permeates through to the metal surface. At the metal surface there are two processes taking place; the generation of electrons, creating  $\text{Fe}^{2+}$  and the reduction of the oxygen in the presence of water to Hydroxide ions<sup>126</sup>. The presence of sodium chloride acts to increase the rate of corrosion acting as charge carriers<sup>127</sup>. The dissolution of iron results in pit formations and crevices and eventual precipitation and formation of rust with further reactions with the oxygen<sup>128</sup>, which will act to change the surface morphology. One speculation is that upon the reduction of oxygen, highly reactive oxygen radical species at the polymer/metal interface are generated, these possible having destructive effect on the organic coating and also reacting with the metal surface<sup>129</sup>. Therefore physical changes at the metal surface occur; changing the chemical properties of the surface, the adhesive properties of the surface and even the morphology at the interface, all promoting the lifting and peeling of the film from the surface. Figure 82 illustrates the delaminating event, showing conditions and processes.

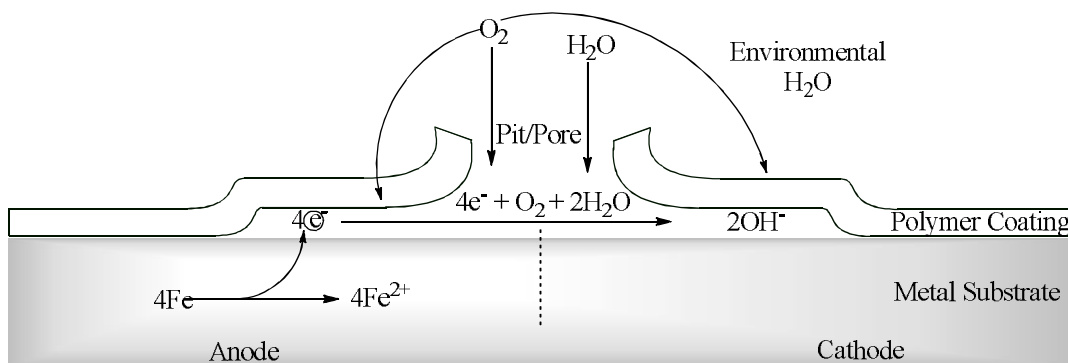


Figure 82: Cathodic Delamination at the Metal/Polymer interface.

#### 5.1.3.2.2 Literature standard phosphoric acid diester's films and their morphology.

Comparative studies were conducted between the phosphate dopants synthesised and phosphate dopants which have been mentioned in literature as good dopants. One of the dopants was functionalised with acrylic end groups on an aliphatic chain similar to the dopants synthesised, the other just contained simple aliphatic chains.

#### Literature standard phosphoric acid diester dopants

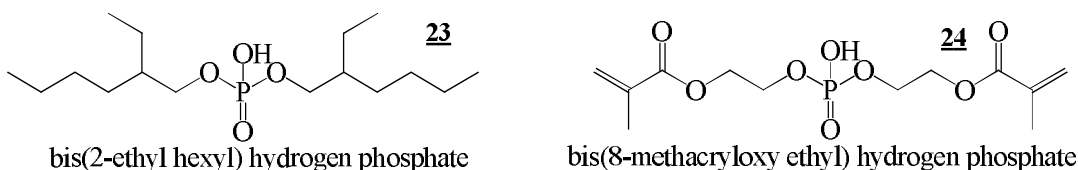


Figure 83: Structures of the literature standard phosphoric acid diester dopants used.

Figure 84 represent the morphology of a film produced by doped PANI (**23**). The image was taken at a site with a huge crack within the coating, looking to be around 10 microns in width. At this magnification (1422x mag.) it was clear to see that there appeared to be much smaller scaled cracks within the film. The cracks appear to be within the nano region, although less than a micron this can still be problematic. Permeation of water and ionic species may well be prevented crossing through to the metal surface either by physical means or electrochemical barrier exerted by materials such as doped PANI but access points such as cracks allow the free movement of water and ionic species into and under the film reaching the metal surface allowing for corrosion to take place and even initiating delamination of the coating.

In terms of smoothness, the film appeared quite smooth with little to no protrusion and no vast peak elevations; however the film contained a considerable number of

wells which could be observed more on the darker grey shaded area. The distribution was quite uniform but the size and shape differed vastly even looking carefully at the lighter grey area. This could suggest that the film was a collection of globules/spheres<sup>125,130,131</sup> of materials which was also seen with other films investigated. The globules suggest dendritic proliferation around a 'seeding' origin point, scaling up these collections as the film grows, the connections increase until only gaps are left between the spheres, a good example of this is polystyrene.

One explanation to why these conditions were seen with this specific doped PANI and not the others, is due to the functionalised side chains or in the case of this sample the lack of functionalisation; functionality of the side chain could have been selectively tuned and modified to serve a purpose, in the case of this dopant it was not the case, it contained only simple aliphatic chains. The functionality of the side chain increased the processability of the polymer, this being to induce solubility into a range of solvents which were once inaccessible and secondly to increase the interaction with other matrix polymers and resins. The reason why it may be a factor affecting the film casting of this molecule is that here we had a simple aliphatic dopant and as such interactions with other chains of the doped polymer are going to be weak as the interaction will be merely electrostatic and weak electro forces may appear such as Van der Waals forces. In the cases of other dopants namely, hydroxyl and acrylate functionalised dopants the interactions were much stronger.

Considering the hydroxyl functionalised dopants, these can undergo hydrogen bonding with other dopants of its kind. The acrylate functionalised dopants again may display Van der Waal forces but the capabilities and potentials for bonding are increased, these dopants when in the presence of other acrylates will cross-link and form new covalent bonds which again are stronger than hydrogen bonds and as such either of these functionalised dopants will create networks of interlinking polymer chains. Translating this to castings films it simply means that with increased interactivity means decreases in the pores the films.



Figure 84: Steel sheet coated with doped PANI (23).

Figure 85 represents the morphology of the film created by doped PANI (24). It displayed similar morphology and characteristics as it was seen with doped PANI (21), as previously the surface was rough with some spherical objects on top of the coating. Also there seemed to be absence of pores as also seen before; however this is in no way stating that there isn't any pores, it just means at this magnification the pores cannot be seen. With further magnification it would be expected that some pores would become visible.

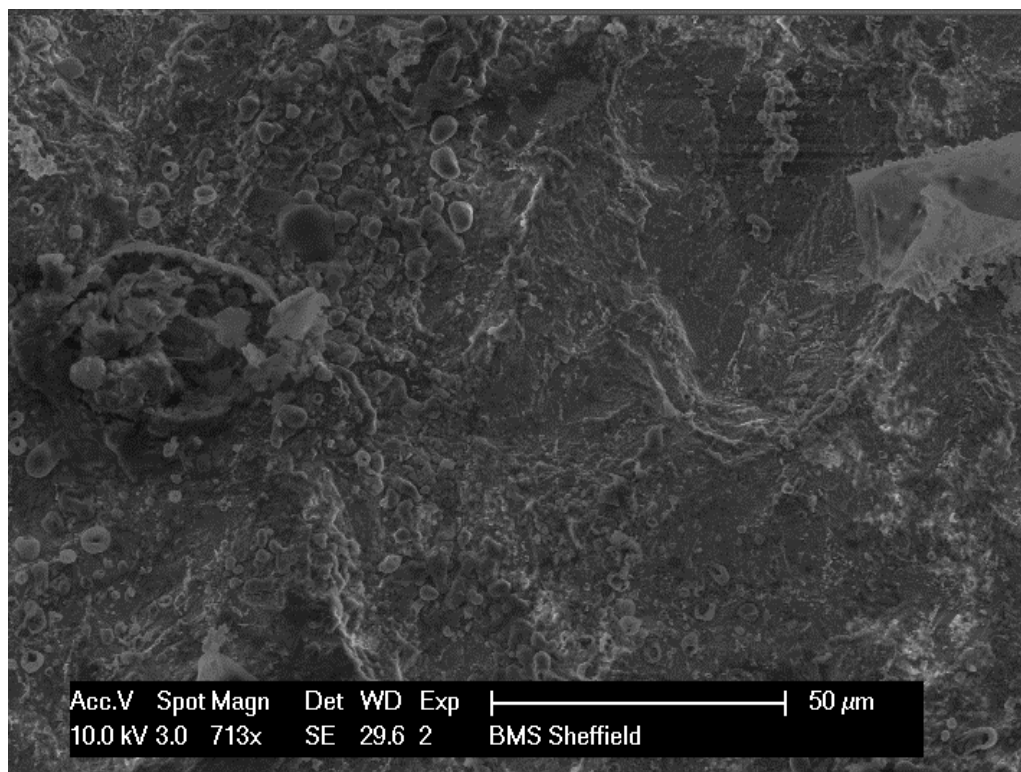


Figure 85: Steel coated with doped PANI (24).

#### 5.1.4 PANI/Polymer resin composites.

In this research it was crucial to investigate and optimise doped PANI/polymer resin matrix formulations for the best achievable anti-corrosion protection looking into volume fractions to determine the lowest weight percentage of doped PANI needed to be incorporated into the resin matrix whilst still presenting active protective, maintaining properties without compromising the integrity of the film and functionality of the composite. The polymer resins investigated are polyvinyl chloride (PVC), epoxide resin namely (Epikote 828™, Bisphenol A diglycidyl ether, CAS # 1675-54-3) and methyl methacrylate.

##### 5.1.4.1 Doped PANI/PVC composites film accelerated corrosion.

PVC is widely known for its uses as a coating material for many applications. It is also known that it has a limited self-life or a limited period where the protection is adequate and as such many metallic objects that have been coated with PVC they soon develop patches of rust, further still cracks and degradation of the coating takes place causing the film to lift, peel, crack and completely dislodge.

Composites of the doped PANI (17, 18, 20 – 23) were successfully created, the process was remarkably easy and plates were produced by dip coating into the

composite solution. The dip mixtures were made by taking aliquots of the doped PANI stock solutions and mixing the PVC into the solution.

Looking at Figure 86, the results are all consistent with each other, showing that when the doped PANI samples were used in combination with a physical barrier, for example PVC there was impedance of corrosion which was attributed to the fact that it is the combination of both constituents that are the most effective method of protection. In these composites the doped PANI exerts electrochemical effects due to its redox properties but PVC was added merely as a device to ensure that the PANI stayed adhered to the surface of the metal, preventing the active polymer from being washed or scratched off the surface. Even though it shows little potential as a corrosion inhibitor, it was beneficial and important to the integrity of the polymer, acting as a sacrificial barrier in order to protect the doped polymer.

It can only be this as the PVC samples and the doped PANI samples alone still showed signs of corrosion. In light of this evidence it can be implied that whilst PANI is not a physical barrier preventing the movement of corrosive agents through to the surface, it does suggest that inhibition of corrosion is via other methods such as the passivation of the metal at the polymer metal interface. It also implies that even though the barrier produced is not effective alone, it does present some barrier qualities that are beneficial when used in combination with PANI. The movement of ions and moisture still occurs and it is the reason why the PVC only coated samples still corrodes. Conclusively one component cannot work without the other effectively but in combination they produce the desired effects.



**Figure 86: Photograph of doped PANI (17) 1 wt% in PVC, dip coated and air dried. From left to right steel submerged, copper submerged in a saline solution (3.5%) after 120 hrs and steel sprayed and copper sprayed with (3.5%) saline solution after 144 hrs.**

All PVC coatings showed cracks within the composite film as evident in Figure 86. It could be speculated at this point that the fact that the film was cracking was not

due to delamination or any other similar process but it was actually a characteristic of PVC films. When the PVC film is cast, at that point the film is still wet and upon the total drying/evaporation of solvent from the film it undergoes shrinkage and as a result it cracks. However delamination then does appear to occur as a result of the cracks.

The films appeared to be a lighter and different shade of green in comparison to the other sulphonic acid doped polymer film composites and the films appear to be striated, as the result of the film casting method. The physical feel of the films before the accelerated corrosion tests resembled the texture of a rubbery material, elastic and soft but after the tests were completed, the films texture changed and it was more rigid and brittle and this was most likely a product of the harsh environment subjected on the samples.

The results of plates coated in the acrylate functionalised doped PANI's (**18** and **20**) and as with the previous samples, the films showed strong adhesion to the steel; nevertheless the adhesion found with the film coated on copper showed lower affinity and disbondment of the film was revealed with the appearance of bubbles and cracks. The films plated on copper also contained more cracks than the films attached to the steel samples. Comparing these films with the ones produced by doped PANI (**17**), it was noticed that they were darker and thinner than the hydroxyl functionalised samples the texture was smooth but unlike the previous they appeared dull, drier and brittle or at least less flexible than the previous samples- This may be due to the functionality of the dopants and the fact the doped PANI (**17**) containing the hydroxyl end groups may be going so far as to retaining moisture by hydrogen bonds, due to their hydrophilicity whilst the situation with these films was that the polymer was likely to be part of a vast array of cross linked chains within PVC leading to much more brittle films.

Films were produced by the mixing of doped PANI (**22**) with PVC at a 2 wt% volume fraction. The samples showed no visible signs of corrosion, delamination or cracking. This dopant as previously stated has been well documented for its ability to change the regime and morphology of PANI from an unprocessable, insoluble globular polymer to one that is crystalline, soluble and electro-active. The fact that there is no evident corrosion suggests that this regime change and the change in the

polymers morphology and electro active properties all play in favour for its efficacy as a corrosion inhibitor. How might this occur? Consider the morphology of the polymer, a more linear polymer is more likely to have greater interaction with other chains than when globular,. It will also aid the formation of a uniform film creating interlocking network and reducing the percolation threshold within the PVC. The change in the electro-active properties only increases the redox properties of the polymer and the process by how it passivates the surface of the metal. Finally the fact that it is more soluble means that producing films with uniform structures are increased. After looking further at the 1 wt% films the same effects were observed and so with the doped polymer lower volume fractions may be achievable for this material whilst still retaining all the desired properties that will efficiently inhibits the progression of corrosion.

Final composite of PVC tested were blended with the phosphate dopants PANI (**21** and **23**). The appearance compared with all of the other PVC samples was significantly different. With all the other PVC composites were various shades of green, but in the case of PANI (**21** and **23**) the PVC composites seemed to be very pale shade of grey which in fact it was only noticeable when looking at copper samples. As with all the other samples there was little to no signs of corrosion visible, with the latter being the case. The films on the steel samples were quite well adhered in both instances but the copper samples showed lower adhesion and the films were beginning to lift off though there were no cracks in the film at this stage.

Lifting of the polymers from the copper surface could be attributed to sheer poor adhesion. It might be argued that there may be delamination occurring under the film but the fact that there are no visible signs of patina's and corrosion suggest otherwise. In order to balance the argument, it must be said that the corrosion which may be happening in this case may not produce visible signs. A second point to make, these composites contained the phosphate doped PANI hence it is then fair to progress on and say that this is direct evidence of some interaction between any released dopant that is cross-linked within the film and the steel surface, examples can be found in literature<sup>81</sup>

#### 5.1.4.1.1 Doped PANI/PVC composite film morphology.

Upon further magnification of the pores, the internal structure became more evident. Figure 87 shows that at 1431x magnification the steel surface was visible within the pore, it can be seen that there was some intermetallic products present, in this case most likely to be rust. The problem with PVC as a resin matrix was sheer down to it being porous. As a physical barrier it would be idealised that water and electrolytes would be prevented from passage to the metal surface, as without water rust cannot be achieved. Oxygen obviously will passively diffuse through to the surface but for rust to form both water and oxygen are needed in combination with the electrolytes acting as charge carriers.

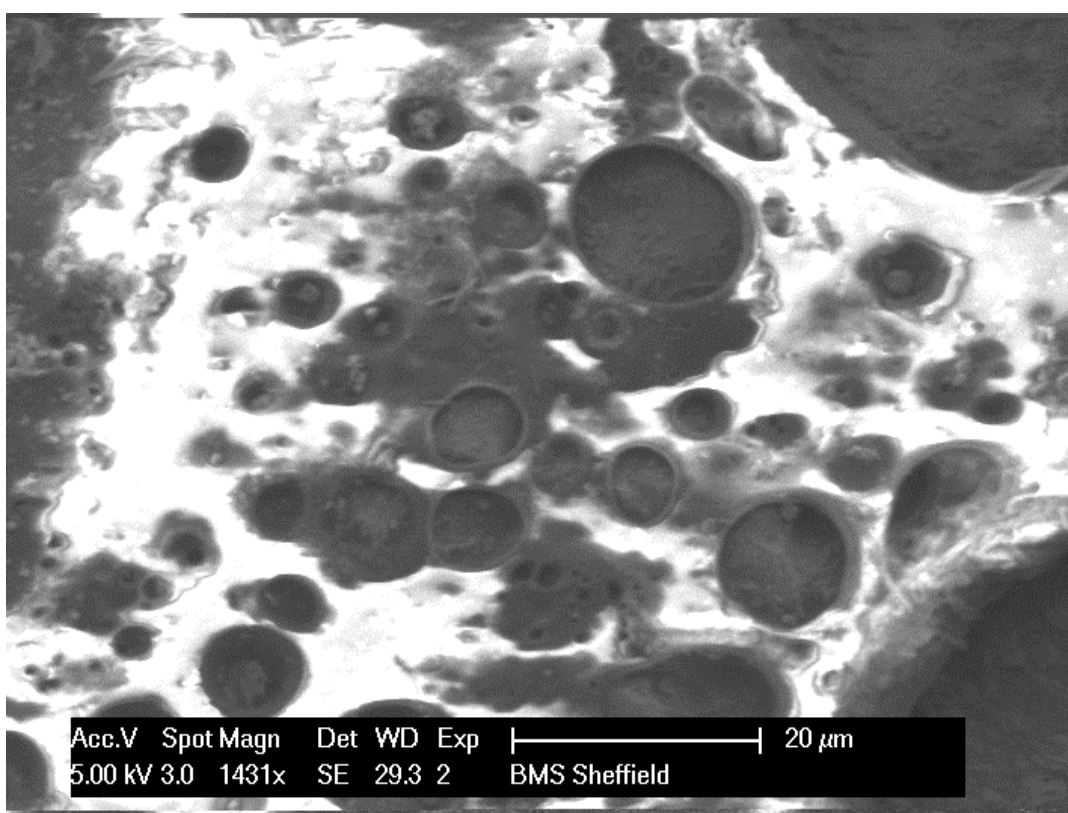


Figure 87: PVC/doped PANI (22) 1 wt% cast onto steel.

What was interesting was the noticed differences in the pore size between samples that contain doped PANI incorporated into the resin mix and the pore size of those without the doped polymer complex present, But what could be determined were the incidences of pores along the film vastly increased, which suggested that the rate of corrosion increases in relation to the number of pores present in the film. However when doped PANI was added to PVC, it showed strong evidence that it had a protective benefits.

#### 5.1.4.2 Doped PANI/epoxy resin composite film accelerated corrosion.

The second composite to be produced was Epikote 282™, an industrial standard epoxide resin that has been used as a material for coatings and adhesives in the past. Doped PANI (**17**) was one of the hydroxyl functionalised dopants created specifically to interact with this resin, upon the curing of the epoxy resin it is hoped that the doped polymer fully blends and integrates into the resin matrix as depicted in Figure 88.

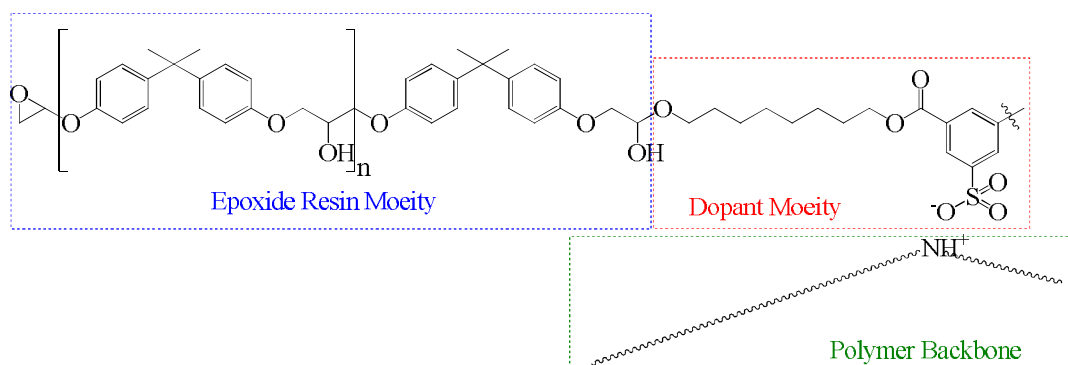


Figure 88: Schematic of cross-linked epoxy resin with the doped PANI (**17**).

One of the first problems noticed with this composite was that upon the curing of the resin, a strong amine was used as the curing agent. This amine not only cures the film but also de-dopes PANI from the doped state being the emeraldine salt to the emeraldine base. However this may not be a problem at all as some articles have reported that not only is the emeraldine salt responsible for the corrosion protection but actually the emeraldine base also has been shown to be responsible to the anti-corrosion properties<sup>81</sup>.

The films produced were the smoothest produced out of all the films cast and showed no signs of cracking, bubbling, lifting and peeling thus the adhesion was the best seen in all the films cast this far.

Unlike all the other films which were produced apart from the acrylates, these were cast by spraying with a solution of the resin/curing agent and the doped PANI solution at the same time which became quite difficult to produce and then the samples were heated slightly to initiate the curing process, before they were placed in the oven for 24 hrs to fully cure and harden.



Figure 89: Photographs of steel and copper coated in doped PANI (17) 1 wt% in Epikote 828™, sampled prior to accelerated corrosion testing.

Accelerated corrosion tests were successfully conducted on all the epoxide resin composites and ran for the full seven days. The results obtained were very promising, with very little corrosion after the 7 days of testing. Again the results showed that the sprayed samples suffered a greater attack than the submerged samples. Figure 90 shows the two steel plates the submerged and the sprayed. Looking firstly and the sprayed plate it is clear to see that the corrosion of the metal substrate was localised to the edges of the plate. It is a fair assumption to say that at the edges the film is likely to be at their weakest; here the coating was likely to be thinner here than in the centre of the plates, rigid and inflexible and the stresses will be greater here than in the centre. At the edges the films may potentially want to pull away from the metal surface however this was not seen at all as two rigid structures to move in opposite directions were expected as opposed to flexibly moving as one. Visually there was no sign of the film lifting; in fact the film was really well intact at the edge which was not to say that there are not any microscopic channels and pores that run underneath the film from the edges. The adhesion of this resin to the metal surface was the strongest of all the composite films which resulted certainly in one of the desirable traits that are being investigated at present and it would ensure any paint formulation using this resin would certainly have a long life before needing to be replenished.



**Figure 90: Photographs of steel and copper samples coated in doped PANI (17) 1 wt% in Epikote 828™, sampled after 7 days of accelerated corrosion testing, from left to right; steel sample sprayed, steel sample submerged and finally the opposite side of the submerged steel sample, bottom left; copper sprayed and bottom; copper submerged.**

At the edges of the sprayed sample rust appeared to be quite aggressive with what it looked to be some localised delamination whilst the submerged sample looked to have corrosion but no form of film disbondment. The submerged sample was quite a special case in that one side showed no signs of corrosion whilst its other side had a solid patch of corrosion it would have been expected that no corrosion to occur whatsoever. Nevertheless, there was one possible explanation, the side of the plate which corroded was facing down and rested on the ledge in the groove of the propagator (Figure 91). Here the movement and flow of water will be lower and far less than that of open waters, due to the restricted and enclosed area, giving rise for a potential of ionic species collecting which with a low flow of water in the area will act to concentrate the aggressive species at this site therefore increasing the rate of corrosion. From looking at the copper samples it was clearly visible that no corrosion was taking place with the film integrity withholding and remaining strong with no cracks, loss of adhesion or delamination.

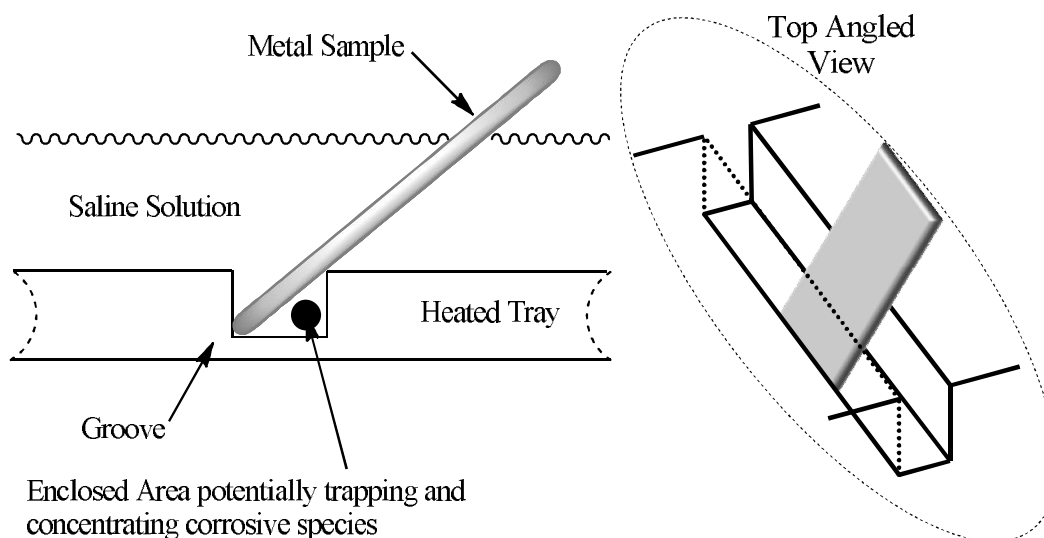


**Figure 91:** Schematic illustration of the accelerated corrosion sampling, A) Side profile and B) a top angled view.

#### 5.1.4.2.1 Morphology of doped PANI/epoxy resin composite film accelerated corrosion.

The incorporation of doped PANI (**17**) was somewhat successful and the results spoke for themselves both Figure 92 and Figure 90 show little to no signs of corrosion. Figure 92 was sampled from centre of the plate, here there was no sign of corrosion at all, and only the presence of what appeared to be grains (represented as white dots). These white dots are likely to be nothing more than trapped air bubble, potentially resulting from the process of curing. Other explanations that could be considered are dust particles trapped under the film present on the metal surface. Another explanation for this is that it may be due to pre-existing pits on the metal surface which have been filled by the resin and in the angle of incidence at which the beam was directed, it may be producing lighter spots. However regardless of what they are, the presence of the spots had no detrimental effects on the film integrity and the protection that the film was casting over the metal.

Unlike the samples which had only Epikote 828™ cast onto them, the samples which contained the doped polymer showed no corrosion at the edges as it was seen in the prior case. It is easy to contemplate that at the edges the levels of adhesion were subsequently lowered due to being a region where the stresses and strains placed on the film were likely to be higher than in the centre of the film. Therefore the incidence of channels and cracks was assumed to be higher in this region. The introduction and flow of corrosive species showed no signs of having any synergistic effects. This alone confirms and it is firm evidence that the presence of

doped PANI has healing properties and it is able to exert protection over areas that may not be necessarily covered by the polymers<sup>118</sup>.

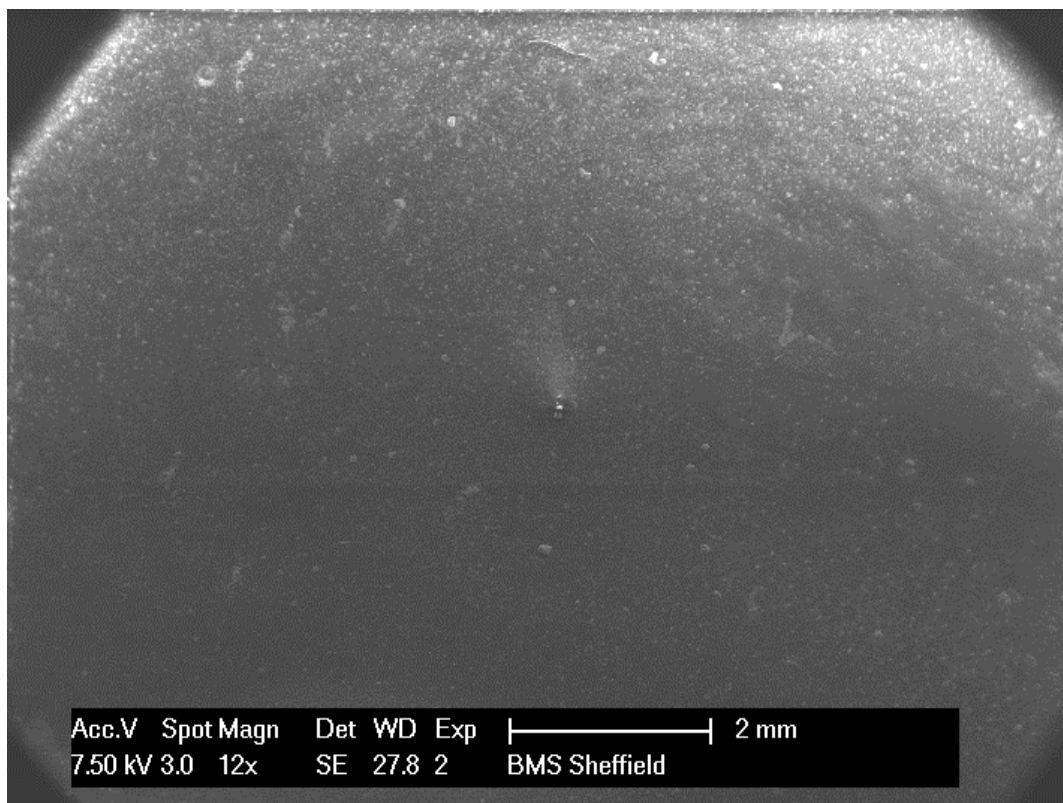


**Figure 92: Epoxy resin/doped PANI (17) 1 wt%, completely clear of rust.**

#### *5.1.4.3 Doped PANI/acrylate resin composite film accelerated corrosion.*

For the final experiments samples were coated in acrylic resin composites with doped PANI (**18**, **20**, **21** and **23**). The process of developing the films was extremely difficult and required weeks to cast. The method of casting used was spot coating, in which the plates were laid flat and horizontal, and spotted with the acrylic solution to produce a film. The curing was very lengthy and it had to be left in the oven overnight until the film cast was dry and then the process started again until adequate films were produced.

The textures of the films were quite rough and bumpy, a vast difference from the epoxy resins and the films produced turned very brittle and crumbly. This problem could be remedied however by lowering the  $T_g$  of the film by addition of other acrylic compounds such as methyl acrylate, with the lowered  $T_g$  the films would be seen to be more flexible and more elastic.

The films produced were very brittle; more so than the epoxy resins and in terms of their morphology, they were very rough with lots of peaks and troughs. The films were almost black and the doped PANI displayed good dispersity in the acrylic resin showing full coverage of the metal surfaces. This is evident in Figure 93; the steel samples seemed to have really good coverage of the film whilst the copper samples showed isolated patches where the doped polymer conglomerated into one area. This was due to the adhesion properties of the acrylic resins and reports in the literature suggest that acrylic resin tends to have poor adhesion and generally do not adhere to anything other than other acrylates. However the adhesion of the films did not seem to be too weak although there did appear to be some delamination of the films especially on the copper samples. The plates in both instances showed no signs of corrosion and appeared to be sufficient coats effectively inhibiting the corrosion of the samples.



**Figure 93:** Photograph of doped PANI (20) 1 wt% in acrylic resin. From left to right steel submerged, copper submerged in a saline solution (3.5%) and steel sprayed and copper sprayed with (3.5%) saline solution after 7 days (168 hrs).

The good results were soon short lived with the samples that were coated with the phosphate doped polymer acrylic composites doped PANI (21 and 23) as with the previous phosphate investigations where these phosphates have appeared react; these samples also follow that trend. As early as 24 hrs, it was noticed that there were reactions going on that involved the doped polymer, water and the salts in the saline solution. Figure 94 shows the same results and the reactions got so bad that after 48 hrs the corrosive solution became contaminated Figure 95. Hence it was decided that the experiment was to be discontinued as the films were literally just dropping off the metal and exposing the surface of the metal to the aggressive environment.

The fact that the films were just dropping off suggests there was very little adhesion if any at all which is contradictory to what was believed regarding the phosphate groups as promoters in the adhesion to steel, but in this case it had the opposite effect. Inspecting the samples films, it was obvious that the film integrity was undergoing extensive delamination, with the films not only lifting but also shrivelling up.

The corrosion of the samples were hard to see visually as the films were very dark sample, though it is clear to see that in both cases the sprayed copper samples had developed patinas, whilst the submerged sample looked to be cleaned from the waterline down.

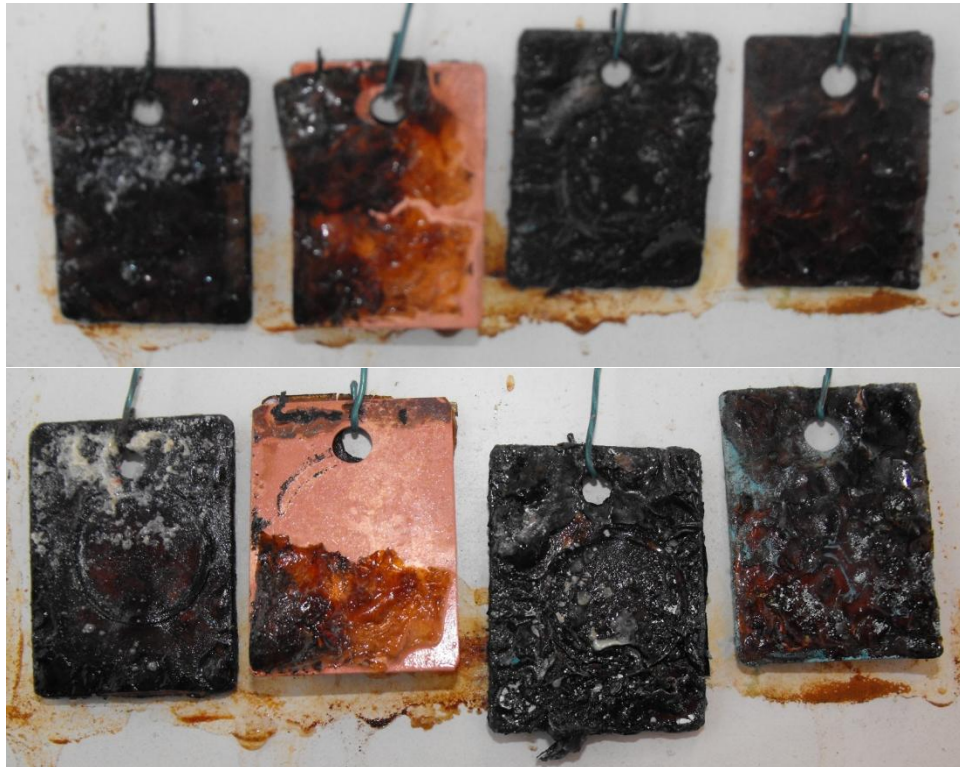


**Figure 94:** Photograph of doped PANI (21) 1 wt% in acrylic resin. From left to right steel submerged, copper submerged in a saline solution (3.5%) and steel sprayed and copper sprayed with (3.5%) saline solution; after 24 hrs (top image) and after 48 hrs for the bottom image samples.



**Figure 95: The contamination of the saline solution used in the accelerated corrosion studies; from the reaction of the phosphate doped polymers, the metal substrates and the saline solution.**

5.1.4.3.1 Morphology of doped PANI/acrylic resin complex coated samples. The samples under magnification showed high levels of delamination and areas where the film had completely peeled off-In these areas it appeared that there was corrosion within the vicinity but in this instance it was hard to determine if it is delamination. The problem with this was whether the corrosion was what initiated delamination of the polymeric coating or whether the fact that it displayed poor adhesion and as result of peeling exposed the surface to the corrosive environment. The latter processability is the most reasonable judgement, looking at these samples as with all the acrylic film samples, the acrylate cast film all peeled prior and during accelerated corrosion testing. It is worth adding at this point that there was some degree of delamination; it became evident during the corrosion testing that the films that did appear to be well adhered seemed to swell in water and dislodge. It was also evident with the phosphate doped samples which were submerged manifested some kind of froth/bubbles around the metal plates- This progressed to contaminate the water and resulted in a milky solution suggesting that there was some kind of unknown chemical reaction taking place.

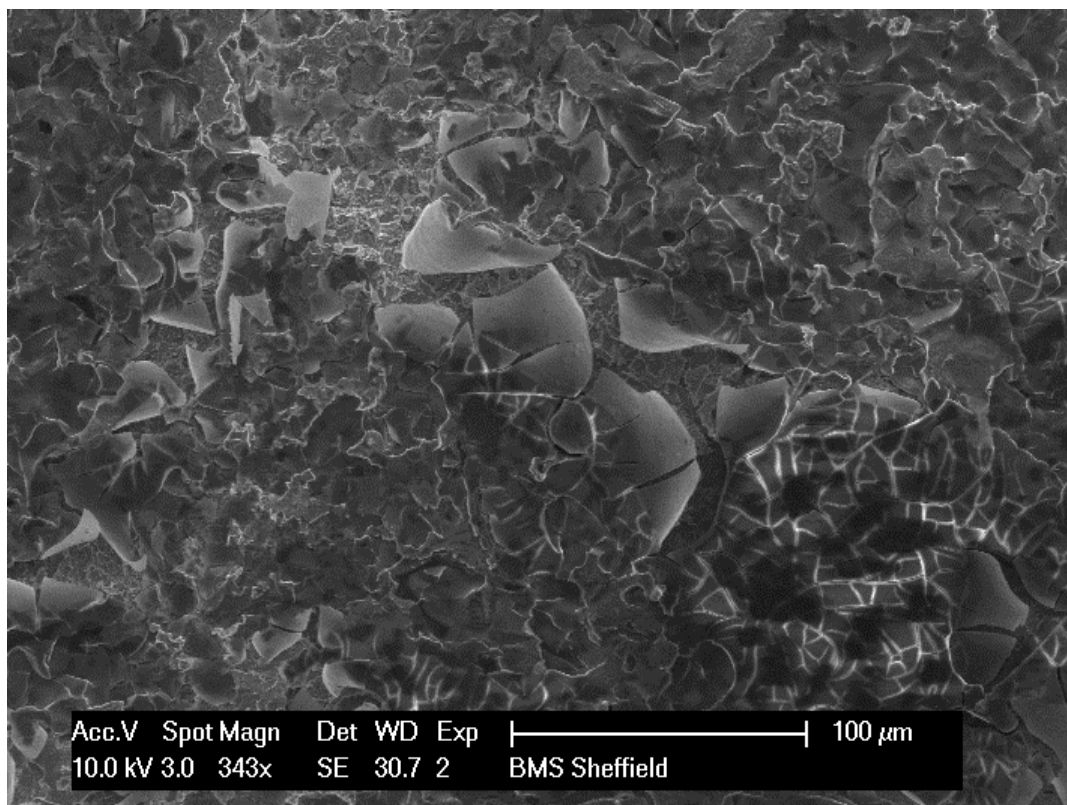


**Figure 96: Acrylate resin/doped PANI (21) 1 wt% cast film displaying delamination**

Looking at the morphology of the acrylate films (Figure 96) it can be seen that the polymeric covering was extremely rough at this magnification (x343) with extensive cracking, which in some areas was highlighted, producing plate like structures which looked to be almost layered. At this magnification it was hard to determine what is happening underneath the film as the image is quite cluttered with visual information; however it looks like there was pitting under the film and so evidently corrosion which will only potentiate the disbondment and delaminating process.

After closer inspection of the intact film, it was apparent that the morphology of the film was similar to that produced by the epoxide resins. The polymer appeared extremely smooth with no pores and very little defects apart from cracks which will be the obvious point of entry for water, oxygen and ions. The film contained no pores at all which again is exactly like the epoxide resin. For such reason, based on the results obtained for the epoxide resin, the acrylic films would produce similar findings. However the fact that the acrylic films were displaying poor adhesion, it means that the doped PANI was exposed to the elements and the film appeared to be lifting the doped polymer and it was carried by the film upon peeling, leaving a

bare surface. The fact that the doped PANI peeled with the film suggested that the polymer was somewhat effectively blended into the resin by mechanisms of acrylic cross linking.

Further examination of areas where samples had fully intact polymer coatings, a vast network of cracks was observed. It was evident that there was peeling with the origin points at the cracked sites indicating that delamination had been initiated. It was expected that PANI exerted protective and healing qualities onto the metal; even sites adjacent to PANI seemed to be passivated but this was providing that the active ingredient was in contact or close proximity for the redox reactions between the doped polymer and the metallic substrate to occur<sup>132</sup>.

Taking a look at the copper sample in Figure 97 the attention is drawn to the acrylic films morphology which unlike most of the other doped PANI samples which were blended into an acrylic matrix, whereby the films exhibited extremely poor adhesive qualities; this sample seemed to stand out. Upon further examination, the film (found at the top of the image) clearly followed the contours of the copper surface, which was found to be two thirds of the image and it appeared almost integral to the surface as though it was part of the structure. The coating was considerably well adhered to the surface and any disbondment and delamination of the film appeared, thus all the above aforementioned made this quite anomalous in comparison to all the other acrylic films.

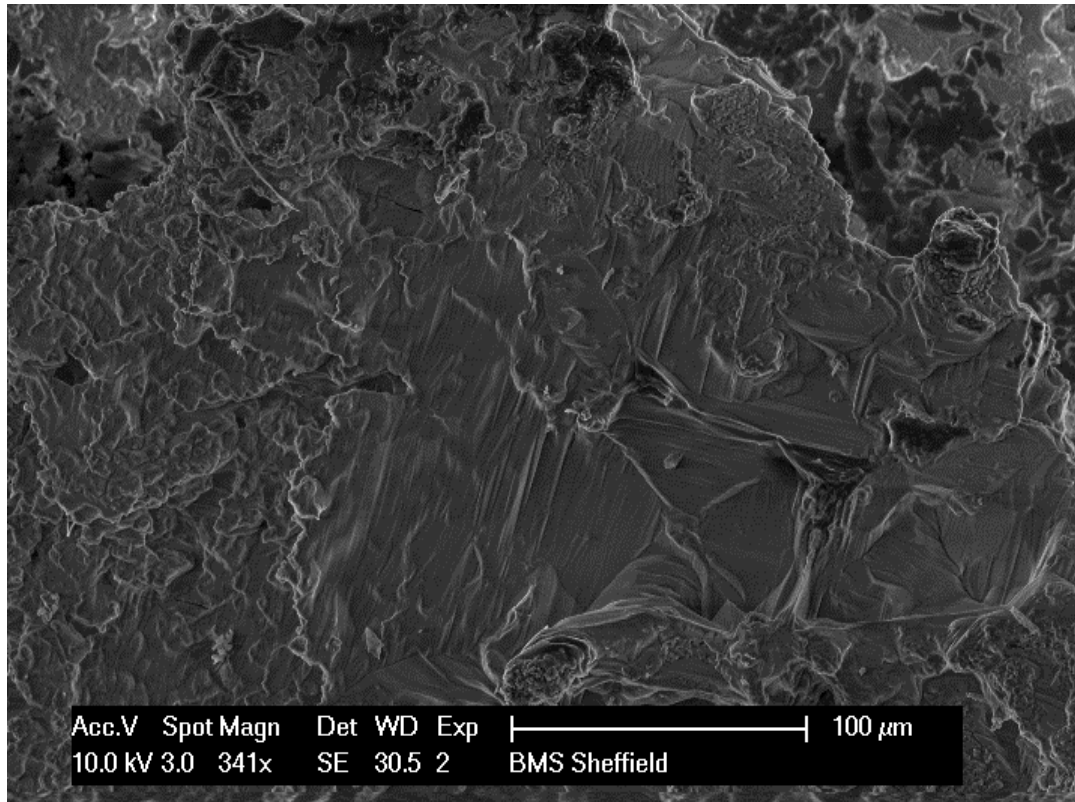


Figure 97: Acrylate resin/doped PANI (23) 1 wt% cast onto copper.

## Chapter 6 CONCLUSIONS AND FUTURE WORK

### 6.1 General Procedures

A series of sulphonic acid and phosphoric acid diester dopants; bis(8-hydroxyoctyl) 5-sulphoisophthalic acid (SIPAOH) (**1**), bis(8-acryloxy octyl) 5-sulphoisophthalic acid (SIPAOA) (**2**), bis[2-(2-hydroxy-ethoxy)-ethyl] 5-sulphoisophthalic acid (SIPADEG) (**3**), bis(8-methacryloxy octyl) 5-sulphoisophthalic acid (SIPAOMA) (**4**), bis(8-acryloxy octyl) hydrogen phosphate (DAOHP) (**5**), bis(8-methacryloxy octyl) hydrogen phosphate (DMOHP) (**6**) have been successfully prepared and have been fully analysed and characterised by NMR spectroscopy, FT-IR spectroscopy, liquid chromatography mass spectroscopy and mass spectroscopy and elemental analysis. The doping of polyaniline (PANI) was successfully achieved producing the appropriate emeraldine salts of PANI the series of sulphonic acid and phosphoric acid diester dopants (**17** – **25**).

#### 6.1.1 Dopant synthesis.

Sulphonic acid series of dopants were successfully created using modified methods of Pron et al<sup>88,92</sup>. The synthesis of bis(8-hydroxyoctyl) 5-sulphoisophthalic acid (SIPAOH) (**1**), was a problematic reaction, the product was found to be a surfactant proving difficult to purify. Methods initially used relied on the vacuum distillation under high vacuum at around 120°C resulting in the alcohol dehydration of the product and upon successive removal of 1,8-octanediol the viscosity of the product increased making it harder for further removal of the reagent, which only become easier by turning up the temperature driving the alcohol dehydration further. The side reaction of alcohol dehydration produced an ether linked side product that was not possible to remove by any method of purification aside from the preparatory high performance liquid chromatography (HPLC). Prep HPLC itself was problematic as it could only purify small amounts of the crude at a time and with the typical run time being over 30 minutes meant that to obtain grams would be too time consuming and not a viable method. Liquid extraction of this compound was difficult, even the salt of the product was not enough to keep the product in aqueous whilst extracting the excess 1,8-octanediol. Several methods of washing were investigated to no avail, however it was first thought that the purification via silica gel column chromatography would be difficult due to the sulphonic acids mobility

on silica in which the acid group sticks, but actually this was going to play to the benefit of purification; 1,8-octanediol showed to be mobile with polar solvents on silica gel. The product on the other hand remained at the top of the column upon passing solvents through; it was only upon the application of a strong polar solvent that it became mobile, in which pure methanol was capable of eluting the product and in a high yield.

The other hydroxyl functionalised dopant bis[2-(2-hydroxy-ethoxy)-ethyl]-5-sulphoisophthalic acid (SIPADEG) (**3**) was fully characterised and synthesised successfully. The product was synthesised exactly as the other hydroxyl functionalised dopant (**1**), the problems that were associated with (**1**) are not seen with dopant (**3**). The product was much more water soluble than the (**1**), therefore the product was not suitable for liquid-liquid extractions; the best method of purification was via silica gel column chromatography. Alcohol dehydration was not noticed with this product due to the initial distillation of the compound to remove excess diethylene glycol being conducted at lower temperatures.

The acrylic functionalised dopant; bis(8-acryloxy octyl) 5-sulphoisophthalic acid (SIPAOA) (**2**) and bis(8-methacryloxy octyl) 5-sulphoisophthalic acid (SIPAOMA) (**4**) were successfully synthesised and characterised though the synthesis was not without inherent problems. Unfortunately, the acrylates were highly sensitive to heat, light and even mechanical movement (sonication and stirring) is enough to promote cross linking of the acrylic groups, however the acrylates were more unstable and more reactive than the methacrylate moieties. The addition of the methyl group seemed to have a somewhat induced stabilising effects on the integrity of the acrylic group. Methacrylate's appeared to be resilient to light and mechanical movement but heating still drove the cross linking reaction. To prevent the cross linking and breakdown of the acrylic groups, *p*-methoxyphenol (anti-oxidant) was added to the products and in the case of methacrylate functionalised dopant, increased resistance to heat degradation of the acrylic group whilst the acrylate showed increase resistance to light and mechanical movement, heat was still a problem. Other problems encountered were due to solubility issues of the starting material (**1**); the starting material showed solubility in methanol, NMP and DMSO; however, these were not compatible for the reaction so THF was used instead as the solubility was increased upon heating; Initial synthesis produced

yields less than half of what were theoretically calculated, this was attributed to the solubility of the starting material, but upon the removal of filtration step the yields improved.

The phosphates were characterised and successfully synthesised by several methods; esterification by the use of water was the least successful with a yield of 0.8%. The fact that the reaction was carried out in chloroform limited the interactivity of the water and phosphorus oxychloride. As a result, it was decided not to carry this out for the synthesis of **(6)** instead another method was employed for the synthesis of **(5 – 6)** relying on the protection of one of the ester sites around the phosphorus and allowing for the acid chlorides to be then substituted with the desired alcohol. Yields were near 70% and easily purified by silica gel column chromatography. The main problem seen with this reaction was with the reagents **(7 – 8)** that contained the acrylic stabilising agent (*p*-methoxyphenol), the anti-oxidant competed with **(7 – 8)** during the esterification process of the protected phosphorodichloridate **(10)**. This resulted in a mix of the products and the contaminants were extremely difficult to separate. Subsequently the acrylic alcohols produced later contained no quenching agent (*p*-methoxyphenol). The last method used for synthesising the phosphate dopants was a relatively simple esterification; the synthesis was conducted in the presence of triethylamine which drove the esterification forward yielding the desired diester at high yields. The product was obtained by liquid extraction of the free acid out of solution; however, by looking at the <sup>31</sup>P-NMR it would be expected that a phosphodiester would produce a signal between -1.0 ppm to 1.0 ppm, but in the case of **(5)** and **(6)** it was noticed that the products produced signals in the region of 4 ppm suggesting the products are in the form of their conjugate salts. Therefore the acid wash was not a sufficient method to desalinate the diesters, accounting for the lower than yields post extraction with diethyl ether. Both methods were successful in synthesising the desired diester; the method of protecting one ester site yielded the highest amount of product however the synthetic procedure was long and was carried out over several days with each stage allowing attributing to loss of product. The fact that the acrylic alcohols were not protected by the anti-oxidant means that the length of time was a crucial factor during the synthesis allowing for gelation and cross linkages to be produced. Thus it was logical to synthesise the phosphodiester via

the final route as opposed to protecting the phosphoryl chloride and esterifying selective ester sites.

The synthesis of the intermediates: 8-hydroxyoctyl acrylate (**7**), 8-hydroxyoctyl methacrylate (**8**), 2-chloromethyl-4-nitrophenyl phosphorodichloridate (**9**), 2-chloromethyl-4-nitrophenyl phosphorodi(octyl acrylate) (**10**), 2-chloromethyl-4-nitrophenyl bis(8-methacryloxy octyl) phosphoridate (**11**) and 2-(*N,N*-dimethylamino)-4-nitrophenol hydrochloride (**12**) were successfully obtained. Products (**7**) and (**8**) were synthesised in the same procedure as dopant (**2**) and (**4**) respectively. Product (**9**) was successfully obtained however the yield was relatively low and the process of distillation via a kugelrohr oven was rather difficult due to the tiny capacity of the vessel. Further problems were encountered such as the charring of the crude within the vessel making distillation problematic. In comparison the synthesis of (**10**) and (**11**) was relatively simple and the procedure showed no signs of complications with yields of around 40%. The alcohol was placed in excess ensuring the formation of the triester that was later deprotected to yield the diester. Compound (**12**) was synthesised as an alternative to 2-chloromethyl-4-nitrophenol. The procedure was relatively simple but there was huge loss at the recrystallisation stage, and the product was obtained in 2.5% yield and the progression to the next stage with phosphorus oxychloride which was unsuccessful. Products (**7**) and (**8**) were also produced and stored without the presence of *p*-methoxy phenol; it was observed that during the reactions in preparation of products (**5**) and (**6**), product (**9**) reacted with the *p*-methoxy phenol with preferentially over products (**7**) and (**8**). This was also the case when preparing products (**5**) and (**6**) from phosphorus oxychloride.

### 6.1.2 Doping of PANI.

PANI emeraldine salts were successfully obtained by the mechanical mixing of the dopant (**17** – **25**) using a mortar and pestle. The process of doping was somewhat difficult initially the dopant is added to the PANI emeraldine base powder; firstly the mixing of heavy oil dopants was relatively easy producing an homogenous mixture, however solid state dopants were much more difficult with the solid dopants requiring heavy pressure application when mixing and more vigorous mixing to grind the dopant down to a fine powder. The solid dopants were mixed until the dopant and PANI powder was well mixed and homogeneity reached.

DCAA was added drop wise to a total of 50 ml maximum which upon the continual addition of the doping solvent it was noticed that the solvent induced gelation of the mixture which became more viscous with each addition, eventually with continual successive addition, the viscosity was seen to decrease with the mixture becoming freer flowing. However the gelation upon the addition of DCAA produced lumps and large masses of PANI which had to be mechanically broken down. This was problematic as the grinding caused splashes of DCAA which caused blisters and aggressive burn upon contact with the skin.

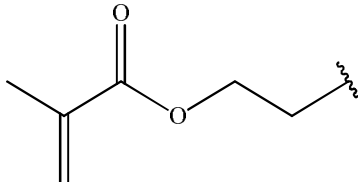
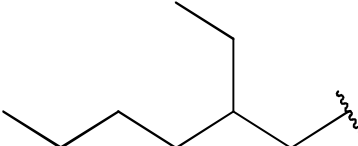
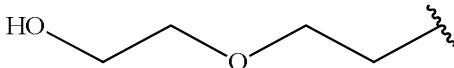
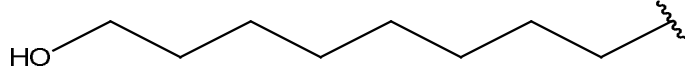
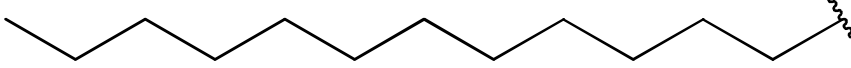
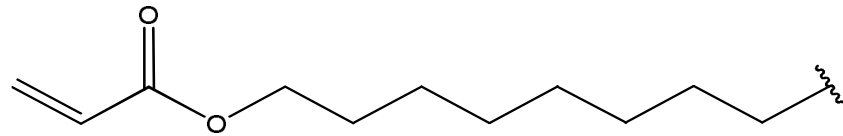
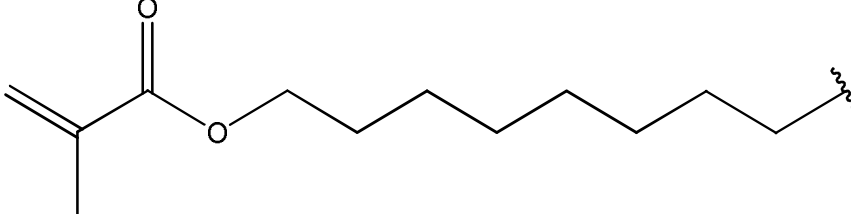
The solution continued mixing over several days at 50°C and then sonicated. After this process the doped polymer fell into solution. Doping initially occurred only when DCAA was added, and the dopant became free moving in solution. Completion of doping resulted in a dark green solution which was added to a fixed volume of DCM and was then successively washed with water until litmus paper showed a neutral pH. The washing stage proved challenging with emulsions forming which were difficult to disperse but upon dispersal, particles of undissolved doped PANI resided at the interface. The use of drying agents was not possible as it promoted the aggregation of the polymer in solution and masses of doped PANI were removed during filtration. The presence of water was seen to have no effects on any of the outcomes of integrity of the solution or the polymer.

### 6.1.3 UV studies of doped PANI (17 – 25).

The doping of PANI with dopants (17 – 25) was successfully achieved and the electronic properties were determined by UV-Visible spectroscopy, working from the ultra-violet region (190 nm) to the infra-red region (1100 nm). The results showed an absorption  $\lambda_{\max}$  of 572 nm for PANI emeraldine base (undoped) in a solution of DCM. This corresponded to the absorption in the green/yellow region of light. Upon the doping of PANI with the sulphonic acid there is a clear red shift in the electronic properties moving from 572 nm up to a  $\lambda_{\max}$  of 917 nm which corresponded to doped PANI (20) system; and the lowest  $\lambda_{\max}$  of the sulphonic acid doped PANI series being at 762 nm correlating to doped PANI (17) system residing at the border of near infra-red region.

In terms of the phosphoric acid doped PANI series, a maximum  $\lambda_{\max}$  of 944 nm was recorded for doped PANI (23) system, this being in the near infra-red region. This

was the highest absorption of all the doped PANI systems of the series, the lowest  $\lambda_{\max}$  of 831 nm in the near infra-red for doped PANI (**25**) system, showing a red shifted band recorded in comparison to the sulphonic acid series of dopants. These results summarised in Table 9 shows a clear correlation between the structure, functionality and chemical properties.

Functionalised dopant side chain (functionalised constituent)	Doped PANI System	$\lambda_{\max}$ (nm) Solution
	<b>24</b>	863
	<b>23</b>	944
	<b>19</b>	764
	<b>17</b>	762
	<b>22</b>	831
	<b>18, 25</b>	865, 831
	<b>20, 21</b>	917, 833

**Table 9:** Table to illustrate the various lengths of the dopant side chains in ascending order of length, correlating the length of the chains to the optical properties observed and recorded. Text in red corresponds to the sulphonic acid doped PANI systems and the blue text refers to the phosphoric acid doped PANI systems.

The highest  $\lambda_{\max}$  recorded belonged to doped PANI (**23**) system. This dopant was a phosphoric acid diester and was relatively smaller than the sulphonic acid series of

dopants. This investigation has highlighted a trend between the dopants structure and the electronic properties, the efficiency and the levels of doping. It was discovered that the most important feature of the dopant was the structure of the side chain; a branched side chain gave a higher order of crystallinity in the polymer by steric effects, uncoiling the chain and opening the polymer to a higher order of linearity. The efficiency and levels of doping depended on the chain length, and their steric hindrance/repulsion, which in the case of sulphonic acid dopants occurred away from the site of doping. This was collaborated by the fact that the smaller branched chains (e.g. doped PANI (**23**)) were more efficacious than those dopants with unbranched chains (e.g. doped PANI (**21**)); both were phosphoric acid diesters. The position of the branching played some importance with the branching at the end of the chains having lower steric effect than those with branch chains closer to the dopant centre.

Regarding side chain length, particular interest was placed on doped PANI (**22**), this system dopant contained the longest chain of all the doped systems and the optical properties showed high good electronic properties and the emergence of a second peak starting at the limit of the detector (1100 nm). This suggested that extensive levels of doping had taken place and the potential presence of a bipolaron, the second peak suggested a delocalisation of the polarons, however without investigating beyond 1100 nm this can only be alluded. The effect of doping was massively amplified in sulphonic acid doped systems by the presence of the aromatic ring. This structure aided with the uncoiling of the polymer structure and the linearity. Evidence has shown in this investigation - and documented throughout literature - that the aromatic rings of the dopant participate a  $\pi$ -bond interaction with those of PANI, known as  $\pi$ -bond stacking.

In terms of the dopant functionality, the chains were designed for two purposes: initially to aid the process of doping and secondly to increase the processability of the material and for these parts were successfully achieved. At first, the chains were functionalised with hydroxyl end groups, designed to increase the processability of the doped PANI system into an epoxide resin matrix. This was achieved by producing cross-links with the epoxy resins. Hydroxyl functionalised systems (**17**) and (**19**) proved effective in the dispersing the polymer into the resin matrix but regarding their doping ability, these doped PANI systems showed some of the

lowest  $\lambda_{\max}$  recorded for doped PANI. The acrylic functionalised systems produced much higher degrees of doping and finally the relatively simple non-functionalised systems (doped PANI (22 - 23)) also gave good electronic properties.

Thin films cast from solutions of DCM onto quartz plates were successfully produced for doped PANI (21) and (25). The optical properties of the solutions sufficiently provided the proof for the concept of doping; however the optical band gap for these systems could not be deduced due to the mobility of the chains in solution hence the optical band gaps were only calculated from the thin films and are summarised in Table 10. The optical properties show distinct red shifts for both systems by around 200 nm and an optical energy gap of 1.21 eV was calculated.

Doped PANI System	Doped PANI cast Film $\lambda_{\max}$ (nm) Film	$\lambda$ Onset Absorbance (nm)	$E_g$ Optical (Band Gap) (eV)
<u>21</u>	<b>1027</b>	Beyond recordable detection	<b>1.21</b>
<u>25</u>	<b>1028</b>		

**Table 10: Summary of optical properties for doped PANI (21) and (25) thin films cast onto quartz plate from a solution of DCM.**

The choice of solvent was crucially important when doping PANI due to a phenomenon known as ‘secondary doping’. Some solvents investigated were shown to potentiate the doping process; *m*-cresol was one such example. Some of the other solvents such as NMP caused the electronic properties to blue shift as a result of the solvent increasing the defects in the conjugation, producing a more coiled structure. Using *m*-cresol moved the absorption deeper into the infra-red region, the result of aromatic ring interactions between the solvent and the polymer known as  $\pi$ -bond stacking, a noticed increase in the crystallinity was evident by the tailing off of the optical properties which correlated to the delocalisation of polarons. Films cast from these solvents also share increased electronic properties. The use of DCM was a great choice of solvent in terms of processing PANI, Volatile and easily released it had several benefits over much heavier solvents (*m*-cresol and NMP) which proved to be difficult to remove from cast film.

#### 6.1.4 Composites

Composites of doped PANI (17 – 24) were created; composites with PVC (17 – 19 and 20 – 24), composites with Epikote 828™ (bisphenol A epoxy resin) (17) and

composites with methyl methacrylate (18, 20, 21, 23 – 24), ranging at volume fractions from 80 wt% to 1wt% of PANI. The successful composites were coated onto metallic substrates for the progression into accelerated corrosion testing, and the potential inhibition of corrosion on the metal surfaces.

PVC composite samples were successfully created; the incorporation of PVC in the doped PANI (17 – 25) solutions at volume fractions of 80, 50, 20, 10, 5, 2 and 1 wt%. Composite solutions produced were thixotropic and gel like at lower volume fractions, whilst at higher volume fractions the solutions showed lower viscosity and were runnier. Upon the addition of PVC at the higher volume fractions the PVC readily dissolved upon sonication of the sample, with the 80 wt% composite not requiring any methods to drive dissolution. The lower volume fractions became difficult to produce; the samples were heated to 50°C and stirred until solutions were homogenous eventually producing dark green solutions. Films were successfully obtained by the dipping method of casting the films. The films showed strong adhesion and were cast very quickly due to the volatility of DCM; however, with progressive drying, the films cracked. UV-Visible spectroscopy was conducted on thin films cast onto quartz plates, the optical properties show slight blue shifts of the films from solutions tested. The blue shift was due to several factors; firstly the doped PANI systems interaction and dispersion of the doped polymer into the PVC matrix.

Composites of the epoxy resin and the doped polymer was not possible due to the curing agent (an amine) acting to strip the proton from the doped PANI and rendering the polymer undoped. Therefore the samples were created as separates with 2 main compositions; a solution of doped PANI and a solution of the epoxy resin with the curing agent, which was quite stable showing no signs of curing until the application of heat or intense UV light. The composites were made up to volume fractions of 20, 10, 5, 2 and 1 wt% successfully. The films were created by spraying the two separate components were sprayed in unison onto the metallic surface and the curing was initiated by heating the sprayed samples with a heat gun before placing into the heated oven. The epoxy resin showed very high adhesion properties during all stages of the film casting process. Films produced were blue, clear, shiny hard structures and were very durable; the blue hue to the films was the result of deprotonation of PANI to its emeraldine base form of the polymer.

Acrylic composites were successfully created at volume fractions of 5, 2 and 1 wt%. The composites were successfully created and were comprised of methyl methacrylate (MMA), methyl acetate (MA), ethylene glycol dimethacrylate (EGDMA), azobisisobutyronitrile (AIBN) and benzophenone in ratios of around; **20:1.6:2:1:0.8** respectively with the doped PANI. The main constituent was methyl methacrylate and made the bulk of the film. The methyl acrylate was added as an adjustment to the glass transition temperature ( $T_g$ ), to produce hard and durable films but with lower glass transition temperatures to ensure flexibility. Ethylene glycol dimethacrylate (EGDMA) was added to increase cross linkage between the methyl methacrylate chains increasing film integrity. Some of the dopants synthesised were selectively functionalised with acrylic groups at the end terminals of the side chains to ensure that upon insertion into the resin matrix that there would be cross linking within the coating.

The most crucial element of the composite is the incorporation of AIBN (azobisisobutyronitrile) into the mixture. AIBN acted as the initiator, initiating the formation of free radical within the mixture that propagated and polymerised the monomers to produce a solid film structure. The final component was benzophenone which stabilised the formulation due to its anti-oxidising properties. This component ensured that polymerisation would only occur upon application of heat. Films were successfully created by a spotting method: the solution was added dropwise onto the metallic surface and placed into an oven set at a high temperature to ensure radical polymerisation. After approximately 6 hours the films were hard enough and dry enough touch but the films were still fragile and therefore the films were left for more than 24 hours until the film was extremely hard. The films produced were very brittle with lots of cracks and the film was easily removed showing that the films adhesion properties were weak and poor.

### 6.1.5 Corrosion testing

The corrosion tests were loosely based on methods already found in literature<sup>68,83,87,112-115</sup>, however no specific method was used. The metal samples used were copper tablets and mild carbon steel tablets which contained eyelets in order to suspend the samples if needed. The metal samples were cleaned by acid pickling; the steel samples were cleaned using concentrated hydrochloric acid

(37%) and the copper samples were cleaned using nitric acid (25%). Once cleaned with 100% scale removal the samples were cast with films. The accelerated corrosion tests were performed over a 7 day period inside a heated propagator, creating a micro-climate within the incubator. Variables such as humidity, air temperature of both in and outside the incubator and solution temperature were all measured. The metallic samples were cast with the films and subjected to the harsh artificial environment created within the incubator; for each sample a test to investigate corrosion upon submersion into a corrosive medium over the 7 day period was conducted, sampling at 1 hour, 24 hours and then every 24 hours up to 7 days.

The other set of samples were designated to investigate the effects of corrosion upon spraying the sample with a corrosive solution, investigating the effects that humidity and temperature has on the movement of corrosive species, again the sampling was carried out as previously described.

The method of accelerated testing was concise and yielding giving lots of information regard the effects that are seen regarding corrosion when the sample is submerged or sprayed showing the effects that humidity and temperature has on the movement of corrosive species and the inhibitory effects that the active film exerts onto the metal surface and how it acts to prevent corrosion.

The films were photographed post testing to document changes before corrosion testing and after to determine the effects. The samples were photographed at the sampling time points to give a timeline in terms of the progression of corrosion and to which levels it is present. For the investigation it was vital to perform corrosion tests on samples that remain uncoated and samples that have been coated with just the resin matrices. This eliminates the effects that the matrices may have on the rate of corrosion therefore upon corrosion testing with doped PANI/Resin films it will be clear to see the effects that the doped polymer may have.

Finally samples that were coated solely with the doped PANI were also tested in order to demonstrate the effects that the polymer has on inhibition of corrosion without any resin matrix. All samples upon completion were then subjected to rigorous surface analysis using a scanning electron microscopy showing the morphology that the films presented. This method also showed the chemical

environments and metallic species that were present prior and post accelerated corrosion test on the metal surfaces.

### 6.1.6 Corrosion results

The accelerated corrosion studies were successfully conducted and completed. The samples were photographed and qualitative analysis of the surface was conducted by scanning electron microscopy. The obtained photographs results indicate that for the different samples and matrices there were different levels of noticed corrosion. The trend was obvious with lower volume fractions showing the lowest anti-corrosion properties and the higher obviously producing the best results.

Looking at the photographs the highest level of protection from the lowest volume fraction was obtained from the samples coated with the epoxy resin with doped PANI (**17**) at 1 wt%. The films cast from epoxy resins alone showed some minimal levels of corrosion and suggested that the resin acted as an excellent physical barrier.

The thin films of the doped PANI were produced onto the metal surfaces and produced porous films that were easily dislodged by mechanical means and contact, however the presence of doped PANI appeared to impede the corrosion and slow down the process in comparison to the experimental controls.

The PVC coated samples showed mixed results but did prove that the presence of doped PANI had inhibitory effects on the levels of corrosion. Samples coated solely with the PVC films showed corrosion and delamination under the film but the film remained intact. Inhibition was seen down to levels as low as 1 wt% doped PANI for (**21** – **23**) with no signs of visible corrosion on the metal surface or under the film.

In comparison to the previous two composites the acrylic resin coatings showed poorer results with low adhesion and severe delamination in some cases. Samples coated with just the acrylic resin showed that the coating formulations needed to be optimised as the films were very brittle and delicate. Beneath the clear films there was extensive corrosion on steel samples and the formation of patinas on the copper samples. Samples coated with the sulphonic acid series doped PANI (**18**) and (**20**) composites showed promising results:, the films were thin but none uniform giving

peaks and troughs and the dispersity of the polymer within the films was poor but the films remained intact and the metal plates showed very little to no signs of corrosion.

In comparison to the sulphonic acid doped PANI composites, the phosphoric acid diester doped PANI composites with the acrylic resin produced very poor results with severe delamination, some areas of the plates showed bare surfaces where the film had completely removed. On all the plates coated with the doped PANI (21, 22 – 23) acrylic resin composites, it appeared that a reaction had occurred between the metal and the cast film in the presence of the saline solution. Further investigation would be needed and tune the composition of the film to produce a durable, relatively softer film which have better adhesion.

To summarise these findings; the epoxide resin films produced durable water tight films with the PANI but at the expense of being undoped. The PVC films produced strong but porous films and there was potentially some signs of corrosion. The films eventually fatigued and cracked during the progression of the testing resulting in delamination. The acrylate composites produced the poorest films which had low adhesive properties and were brittle, but however poor the films were the results in comparison to this were not as bad and the presence of the polymer still went some way to inhibit the corrosion at the metal surface.

The obtained microscopic images indicated that where the polymer was not present mostly showed signs of corrosion. Films cast onto the surfaces appeared to be somewhat smooth; with the exception of the acrylic resin based films which showed rough and layered structured that protruded, with what looked to be delamination at these sites. PVC samples at the microscopic level were highly porous and it was seen that pores existed within the pores in a vast array. Therefore it was assumed that the vast network of pores lead inevitably to channels down to the metal surface.

#### **6.1.7 Overall conclusion.**

In summary, the main conclusions that are derived from this research showed that the presence of PANI in a doped or undoped states inhibit the process of corrosion and showed anti-corrosion properties, this being most likely due to its excellent redox properties.

The doped PANI systems were analysed by UV-Vis spectroscopy showing clear red shifts in the absorptions with the absorption shifting from the visible light region of the spectrum to the near infra-red region for the sulphonic acids and the phosphoric acid diester doped PANI systems. The successful doping of the polymer rendered the intractable and insoluble polymer, soluble in a range of common solvents or at least the solubility potential of the polymer increased.

The successful transfer from DCAA solution to the DCM allowed for easy casting of the films with the solvent quickly evaporating leaving the film intact and set. Therefore these doped polymers make for ideal materials incorporated into paints and would find use in devices where a thin conductive or even semi conductive film would be useful.

PANI alone was not sufficient enough to halt the effect of corrosion, but it did go some way to inhibit the process or at least slow the rate of corrosion down. The film (including the doped polymer) also acts as a physical barrier which mostly prevented the migration of corrosive agents to the surface and working in conjunction with the doped polymer had the added benefit of not only being a physical barrier but also an electrochemical barrier too.

From this investigation it is clear that the best system produced was a PANI/Epoxy resin combination with its high durability, the lack of cracking and the watertight smooth surface all made for desirable properties. The PVC samples showed adequate adhesion properties but were porous and so would not be ideal for the incorporation into a paint formulation. Finally the acrylic films showed the poorest qualities of all the films, showing low durability and many undesirable properties; however, the acrylic coating formulations were not optimised and some future work and optimisation may yield better results.

In terms of the dopants, it became apparent that their presence was less important than first thought. The correlation between the electronic states of PANI and their respective anti-corrosion properties was not clear and it needs further investigation. The dopants and the doping process appeared to be necessary solely for the purposes of processability. Overall, this study has highlighted that the process of doping can be used to obtain a conductive form of PANI in a processable form which gives rise to the new potential for this material and its potential uses.

## 6.2 Future work

During this research a few issues have been raised, primarily that the electronic state of PANI appeared to have little consequence or effect on the ability to inhibit corrosion, but has however shown that PANI alone was not sufficient to prevent corrosion as the PANI films themselves are delicate and can be easily removed just. It was shown that the use of a resin was integral, which would act to deliver the PANI to the metal surface providing not only an electrochemical barrier resulting from the PANI but also a physical barrier with a sacrificial role.

Further investigations should look at the acrylic resin formulations and films; the films produced displayed poor adhesion properties, low durability and were extremely brittle. Further investigations of the acrylic resin formulation are needed to optimise the ideal composition that would give benefits of a lower the glass transition temperature, reduced brittleness and increased flexibility for a more durable coating. This can be achieved by looking at the ratios of methyl methacrylate, methyl acrylate and other potential acrylic monomers to see what composition gives the best film.

Other investigations should be progressed into the further development of the sulphonic acid series of dopants and the phosphoric acid diester series of dopants. In this research the most effective dopants were the sulphonic acid dopants functionalised with the acrylate end groups, and long side chains whilst the phosphates favoured shorter and branched chains producing remarkable changes in the optical properties. Therefore it is appropriate to develop and extend the family of acrylate functionalised dopants of both the sulphonic acid dopants and of the phosphoric acid diesters. Secondly to develop dopants with branching side chain in which this research indicates that longer side chains are beneficial for the sulphonic acid dopants, whilst shorter branched chains had higher benefits for the phosphates. The UV-Vis studies conducted were limited to a narrow range of the spectrum, further studies into the electronic properties would benefit from instrumentation with much broader detection range into the infra-red region (2000 nm) and allowing more detailed analysis of both the films and solutions.

It would be interesting to see the effects of phosphoric acid diesters containing aromatic groups. Potentially the addition of the aromatic groups to the phosphate

dopants may give increased interaction with the polymer backbone similar to the effects noticed in the presence of *m*-cresol.

Another topic for investigation is the idea of ‘self-doping’ polyaniline, where the dopant is incorporated into the structure of the polymer; either onto the aromatic ring or the amine (such as *N*-alkylated PANI) to give self-dispersing polymers capable dissolving into a solvent system or dispersing the self-doped polymer to low particle size in solvent. The most interesting idea is that the self-doping PANI’s may even be capable of rendering the system compatible with an aqueous medium giving rise to water borne systems and emulsions<sup>55,133-140</sup>.

## References

- 1 Alan, J. H. Semiconducting and Metallic Polymers: The Fourth Generation of Polymeric Materials (Nobel Lecture)13. *Angewandte Chemie International Edition* 40, 2591-2611 (2001).
- 2 Gerard, M., Chaubey, A. & Malhotra, B. D. Application of conducting polymers to biosensors. *Biosensors and Bioelectronics* 17, 345-359 (2002).
- 3 Zarras, P. *et al.* Progress in using conductive polymers as corrosion-inhibiting coatings. *Radiation Physics and Chemistry* 68, 387-394 (2003).
- 4 Salaneck, W. R. & Brédas, J. L. Conjugated polymers. *Solid State Communications* 92, 31-36 (1994).
- 5 Kraft, A., Grimsdale, A. C. & Holmes, A. B. Electroluminescent conjugated polymers-seeing polymers in a new light. *Angewandte Chemie, International Edition* 37, 403-428 (1998).
- 6 Osiele, O. M. *et al.* Defect structural characterization of organic polymer layers. *J. Non-Cryst. Solids* 338-340, 612-616 (2004).
- 7 MacDiarmid, A. G. Synthetic metals: a novel role for organic polymers. *Synthetic Metals* 125, 11-22 (2001).
- 8 Salaneck, W. R., Friend, R. H. & Bredas, J. L. Electronic structure of conjugated polymers: consequences of electron-lattice coupling. *Physics Reports* 319, 231-251 (1999).
- 9 Anand, J., Palaniappan, S. & Sathyanarayana, D. N. Conducting polyaniline blends and composites. *Progress in Polymer Science* 23, 993-1018 (1998).
- 10 Stenger-Smith, J. D. Intrinsically electrically conducting polymers. Synthesis, characterization, and their applications. *Progress in Polymer Science* 23, 57-79 (1998).
- 11 Shirakawa, H., Louis, E. J., MacDiarmid, A. G., Chiang, C. K. & Heeger, A. J. Synthesis of electrically conducting organic polymers: halogen derivatives of polyacetylene, (CH)<sub>x</sub>. *J. Chem. Soc., Chem. Commun.*, 578-580 (1977).
- 12 Pron, A. & Rannou, P. Processible conjugated polymers: from organic semiconductors to organic metals and superconductors. *Progress in Polymer Science* 27, 135-190 (2002).
- 13 Stenger-Smith, J. D. Intrinsically electrically conducting polymers. Synthesis, characterization, and their applications. *Progress in Polymer Science* 23, 57-79 (1998).
- 14 Walatka, V. V., Jr., Labes, M. M. & Perlstein, J. H. Poly(sulfide nitride), a one-dimensional chain with a metallic ground state. *Physical Review Letters* 31, 1139-1142 (1973).
- 15 Chiang, C. K. *et al.* Electrical conductivity in doped polyacetylene. *Physical Review Letters* 39, 1098-1101 (1977).
- 16 Anand, J., Palaniappan, S. & Sathyanarayana, D. N. Conducting polyaniline blends and composites. *Progress in Polymer Science* 23, 993-1018 (1998).
- 17 Heeger, A. J. Semiconducting and metallic polymers: The fourth generation of polymeric materials (Nobel Lecture). *Angewandte Chemie, International Edition* 40, 2591-2611 (2001).
- 18 Heeger, A. J. Nobel Lecture: Semiconducting and metallic polymers: The fourth generation of polymeric materials. *Reviews of Modern Physics* 73, 681 (2001).
- 19 Kohlman, R. S., Joo, J. & Epstein, A. J. Conducting polymers: Electrical conductivity. *Phys. Prop. Polym. Handb.*, 453-478 (1996).

- 20 Salaneck, W. R., Friend, R. H. & Brédas, J. L. Electronic structure of conjugated polymers: consequences of electron-lattice coupling. *Physics Reports* 319, 231-251 (1999).
- 21 Berlinsky, A. J. The band structure and optical properties of sulfur nitride polymer. Comments. *J. Phys. C* 9, L283-L287 (1976).
- 22 Yang, S., Olishovski, P. & Kertesz, M. Bandgap calculations for conjugated polymers. *Synthetic Metals* 141, 171-177 (2004).
- 23 MacDiarmid, A. G. & Epstein, A. J. Polyanilines: a novel class of conducting polymers. *Faraday Discuss. Chem. Soc.* 88, 317-332 (1989).
- 24 MacDiarmid, A. G. "Synthetic metals": A novel role for organic polymers (Nobel Lecture). *Angewandte Chemie, International Edition* 40, 2581-2590 (2001).
- 25 Bundgaard, E. & Krebs, F. C. Low band gap polymers for organic photovoltaics. *Solar Energy Materials and Solar Cells* 91, 954-985 (2007).
- 26 Walatka, V. V., Labes, M. M. & Perlstein, J. H. Polysulfur Nitride; a One-Dimensional Chain with a Metallic Ground State. *Physical Review Letters* 31, 1139 (1973).
- 27 Atwani, O., Baristiran, C., Erden, A. & Sonmez, G. A stable, low band gap electroactive polymer: Poly(4,7-dithien-2-yl-2,1,3-benzothiadiazole). *Synthetic Metals* 158, 83-89 (2008).
- 28 Salzner, U., Karalti, O. & Durdagi, S. Does the donor-acceptor concept work for designing synthetic metals? III. Theoretical investigation of copolymers between quinoid acceptors and aromatic donors. *Journal of Molecular Modeling* 12, 687-701 (2006).
- 29 Rannou, P., Dufour, B., Travers, J. P. & Pron, A. New PANI/dopant/solvent associations for processing of metallic PANI. *Synthetic Metals* 119, 441-442 (2001).
- 30 Bredas, J. L. & Street, G. B. Polarons, bipolarons, and solitons in conducting polymers. *Acc. Chem. Res.* 18, 309-315 (1985).
- 31 Chance, R. R., Brédas, J. L. & Silbey, R. Bipolaron transport in doped conjugated polymers. *Physical Review B* 29, 4491 (1984).
- 32 Epstein, A. J. & MacDiarmid, A. G. Polyanilines: From solitons to polymer metal, from chemical curiosity to technology. *Synthetic Metals* 69, 179-182 (1995).
- 33 MacDiarmid, A. G. Synthetic metals: a novel role for organic polymers. *Synthetic Metals* 125, 11-22 (2001).
- 34 Wolszczak, M., Kroh, J. & Abdel-Hamid, M. M. Effect of ionizing radiation on polyaniline solutions. *Radiation Physics and Chemistry* 47, 859-867 (1996).
- 35 Phang, S.-W., Hino, T., Abdullah, M. H. & Kuramoto, N. Applications of polyaniline doubly doped with p-toluene sulphonic acid and dichloroacetic acid as microwave absorbing and shielding materials. *Materials Chemistry and Physics* 104, 327-335 (2007).
- 36 Lindfors, T., Ervela, S. & Ivaska, A. Polyaniline as pH-sensitive component in plasticized PVC membranes. *Journal of Electroanalytical Chemistry* 560, 69-78 (2003).
- 37 Shimano, J. Y. & MacDiarmid, A. G. Polyaniline, a dynamic block copolymer: key to attaining its intrinsic conductivity? *Synthetic Metals* 123, 251-262 (2001).
- 38 Pron, A. & Rannou, P. Processible conjugated polymers: from organic semiconductors to organic metals and superconductors. *Progress in Polymer Science* 27, 135-190 (2002).
- 39 Epstein, A. J. & MacDiarmid, A. G. Polyanilines: From solitons to polymer metal, from chemical curiosity to technology. *Synthetic Metals* 69, 179-182 (1995).

- 40 Stejskal, J., Kratochvil, P. & Jenkins, A. D. The formation of polyaniline and the nature of its structures. *Polymer* 37, 367-369 (1996).
- 41 Aoki, K., Kawaguchi, F., Nishiumi, T. & Chen, J. Electrically conducting suspensions formed by polyaniline. *Electrochimica Acta* 53, 3798-3802 (2008).
- 42 Mohilner, D. M., Adams, R. N. & Argersinger, W. J., Jr. Investigation of the kinetics and mechanism of the anodic oxidation of aniline in aqueous sulfuric acid solution at a platinum electrode. *Journal of the American Chemical Society* 84, 3618-3622 (1962).
- 43 Kim, M. S. & Levon, K. Blend of electroactive complexes of polyaniline and surfactant with alkylated polyacrylate. *Journal of Colloid and Interface Science* 190, 17-36 (1997).
- 44 Paul, R. K. & Pillai, C. K. S. Melt/solution processable conducting polyaniline with novel sulfonic acid dopants and its thermoplastic blends. *Synthetic Metals* 114, 27-35 (2000).
- 45 Stafstrom, S. *et al.* Polaron lattice in highly conducting polyaniline: theoretical and optical studies. *Phys. Rev. Lett.* 59, 1464-1467 (1987).
- 46 MacDiarmid, A. G. Polyaniline and polypyrrole: Where are we headed? *Synthetic Metals* 84, 27-34 (1997).
- 47 Kwon, O. & McKee, M. L. Calculations of Band Gaps in Polyaniline from Theoretical Studies of Oligomers. *J. Phys. Chem. B* 104, 1686-1694 (2000).
- 48 Huang, W. S., Humphrey, B. D. & MacDiarmid, A. G. Polyaniline, a novel conducting polymer. Morphology and chemistry of its oxidation and reduction in aqueous electrolytes. *J. Chem. Soc., Faraday Trans. 1* 82, 2385-2400 (1986).
- 49 de Oliveira, Z. T. & dos Santos, M. C. Relative stability of polarons and bipolarons in emeraldine oligomers: a quantum chemical study. *Solid State Communications* 114, 49-53 (2000).
- 50 Wang, X. H. *et al.* Polyaniline as marine antifouling and corrosion-prevention agent. *Synthetic Metals* 102, 1377-1380 (1999).
- 51 Sergeyeva, T. A., Lavrik, N. V., Piletsky, S. A., Rachkov, A. E. & El'skaya, A. V. Polyaniline label-based conductometric sensor for IgG detection. *Sensors and Actuators B: Chemical* 34, 283-288 (1996).
- 52 Shimano, J. Y. & MacDiarmid, A. G. Polyaniline, a dynamic block copolymer: key to attaining its intrinsic conductivity? *Synthetic Metals* 123, 251-262 (2001).
- 53 Quadrat, O. *et al.* Electrical properties of polyaniline suspensions. *Synth. Met.* 97, 37-42 (1998).
- 54 Hua, M. Y., Hwang, G. W., Chuang, Y. H., Chen, S. A. & Tsai, R. Y. Soluble n-Doped Polyaniline: Synthesis and Characterization. *Macromolecules* 33, 6235-6238 (2000).
- 55 Chen, S.-A. & Hwang, G.-W. Synthesis of Water-Soluble Self-Acid-Doped Polyaniline. *J. Am. Chem. Soc.* 116, 7939-7940 (1994).
- 56 MacDiarmid, A. G. Polyaniline and polypyrrole: Where are we headed? *Synthetic Metals* 84, 27-34 (1997).
- 57 Monkman, A. P., Adams, P. N., Laughlin, P. J. & Holland, E. R. Polyaniline, air stable organic metal: fact, no longer fiction. *Synthetic Metals* 69, 183-186 (1995).
- 58 Pron, A., Luzny, W. & Laska, J. Thermally processable polyaniline protonated with diphenyl phosphate -- preparation and structural aspects. *Synthetic Metals* 80, 191-193 (1996).
- 59 Pron, A., Dufour, B., Rannou, P. & Travers, J. P. Use of sulfonic, phosphonic acids as doping agents of polyaniline, and conducting composite materials based on polyaniline. Application: FR

- 2830535 (2003).
- 60 MacDiarmid, A. G. & Epstein, A. J. Secondary doping in polyaniline. *Synthetic Metals* 69, 85-92 (1995).
- 61 Koul, S., Chandra, R. & Dhawan, S. K. Conducting polyaniline composite for ESD and EMI at 101 GHz. *Polymer* 41, 9305-9310 (2000).
- 62 Cai, Z., Geng, M. & Tang, Z. Novel battery using conducting polymers: Polyindole and polyaniline as active materials. *Journal of Materials Science* 39, 4001-4003 (2004).
- 63 Koul, S., Chandra, R. & Dhawan, S. K. Conducting polyaniline composite for ESD and EMI at 101 GHz. *Polymer* 41, 9305-9310 (2000).
- 64 Makela, T., Pienimaa, S., Jussila, S. & Isotalo, H. Lithographic patterning of conductive polyaniline. *Synth. Met.* 101, 705-706 (1999).
- 65 Makela, T., Pienimaa, S., Taka, T., Jussila, S. & Isotalo, H. Thin polyaniline films in EMI shielding. *Synth. Met.* 85, 1335-1336 (1997).
- 66 Wang, J., Torardi, C. C. & Duch, M. W. Polyaniline-related ion-barrier anticorrosion coatings: II. Protection behavior of polyaniline, cationic, and bipolar films. *Synthetic Metals* 157, 851-858 (2007).
- 67 Tallman, D., Spinks, G., Dominis, A. & Wallace, G. Electroactive conducting polymers for corrosion control. *Journal of Solid State Electrochemistry* 6, 73-84 (2002).
- 68 Armelin, E. *et al.* Corrosion protection with polyaniline and polypyrrole as anticorrosive additives for epoxy paint. *Corrosion Science* 50, 721-728 (2008).
- 69 Sangaj, N. S. & Malshe, V. C. Permeability of polymers in protective organic coatings. *Progress in Organic Coatings* 50, 28-39 (2004).
- 70 Vannerberg, N. G. Solution chemistry and corrosion. *Pure Appl. Chem.* 60, 1831-1840 (1988).
- 71 Mendoza, A. R. & Corvo, F. Outdoor and indoor atmospheric corrosion of carbon steel. *Corrosion Science* 41, 75-86 (1999).
- 72 Mendoza, A. R. & Corvo, F. Outdoor and indoor atmospheric corrosion of nonferrous metals. *Corrosion Science* 42, 1123-1147 (2000).
- 73 Bierwagen, G. P. Reflections on corrosion control by organic coatings. *Progress in Organic Coatings* 28, 43-48 (1996).
- 74 Okayasu, M., Sato, K., Okada, K., Yoshifuji, S. & Mizuno, M. Effects of atmospheric corrosion on fatigue properties of a medium carbon steel. *Journal of Materials Science* 44, 306-315 (2009).
- 75 Núñez, L., Reguera, E., Corvo, F., González, E. & Vazquez, C. Corrosion of copper in seawater and its aerosols in a tropical island. *Corrosion Science* 47, 461-484 (2005).
- 76 Fitzgerald, K. P., Nairn, J. & Atrens, A. The chemistry of copper patination. *Corrosion Science* 40, 2029-2050 (1998).
- 77 Zhang, J., Klasky, M. & Letellier, B. C. The aluminum chemistry and corrosion in alkaline solutions. *Journal of Nuclear Materials* 384, 175-189 (2009).
- 78 Namazi, H., Kabiri, R. & Entezami, A. Determination of extremely low percolation threshold electroactivity of the blend polyvinyl chloride/polyaniline doped with camphorsulfonic acid by cyclic voltammetry method. *European Polymer Journal* 38, 771-777 (2002).
- 79 Chen, Y., Wang, X. H., Li, J., Lu, J. L. & Wang, F. S. Long-term anticorrosion behaviour of polyaniline on mild Steel. *Corrosion Science* 49, 3052-3063 (2007).
- 80 Spinks, G., Dominis, A., Wallace, G. & Tallman, D. Electroactive conducting polymers for corrosion control. *Journal of Solid State Electrochemistry* 6, 85-100 (2002).

- 81 Ahmad, N. & MacDiarmid, A. G. Inhibition of corrosion of steels with the exploitation of conducting polymers. *Synthetic Metals* 78, 103-110 (1996).
- 82 Tanner, J., Ikkala, O. T., Passiniemi, P. & Österholm, J. E. Conductivity tailoring of blends of fusible polyaniline and polyolefins by viscosity ratio. *Synthetic Metals* 84, 763-764 (1997).
- 83 Armelin, E. *et al.* Marine paint formulations: Conducting polymers as anticorrosive additives. *Progress in Organic Coatings* 59, 46-52 (2007).
- 84 Wessling, B. Dispersion as the link between basic research and commercial applications of conductive polymers (polyaniline). *Synthetic Metals* 93, 143-154 (1998).
- 85 Li, X.-G., Huang, M.-R., Zeng, J.-F. & Zhu, M.-F. The preparation of polyaniline waterborne latex nanoparticles and their films with anti-corrosivity and semi-conductivity. *Colloids and Surfaces A: Physicochemical and Engineering Aspects* 248, 111-120 (2004).
- 86 Pan, W., Yang, S. L., Li, G. & Jiang, J. M. Electrical and structural analysis of conductive polyaniline/polyacrylonitrile composites. *European Polymer Journal* 41, 2127-2133 (2005).
- 87 Armelin, E. *et al.* Study of epoxy and alkyd coatings modified with emeraldine base form of polyaniline. *Progress in Organic Coatings* 58, 316-322 (2007).
- 88 Kulszewicz-Bajer, I., Zagórska, M., Niziol, J., Pron, A. & Luzny, W. Esters of 5-sulfo-i-phthalic acid as new dopants improving the solution processibility of polyaniline: spectroscopic, structural and transport properties of the doped polymer. *Synthetic Metals* 114, 125-131 (2000).
- 89 Jadwiga Laska, A. P., nacute & Lefrant, S. Phosphoric acid diesters protonated polyaniline: Preparation, spectroscopic properties, and processability. *Journal of Polymer Science Part A: Polymer Chemistry* 33, 1437-1445 (1995).
- 90 Proń, A., Laska, J., Österholm, J.-E. & Smith, P. Processable conducting polymers obtained via protonation of polyaniline with phosphoric acid esters. *Polymer* 34, 4235-4240, doi:http://dx.doi.org/10.1016/0032-3861(93)90182-A (1993).
- 91 Ikkala, O. T., Lindholm, T. M., Ruohonen, H., Seläntaus, M. & Väkiparta, K. Phase behavior of polyaniline/dodecyl benzene sulphonic acid mixture. *Synthetic Metals* 69, 135-136 (1995).
- 92 Kulszewicz-Bajer, I., Zagórska, M., Bany, A. & Lukasik, L. Spectroscopic studies of polyaniline protonated with esters of 5-sulfoisophthalic acid 1. *Synthetic Metals* 101, 713-714 (1999).
- 93 Levon, K. *et al.* Thermal doping of polyaniline with dodecylbenzene sulfonic acid without auxiliary solvents. *Polymer* 36, 2733-2738 (1995).
- 94 Olinga, T. E., Fraysse, J., Travers, J. P., Dufresne, A. & Pron, A. Highly Conducting and Solution-Processable Polyaniline Obtained via Protonation with a New Sulfonic Acid Containing Plasticizing Functional Groups. *Macromolecules* 33, 2107-2113, doi:doi:10.1021/ma991525i (2000).
- 95 Rannou, P. *et al.* Spectroscopic, Structural and Transport Properties of Conductive Polyaniline Processed from Fluorinated Alcohols. *Macromolecules* 31, 3007-3015, doi:doi:10.1021/ma971365f (1998).
- 96 Dufour, B. *et al.* Effect of Plasticizing Dopants on Spectroscopic Properties, Supramolecular Structure, and Electrical Transport in Metallic Polyaniline. *Chemistry of Materials* 13, 4032-4040, doi:doi:10.1021/cm001224j (2001).
- 97 Hopkins, A. R., Rasmussen, P. G. & Basheer, R. A. Characterization of Solution and Solid State Properties of Undoped and Doped Polyanilines Processed from Hexafluoro-2-propanol. *Macromolecules* 29, 7838-7846, doi:doi:10.1021/ma9606519 (1996).

- 98 Davies, S. J., Ryan, T. G., Wilde, C. J. & Beyer, G. Processable forms of conductive polyaniline. *Synthetic Metals* 69, 209-210 (1995).
- 99 John, A., Palaniappan, S., Djurado, D. & Pron, A. One-step preparation of solution processable conducting polyaniline by inverted emulsion polymerization using didecyl ester of 4-sulfophthalic acid as multifunctional dopant. *Journal of Polymer Science Part A: Polymer Chemistry* 46, 1051-1057, doi:10.1002/pola.22448 (2008).
- 100 Palaniappan, S. & Ajit, S. Didecyl ester of 4-sulfophthalic acid as a plast dopant and emulsifier in the chemical polymerization of aniline into polyaniline salt. *Journal of Applied Polymer Science* 118, 2704-2711, doi:10.1002/app.32636 (2010).
- 101 Kulszewicz-Bajer, I., Zagórska, M. & Różalska, I. Polyaniline doped with esters of 5-sulfo-i-phthalic acid and its blends with nonconducting polymers. *Synthetic Metals* 119, 69-70, doi:http://dx.doi.org/10.1016/S0379-6779(00)00693-7 (2001).
- 102 Laco, J. I. I., Villota, F. C. & Mestres, F. L. Corrosion protection of carbon steel with thermoplastic coatings and alkyd resins containing polyaniline as conductive polymer. *Progress in Organic Coatings* 52, 151-160 (2005).
- 103 Wang, J. Polyaniline coatings: anionic membrane nature and bipolar structures for anticorrosion. *Synthetic Metals* 132, 53-56 (2002).
- 104 Hata, T., Mushika, Y. & Mukaiyama, T. New phosphorylating reagent. I. Preparation of alkyl dihydrogen phosphates by means of 2-chloromethyl-4-nitrophenyl phosphorodichloridate. *J. Amer. Chem. Soc.* 91, 4532-4535, doi:10.1021/ja01044a037 (1969).
- 105 Mushika, Y., Hata, T. & Mukaiyama, T. New phosphorylating reagent. III. Preparation of mixed diesters of phosphoric acid by the use of an activatable protecting group. *Bull. Chem. Soc. Jap.* 44, 232-235, doi:10.1246/bcsj.44.232 (1971).
- 106 Jang, J. & Jeong, Y.-K. Synthesis and flame-retardancy of UV-curable methacryloyloxy ethyl phosphates. *Fibers Polym* 9, 667-673, doi:10.1007/s12221-008-0105-2 (2008).
- 107 Hata, T., Mushika, Y. & Mukaiyama, T. New phosphorylating reagent. II. Preparation of mixed diesters of phosphoric acid by the use of alkyl 2-chloromethyl-4-nitrophenyl hydrogen phosphates. *Tetrahedron Letters*, 3505-3508 (1970).
- 108 Vikki, T. *et al.* Molecular Recognition Solvents for Electrically Conductive Polyaniline. *Macromolecules* 29, 2945-2953, doi:doi:10.1021/ma951555v (1996).
- 109 Ikkala, O. T. *et al.* Processible polyaniline complexes due to molecular recognition: Supramolecular structures based on hydrogen bonding and phenyl stacking. *Synthetic Metals* 84, 55-58 (1997).
- 110 Chen, S.-A. & Lee, H.-T. Polyaniline-acid dopant interaction in the presence of 1-methyl-2-pyrrolidone. *Synthetic Metals* 47, 233-238, doi:http://dx.doi.org/10.1016/0379-6779(92)90390-5 (1992).
- 111 Geng, Y., Li, J., Jing, X. & Wang, F. Interaction of N-methylpyrrolidone with doped polyaniline. *Synthetic Metals* 84, 97-98, doi:http://dx.doi.org/10.1016/S0379-6779(97)80665-0 (1997).
- 112 Kinlen, P. J., Ding, Y. & Koncki, K. F. Synthesis and applications of intrinsically conductive polymer salts of polyphosphonic acids in anti-corrosion coatings. Application: WO

WO patent 98-EP7202

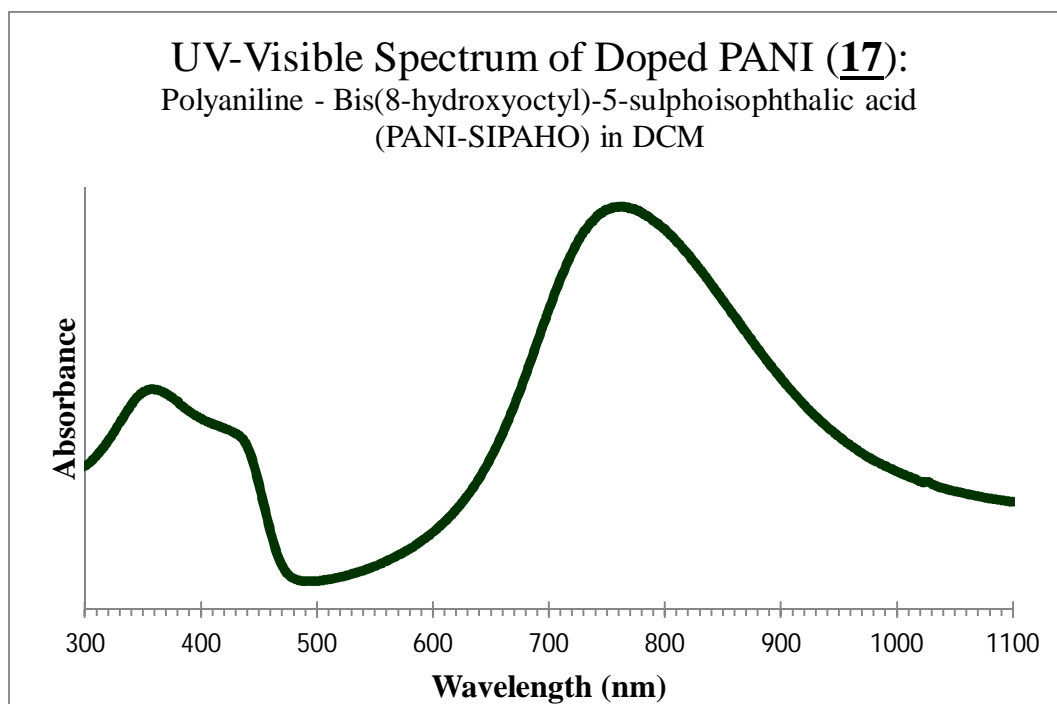
9925778 (1999).

- 113 Samui, A. B., Patankar, A. S., Rangarajan, J. & Deb, P. C. Study of polyaniline containing paint for corrosion prevention. *Progress in Organic Coatings* 47, 1-7, doi:http://dx.doi.org/10.1016/S0300-9440(02)00117-0 (2003).
- 114 Kalendová, A., Sapurina, I., Stejskal, J. & Veselý, D. Anticorrosion properties of polyaniline-coated pigments in organic coatings. *Corrosion Science* 50, 3549-3560 (2008).
- 115 Armelin, E., Alemán, C. & Iribarren, J. I. Anticorrosion performances of epoxy coatings modified with polyaniline: A comparison between the emeraldine base and salt forms. *Progress in Organic Coatings* 65, 88-93 (2009).
- 116 Polyzois, G. L., Andreopoulos, A. G. & Lagouvardos, P. E. Acrylic resin denture repair with adhesive resin and metal wires: Effects on strength parameters. *The Journal of Prosthetic Dentistry* 75, 381-387, doi:http://dx.doi.org/10.1016/S0022-3913(96)90029-3 (1996).
- 117 Radhakrishnan, S., Sonawane, N. & Siju, C. R. Epoxy powder coatings containing polyaniline for enhanced corrosion protection. *Progress in Organic Coatings* 64, 383-386 (2009).
- 118 Lu, W.-K., Elsenbaumer, R. L. & Wessling, B. Corrosion protection of mild steel by coatings containing polyaniline. *Synthetic Metals* 71, 2163-2166 (1995).
- 119 Ikkala, O. T. *et al.* Counter-ion induced processibility of polyaniline: Conducting melt processible polymer blends. *Synthetic Metals* 69, 97-100, doi:http://dx.doi.org/10.1016/0379-6779(94)02376-A (1995).
- 120 Puzari, A. *et al.* Synthesis and characterization of processible polyaniline containing plasticizing dendron-type dopants. *Synthetic Metals* 157, 611-618 (2007).
- 121 James, D. The use of phosphate coatings in the fight against corrosion. *Anti-Corrosion Methods and Materials* 23, 3, 7, doi:10.1108/eb007007 (1976).
- 122 Quitmeyer, J. Grasping the phosphate coating process: A properly maintained solution is key to achieving adhesion, corrosion protection, and lubrication. *Metal Finishing* 104, 47-50, doi:http://dx.doi.org/10.1016/S0026-0576(06)80303-X (2006).
- 123 Palraj, S., Selvaraj, M. & Jayakrishnan, P. Effect of phosphate coatings on the performance of epoxy polyamide red oxide primer on galvanized steel. *Progress in Organic Coatings* 54, 5-9, doi:http://dx.doi.org/10.1016/j.porgcoat.2004.03.012 (2005).
- 124 Lin, C. T., Lin, P., Hsiao, M. W., Meldrum, D. A. & Martin, F. L. Chemistry of a single-step phosphate/paint system. *Industrial & Engineering Chemistry Research* 31, 424-430, doi:10.1021/ie00001a058 (1992).
- 125 Paliwoda-Porebska, G. *et al.* On the development of polypyrrole coatings with self-healing properties for iron corrosion protection. *Corrosion Science* 47, 3216-3233, doi:http://dx.doi.org/10.1016/j.corsci.2005.05.057 (2005).
- 126 Hoffmann, K. & Stratmann, M. The delamination of organic coatings from rusty steel substrates. *Corrosion Science* 34, 1625-1645, doi:http://dx.doi.org/10.1016/0010-938X(93)90037-H (1993).
- 127 Han, J., Carey, J. W. & Zhang, J. Effect of sodium chloride on corrosion of mild steel in CO<sub>2</sub>-saturated brines. *J Appl Electrochem* 41, 741-749, doi:10.1007/s10800-011-0290-3 (2011).
- 128 Cushman, A. S. The corrosion of steel. *Journal of the Franklin Institute* 165, 111-120 (1908).
- 129 Leng, A., Streckel, H., Hofmann, K. & Stratmann, M. The delamination of polymeric coatings from steel Part 3: Effect of the oxygen partial pressure on the delamination reaction and current distribution at the metal/polymer interface.

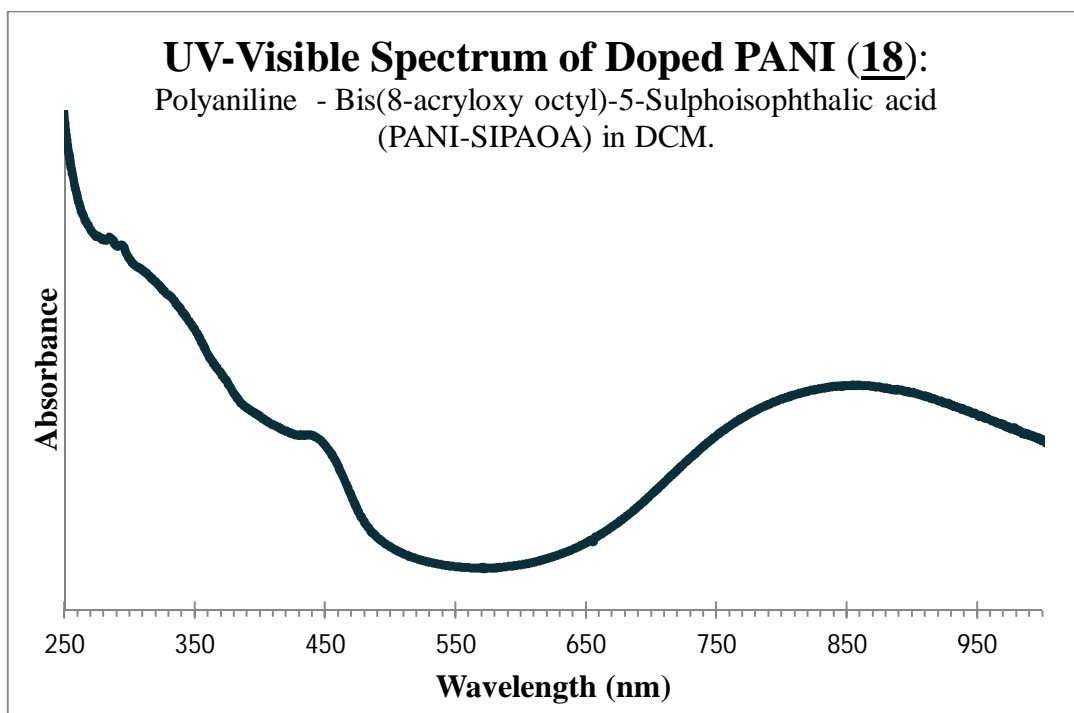
- Corrosion Science* 41, 599-620, doi:[http://dx.doi.org/10.1016/S0010-938X\(98\)00168-1](http://dx.doi.org/10.1016/S0010-938X(98)00168-1) (1998).
- 130 Tan, C. K. & Blackwood, D. J. Corrosion protection by multilayered conducting polymer coatings. *Corrosion Science* 45, 545-557 (2003).
- 131 Xiong, S. *et al.* Covalent bonding of polyaniline on fullerene: Enhanced electrical, ionic conductivities and electrochromic performances. *Electrochimica Acta* 67, 194-200, doi:<http://dx.doi.org/10.1016/j.electacta.2012.02.026> (2012).
- 132 Kinlen, P. J., Silverman, D. C. & Jeffreys, C. R. Corrosion protection using polyaniline coating formulations. *Synthetic Metals* 85, 1327-1332 (1997).
- 133 Zheng, W.-Y., Levon, K., Laakso, J. & Oesterholm, J.-E. Characterization and Solid-State Properties of Processable N-Alkylated Polyanilines in the Neutral State. *Macromolecules* 27, 7754-7768 (1994).
- 134 Yue, J., Wang, Z. H., Cromack, K. R., Epstein, A. J. & MacDiarmid, A. G. Effect of sulfonic acid group on polyaniline backbone. *Journal of the American Chemical Society* 113, 2665-2671, doi:10.1021/ja00007a046 (1991).
- 135 Yue, J. & Epstein, A. J. Synthesis of self-doped conducting polyaniline. *Journal of the American Chemical Society* 112, 2800-2801, doi:10.1021/ja00163a051 (1990).
- 136 Chen, S.-A. & Hwang, G.-W. Water-Soluble Self-Acid-Doped Conducting Polyaniline: Structure and Properties. *Journal of the American Chemical Society* 117, 10055-10062, doi:10.1021/ja00145a017 (1995).
- 137 Lin, H.-K. & Chen, S.-A. Synthesis of New Water-Soluble Self-Doped Polyaniline. *Macromolecules* 33, 8117-8118, doi:10.1021/ma000660o (2000).
- 138 Ke, W.-J. *et al.* Solution processable self-doped polyaniline as hole transport layer for inverted polymer solar cells. *Journal of Materials Chemistry* 21, 13483-13489 (2011).
- 139 Deore, B. A., Yu, I. & Freund, M. S. A Switchable Self-Doped Polyaniline: Interconversion between Self-Doped and Non-Self-Doped Forms. *Journal of the American Chemical Society* 126, 52-53, doi:10.1021/ja038499v (2003).
- 140 Malinauskas, A. Self-doped polyanilines. *Journal of Power Sources* 126, 214-220, doi:<http://dx.doi.org/10.1016/j.jpowsour.2003.08.008> (2004).

# Appendix

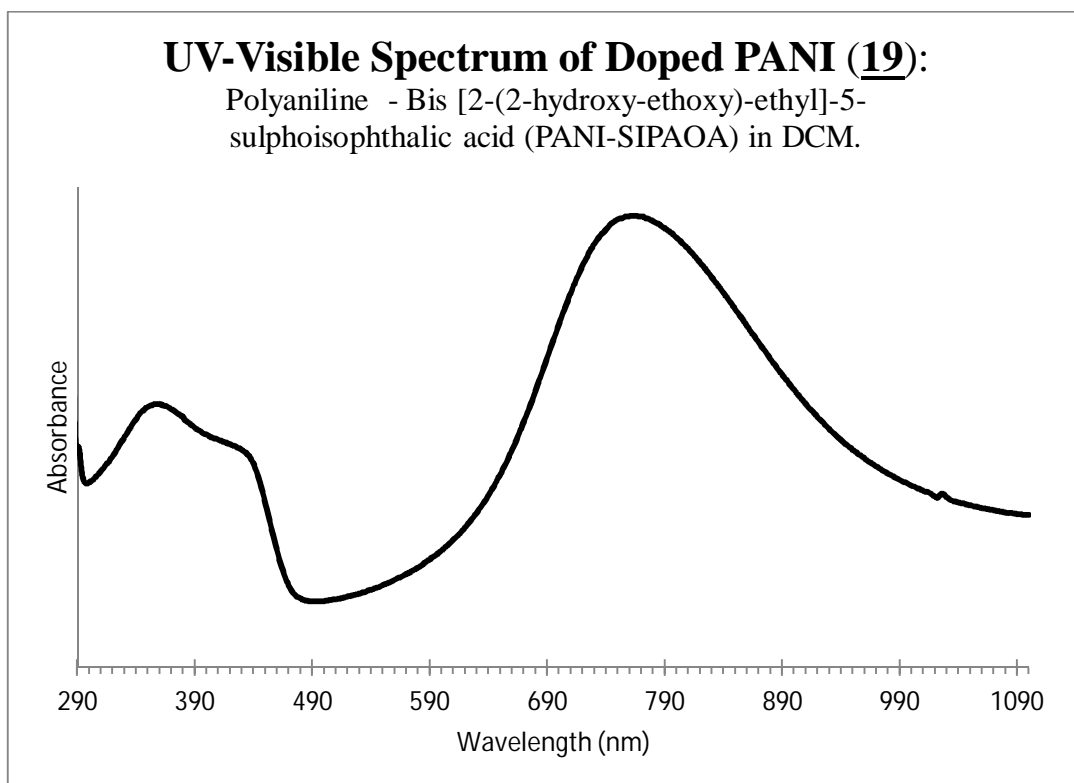
## 1. UV/Visible Spectroscopy (supplementary)



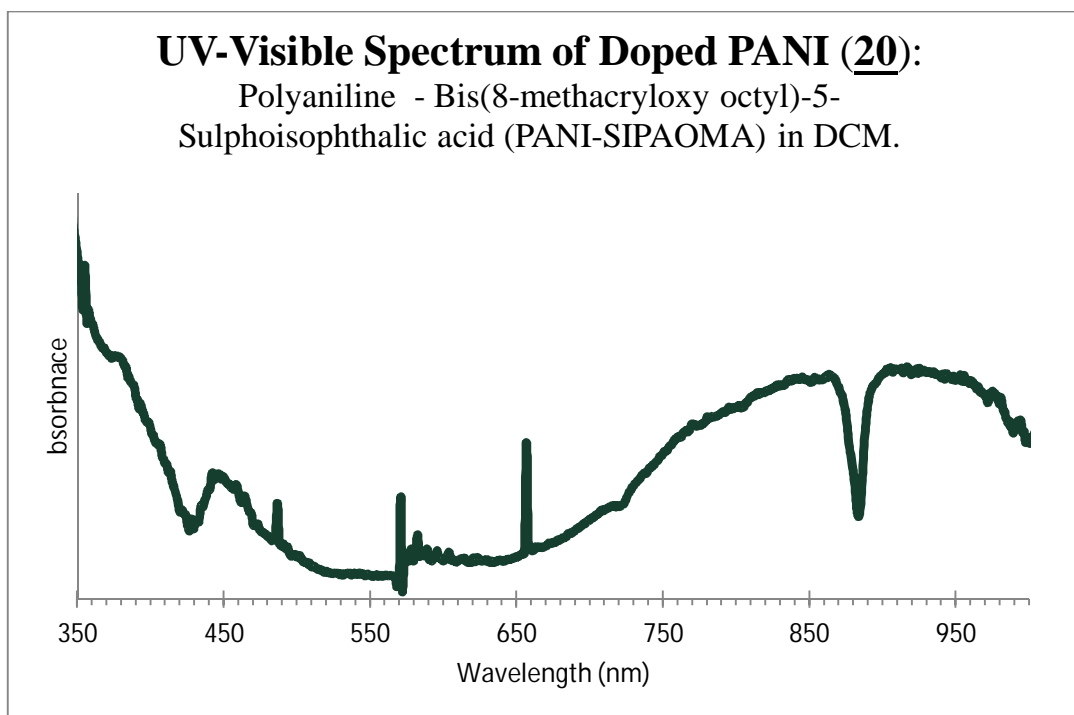
**Appendix 1: UV/Vis spectroscopy displaying the electronic properties of polyaniline doped with bis(8-hydroxyoctyl)-5-sulphoisophthalic acid (**17**).**



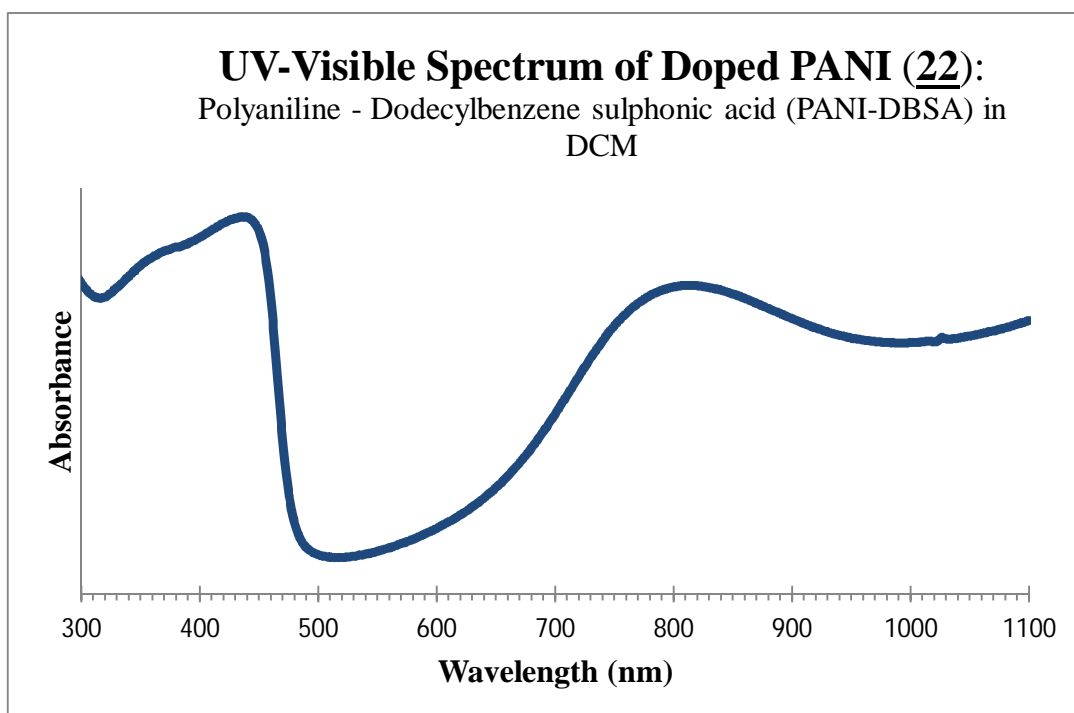
Appendix 2: UV/Vis spectroscopy displaying the electronic properties of polyaniline doped with bis(8-acryloxy octyl) 5-sulphoisophthalic acid doped PANI (18) (PANI- SIPAOA) in solution.



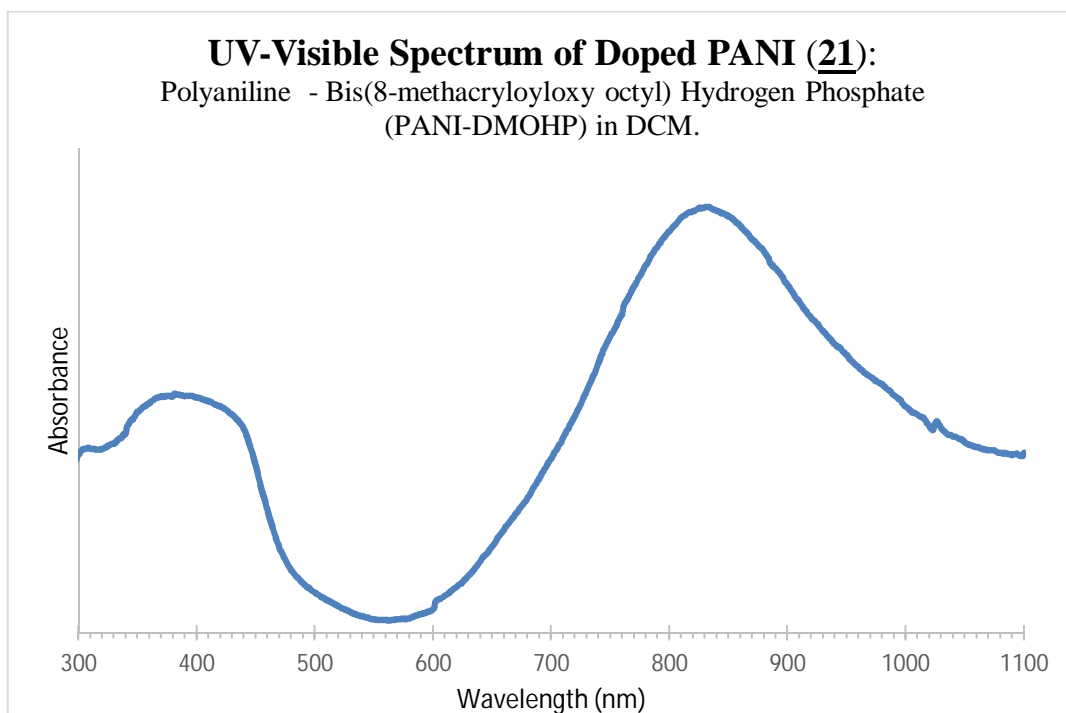
Appendix 3: UV/Vis spectroscopy displaying the electronic properties of polyaniline doped with bis[2-(2-hydroxy-ethoxy)-ethyl]-5-sulphoisophthalic acid (PANI-SIPAOA).



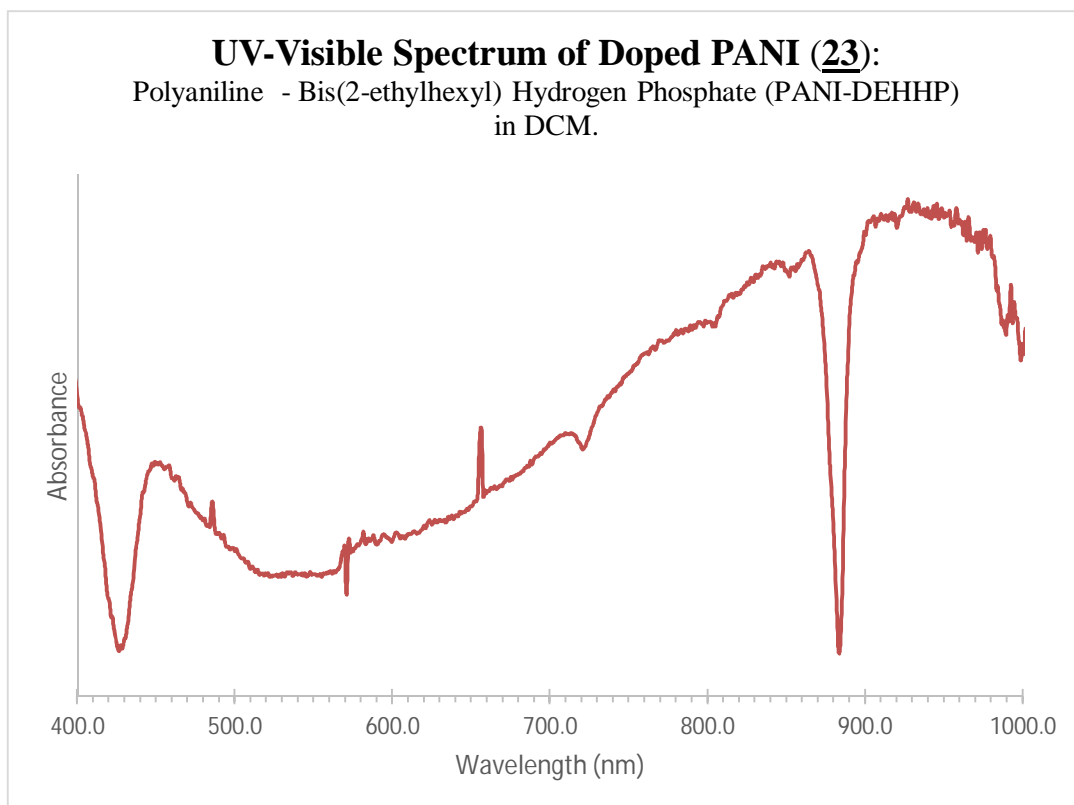
**Appendix 4: UV/Vis spectroscopy displaying the electronic properties of polyaniline doped with bis(8-methacryloxy octyl)-5-Sulphoisophthalic acid (PANI-SIPAOMA).**



**Appendix 5: UV/Vis spectroscopy displaying the electronic properties of polyaniline doped with dodecylbenzene sulphonic acid doped PANI (22) (PANI-DBSA).**



**Appendix 6: UV/Vis spectroscopy displaying the electronic properties of polyaniline doped with bis(8-methacryloyloxy octyl) Hydrogen Phosphate (PANI-DMOHP) (21).**



**Appendix 7: UV/Vis spectroscopy displaying the electronic properties of polyaniline doped with bis(2-ethylhexyl) Hydrogen Phosphate (PANI-DEHHP) (23).**

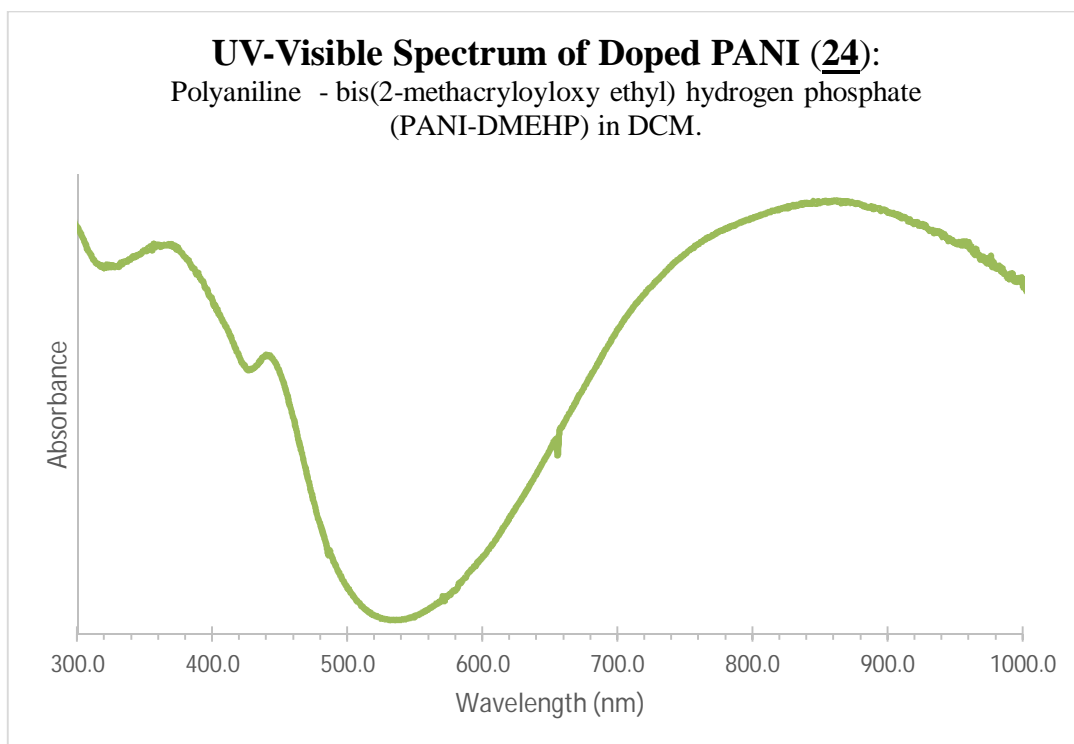
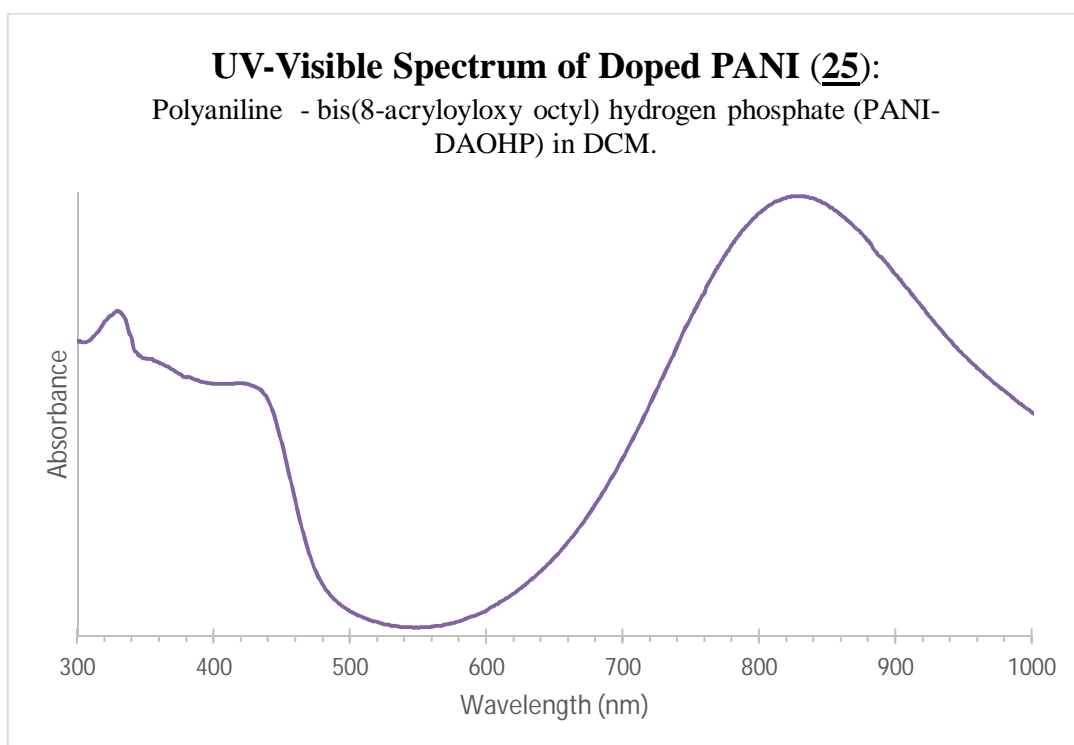
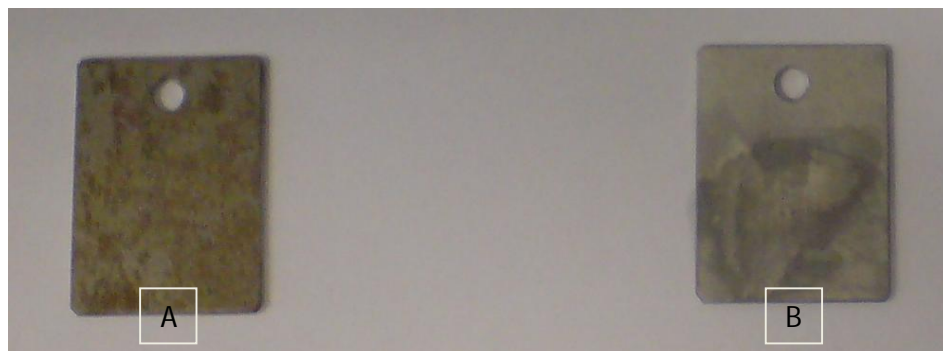


**Figure 98: UV/Vis spectroscopy displaying the electronic properties of polyaniline doped with bis(2-methacryloyloxy ethyl) Hydrogen Phosphate (PANI-DMEHP) (24).**

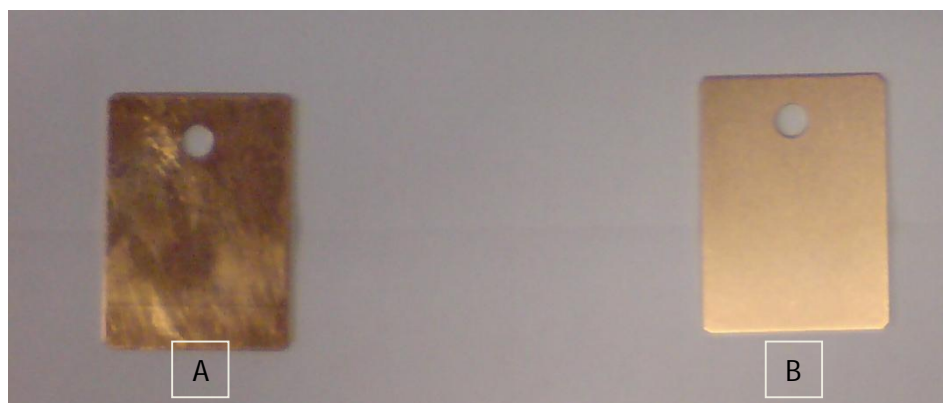


**Appendix 8: UV/Vis spectroscopy displaying the electronic properties of polyaniline doped with bis(8-acryloyloxy octyl) hydrogen phosphate (PANI-DAOHP) (25).**

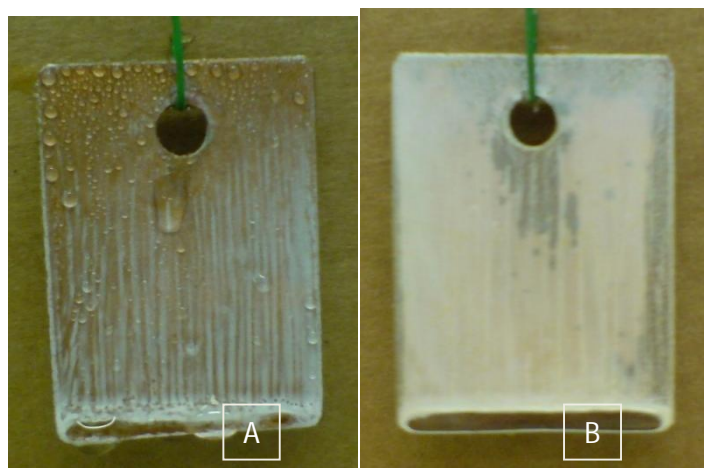
2. Accelerated corrosion (supplementary)



**Appendix 9: Photograph of A) Mild Steel before acid pickling and B) After acid pickling.**



**Appendix 10: Photograph of A) Copper before acid pickling and B) After acid pickling**



**Appendix 11: Photographs of PVC cast Film onto copper; sampling A) 7 days after being sprayed with a 3.5% saline solution and B) 7days after being submerged into a 3.5% saline solution.**



**Appendix 12: Metal samples coated in epoxide resin cast films, from left to right; mild steel submerged, mild steel sprayed (3.5% saline), copper submerged and copper sprayed after 7 days incubation.**



**Appendix 13: Metal plates coated in acrylic resin alone prior to accelerated corrosion testing, from left to right; steel then copper for submersion and steel and copper for spraying.**



Appendix 14: Photograph of A) Copper after 48 hrs submersion in 3.5% Saline Solution and B) Copper after 1 hr post saline spray Doped PANI (17).



Appendix 15: Photograph of both steel and copper prior to testing (top image) and corrosion noticed after 24hrs; from left to right Steel submerged, copper submerged, steel sprayed and copper sprayed with (3.5%) saline solution and coated doped PANI (18).



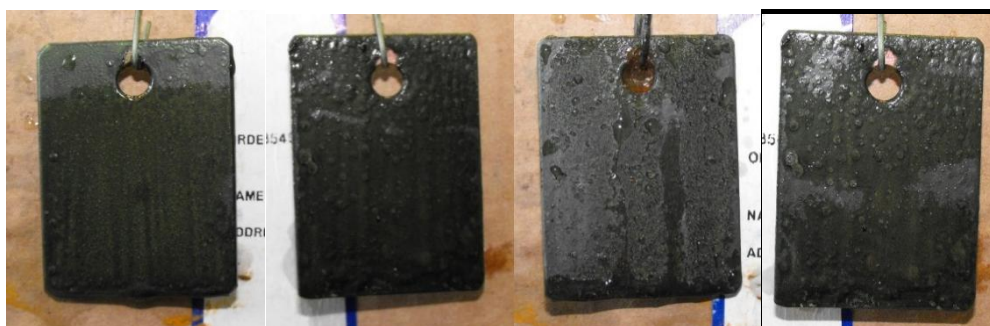
Appendix 16: : Photograph of both steel and copper prior to testing (top image) and corrosion noticed after 24hrs; from left to right steel submerged, copper submerged, steel sprayed and copper sprayed with (3.5%) saline solution and coated doped PANI (20).



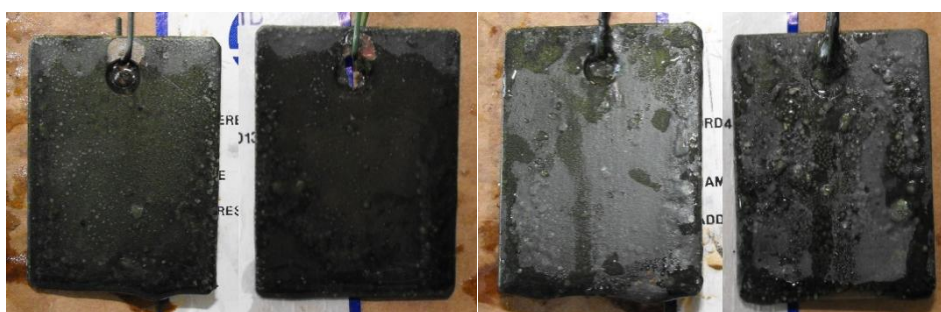
Appendix 17: Photograph of both steel and copper coated with doped PANI (18) 1 wt% in PVC after 7 days (168 hrs) of testing, from left to right; steel submerged, copper submerged in a saline solution (3.5%) and steel sprayed and copper sprayed with (3.5%) saline solution.



**Appendix 18:** Photograph of both steel and copper coated with doped PANI (20) 1 wt% in PVC after 7 days (168 hrs) of testing, from left to right; steel submerged, copper submerged in a saline solution (3.5%) and steel sprayed and copper sprayed with (3.5%) saline solution.



**Appendix 19:** Photograph of doped PANI (22) 2 wt% in PVC, dip coated and air dried. From left to right steel submerged, copper submerged in a saline solution (3.5%) after 7 days (168 hrs) and steel sprayed and copper sprayed with (3.5%) saline solution. after 7 days (168 hrs).



**Appendix 20:** Photograph of doped PANI (22) 1 wt% in PVC, dip coated and air dried. From left to right steel submerged, copper submerged in a saline solution (3.5%) after 7 days (168 hrs) and steel sprayed and copper sprayed with (3.5%) saline solution after 7 days (168 hrs).



Appendix 21: Photograph of doped PANI (21) 1 wt% in PVC, dip coated and air dried. From left to right steel submerged, copper submerged in a saline solution (3.5%) after 7 days (168 hrs) and steel sprayed and copper sprayed with (3.5%) saline solution after 7 days (168 hrs).



Appendix 22: Photograph of doped PANI (23) 1 wt% in PVC, dip coated and air dried. From left to right steel submerged, copper submerged in a saline solution (3.5%) after 7 days (168 hrs) and steel sprayed and copper sprayed with (3.5%) saline solution after 7 days (168 hrs).

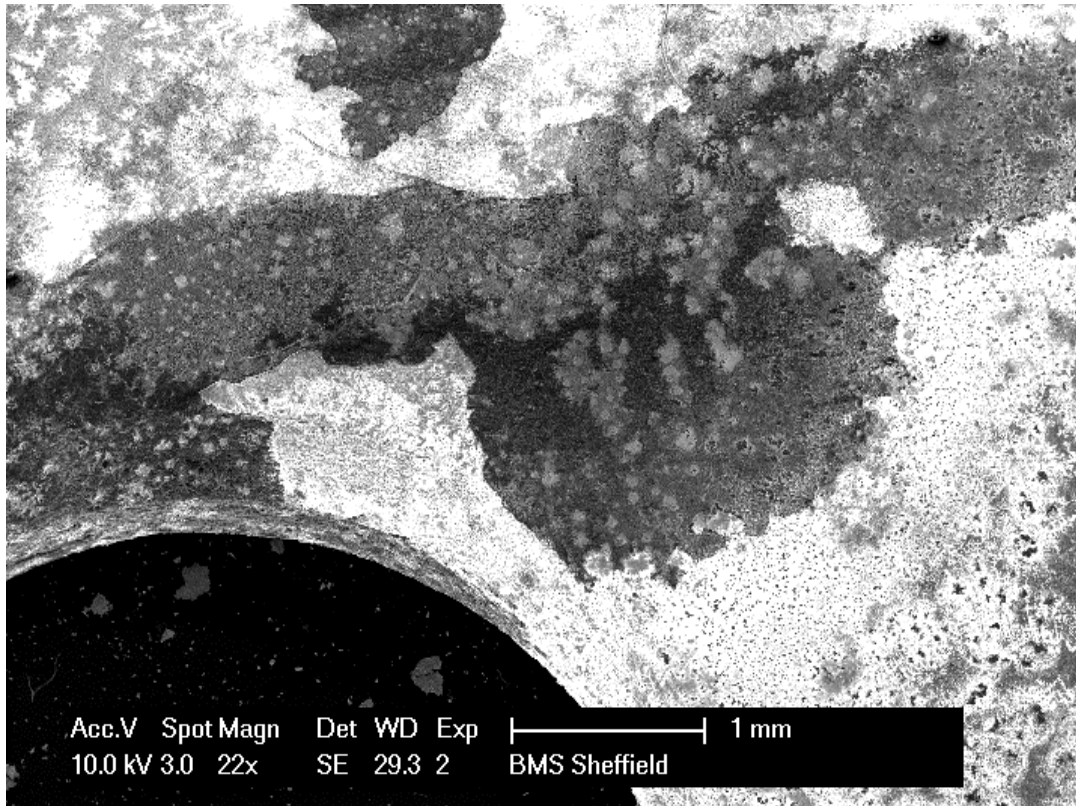


Appendix 23: Photograph of doped PANI (18) 1 wt% in acrylic resin. From left to right steel submerged, copper submerged in a saline solution (3.5%) and steel sprayed and copper sprayed with (3.5%) saline solution after 7 days (168 hrs).

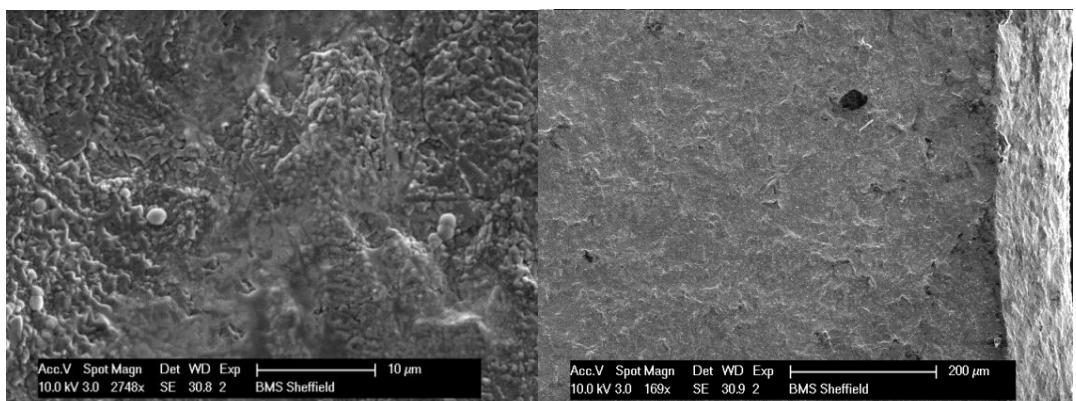


**Appendix 24: Photograph of doped PANI (23) 1 wt% in acrylic resin. From left to right steel submerged, copper submerged in a saline solution (3.5%) and steel sprayed and copper sprayed with (3.5%) saline solution after 24 hrs Top image. and after 48 hrs for the bottom image samples.**

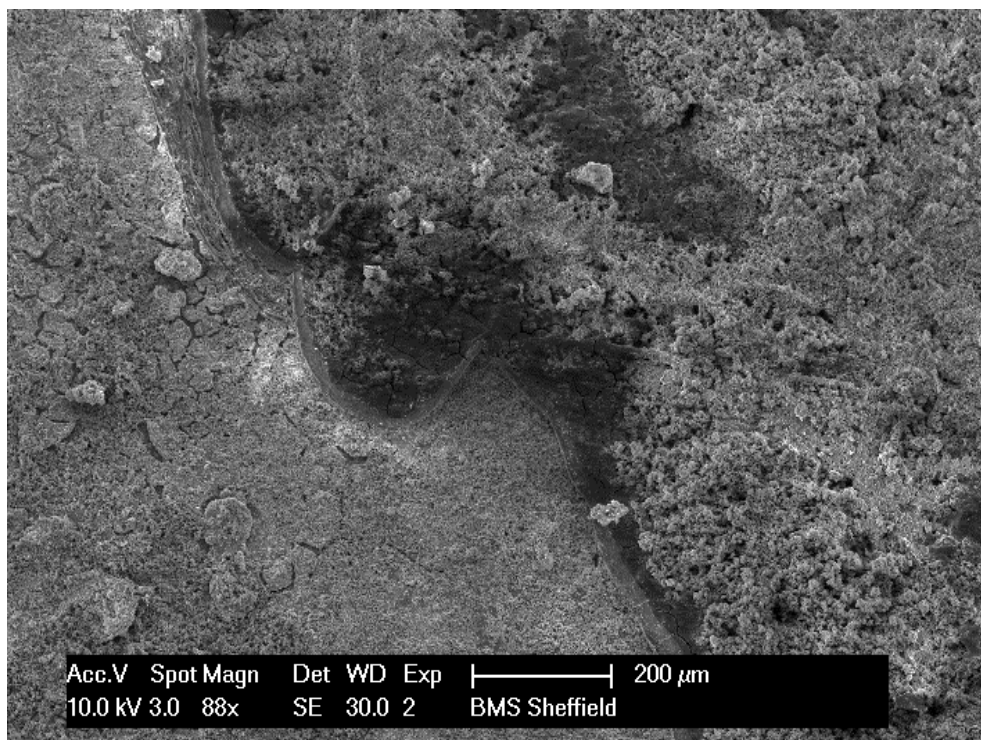
## 3. Electron Microscopy images (supplementary)



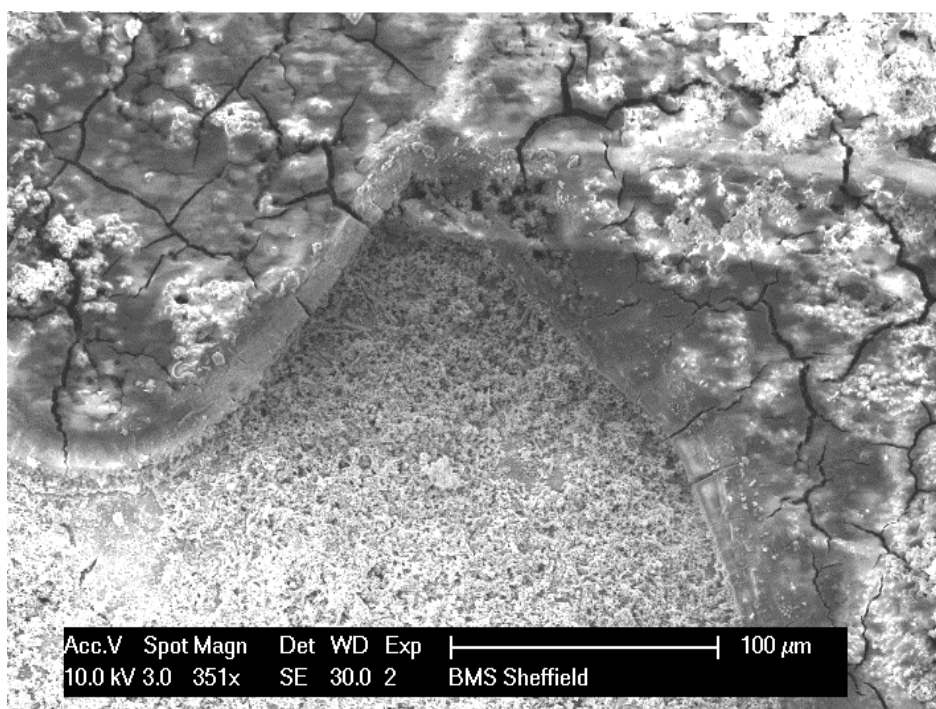
**Appendix 25:** Uncoated steel sample taken at the eyelet, situated at the top centre of the plate. The surface of the metal in this zone illustrates both corroded (rust) metal, seen as brighter areas and the duller areas represent rust free zones.



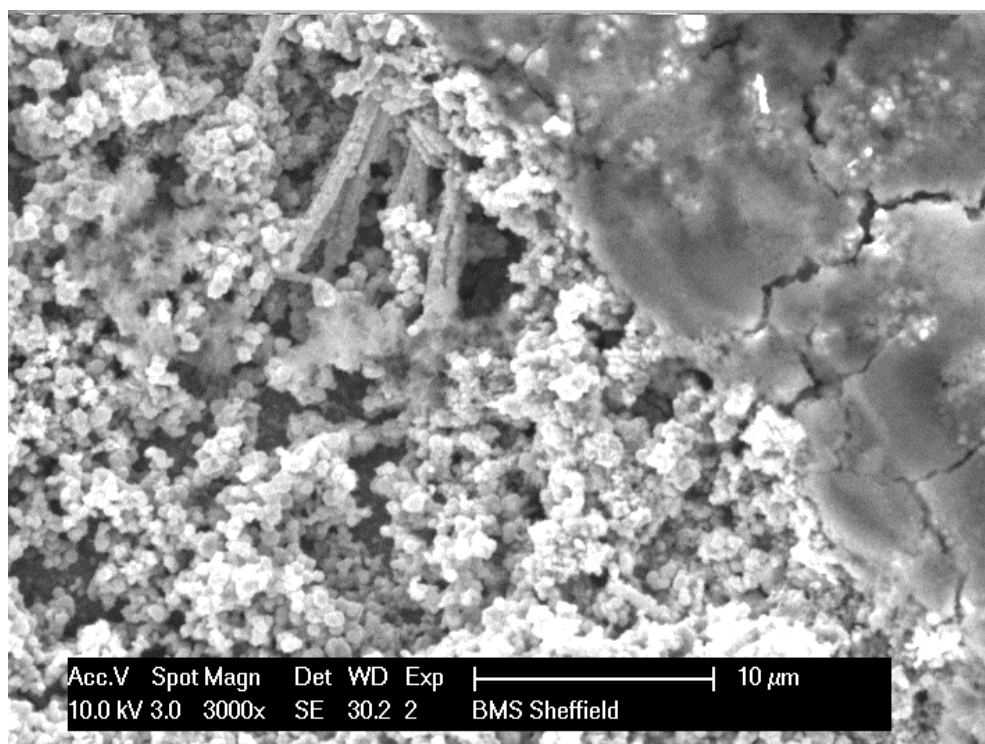
**Appendix 26:** Bare copper surface at; A) 2748x magnification and B) 169x magnification



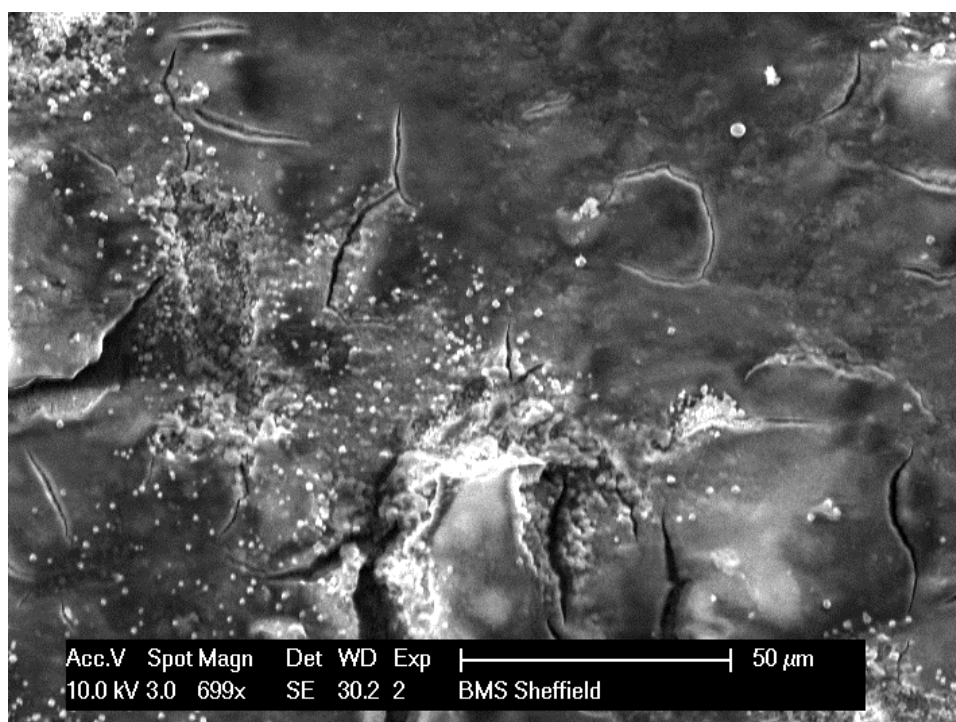
**Appendix 27: Steel sample coated with hydroxyl functionalised doped PANI (17). Image shows Polymer (dark area) and Rust (lighter area). Image obtained at 88x magnification.**



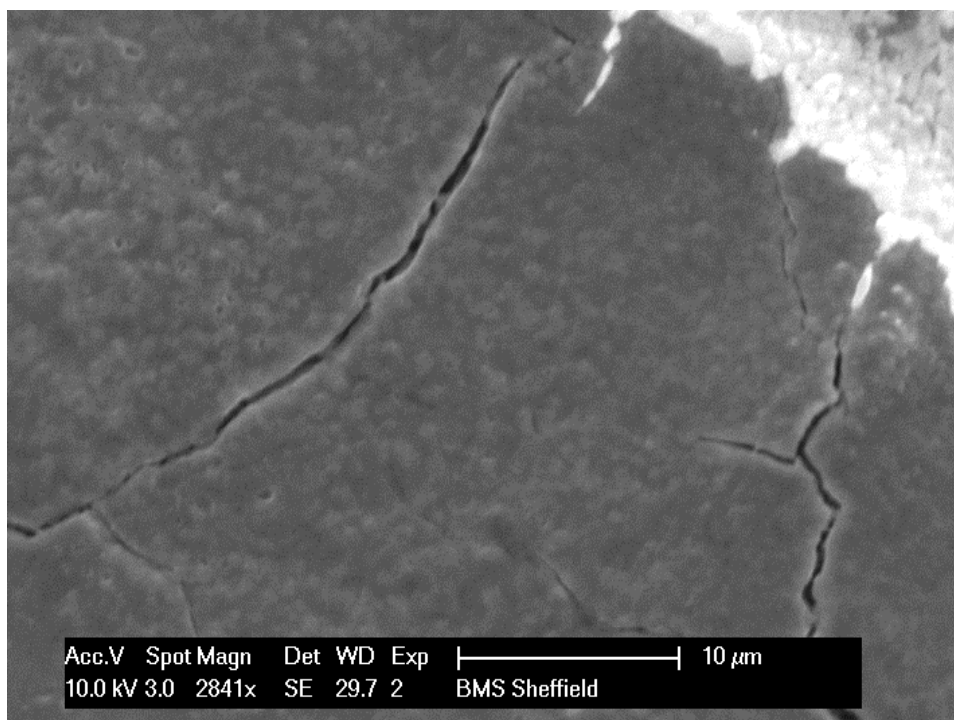
**Appendix 28: Further magnification of the same area shown in (Appendix 27). 351x magnification.**



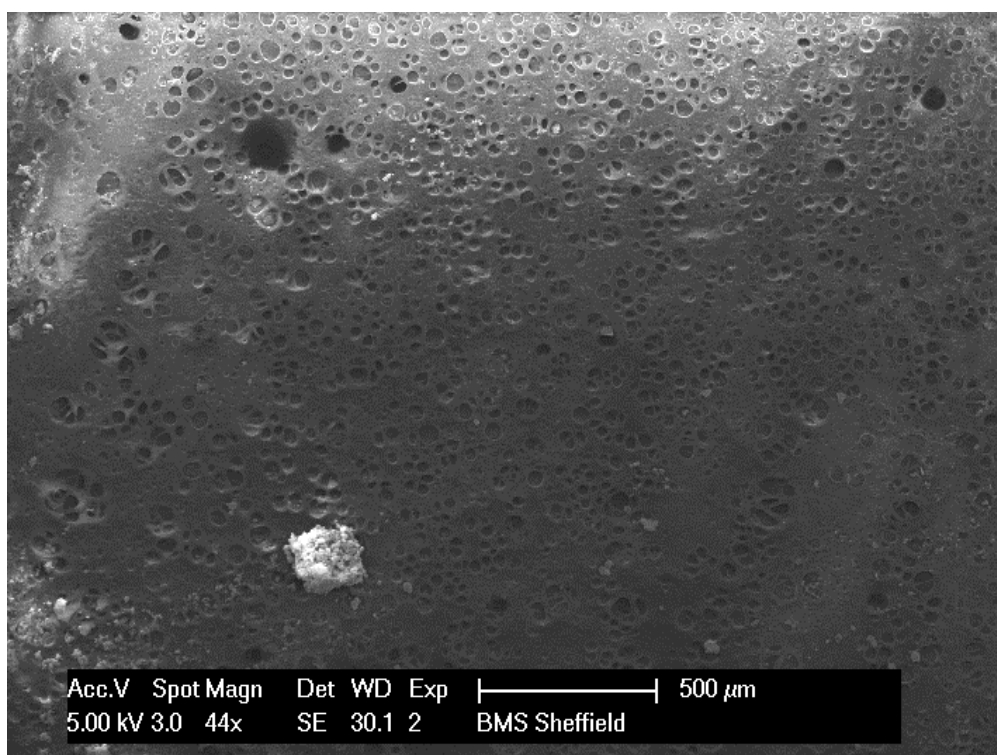
**Appendix 29: Further magnification of Appendix 28 demonstrating the morphology of the polymer and the corroded steel at the interface.**



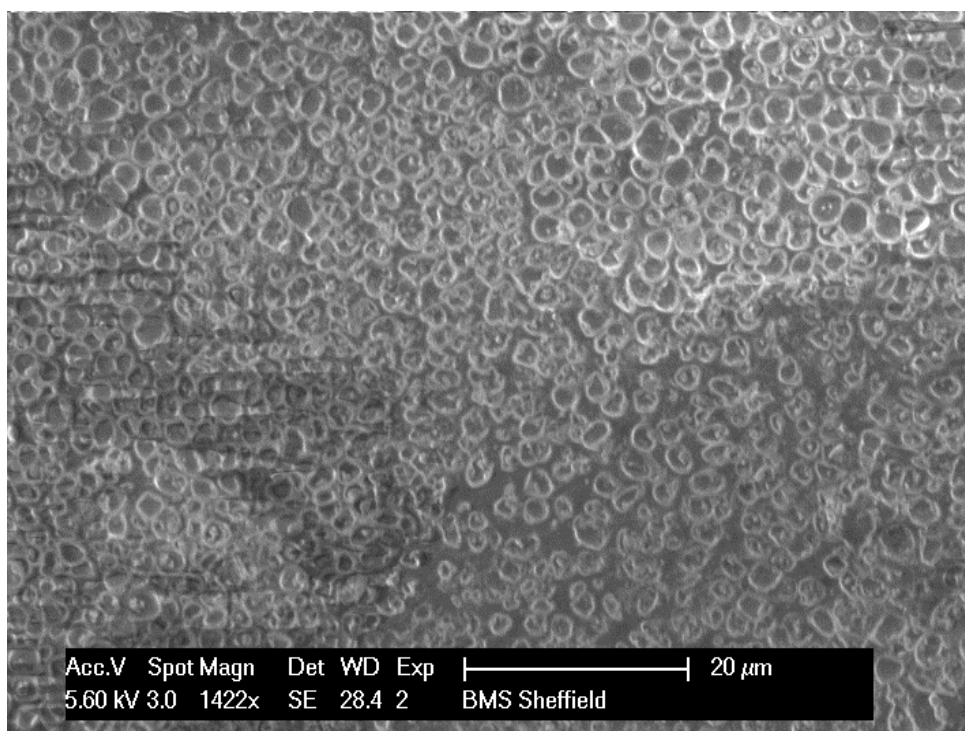
**Appendix 30: Copper sample coated with doped PANI (17).**



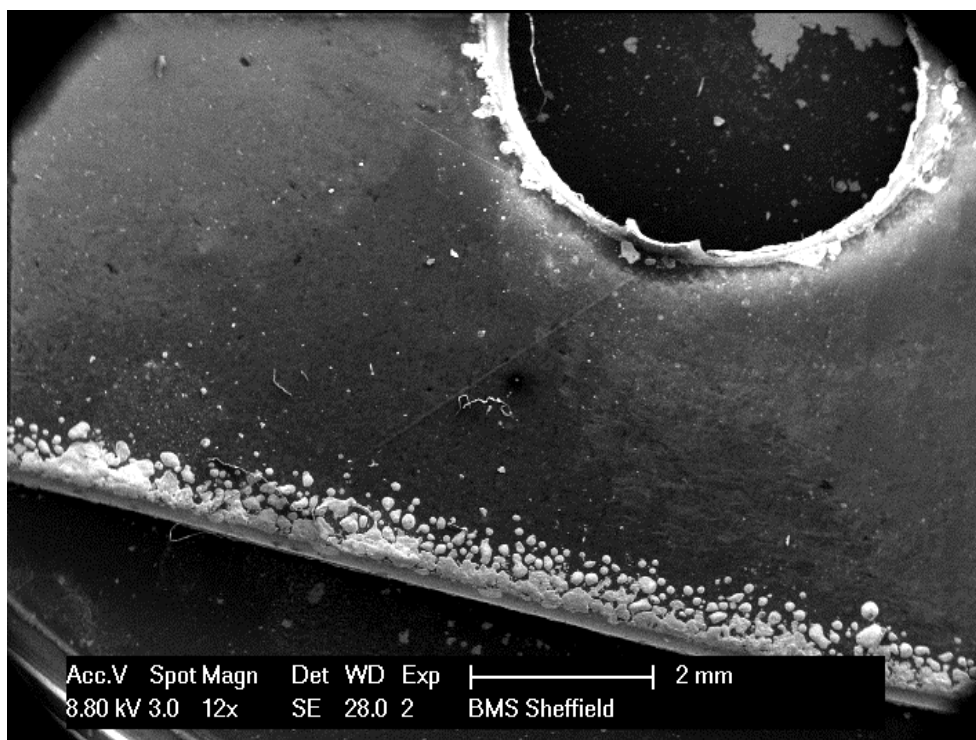
Appendix 31: Doped PANI (23) film on copper.



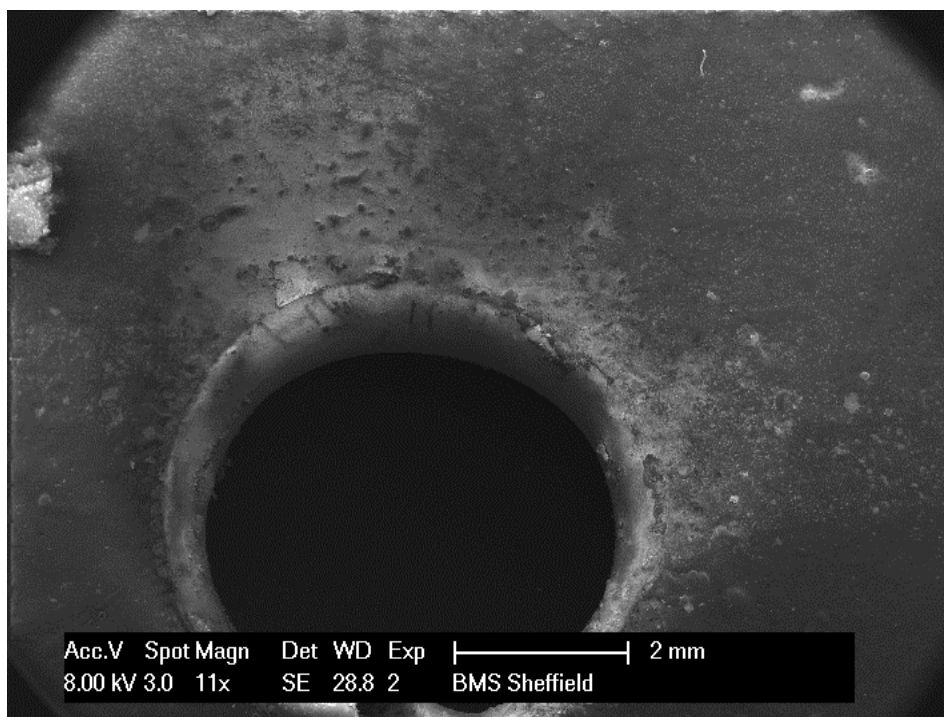
Appendix 32: PVC (Polyvinyl chloride) cast onto pre-cleaned steel.



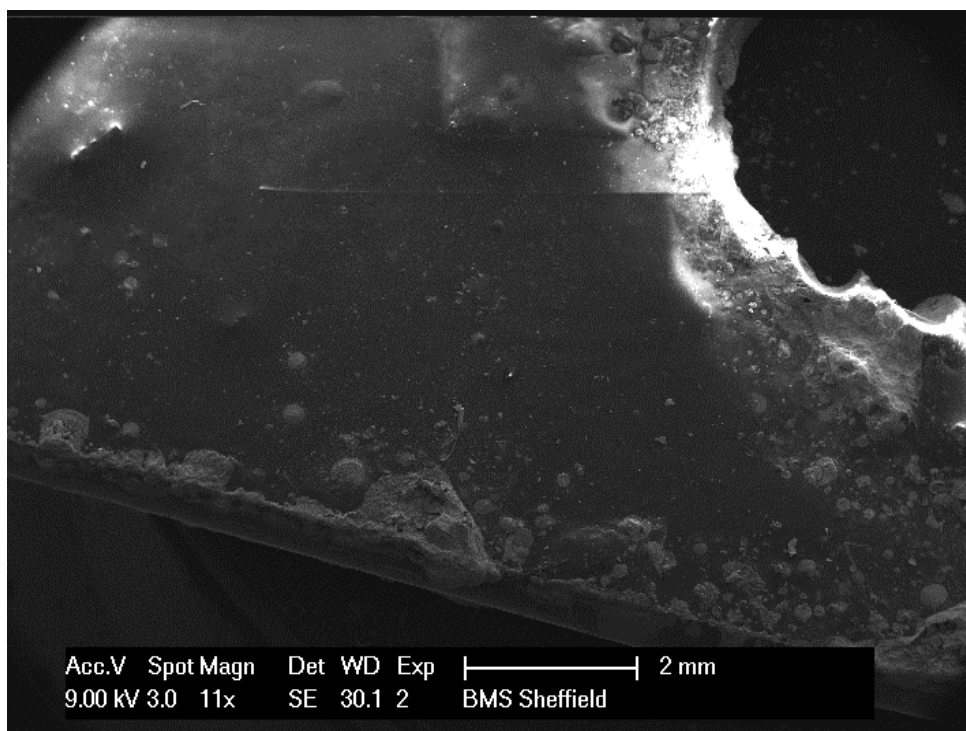
Appendix 33: PVC/doped PANI (22) 1 wt% cast onto steel.



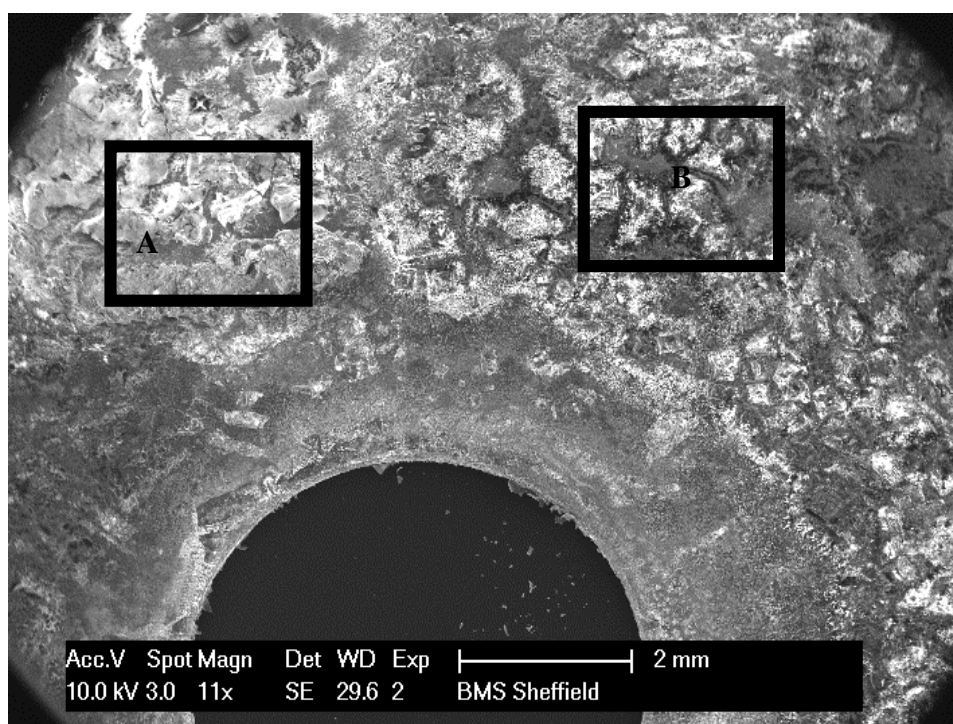
Appendix 34: Pre-cleaned copper sample with epoxy resin matrix cast film coating.



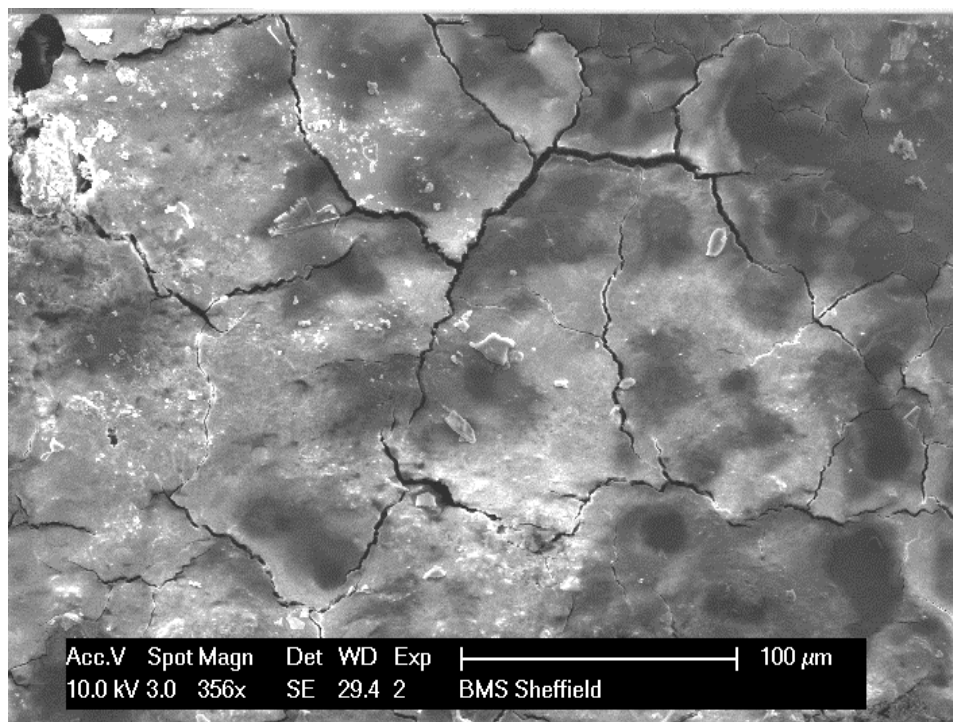
**Appendix 35: Epoxy resin/doped PANI (17) 1 wt%, displaying no rust at the edge of metal sheet**



**Appendix 36: Epoxy resin cast film on pre cleaned steel sample.**



**Appendix 37: Acrylate resin/doped PANI (21) 1 wt% cast film, displaying A) organic coat delamination (top left corner) and B) rust (mid-centre to the right).**



**Appendix 38: Intact acrylate resin/doped PANI (21) 1 wt% cast film on steel**